A thesis submitted in part fulfilment of the requirements of the degree
Doctor of Philosophy

Development of Photoredox Catalysed Transformation of Enamides and Allenamides

Olusesan Kayode Koleoso

Department of Chemistry

Loughborough University

Supervisor:

Dr Marc C. Kimber

ABSTRACT

Enamides and allenamides are two versatile functional groups that offer a wide variety of alternatives for the inclusion of nitrogen-based moiety into an organic system. Nitrogen-containing structures are prevalent among medicinally interesting natural and unnatural products and, thus, are useful in developing new therapeutics. Their chemical utilities have been exploited by a number of research groups. They represent interesting functional groups and useful in organic synthesis.

Photoredox catalytic approach was develop to synthetically transform enamides into useful products, *N*-acyl-*N'*-aryl-*N,N'*-aminals. A novel approach using iridium polypyridyl complex photoredox catalyst to initiate a three-component domino transformation of enamides to *N*-acyl-*N'*-aryl-*N,N'*-aminals *via* photoredox catalysed β-alkylation of enamide intermediates and their subsequent trapping with an arylamine was successfully developed. The *N*-acyl-*N'*-aryl-*N,N'*-aminal structural motif is prevalent within a wide range of biologically important compounds and have attracted considerable attention as building blocks for the synthesis of drug candidates.

This method uses the addition of a radical precursor to an enamide, with subsequent interception of the cationic iminium intermediate with an arylamine. The reaction was found to be compatible with both electron-rich and electron-deficient arylamines, and moderate to good levels of diastereoselectivity were attained using a chiral enamide. The *N*-acyl-*N'*-aryl-*N,N'*-aminals formed were used as precursors to synthesis of valuable γ-lactams building blocks under a mild condition by cyclization. The γ-lactams were obtained by intramolecular cyclization of the *N,N'*-aminals with the lone pair of the nitrogen atom of the arylamine as the nucleophilic centre attacking the electrophilic carbon of the carbonyl carbon of the ester in the molecule. This is a novel synthetic route to these valuable γ-lactams.

The photoredox reaction procedure developed was also applied on allenamides. There are limited reports of radical reactions on allenamides, the major and seemingly single intermolecular radical cyclization involving allenamides was the one reported by Hsung. There are no reports of radical photoredox reactions on allenamides in the literature. The addition reaction was initiated by the electrophilic malonate radical generated by irradiation with blue light in the presence of iridium photoredox catalyst. The malonate radical attacked the central carbon of the allenic group which led to the formation of β-alkyl allenamide

radical that was oxidized to an iminium ion intermediate. The iminium intermediate was subsequently trapped with an arylamine giving rise to α,β-addition product (*N*-acyl-*N'*-aryl-*N*,*N'*-aminals) with *exo*-methylene or β,γ-addition product leading to the formation of double bond substituted enamides. It was found that the α,β-adduct product is more favourable, however, the alternative product was formed when the α-position is sterically hindered by the substituents on the allenamide or the arylamine nucleophile.

ACKNOWLEDGEMENTS

List of Abbreviations

AcO $^-$	Acetate ion
ATRA	Atom transfer radical addition
BET	Back Electron Transfer
BNAH	1-Benzyl-1,4-dihydronicotinamide
Boc	*t*-Butyloxycarbonyl
bpy	2,2'-Bipyridyl
bpz	2,2'-Bipyrazyl (2,2'-bipyrazine)
COSY	Correlation Spectroscopy
CSA	Camphorsulfonic acid
DCM	Dichloromethane
DEPT	Distortionless Enhancement by Polarization Transfer
DME	Dimethoxyethane
DMSO	Dimethylsulfoxide
DNA	Deoxyribonucleic acid
DPP	4,7-diphenyl-1,10-phenanthroline
dtbbpy	4,4'-Di-*tert*-butyl-2,2'-bipyridine
Et	Ethyl
ET	Electron Transfer
EWG	Electron withdrawing group

FTIR	Fourier Transform Infrared
HE	Hantzsch ester
HMQC	Heteronuclear Multiple Quantum Coherence
HOMO	Highest Occupied Molecular Orbital
HRMS	High Resolution Mass Spectroscopy
IR	Infrared
LAS	Light Absorption Sensitizer
LED	Light Emitting diode
LUMO	Lowest Un-occupied Molecular Orbital
m	meta
mg	milligramme
mL	millilitre
MLCT	Metal to Ligand Charge Transfer
MRSA	Meticillin-Resistant *Staphylococcus aureus*
n	normal
NADH	1,4-Dihydronicotinamide dinucleotide
NMR	Nuclear Magnetic Resonance
NOE	Nuclear Overhauser Effect
o	ortho
ORTEP	Oak Ridge Thermal-Ellipsoid Plot Program

p	para
PDE	Phosphodiesterase
PET	Photo-induced Electron Transfer
phen	1,10-Phenanthroline
PKR	Pauson-Khand reaction
ppm	Part per million
PPTS	Pyridinium *p*-toluenesulfonate
ppy	2-Phenylpyridine
rt	Room temperature
SET	Single Electron Transfer
t-**Bu**	*tert*-butyl
TEA	Triethylamine
Tf	Triflate
TLC	Thin Layer Chromatography
TMS	Trimethylsilyl
TSA	*p*-Toluenesulfonic acid
UV	Ultra-violet
δ	Chemical shift

Table of Contents

1.0   Introduction

1.1   Photocatalysis

Catalysis, the action of a catalyst, is a process in which the rate of a reaction is altered (usually enhanced) by the presence of a different substance (catalyst) that does not undergo any permanent change itself in the course of the reaction. Thus, catalysis is simply the "acceleration of a chemical reaction by the presence of a catalyst". A catalyst does not change in itself or being consumed in the chemical reaction. A substance can be thought to be a catalyst when it alters the rate of a chemical reaction without being consumed as a reactant; though it appears in the rate expression describing a thermal reaction without appearing in the stoichiometric equation.

According to Castellote M. and Bengtsson N. in 2011, in a book titled *Application of Titanium Dioxide Photocatalysis to Construction Materials:* State-of-the-Art Report of the RILEM Technical Committee 194-TDP, edited by Ohama Y. and Van Gemert D.,[1] catalysis refers simply to a "process in which a substance (the catalyst) accelerates, through intimate interaction(s) with the reactant(s) and concomitantly providing a lower energy pathway, an otherwise thermodynamically favoured but kinetically slow reaction with the catalyst fully regenerated quantitatively at the conclusion of the catalytic cycle." A catalyst alters the rate of a reaction by providing an alternative pathway that lowers the free activation enthalpy necessary for the reaction to proceed along the reaction pathway. It increases the rate of a reaction without modifying the overall standard Gibbs energy change (the driving force for a reaction to occur) of the reaction. A catalyst will not ordinarily make a reaction that is not thermodynamically favoured to occur. It can only alter the rate of a reaction that is thermodynamically feasible.

When photons (discrete packets of energy associated with electromagnetic radiation (light)) are involved in the acceleration of a reaction, without the implication of any specific mechanism, the expression photocatalysis can be used to describe the acceleration. Photocatalysis can then be described as a change in the rate of chemical reactions under the action of light in the presence of substances -called photocatalysts- that absorb light quanta and are involved in the chemical transformations of the reaction participants.[2]   A photocatalyst is a substance that is able to produce, by absorption of light quanta, chemical

transformations of the reaction participants, repeatedly coming with them into the intermediate chemical interactions and regenerating its chemical composition after each cycle of such interactions.[2] The catalyst may accelerate the photoreaction by interacting with the substrate(s) either in its ground state or in its excited state or with the primary product (of the catalyst), depending on the mechanism of the photoreaction.[3,4] Chlorophyll of plants is a type of photocatalyst (**Figure 1**). Photocatalysis compared to photosynthesis, in which chlorophyll captures sunlight to turn water and carbon dioxide into oxygen and glucose. Therefore, photocatalysis, as a part of photochemistry, refers to reactions promoted by synergetic effect of light and a catalyst but keeping the same essence as a thermal reaction.

Figure 1: Chemical structure of chlorophyll
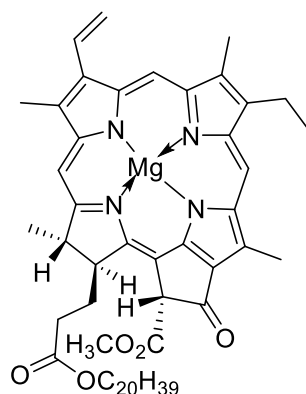
Clarification needs to be made between a sensitized and a catalysed photoreaction. A photosensitization is a process in which a photochemical alteration occurs in one molecular entity as a result of initial absorption of radiation (light) by another molecular entity called the photosensitizer. This is catalytic in photons. Whereas in a catalysed photoreaction which is non-catalytic in photons, either the nominal catalyst or the substrate or both are in an excited state during the catalytic step.

Depending on the specific photoreaction, the catalyst may accelerate the photoreaction by interaction with the substrate in its ground or excited state and/or with a primary photoproduct. When the light is absorbed by the catalyst ([cat]), the system represents a sensitized photoreaction, the reaction may occur through two different ways:

1. *via* energy transfer, by forming an activated state of the reactant of interest (R), which is more reactive than its ground state:[1]

Scheme 1: Energy Transfer Activity of a Photocatalyst

$$[cat] \ + \ h\nu \longrightarrow [cat]^*$$

$$[cat]^* \ + \ R \longrightarrow [cat] \ + \ R*$$

$$R* \longrightarrow P$$
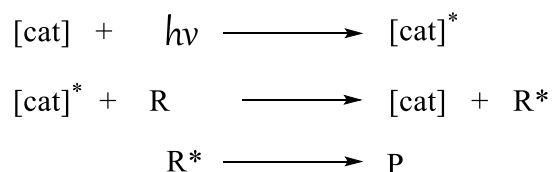
In this case, when the photocatalyst absorbs photon quanta, it is activated and raised to its excited state. This activated or excited entity interacts with the reactant of interest R and in the process, energy is transferred between them. The activated catalyst loses energy to the reactant and returns to its ground state in the process called quenching whereas the reactant R becomes energized and activated. The excited reactant then undergoes transformations that lead to the formation of the product(s).

2. *via* electron transfer, by acting either as an electron donor or electron acceptor.[1]

Scheme 2: Electron Transfer Activity of a Photocatalyst

$$[cat] \ + \ h\nu \longrightarrow [cat]^*$$

$$[cat]^* \ + \ R \longrightarrow [cat]^+ \ + \ R^-$$

$$R^- \longrightarrow P^-$$

$$P^- \ + \ [cat]^+ \longrightarrow P \ + \ [cat]$$
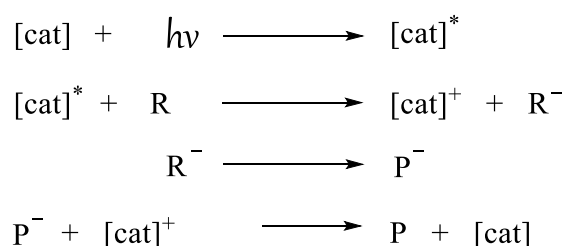
In the case of energy transfer, the product P is formed from the activated substrate along the potential energy curve, while a new reaction path is opened when the photosensitizer transfers an electron to the substrate.[1] In considering excited-state redox reactivity, particularly that involved in organic photocatalysis, the direct occurrence of electron transfer will be of greater concern than involving energy transfer. Chemical reactions involving electron(s) transfer are referred to as oxidation-reduction (redox) reactions and when it involves photocatalysis it is referred to as photoredox catalysis. Photoredox catalysis is therefore a branch of catalysis that harnesses the energy of visible light to accelerate a chemical reaction via electron transfer, most often a single-electron transfer (SET).

1.2   Need for Photoredox Catalysis

Carbon-carbon bond formation is the core of organic synthesis. Many organic synthetic methodologies are based on the ease of generation of radicals. Generation of a radical is

achieved traditionally by heating, irradiation by light or a redox reaction. These conventional methods of radical generation often need the use of harmful or explosive reagents, use of high-energy UV radiation etc.[5,6] In addition, the traditional methods often have a poor atom economy. During the process, considerable amounts of waste are generated which may cause environmental problems, and sometimes special equipment is required. Clearly, the use of a catalyst rather than a stoichiometric reagent is preferable. However, most of the catalysts used often are labile compounds and require that carefully controlled conditions are used (e.g., with regard to the exclusion of air, moisture, impurities), as well as in many cases co-catalysts or additives. Considering the environmental factor, the atom economy and energy requirement, new methods for the formation of the C-C bond have to be developed. These methods/protocols, according to the principles of "Green Chemistry", need to be easy and safe to use and are expected to be efficient (both in terms of energy and atoms) and selective in their outcomes.[7]

Nature's ability to use various visible light absorbing chromophores/photocatalysts for converting solar energy to chemical energy has inspired various research groups to develop a plethora of hosts involving photoredox systems in an effort to mimic natural photosynthesis. However, despite the obvious, practical advantages of visible light as an "infinitely available" promoter for chemical synthesis, the simple inability of most organic molecules to absorb light in the visible range of the spectrum has greatly limited the potential applications of photochemical reactions.

The challenge to mimic and understand enzymatic transformations, organocatalysis has now become an important tool in modern organic synthesis with new reactivity that complements that of enzyme and metal catalysis. The major driving force being the increasing need for more efficient synthetic methods, sustainable processes. It also stimulates the creative rethinking of known concepts, which, in turn, will lead to the development of innovative chemistry.[4,6,7]

Photochemical transformations/reactions, using photocatalysts, generally require mild conditions for substrate activation—ideally light alone—and are suitable for "green reactions".[4] These systems have provided a platform to understand and elucidate the electron or energy transfer pathways involved in natural photosynthesis.[8-12] This, therefore, is employed as a strategy to overcome the barrier posed by the inability of most organic compounds to absorb visible light. Hence, the development of new efficient processes using

photosensitizers and/or photocatalysts.[13] This involves the employment of visible light absorbing photocatalysts and utilizing their electron/energy transfer processes to sensitize organic molecules to carry out required photochemical reactions. Photocatalysts, unlike thermal catalysts, are only effective while in the excited state, activate the substrate through a chemical process, such as photoinduced electron transfer (PET), in lieu of a physical energy transfer such as photosensitization. In particular, photoredox catalysis employs small quantities of a light-sensitive compound that, when excited by light, can mediate the transfer of electrons between chemical compounds that otherwise would not react.[14]

Photocatalysis involves an ever-increasing number of generic activation modes in which photonic energy is selectively targeted to a specifically designed photon-absorbing catalyst (a photocatalyst) which, upon excitation by irradiation with visible light of the appropriate wavelength, is able to induce an accompanying substrate, reagent, or secondary catalyst to participate in unique reaction pathways that were previously unattainable under thermal control.[15,16] Upon irradiation, these molecules are converted into their photoexcited states, which are chemically more reactive because of the significantly altered electronic distribution.

In the recent development of photocatalysis is the recognition that readily accessible (transition) metal polypyridyl complexes and organic dyes can facilitate the conversion of visible light into chemical energy under exceptionally mild conditions[15-17] and as such they can be used as photocatalysts. Most of the commonly employed transition metal polypyridyl complex visible light photocatalysts are those of ruthenium and iridium metals. These complexes can be represented by the general formula ML_3^{n+}, where M is the metal, L the ligand and n is the oxidation state of the metal. In fact, these complexes have played and are still playing a key role in the development of photochemistry, photophysics, photocatalysis, electrochemistry, photoelectrochemistry, chemi- and electrochemi-luminescence, and electron and energy transfer. They allow access to unique chemistries and a broad range of substrates that are unreactive in most synthetic contexts.

The most common mechanisms by which photocatalysts are able to convert light into chemical energy and at the same time perform selective molecular activation include (i) energy transfer, (ii) organometallic excitation, (iii) light-induced atom transfer, and (iv) photoredox catalysis involving single electron transfer.[17] The photophysical properties of an electronically excited molecule in the end determine its photochemical reactivity.

Accordingly, consideration of the properties of a photoredox catalyst in both the excited and ground states is crucial in effecting a desired reactivity.

The first act of any photochemical and photophysical process, including photocatalysis, is the absorption of a photon by a molecule. Absorption of light ($+hv$) produces an electronically excited molecule, the promotion of an electron in the molecule to a higher energy level, from a ground state singlet to a singlet excited state. The excited state that is formed in this way is a high energy, unstable species that must undergo some type of deactivation. As shown in **Figure 2** below, the excited state deactivation can occur *via* (i) disappearance of the original molecule (photochemical reaction), (ii) emission of light ($-hv$) (luminescence), (iii) degradation of the excess energy into heat (nonradiative deactivation), and (iv) some type of interaction with other species (**R**) present in the reaction mixture (quenching process).[18]

Figure 2: Schematic representation of excited state deactivation processes
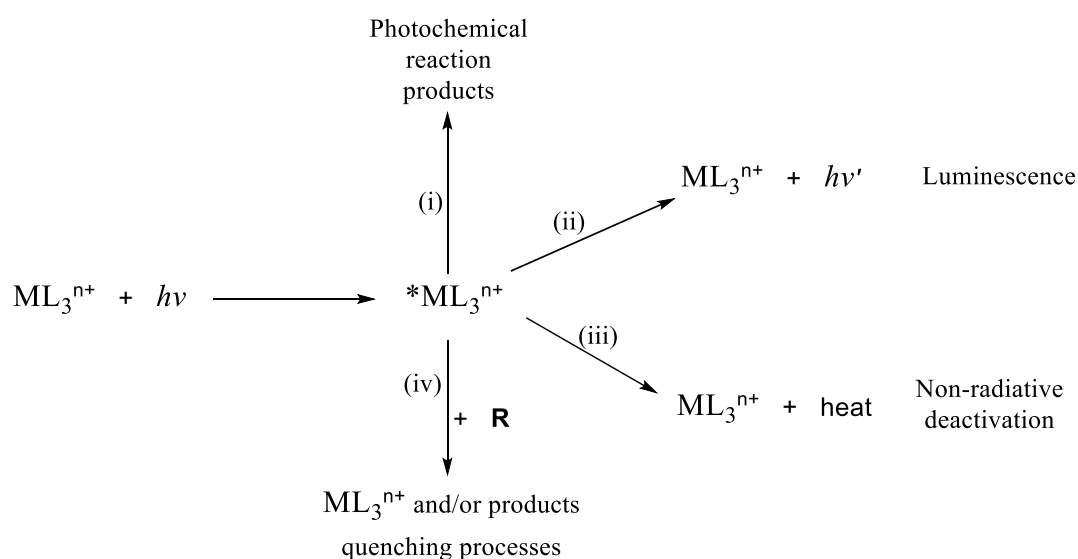
The probability of light (photon) absorption (and thus the intensity of the correspondent absorption band) is related to the characteristics of the states involved and particularly to their spin quantum number. Transitions from the ground state to excited states having the same spin value are allowed and give rise to intense bands, whereas transitions to excited states of different spin value are forbidden and can hardly be observed in the absorption spectra (**Figure 3**).

Upon absorption of a photon in the visible region, an electron in one of the photocatalyst's metal-centered (M^{n+}) orbitals, the highest occupied molecular orbital HOMO, (e.g. a *d*

orbital), is excited to a ligand-centered π^* (L) orbital, the lowest unoccupied molecular orbital, LUMO, (e.g. the π^* orbital of an aromatic ligand), having the same spin allowed value.[8,19,20] This transition is thus termed a metal to ligand charge transfer (MLCT) and results in a species in which the metal has effectively been oxidized (due to a loss of an electron) and the ligand framework has undergone a single-electron reduction (an electron gain).[21] In most molecules, the ground state is a singlet and the lowest excited state is a triplet that cannot be directly populated by light absorption but can be obtained from the deactivation of upper excited states. For this reason, at least three states (e.g., ground state singlet and excited singlet and triplet) are involved in a photochemical process.

Figure 3: Simplified molecular orbital depiction of photoredox catalyst
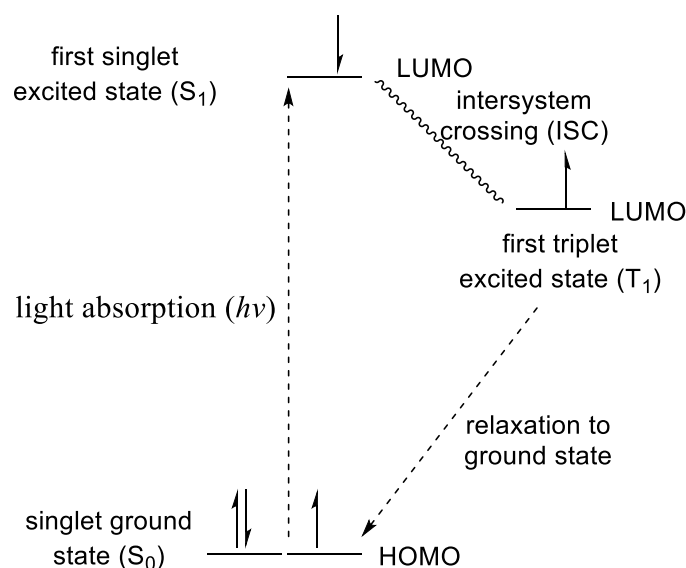
As stated above, the excited state that is formed in this way is a high energy, unstable species that must undergo some type of deactivation to be stabilized. Deactivation of the excited singlet can occur by a number of familiar routes including emission (radiative deactivation), internal conversion, IC or intersystem crossing, ISC (nonradiative deactivation/radiationless decay). Emission of light (luminescence) which could be fluorescence or phosphorescence depending on whether the excited state has the same or different spin compared to the ground state respectively. In the same way, radiationless deactivation is called internal conversion when it occurs between states of the same spin and intersystem crossing when it occurs between states of different spin. Fluorescence and internal conversion are spin-allowed steps, whereas phosphorescence and intersystem crossing are spin-forbidden steps. All these are

referred to as intramolecular deactivation processes or steps. They occur at a very high rate, i.e. they occur very fast within picoseconds.

However, when the intramolecular deactivation steps are not too fast, i.e. when the lifetime of the excited state is sufficiently long, the excited molecule may have a chance to encoun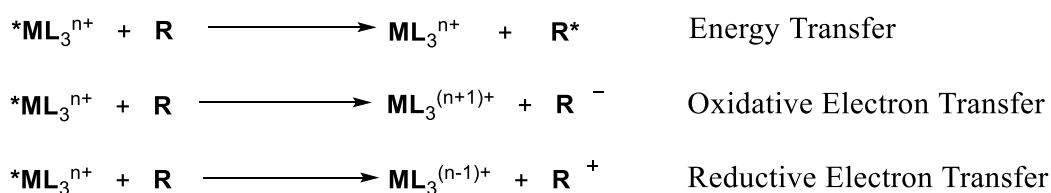ter a molecule of another solute in the reaction mixture. In such a case, some specific interaction may occur and the process taking place is called a bimolecular process (**Scheme 3**) [18].

Scheme 3: Schematic representation of bimolecular processes that may take place between an excited state **M*** and another chemical species/reactant **R**
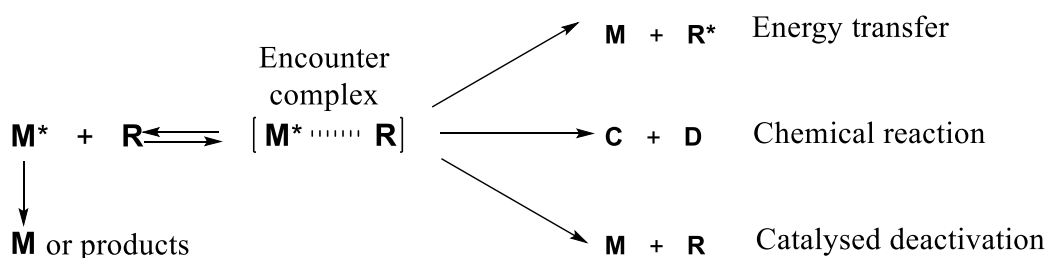
Simple kinetic arguments show that only those excited states that live longer than 10^{-9} s may have a chance to be involved in encounters with other substrate molecules.[19] For transition metal complexes, only the lowest spin-forbidden excited state satisfies this requirement. The triplet state is the long-lived photoexcited species that engages in single-electron transfer; its long lifetime derives from the fact that decay to the singlet ground state is spin-forbidden. These complexes absorb light in the visible region of the electromagnetic spectrum to give stable, long-lived photoexcited states.[19] The lifetime of the excited species is sufficiently long (e.g. 1100 ns for $Ru(bpy)_3^{2+}$)[19] that it may engage in bimolecular electron-transfer reactions in competition with intramolecular deactivation pathways.[18] Photoinduced electron transfer, or PET, is a term used to refer to the overall process of excitation and electron transfer between the excited state molecule and a ground state molecule.

The most important bimolecular processes are energy transfer and electron transfer [22,23]; the latter process may involve either the oxidation or the reduction of the excited state.

$$*ML_3^{n+} + R \longrightarrow ML_3^{n+} + R* \qquad \text{Energy Transfer}$$

$$*ML_3^{n+} + R \longrightarrow ML_3^{(n+1)+} + R^- \qquad \text{Oxidative Electron Transfer}$$

$$*ML_3^{n+} + R \longrightarrow ML_3^{(n-1)+} + R^+ \qquad \text{Reductive Electron Transfer}$$

The unique pathway involving complete electron transfer with concomitant radical ion formation offers a way to return the excited molecule to the ground-state manifold.

It is the conversion of these bench stable transition metal polypyridyl complex, benign catalysts to redox-active species upon irradiation with simple household light bulbs that triggered the use of these transition metal-ligand complexes to induce unique and valuable catalytic processes.[19] In addition, the technological progress and broad commercial availability of light-emitting diodes (LED) that are able to provide high-intensity visible light in a narrow wavelength range arouse the interest of many research groups in the study.[6]

1.3   Mechanism of Photocatalysis

As stated above, most organic compounds, especially the aliphatic derivatives, do not absorb in the near UV. Their excitation requires the use of high-energy radiation (e.g., $\lambda < 220$ nm), for which cheap lamps are presently not available. Furthermore, because of their high energy, the corresponding excited states often undergo various fragmentation processes, scarcely useful in synthesis. These compounds can, however, be activated using photochemical methods. Irradiation in the UV or visible region is a convenient way for generating electronically excited states and exploiting their high energy and different electronic structure for useful chemical reactions (as shown for compound **R** in **Scheme 4a**).[24] However, activation of a compound by light does not necessarily imply that the reagent is directly irradiated. A variation that is often used in photochemistry, for example, when a reaction from the triplet is desired and the reagent considered intersystem crosses inefficiently, is the use of a sensitizer, a photocatalyst such as organic photocatalysts or a transition metal polypyridyl complex of the type $\mathbf{ML_3^{n+}}$ (**M** for simplicity), that absorbs light and transfers energy to the reagent (**R**), so that the (triplet) excited-state of the latter is reached indirectly (photosensitization, **Scheme 4b**).

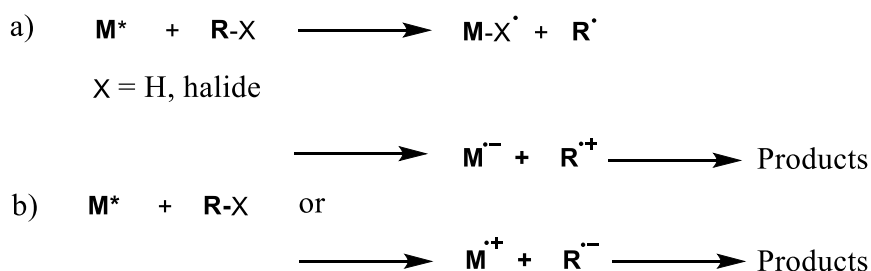**Scheme 4:** Mechanisms of photochemical reactions
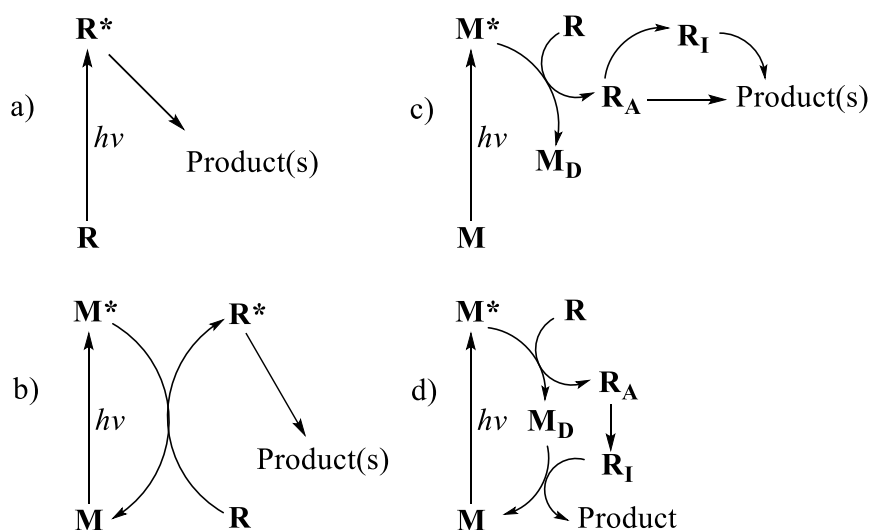
R = reagent/substrate; R* = activated or energized reagent;
R_A and R_I = reactive intermediates; M = photomediator molecule;
M* = excited/activated photomediator; M_D = deactivated photomediator

Apart from energy transfer, there are other ways through which the light-absorbing molecule **M**, which might then generically be indicated as a photomediator, activates the reagent **R**. In particular, some chemical reaction may transform inactive **R** into a highly reactive intermediate R_A that will give the final products, possibly *via* further intermediates (e.g., R_I, see **Scheme 4c**; this mode of action has also been included among photosensitizations, but is distinguished because activation is based on a chemical reaction, as opposed to energy transfer, a physical phenomenon).[24] Differently from direct irradiation or energy transfer, here the excited-state surface of reagent **R** is never attained, and, as far as this is concerned, the reaction path involves the lowest potential energy surface at any configuration, as it occurs in thermal reactions and contrary to photochemical reactions, where part of the path occurs on an excited surface. However, at least one photon is consumed per every molecule converted in all of the three cases (**Scheme 4a-c**). In the favourable case, the further condition applies that (one of) the intermediate(s) thus formed (R_I) interact(s) with the deactivated photomediator M_D giving the final product(s) and regenerate(s) **M** in the initial state. Then, **M** is not consumed in the overall process, exactly as it happens with a thermal catalyst (**Scheme 4d**). It seems, therefore, appropriate to label such a process as photocatalytic.[24] As mentioned, **M** is used in an amount lower than stoichiometric, but light is a stoichiometric reagent.

Activation by a photocatalyst (**M**) results through one of the following three mechanisms. In the first one, an atom, or a group, is transferred from the reagent R-X to the excited photocatalyst generating a radical R$^\bullet$. This intermediate undergoes some reaction (e.g., coupling, addition), which leads to the desired product (**Scheme 5a**). In the process, the photocatalyst is regenerated, typically by back atom transfer to a reaction intermediate.

Scheme 5: Mechanisms of activation by a photocatalyst

a)   **M*   +   R-X** $\longrightarrow$ **M-X**$^\bullet$ **+ R**$^\bullet$

   X = H, halide

b)   **M*   +   R-X**   or $\begin{array}{l} \longrightarrow \textbf{M}^{\bullet-} + \textbf{R}^{\bullet+} \longrightarrow \text{Products} \\ \\ \longrightarrow \textbf{M}^{\bullet+} + \textbf{R}^{\bullet-} \longrightarrow \text{Products} \end{array}$

In the second mode, an electron is transferred, forming the radical cation or anion of the substrate (electron transfer, ET). Thus, redox processes, a rare occurrence when only ground state organic molecules are involved, are often operating in photoinduced reactions and are a typical mechanism in photocatalysis (**Scheme 5b**).[24] The ensuing reactions of the radical ions, for example, (cyclo)addition reactions, or of further intermediates resulting from them may give useful reactions, obviously including at some stage of the process a back electron transfer (BET) step regenerating the photocatalyst. In some cases, 'sacrificial' donors or, respectively, acceptors, have to be used to regenerate the starting photocatalyst.

Finally, in the third mode, the reaction occurs on a metal centre.[18,24] As an example, a reagent adds onto a metal centre that has been activated by a photochemical reaction, and under these conditions, a C-C bond is formed. Then, liberation of the final product regenerates the starting metal catalyst so that the absorption of a further photon is required for initiating a second cycle. This distinguishes photocatalysis from photogeneration of a thermal catalyst.

Our present concern is the second mode that involves single electron transfer (SET), forming the radical cation or anion of the substrate (electron transfer, ET). Here photoredox catalysis relies on the general property of excited states to be both more easily reduced as well as more easily oxidized than their corresponding ground states, and so the photocatalyst can serve

either as an electron donor or an electron acceptor to be regenerated in the catalytic cycle (**Scheme 6**). The photocatalyst undergoes two distinct electron-transfer steps; both the "quenching" and the "regenerative" electron transfer. The two can be productive with respect to a desired chemical transformation.[7] Ideally, the two electron transfer processes are connected by the substrates or intermediates of the catalysed reaction and therefore do not require any sacrificial electron donor or acceptor.

**Scheme 6:** Photoredox catalysis by SET pathways
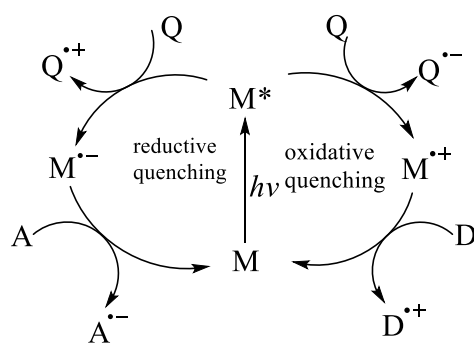
M = photocatalyst, A = electron acceptor
D = electron donor, Q = quencher

1.4   Common Photoredox Catalysts

A potential photochemical reaction can be induced (or sensitized) by a species which possesses specific redox, spectroscopic, and excited state properties upon light absorption. Such species or compounds can be called light absorption sensitizers (LAS)[18] or simply as organic photocatalysts (**M**). Juris and co-workers[19] opined that such a compound must perform as shown schematically below (**Scheme 7**): (i) it must absorb light so as to give an excited state; (ii) this excited state must be able to oxidize (or reduce) one of the reactants; (iii) the reduced (or oxidized) form of the photosensitizer must be able to reduce (or oxidize) the other reactant in order to complete the redox process and to regenerate the LAS. According to this group of researchers, the requirements for an ideal LAS should include the following: (1) reversible redox behaviour; (2) suitable ground and excited state potentials; (3) stability towards thermal and photochemical decomposition; (4) intense absorption in a suitable spectral region; (5) small energy gap between relevant excited states; (6) high efficiency of population of the reactive excited state; (7) suitable lifetime of the reactive excited state; (8) high energy content of the reactive excited state; (9) good kinetic factors for outer sphere electron transfer reactions.

Scheme 7: Schematic representation of a photosensitized electron transfer reaction.

Reductive Quenching Cycle   Oxidative Quenching Cycle
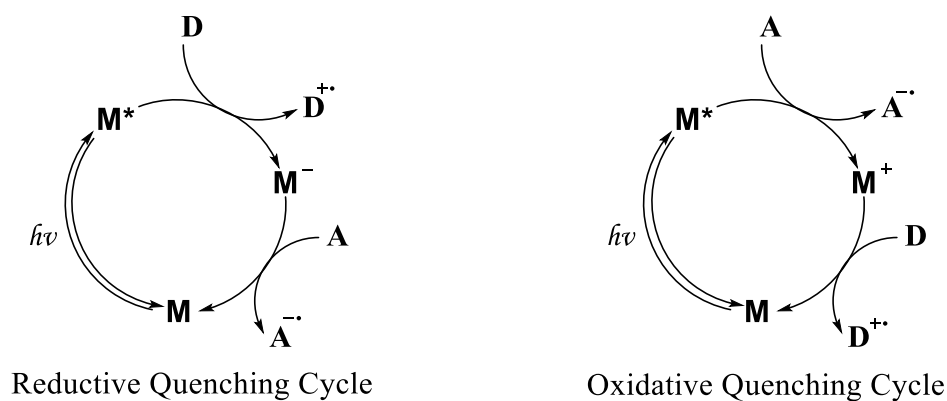
M = light absorption sensitizer/photoredox catalyst
A = Electron acceptor and **D** = Electron donor

Fagnoni, *et. al* [24] explained further that for a compound to be useful as a photocatalyst **M**, it obviously must undergo neither a thermal reaction nor a monomolecular photochemical reaction. Most importantly, the 'deactivated' state M_D (in Scheme 4 above) form, resulting from the initial photochemical step, must be a persistent species that is sufficiently stable to avoid interfering with the (on the contrary highly reactive) activated substrate R_A and with the other intermediates involved in the process, yet capable of being reconverted into the original form at some stage, so that absorption of a new photon initiates a new cycle.
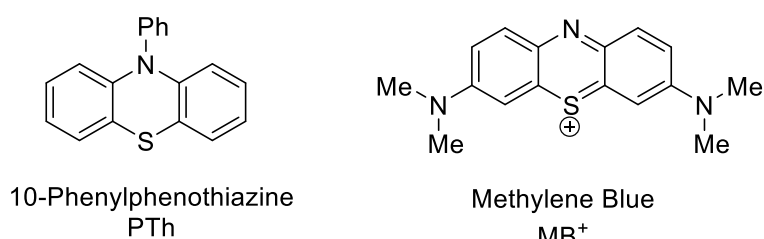
Classes of chemical compounds that have been shown to operate efficiently in this role, with little or no photodecomposition, and to be able to function for many catalytic cycles include the following: transition metal-ligand complexes and aromatic compounds, in particular those bearing strongly electron-withdrawing (to a lesser degree, donating) substituents: cyanoarenes; quinones; benzophenones; thiazines; electron-poor heterocycles. These compounds act *via* electron transfer (ET). Electron transfer to organic molecules can occur both ways, to the valence band or from the conduction band, and generates both (single electron) oxidized and reduced intermediates, respectively. Semiconductor oxides and sulfides such as TiO_2, ZnS, and CdS may also act *via* ET, being both strong oxidant and strong reducing agents.

However, most of the photoredox catalysts used in recent times are metal-ligand complex molecules. Metals, especially the transition metals, like ruthenium (Ru), iridium (Ir), chromium (Cr), rhodium (Rh), and cobalt (Co). The ligands mostly in use include 2,2'-
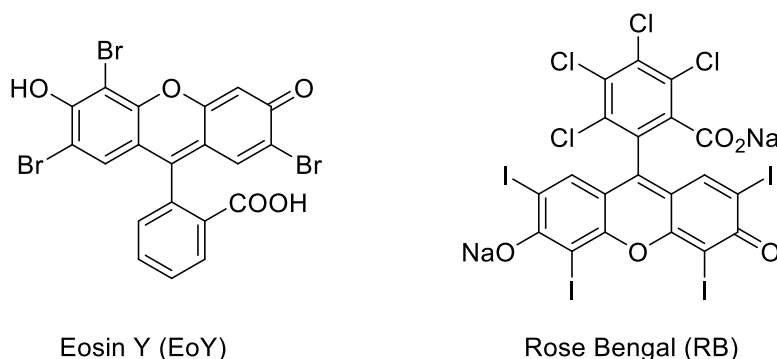
bipyridine (bpy), 2-phenylpyridine (ppy), 4,4'-di-*tert*-butyl-2,2'-bipyridine (dtbpy), 2,2'-bipyrimidine (bpm), 2,2'-bipyrazine (bpz), and 1,10-phenanthroline (phen). The recent literature reviews on photoredox catalysis focus mainly on transition metal chromophores with ruthenium and iridium polypyridyl complexes standing out. They are well studied and employed in organic synthesis.[18] Among them, Ru(bpy)$_3^{2+}$ is the most studied one-electron photoredox catalyst. Some commonly used photoredox catalysts are shown in **Figure 4**.[24-26]

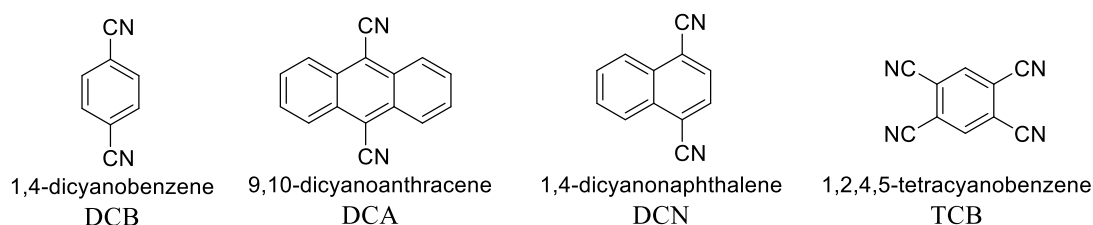**Figure 4**: Some commonly used photoredox catalysts

Thiazines

10-Phenylphenothiazine
PTh

Methylene Blue
MB$^+$

Xanthenes

Eosin Y (EoY)

Rose Bengal (RB)

Cyanoarenes

1,4-dicyanobenzene
DCB

9,10-dicyanoanthracene
DCA

1,4-dicyanonaphthalene
DCN

1,2,4,5-tetracyanobenzene
TCB

Metal-polypyridyl complexes

Ru(bpy)$_3$$^{2+}$ (Ru-**1**)

Ru(bpz)$_3$$^{2+}$ (Ru-**2**)

Ru(phen)$_3$$^{2+}$ (Ru-**3**)

Ir(ppy)$_2$(dtbbpy)$^+$ (Ir-**2**)

Ir(ppy)$_3$ (Ir-**1**)

Ir(bpy)(ppy)$_2$$^+$ (Ir-**3**)

Ir[dF(CF)$_3$ppy]$_2$(dtbbpy)$^+$ (Ir-**4**)

Benzophenones

benzophenone
BP

Michler's Ketone
MK

fluorenone
FLN

xanthone (X=O)
XO
thioxanthone (X=S)
TXO

Quinones

anthraquinone
AQ

2,3-dichloro-5,6-
dicyano-1,4-
benzoquinone
DDQ

o-Chloranil
(2,3,5,6-tetrachlorobenzoquinone)
TCBQ

While each class of materials has advantages, soluble transition-metal complexes are used most often. The reasons for this is that this class of photoredox catalysts are often less toxic

15

than other reagents frequently used to generate free radicals, such as organotin reagents. In addition, they generate potent redox agents while exposed to light, they are innocuous under ordinary conditions. Their photoredox catalytic properties can be modified by changing ligands and the metal (**Table 1**), reflecting the somewhat modular nature of the catalysts.

Table 1. Redox potentials of some visible-light photocatalysts.[25]

Photocatalyst (**M**)	$E_{1/2}$ **M**$^+$/**M***	$E_{1/2}$ **M***/**M**$^-$	$E_{1/2}$ **M**$^+$/**M**	$E_{1/2}$ **M**/**M**$^-$
Ru(bpy)$_3$$^{2+}$	-0.81	+0.77	+1.29	-1.33
Ru(bpz)$_3$$^{2+}$	-0.26	+1.45	+1.86	-0.80
Ru(phen)$_3$$^{2+}$	-0.87	+0.82	+1.26	-1.36
fac-Ir(ppy)$_3$	-1.73	+0.31	+0.77	-2.19
Ir(ppy)$_2$(dtbbpy)$^+$	-0.96	+0.66	+1.21	-1.51
Rose Bengal	-0.68	+0.99	+1.09	-0.78
Eosin Y	-1.60	+1.18	+0.72	-1.14

In V in CH$_3$CN vs. SCE.

1.5 Applications of Photoredox Catalysis in Organic Synthesis

Since the beginning of scientific chemistry, chemists have been interested in light as an energy source to induce chemical reactions.[27] Harnessing visible light as the driving force for chemical transformations generally offers a more environmentally friendly alternative compared with classical synthetic methodology.[28] Absorbing light, molecules reach an electronically excited state. As a result, the distribution of electrons in the molecules is significantly different at these states when compared to the ground state. The transition metal-polypyridyl complexes based photocatalysts commonly employed in photoredox catalysis absorb efficiently in the visible spectrum allowing for orthogonal excitation. The chemical properties and more particularly the reactivity of the molecules also change, and the reaction spectrum of a family of compounds is considerably broadened. In some instances, using photochemical steps significantly shortens a total synthesis, and frequently complex, polycyclic, or highly functionalized structures can be obtained from simple substrates. New product families or libraries difficult to achieve with ground-state reactions are thus available, opening new perspectives in the search of biologically active compounds.

Irradiation of a chemical reaction components or mixture with UV or visible light frequently improves the yields of metallocatalysed reactions.[29] For instance, ligand-exchange steps are often accelerated, and irradiation with light has become part of the standard reaction

conditions. Irradiation is also used to initiate radical chain processes under mild conditions.[29] Molecular chlorine and bromine, for example, undergo homolytic cleavage to form radicals when irradiated with UV light. Halogenated amide *N*-bromosuccinide (NBS also form radicals when exposed to light (**Scheme 8**). Thus, particularly complex radical reactions such as certain radical tandem or multicomponent transformations can be made possible.[29]

Scheme 8: Photo induced homolytic bond cleavage/radical initiation

N-bromosuccinide (NBS)
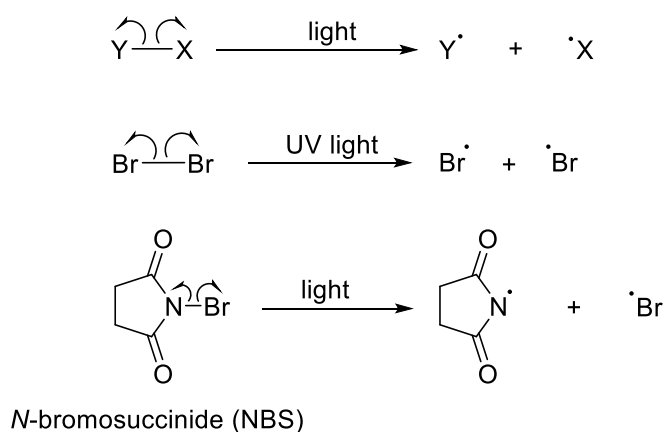
The use of photocatalysis in organic synthesis continues to receive the attentions of many research groups. The applications range from simple transformation of compounds to complex multicomponent transformations with very high selectivity. These include natural products syntheses[8] to late-stage pharmaceutical functionalization and polymer synthesis.[4] There are several reasons researching into the application of photocatalytic methods to synthetic issues such as carbon-carbon bond formation and carbon-heteroatom bond formation. First, it is a useful way to take advantage of the high energy of the photon. Second, the reactive intermediates involved (radicals, ions, radical ions) are the same that are generated in thermal reactions (though generally from different precursors) or can be likened with them (as it may be the case for the photocatalytic generation of an ion, which is similar to imparting an ionic character to a group in an organic molecule by forming a metal complex). The advantages of this are twofold. From the mechanistic point of view, obtaining the same intermediates under conditions that are much milder than in thermal reactions and more easily amenable to the characterization of the path followed may help in the rationalization also of alternative thermal processes. On the other hand, because the course of the reaction is (at least partially) the same, this enables chemists to exploit the available

knowledge on thermal reactions (much larger than that on photochemical reactions) for making the best synthetic use of the photocatalytic methods.[6] Another fascinating aspect of photochemistry, according to Cambie *et al.*, is the use of photons as "traceless and green reagents", hence rendering photochemical processes green and sustainable.[30]

Much of the promise of visible light photoredox catalysis hinges on its ability to achieve unique exotic bond constructions that are not possible using established protocols. For instance, photoredox catalysis may be employed to perform overall redox neutral reactions. As both oxidants and reductants may be transiently generated in the same reaction vessel, photoredox approaches may be used to develop reactions requiring both the donation and the reception of electrons at disparate points in the reaction mechanism. This approach stands in contrast to methods requiring stoichiometric chemical oxidants and reductants, which are often incompatible with each other, as well as to electrochemical approaches, which are not amenable to redox neutral transformations. Furthermore, single-electron-transfer events often provide access to radical ion intermediates having reactivity patterns fundamentally different from those of their ground electronic or excited states.[31] Access to these intermediates using other means of activation is often challenging or requires conditions under which their unique reactivity cannot be productively harnessed.

At the same time, these photoredox catalysts such as those of Ru- and Ir-polypyridyl complexes may also be employed to generate radicals for use in a diverse range of established radical chemistries. The irradiation source is typically a commercial household light bulb, a significant advantage over the specialized equipment required for processes employing high-energy ultraviolet (UV) light. Additionally, for the fact that organic molecules generally do not absorb visible light, there is little potential for deleterious side reactions that might arise from photoexcitation of the substrate itself. Finally, photoredox catalysts are employed at very low loadings, with 1 mole % or less.

The application of photocatalysis in organic synthesis can be grouped into two broad classes: reactions involving electron transfer (i.e., photoredox catalysis) and the energy transfer reactions. Most photoredox catalysis involving electron transfer follow one of the two mechanistic schemes depicted in **Scheme 9** below. Each of these photoinduced electron transfer cycles is categorized by the primary direction of the electron transfer with respect to the excited state catalyst **M***. Based on the stronger reduction or oxidation capability of the excited state than the corresponding ground state, photoredox catalyst takes advantage of the

electron transfer pathway of photocatalysis, donating an electron to an oxidative quencher or accepting an electron from a reductive quencher: in an oxidative quenching cycle, the excited state **M*** is quenched by donating an electron either to a substrate **R** or an oxidant [ox] present in the reaction mixture; in a reductive quenching cycle, **M*** is quenched by accepting an electron from the substrate **R** or a reductant [red]. The catalyst turnover step involves reduction of the oxidized [**M**]$^{\bullet+}$ in the oxidative cycle and oxidation of the reduced [**M**]$^{\bullet-}$ in the reductive cycle. In either case, the substrate **R**, an external redox-active reagent, or an intermediate may be responsible for catalyst turnover.[17]

Radical ion intermediates (e.g. both quenchers) that are formed from a single-electron transfer step through either oxidative quenching or reductive quenching, subsequently undergo the second chemical step to transform into either radicals or ions quite fast, serving as the real key reactive species to react with other molecules. However, some radical ions still do remain as key species directly participating in some chemical reactions. Overall, photoredox catalytic reactions typically involve a radical ion, a radical, or an ion as the key reactive intermediate.[15] Radical ion mediated transformations are a unique and valuable type of organic reaction because of their umpolung nature, especially in organic synthesis.

Scheme 9: Oxidative and reductive quenching cycle of a
photoredox catalyst
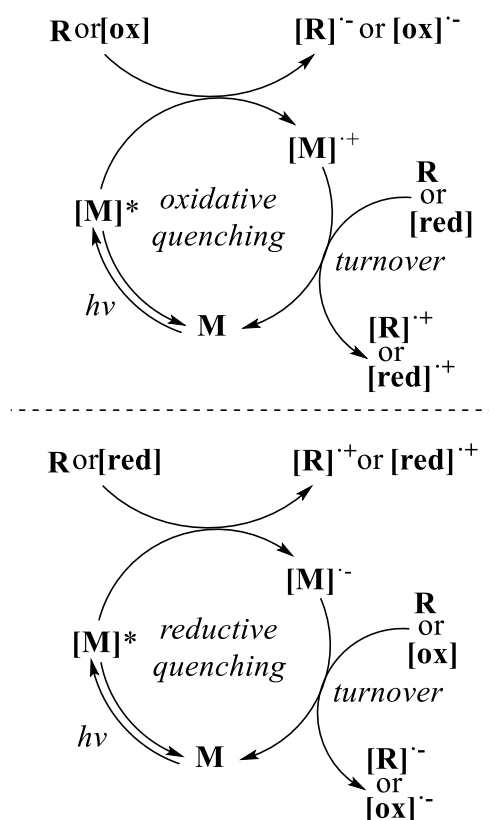
Regardless of whether the substrate undergoes an electron transfer **ET** reaction in the photoinduced electron transfer **PET** step or in the turnover step, there are three general redox outcomes possible for the substrate in either quenching manifold: net oxidative, net reductive, and net redox-neutral. A net oxidative reaction requires an external oxidant, which can accept electrons in either the PET step or the turnover step. Likewise, net reductive reactions involve an external reductant donating electrons during the PET or turnover steps. Net redox-neutral processes are more complex and often involve return electron transfer with the oxidized or reduced catalyst, sometimes mediated by a redox-active co-catalyst.[17]

The mechanism explained above are idealized representations of reactions through PET manifolds, but in reality, however, an intermediate may be capable of donating or accepting an electron to initiate a new chain thereby rendering the quantum yield of reactions values greater than unity which are observed in some photoredox catalysis (**Scheme 10**). Yoon and Cismesia demonstrated that a number of transition metal photoredox reactions exhibit a significant component of chain transfer.[4]

Scheme 10: Yoon and Cismesia[4] proposed chain propagation
mechanism in photoredox reactions
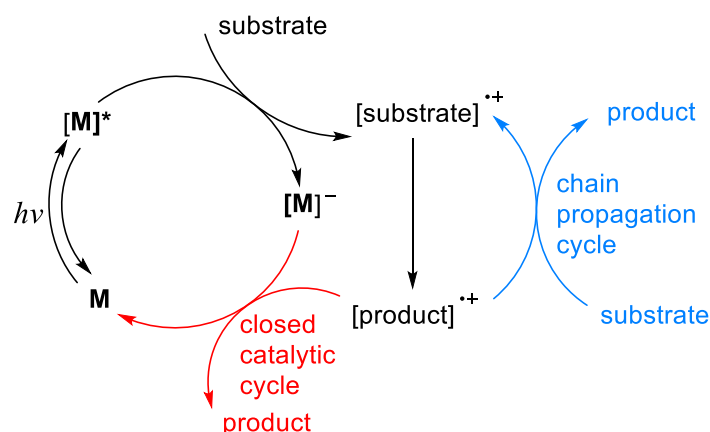
1.6   Net Reductive Photoredox Reactions

A net reductive photoredox reaction involves an external reductant donating electrons during
the photoinduced electron transfer PET or turnover steps (**Scheme 11**). The first reactions
demonstrating the potential utility of visible light photoredox catalysis in organic synthesis
were net reductive reactions, in which an electron donor is required to serve as the
stoichiometric reductant.[14,19,31]

Scheme 11: Net reductive photoredox process
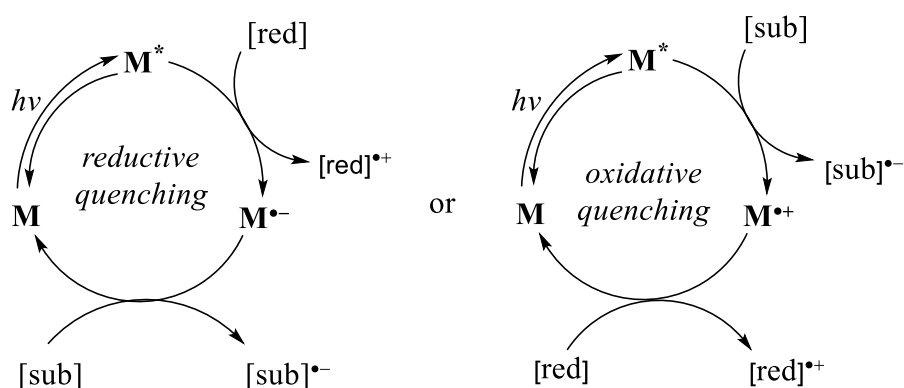
1.6.1   Reduction of Electron-Poor Olefins[14]

Pac and co-workers in 1981 demonstrated the potential utility of visible light photoredox
catalysis and reported the Ru(bpy)$_3{}^{2+}$-mediated reduction of electron deficient olefins.[19] The
terminal reductant employed in these studies, 1-benzyl-1,4-dihydronicotinamide (BNAH, **1**),
was of interest for its analogy to the biological reductant 1,4-dihydronicotinamide adenine

dinucleotide (NADH), with both molecules sharing the redox-active 1,4-dihydropyridine moiety. The research group found that a catalyst system comprising 2 equiv. of BNAH and catalytic quantities of Ru(bpy)$_3^{2+}$ was capable, upon irradiation with visible light, of reducing dimethyl maleate (**2**) to the saturated product dimethyl succinate (**3**) (**Scheme 12**).

They proposed that as in all photoredox reactions, this process is initiated by absorption of visible light by the photocatalyst Ru(bpy)$_3^{2+}$ (**M**) to give the photoexcited species *Ru(bpy)$_3^{2+}$ (**M***). Photoexcitation renders this species sufficiently oxidizing to accept an electron from BNAH, generating the BNAH radical cation **4** and concurrently reducing the photocatalyst to Ru(bpy)$_3^+$ (**M⁻**). This Ru(I) intermediate is highly reducing, enabling transfer of an electron to dimethyl maleate. This event oxidizes the photocatalyst back to Ru(bpy)$_3^{2+}$ (**M**) and completes the photocatalytic cycle (**Scheme 12**). Meanwhile, single-electron reduction of **2** gives the radical anion **5**, which may be protonated to yield α-carbonyl radical **6**. This radical is then believed to undergo a second single-electron reduction followed by protonation to give dimethyl succinate (**3**). The single-electron donor for this step may be another equivalent of Ru(bpy)$_3^+$ (**M⁻**), or it may be dihydropyridyl radical **7**, the product of deprotonation of radical cation **4** and itself a strong reductant.[19] Upon loss of an electron, radical **7** is converted to pyridinium **8**, the ultimate product of two-electron oxidation of BNAH. BNAH (**1**) was observed to quench *Ru(bpy)$_3^{2+}$ (**M***), while dimethyl maleate (**2**) did not. This observation provided strong evidence that the reaction proceeded *via* reductive quenching of *Ru(bpy)$_3^{2+}$ (**M***) to give a Ru(bpy)$_3^+$ (**M⁻**) intermediate, rather than via oxidative quenching to give a Ru(bpy)$_3^{3+}$ (**M⁺**) intermediate. The reaction was additionally found to be amenable to the reduction of alkenes bearing a range of electron-withdrawing groups, such as esters, ketones, arenes, and nitriles.[19]

**Scheme 12**: Photoredox reduction of dimethyl maleate
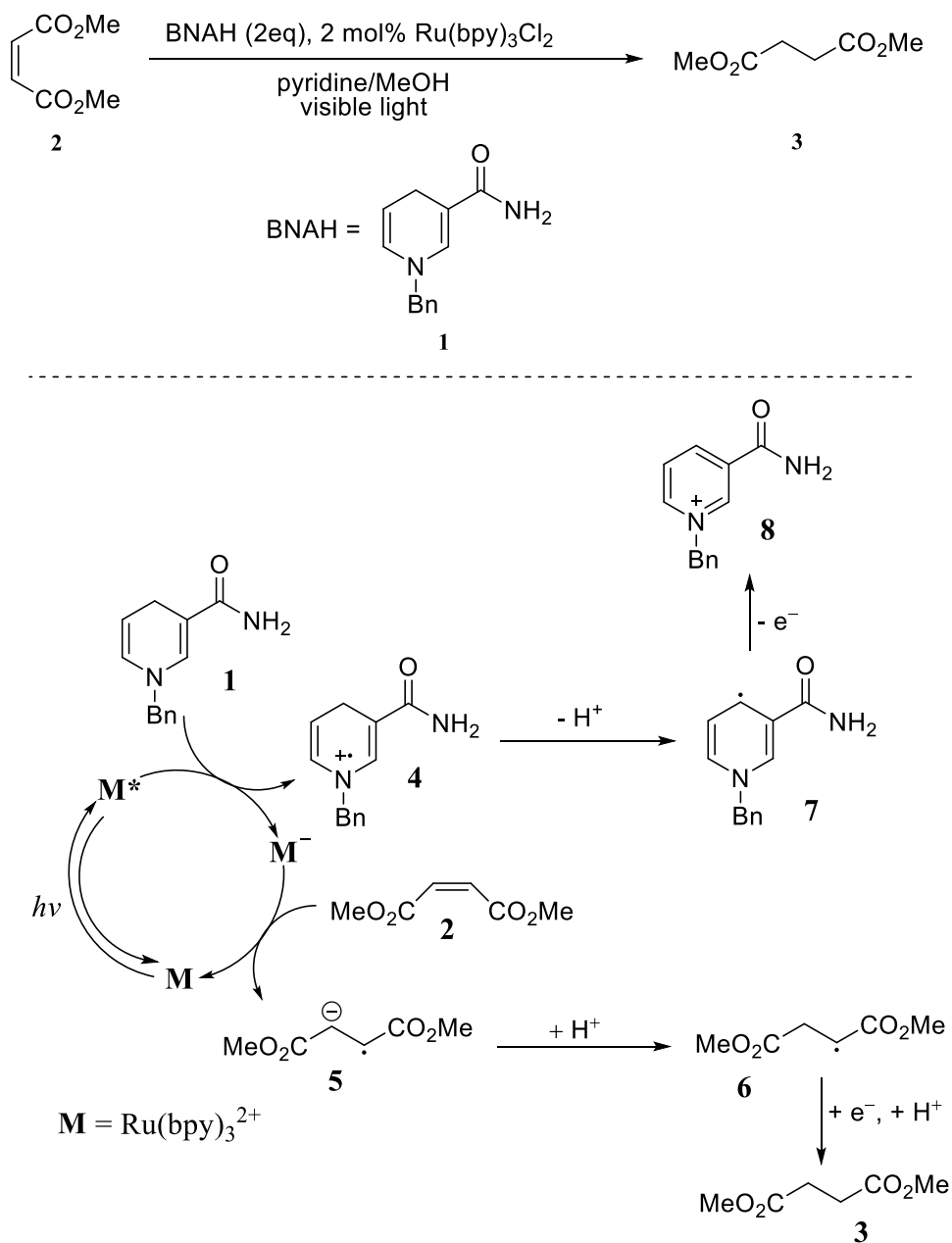
1.6.2 Reductive Dehalogenation

Reductive dehalogenation reactions, mediated by visiblelight photoredox catalysis, were pioneered by Kellogg and co-workers, as well as others since 1978.[32] The photoredox-mediated reductive dehalogenation, in which a C−X bond is reduced to a C−H bond, first observed by Fukuzumi for α-haloacetophenones,[27] was later developed by Stephenson and

co-workers into a synthetically useful transformation.[24] Fukuzumi and co-workers in 1990 demonstrated the reduction of phenacyl bromides using visible light, Ru(bpy)$_3^{2+}$ as a photocatalyst, and 9,10-dihydro-10-methylacridine as the stoichiometric reductant.[27] In the net transformation, the phenacyl bromide (**9**) is reduced by two electrons to give acetophenone (**10**), while the dihydroacridine (**11**) is oxidized by two electrons to give the acridinium by-product (**12**) (**Scheme 13**). Halogens α- to a carbonyl, electron withdrawing or aryl group could be selectively reduced under these conditions. Halogens α- to a carbonyl, electron withdrawing or aryl group are considered to be activated, because the radical they produce upon fragmentation is stabilized by conjugation with these groups.

Scheme 13: Reductive dehalogenation
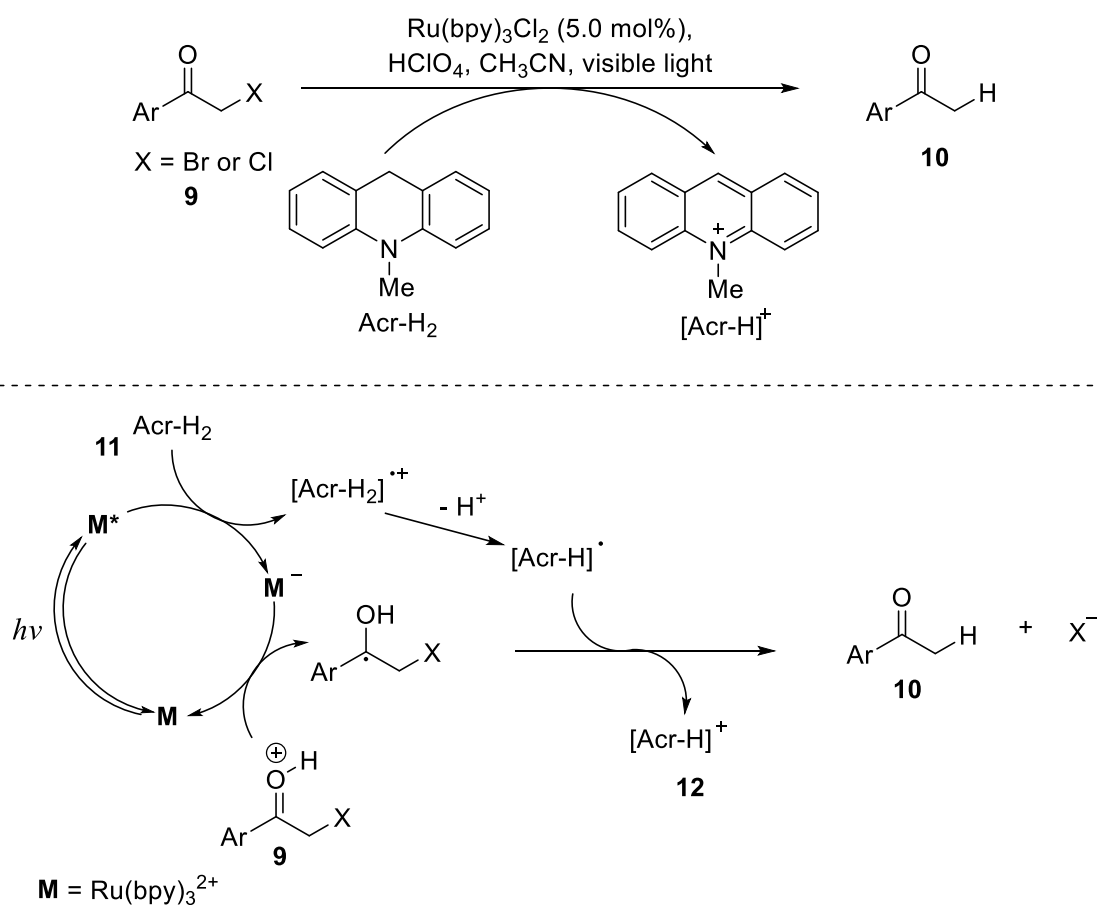
Conceptually, this reaction proceeds *via* reductive quenching of photoexcited *Ru(bpy)$_3^{2+}$ to Ru(bpy)$_3^+$ and subsequent electron transfer to C–X bond α- to an electron-withdrawing group, followed by hydrogen abstraction. The reductive dehalogenation using photoredox catalysis at this stage was only limited to *activated* halogen compounds. Stephenson and co-workers extended it to the reduction of less *activated* (or un-activated) halogen substrates

such as alkyl iodides by simply modifying redox potentials of the photocatalysts using the strongly reducing photocatalyst tris-(2,2'-phenylpyridine)iridium (Ir(ppy)$_3^{2+}$).[33] This updated reaction is mechanistically distinct from the previous transformation of activated bromides and chlorides. The increased reduction potential of this catalyst compared to Ru(bpy)$_3^{2+}$ allows direct reduction of the carbon-iodine bond without first interacting with a stoichiometric reductant. Thus, the iridium complex transfers an electron to the substrate, causing fragmentation of the substrate and oxidizing the catalyst to the Ir(IV) oxidation state. The oxidized photocatalyst is then easily returned to its original oxidation state through interaction with one of the reaction additives, tributylamine (**Scheme 14**). This shows that photocatalytic generation of a radical by the reduction of a C–X bond has great potential as an alternative for C–C bond forming reactions *via* the chemistry of alkyl free-radicals.

Scheme 14: Reductive iodination
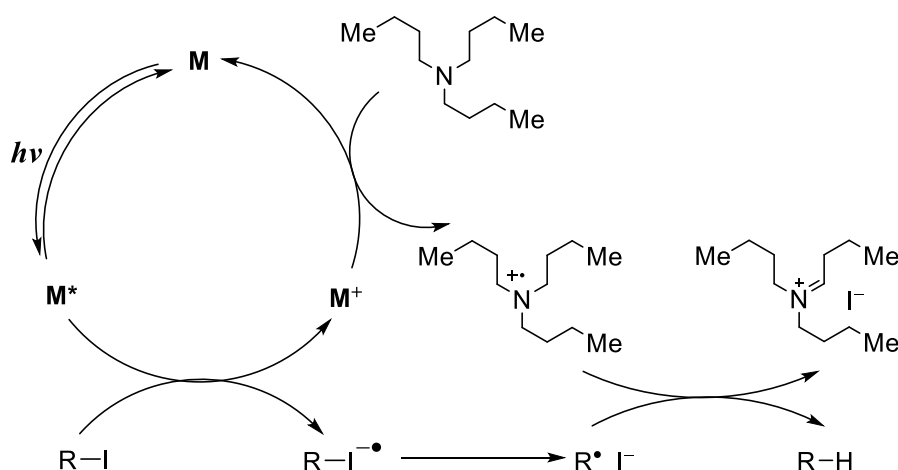
Just as Sn-mediated radical dehalogenation reactions can be used to initiate cascade cyclizations to rapidly generate molecular complexity, the photocatalytic reductive dehalogenation allows access to the same types of complex products. Visible-light-mediated dehalogenation reactions, when compared with those that employ conventional radical-based methods, not only provide the desired products in excellent yields under mild reaction conditions, but also exhibit superior chemoselectivity and excellent functional-group tolerance (**Scheme 15 (a)**). In the work of Stephenson,[34] a radical cascade cyclization that closed two five-membered rings and formed two new stereocenters with good yield was also achieved using visible light photoredox catalyst (**Scheme 15 (b)**). It was observed that the reductive dehalogenation protocol could be a key step in a total synthesis of the natural product (+)-gliocladin C (**Scheme 15 (c)**).[32,35]

**Scheme 15**: A visible-light-mediated reductive dehalogenation reaction.

a)

1 mol% [Ru(bpy)$_3$Cl$_2$]

10 equiv iPr$_2$NEt
10 equiv HCOOH
DMF, 14W fluorescent bulb

13 → **14**

b)

Ru(bpy)$_3$Cl$_2$ (1 mol%)
Et$_3$N (2 equiv)
DMF, blue LED

15 → **16**

c)

18

1 mol% [Ru(bpy)$_3$Cl$_2$]
2 equiv Bu$_3$N
DMF, blue LEDs
Key step

82%

17 → **19**

3 steps

Boc-D-tryptophan methyl ester

6 steps

gliocladin C
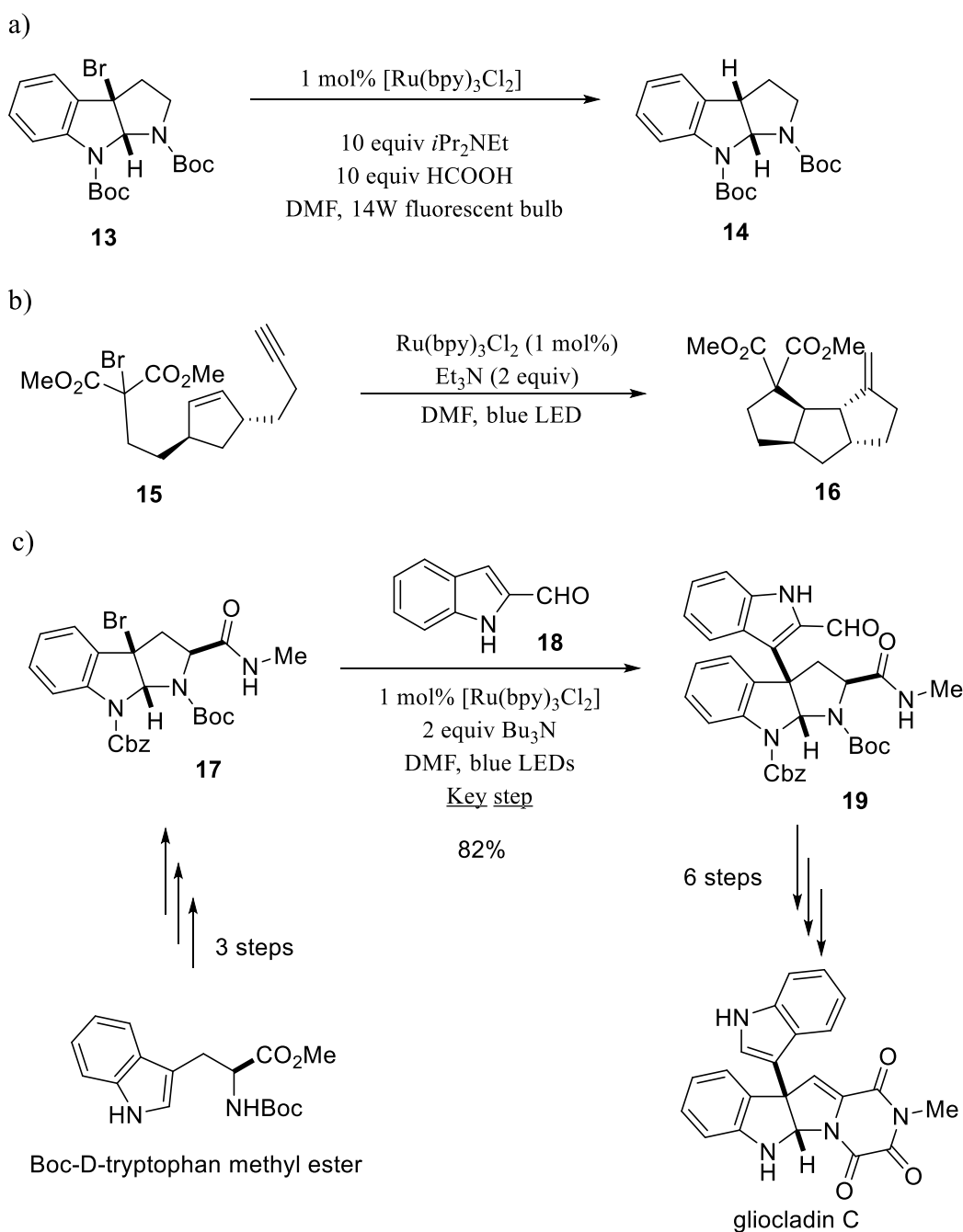
1.6.3 *[2 + 2] Photocycloadditions*: *Formation of Cyclobutanes*

Cycloadditions and other pericycle reactions are powerful transformation in organic synthesis because of their potential to rapidly generate complex molecular architectures and particularly because of their capacity to set multiple adjacent stereocenters in a highly controlled manner. Cycloadditions that are not thermally allowed, such as the [2+2]-

cycloaddition, can be enabled by photochemical activation of the reaction. Among photochemical reactions, the [2+2]-photocycloaddition of α,β-unsaturated ketones or esters to alkenes, alkynes, or allenes leading to cyclobutanes is certainly the most applied reaction in organic synthesis.[14,29,31,36] With α,β-unsaturated ketones, the reaction can be induced by simple light absorption. In contrast, a sensitized reaction is preferred in the case of α,β-unsaturated esters. The transformation is then frequently performed with acetone as solvent and sensitizer. In many cases, the unsaturated carbonyl compounds react at the $^3\pi\pi^*$ state with alkenes and 1,4-biradical intermediates are generated.[29] As shown in the following example, complex structures are accessible in only one step without using expensive and/or toxic reagents. This considerably simplifies the total synthesis of complex molecules such as natural products.

Scheme 16: [2 + 2] Photocycloaddition in the total synthesis of solaneclepin A

solanoeclepin A
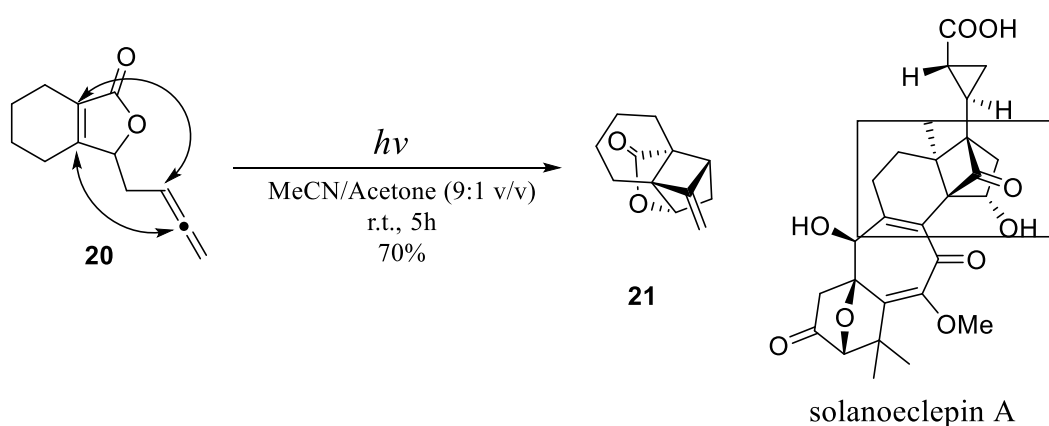
Yoon and co-workers in 2008 reported a visible-light photocatalytic [2+2] cycloaddition reaction of αβ-unsaturated ketones (enones), inspired by Krische's pioneering work on metal-catalysed formal [2+2]-cycloaddition.[36] By irradiation in the presence of 5 mol% Ru(bpy)$_3$Cl$_2$ (a photoredox catalyst), ^{i}Pr$_2$NEt as a terminal electron donor, and LiBF$_4$ as a mild Lewis acid, intramolecular [2+2]-cycloaddition reactions could be achieved in high yield together with promising diastereoselectivity (d.r. > 10 : 1). In their initial report, Yoon demonstrated that introducing lithium salt as the additive effectively promoted the reaction by not only activating the carbonyl group toward oxidation but also stabilizing the radical anion intermediate. Unfortunately, only aryl enones underwent this type of transformation while aliphatic enones remained intact, presumably attributable to the more negative reduction potential. The proposed mechanism of this visible-light photocatalytic formal [2+2]-cycloaddition of enones is shown in **Scheme 17**.[15]

Scheme 17: Visible-light-mediated intramolecular [2 + 2] cycloaddition of enones.
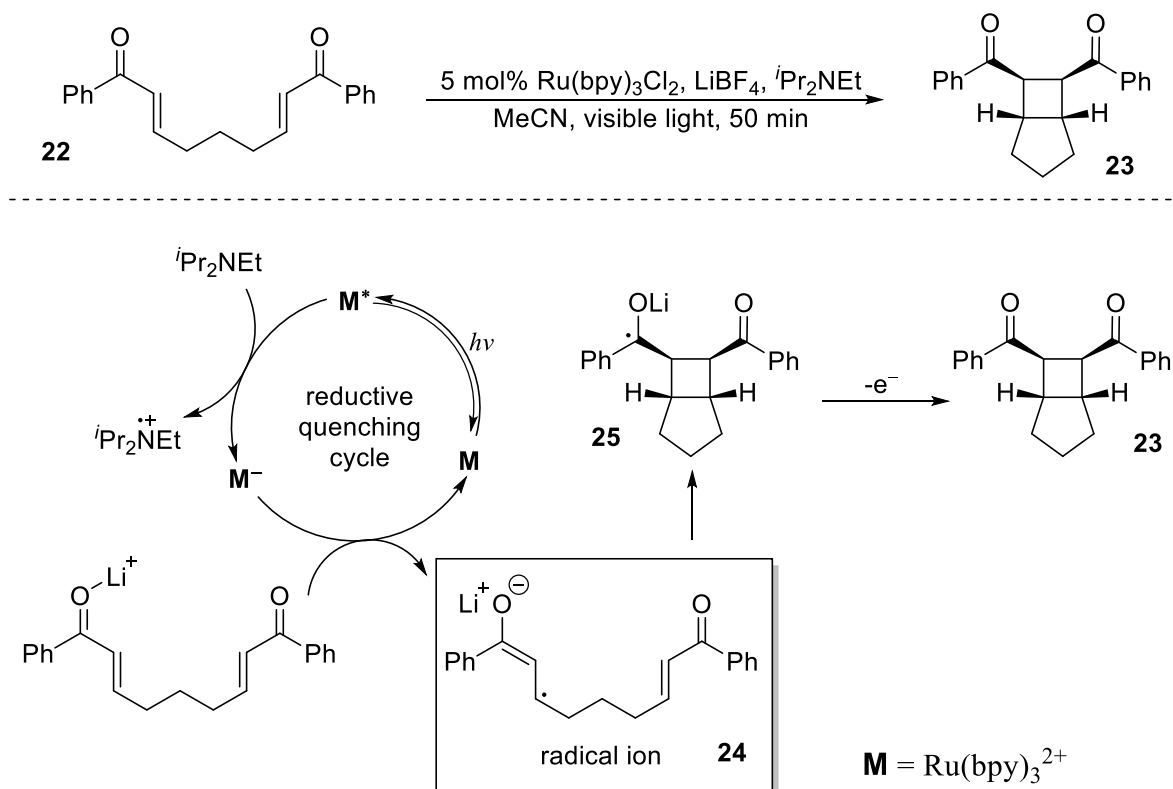
The sensitized [2+2]-photocycloaddition of various α,β-unsaturated lactones such as **20** has been studied and reported in the context of an application to the total synthesis of solanoeclepin A.[29]

A [2+2] photocycloaddition was also used by Crimmins and co-workers as one of the key steps in the synthesis of ginkgolide B1.[37] This natural product possesses a propellane core structure, and photochemical reactions have frequently been applied for the synthesis of such derivatives.[29] Cyclobutane **27** was obtained in quantitative yield from the nonsensitized photocycloaddition of **26**. Under similar conditions, the cinnamic acid derivative **28** was transformed in high yields *via* a [2+2]-photocycloaddition followed by hydrogenation into littoralisone.[38] The reaction also occurs but less efficiently with visible light, which may indicate that the photochemical generation of the cyclobutane ring is part of the biosynthesis of this compound.[33] Currently, the acetone-sensitized [2+2]-photocycloaddition is studied as a key step in the synthesis of bielschowskysin, a diterpene possessing a [9.3.0.0]-tetradecane ring system with 11 stereocenters.[34]

Scheme 18: [2+2]-Photocycloaddition in the synthesis of ginkgolide B1 and littoralisone
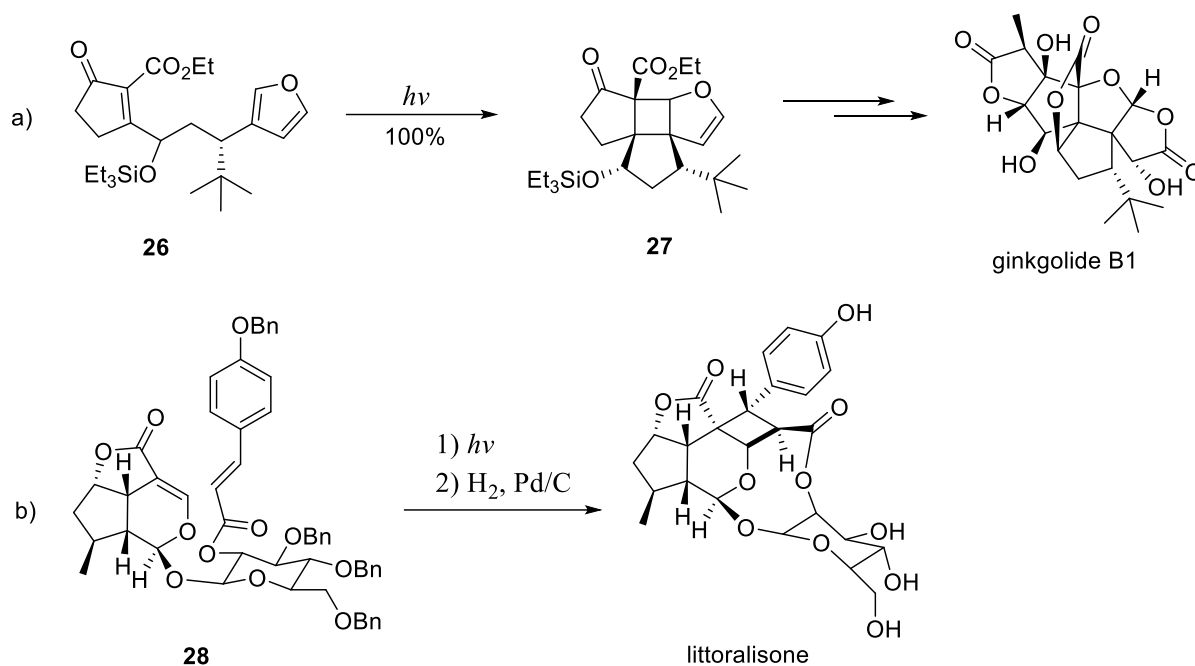
A versatile variant of the [2+2]-photocycloaddition in synthetic applications is the DeMayo reaction. The DeMayo reaction is a photochemical reaction in which the enol of a 1,3-diketone (a β-diketone) reacts as an α,β-unsaturated ketone with an alkene (or another similar species with a C=C bond) resulting in the formation of a cyclobutane ring. This step is followed by a retro-aldol reaction by the resulting cyclobutane ring to yield a 1,5-diketone. The ensuing retro-aldol cleavage is favoured by the relative instability of the cyclobutane ring.

An example is presented below. In its enol form, a β-diketone reacts as an α,β-unsaturated ketone with an alkene. This step is followed by a retro-aldol reaction. In the compound **29**, the mono-enolized β-diketone chromophore adds to the enamine part of the isoquinolone moiety and the tetracyclic aldol **30** is obtained as an intermediate.[29] Due to the cyclobutane ring strain, the intermediate is immediately transformed to **31** and the more stable tetracyclic hydroxyketone derivative **32** is isolated. This compound possesses the galathane skeleton which is encountered in lycorine alkaloids isolated from *Amaryllidaceae*.
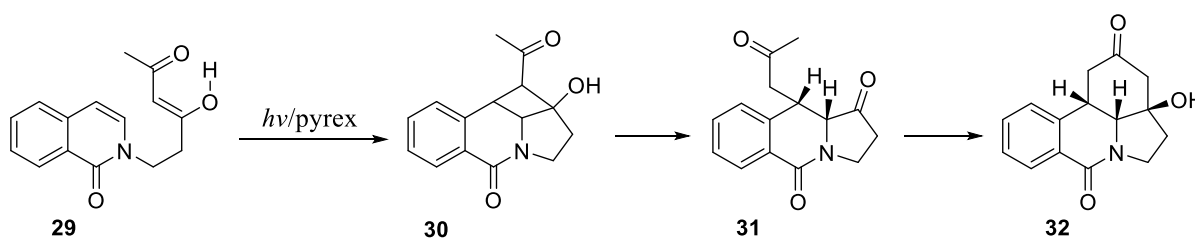
1.6.4 Reduction of Nitrogen Functional Groups

Photoredox catalysis has also been employed in the reduction of some nitrogen-containing functional groups. Hirao and co-workers were reported to use the method in the reduction of nitrobenzenes to anilines using either $Ru(bpy)_3^{2+}$ or the related photocatalyst $Ru(bpy)_2(MeCN)_2(PF_6)_2$.[19] In these reactions, hydrazine was employed as the stoichiometric reductant, the source of the electrons that were ultimately transferred to the nitro-arene. The reduction of nitrobenzenes to anilines has also been achieved using a resin loaded with the organic photocatalyst Eosin Y. Liu was also able to accomplish the reduction of azides to amines by using a catalytic system comprising $Ru(bpy)_3^{2+}$, Hünig's base, and Hantzsch ester.[39] The reaction was proposed to proceed first *via* reductive quenching of $*Ru(bpy)_3^{2+}$ by the tertiary amine *i*-Pr$_2$NEt to give $Ru(bpy)_3^+$. Single-electron reduction of the azide by $Ru(bpy)_3^+$ gives an azide radical anion, which upon expulsion of dinitrogen and protonation affords the aminyl radical. This intermediate may then abstract a hydrogen atom (from either Hantzsch ester or the radical cation of Hünig's base) to furnish the primary amine product (**Scheme 20**). Aryl as well as aliphatic azides may be reduced following this protocol. The reaction was also shown to be compatible with biomolecules, as demonstrated by the reduction of an azide tethered to a DNA oligonucleotide.[19]

Scheme 20: Photoredox catalytic mediated azide reduction reaction
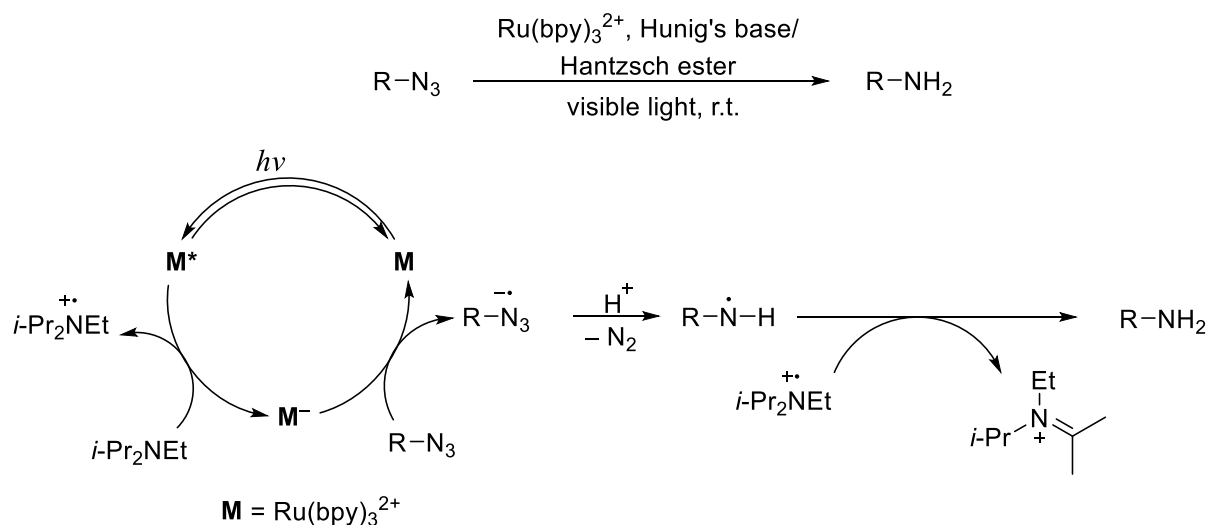
Zheng also reported the reduction of hydrazides and hydrazines under visible light photoredox catalysis using $Ru(bpz)_3^{2+}$, a tris(bipyrazyl) analogue of $Ru(bpy)_3^{2+}$.[39] Using the photoredox catalyst, *N*-phenyl-*N*-benzoylhydrazine (**33**) undergoes efficient reduction to *N*-phenylbenzamide (**34**), and *N*-methyl-*N*-phenylhydrazine (**35**) is reduced to *N*-methylaniline (**36**) (**Scheme 21**).

Scheme 21: Photoredox catalytic reduction of hydrazide and hydrazine
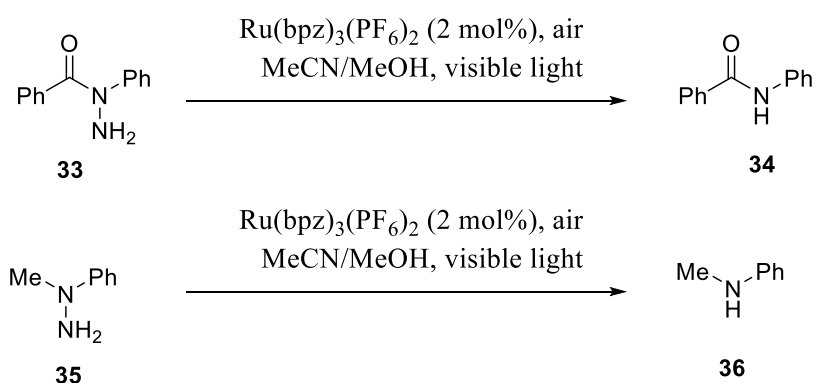
1.6.5 Reductive Epoxide and Aziridine Opening

Although an epoxide functional group is not readily reduced, MacMillan and co-workers exploited the ability to reduce carbonyls using photoredox catalysis to achieve the reductive opening of epoxides and aziridines. Epoxides and aziridines containing an α-carbonyl moiety undergo epoxide and aziridine ring-opening reactions through visible-light-mediated

electron-transfer pathways a photocatalyst and Hantzsch ester (HE) (diethyl 1,4-dihydro-2,6-dimethyl-3,5-pyridinedicarboxylate) as the stoichiometric reductant.[20,31] In the catalytic cycle, reductive quenching of the excited photocatalyst, $*Ru(bpy)_3^{2+}$, generates $Ru(bpy)_3^{+}$ (**Scheme 22**). $Ru(bpy)_3^{+}$ is sufficiently reducing to donate an electron to α-ketoepoxide **37** to give ketyl radical **38**. The cleavage of C−O bond that follows provides radical anion **39**, which after protonation and abstraction of a hydrogen atom gives the β-hydroxyketone product **40**. Hantzsch ester (HE) may potentially act as a hydrogen atom donor and reductive quencher as described in **Scheme 22**, ultimately undergoing conversion to Hantzsch pyridine (HP). This reductive protocol was additionally found to ring-open α-ketoaziridines such as **41** to provide β-aminoketones such as **42**. However, in both cases of the ring-opening, an aryl substituent is required on the ketone, probably to facilitate single-electron reduction to the ketyl radical. $[Ir(dtb-bpy)(ppy)_2]PF_6$ as a single-electron transfer (SET) photosensitizer, was utilized to bring about the ring-opening reactions of the sterically hindered β-epoxyketones.

Scheme 22: Reductive opening of epoxide and aziridines

HE = Hantzsch ester; HP = Hantzsch pyridine
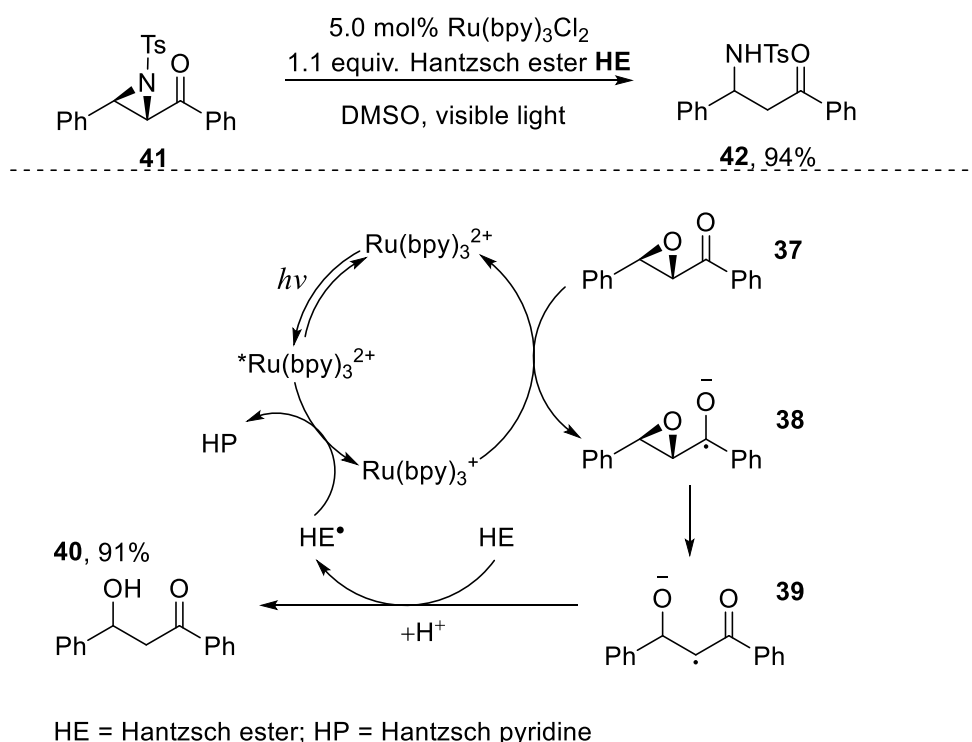
1.7 Net Oxidative Photoredox Reactions

Photoredox catalysis has also been used to perform net oxidative reactions as it is used to achieve net reductive reaction. A net oxidative reaction requires an external oxidant, which

can accept electrons in either the photoinduced electron transfer (PET) step or the catalyst turnover step. Reactions in this category typically hinge on the single-electron oxidation of particularly electron-rich functional groups, such as electron-rich arenes and amines.[18,24,39]

The Ru(II) polypyridyl complex (RL_3^{2+}) effectively catalysed the photo-oxidation by visible light of some carbinols to aldehydes in the presence of a diazonium salt as quencher and a basic agent in acetonitrile.

1.7.1 Functional group oxidation

Single-electron oxidation pathways have enabled the oxidation of several common functional groups *via* photoredox catalysis. In 1984, Cano-Yelo and Deronzier reported the use of ruthenium(II) photocatalyst to effect the oxidation of benzylic alcohols to their corresponding aldehydes using aryldiazonium salts as sacrificial electron acceptors (quencher).[40] The reaction was carried out in acetonitrile in the presence of a basic agent, collidine. (**Scheme 23**)

Scheme 23: Photoredox Catalytic Oxidation of Benzylic Alcohol
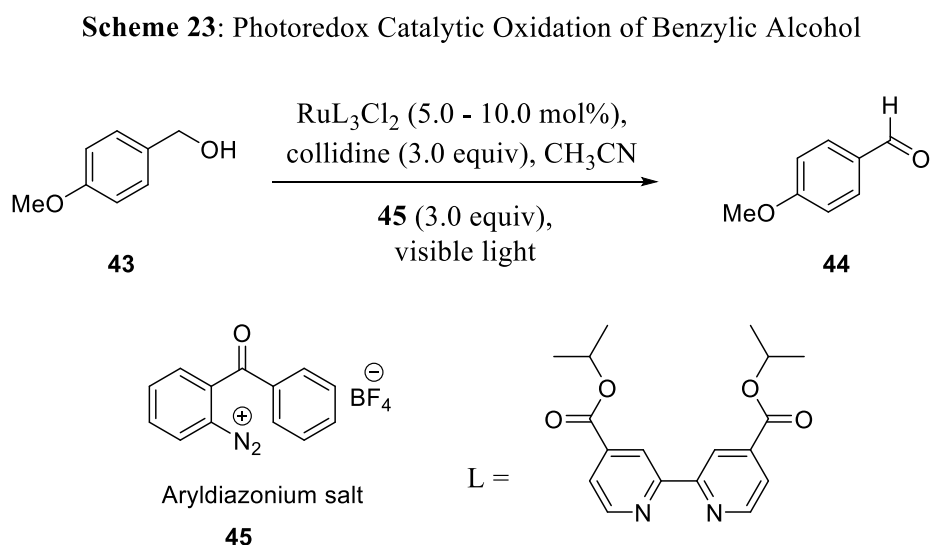
Cano-Yelo and Deronzier observed that the efficiency of alcohol oxidation by the method largely depends on the redox properties of the photocatalyst that can be modulated *via* the instalment of substituents on the ligand framework of the catalyst. The presence of electron-withdrawing groups on the bipyridine ligands renders the catalyst RuL_3Cl_3 significantly more oxidizing than $Ru(bpy)_3^{2+}$.

Much more later after the Deronzier's first application of photoredox catalysis for the synthesis of organic compounds, Zen and co-workers reported the selective and efficient photocatalytic oxidation of sulfides to sulfoxides.[19] For this oxidation, a Nafion membrane doped with a lead ruthenate pyrochlore (Pyc) catalyst and $Ru(bpy)_3^{2+}$ (designated as |NPycx–Ru(bpy)|) was used. When the sulphide **46** was irradiated with visible light in the presence of the catalyst in CH_3CN/H_2O and continuous purging with O_2 for 3 h the sulfoxide **47** was obtained in 97% yield (**Scheme 24**). No over oxidation of sulfoxide to sulfone was observed.

A proposed reaction mechanism is shown in **Scheme 24**, where Pyc plays a dual catalytic role as the reducing agent in the oxygen reduction reaction (ORR) to produce H_2O_2 and also as an electron acceptor from the excited $*Ru(bpy)_3^{2+}$ to form $Ru(bpy)_3^{3+}$. Hydrogen peroxide generated *in situ* oxidizes the sulfide to sulfoxide while regenerating $Ru(bpy)_3^{2+}$ to complete the catalytic cycle of the catalyst.

Scheme 24: Photocatalytic Oxidation of Sulfides to Sulfoxides
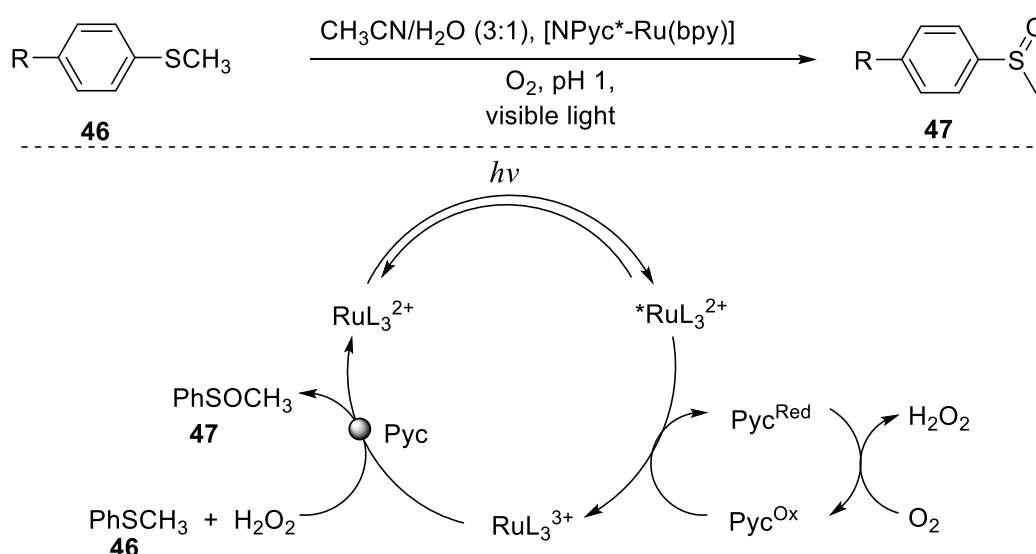
1.7.2 Oxidative Generation of Iminium Ions

Sequel to their previous work on reductive quenching cycle of photoredox catalysis, Stephenson and co-workers in 2012 reported their achievement of Friedel−Crafts amidoalkylation **51** by oxidation of dialkylamides **48** using persulfate ($S_2O_8^{2-}$) in the presence of the visible light catalyst, $Ru(bpy)_3Cl_2$, at room temperature, *via* a reactive *N*-acyliminium intermediate **50**. Alcohols and electron-rich arenes served as effective nucleophiles, forming new C−O or C−C bonds. Though the same reaction could be carried

out by mild heating of the dialkylamides and persulfate, photocatalysis provided higher yields and better selectivities.[41] *N*-Acyliminium ions are very important in the synthesis of alkaloid natural products.

Scheme 25: α-C-H functionalization of amides *via* visible light-mediated photocatalysis
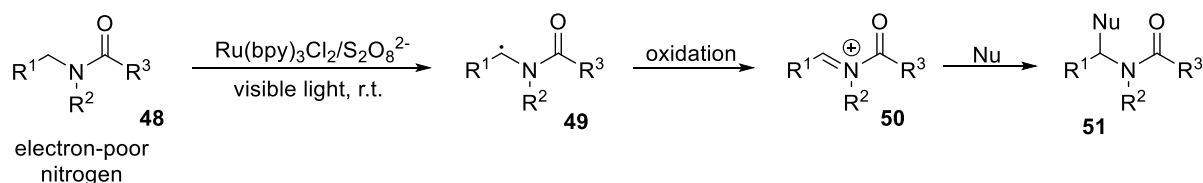
There is precedence that persulfate ($S_2O_8^{2-}$) is an effective oxidative quencher of $*Ru(bpy)_3^{2+}$, and the generated sulfate radical anion ($SO_4^{\cdot-}$) is a reactive intermediate known to abstract activated hydrogen atoms and also to be a strong oxidant.[41]

1.7.3 Aza-Henry Reactions

Stephenson and co-workers reported in 2010, the use of photoredox reductive reaction to achieve Aza-Henry reactions, oxidative coupling of nitroalkanes with tertiary *N*-arylamines, by taking the advantage of the iminium ions generated in the reaction using tertiary amines as reductants. With an appropriately chosen oxidant, the iminium ion generated in the reductive quenching cycle of the photoredox catalyst could be trapped by a variety of nucleophiles under the photoredox conditions. In their study, the group used nitroalkanes (as nucleophiles) and *N*-arylamines to achieve the oxidative coupling using visible-light photoredox catalysis. The photocatalyst employed is the iridium complex $Ir(ppy)_2(dtbbpy)PF_6$, which upon photoexcitation is capable of oxidizing *N*-phenyltetrahydroisoquinoline **52** to its radical cation **53** (**Scheme 26**). The intermediate Ir(II) species is proposed to reduce dioxygen to complete the photoredox cycle. Superoxide may then abstract a hydrogen atom at the α-position of the amine to generate the key iminium intermediate **54**. Addition of the nitromethane anion **55** yields the aza-Henry adduct **56**.[19,42]

Scheme 26: Photoredox aza-Henry reaction *via* iminium intermediate
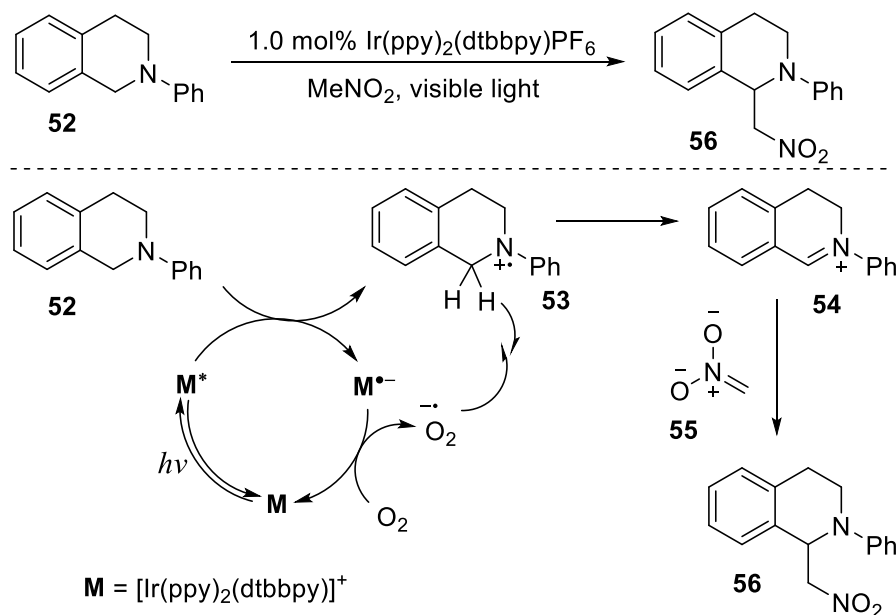
1.7.4 Azomethine Ylide [3+2] Cycloadditions

Iminium ions generated *via* photoredox catalysis had been used to achieve azomethine ylide [3+2] cycloadditions by some research groups. Azomethine ylides are nitrogen-based 1,3-dipoles, consisting of an iminium ion next to a carbanion. They are usually used in 1,3-dipolar cycloaddition reactions to form 5-membered heterocycles,[43] including pyrrolidines and pyrrolines by reacting them with electron-deficient alkenes. Xiao and co-workers were reported[19] to couple this reaction with an oxidative aromatization sequence to convert tetrahydroisoquinolines to polycyclic adducts such as **57** (**Scheme 27**). In the transformation, tetrahydroisoquinoline **58** undergoes single-electron oxidation by *Ru(bpy)$_3$$^{2+}$ to give radical cation **59**. Hydrogen atom abstraction, presumably by superoxide generated during catalyst turnover, then furnishes iminium **60**. Deprotonation adjacent to nitrogen forms the azomethine ylide **61**, which may engage a host of electron-deficient alkenes in [3+2] cycloaddition reactions. Thus, cycloaddition with *N*-phenylmaleimide **62** furnishes the pyrrolidine-containing adduct **63**.[19]

Scheme 27: Photoredox-promoted azomethine ylide [3+2]-cycloaddition
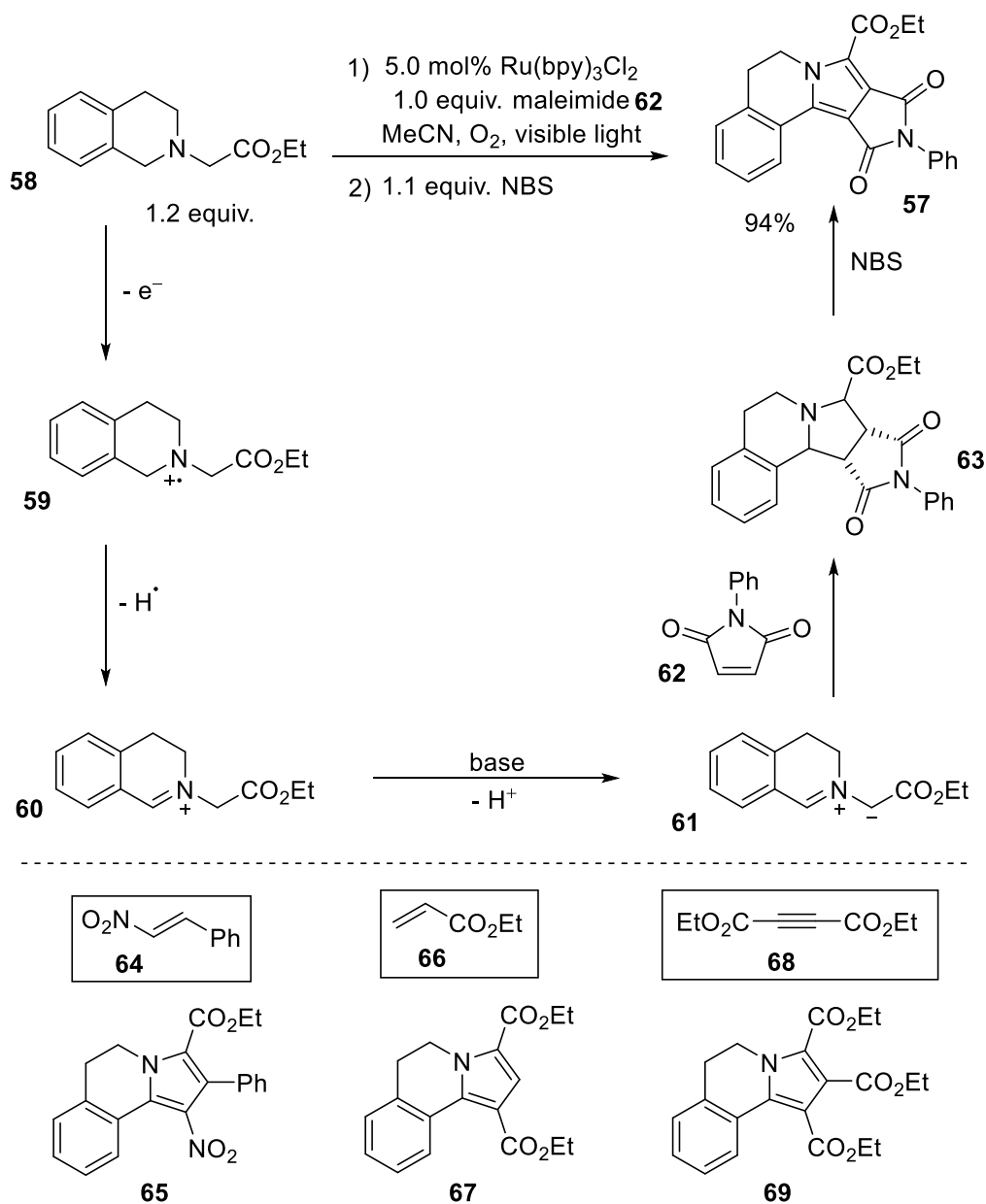
1.8 Net Redox-Neutral Reactions

In both the net reductive and net oxidative reactions discussed above, there is a need for the use of a stoichiometric quantity of a molecule that can serve as a source or reservoir of electrons, respectively. However, there are situations where the substrate or substrates undergo both a single-electron oxidation and a single-electron reduction at separate points in the reaction mechanism. As a result, there is no net oxidation state change between starting materials and products, and no stoichiometric external components are required to turn over the photocatalytic cycle. Net redox-neutral processes are more complex than the net

reductive and net oxidative reactions and are sometimes mediated by a redox-active co-catalyst.[17]

1.8.1   *Atom Transfer Radical Addition (ATRA)*

The redox neutral approach is perhaps best exemplified by atom transfer radical addition (ATRA) reactions.[19] In ATRA reaction, an atom transfer reagent formally undergoes σ bond cleavage and addition across a π bond of an alkene or alkyne, in the process forming two new σ bonds.[44] In 1994, Barton, *et al* reported an atom transfer radical addition of Se-phenyl *p*-tolueneselenosulfonate to a range of vinyl ethers using $Ru(bpy)_3^{2+}$ photoredox catalyst producing β-phenylselenosulfones in high yields.[45]   Stephenson and co-workers[44] accomplished similar results using the photoredox catalyst $[Ir(dF(CF_3)ppy)_2(dtbbpy)]PF_6$ (**M**) on a broader range of atom transfer reagents to olefins using α-halocarbonyls such as diethyl 2-bromomalonate   and   ethyl   bromodifluoroacetate   and   haloalkanes   such   as trifluoromethyliodide and perfluoroalkyl iodides.   Their protocol is capable of coupling a wide variety of halogenated compounds to terminal olefins and disubstituted olefins under mild conditions.[19] Based on their findings, Stephenson and co-workers proposed the mechanism outlined in **Scheme 28**. Oxidative quenching of the visible light-induced excited state of the photoredox catalyst, **M*** by the haloalkane **70** generates an electrophilic radical **71** along with the **M**$^+$ complex, bearing the halide as a counterion. This radical then undergoes an addition to the alkene **72**. The ATRA product **74** can then be formed *via* two potential pathways. First, oxidation of the alkyl radical **73** by **M**$^+$ generates the carbocation **73**, pre-associated with the halide, which combine to provide the final product **74** selectively. Alternatively, a radical chain transfer mechanism may also be operative.[44] The reactions are amenable to addition across a range of terminal alkenes, as well as cyclic internal alkenes and terminal alkynes.[46]

Scheme 28: Proposed mechanism for atom transfer radical addition[44]

Nucleophilic trapping

Radical propagation

$M = Ir(dF(CF_3)ppy)_2(dtbbpy)PF_6$
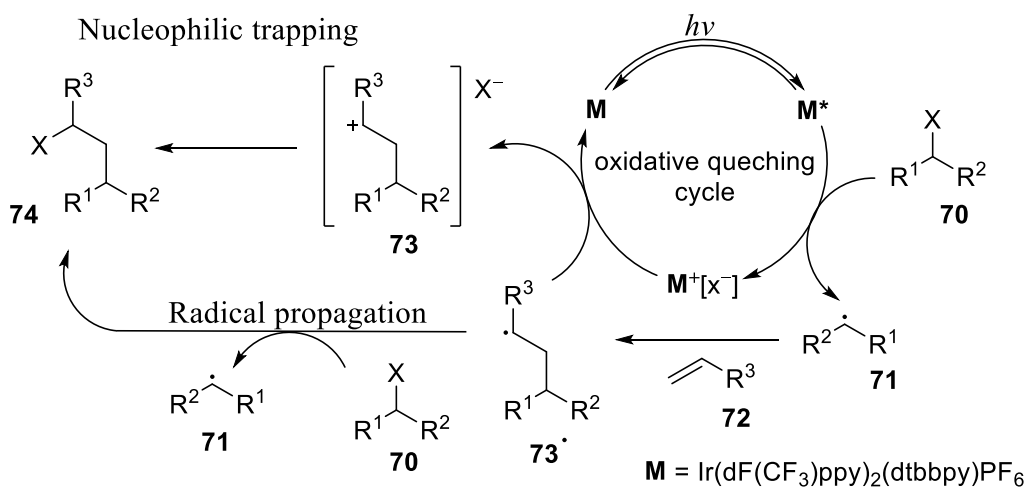
CHAPTER TWO

2.0　Aims

Alkenes and allenes represent versatile functional groups that can be utilized as a useful precursors in a variety of synthetic transformations, leading to complex structures that are useful for constructing natural and unnatural products.[47,48] When one of the hydrogen atoms of these functional groups is replaced with an amine, enamines and allenamines are obtained respectively. Both enamines and allenamines are unsaturated compounds and are highly nucleophilic due to the electron-donating ability of the nitrogen lone pair to the C=C double bond which increases its electron density. This electron rich C=C double bond makes them powerful synthetic intermediates and find wide applications in organic synthesis.[49] However, this factor also makes enamines and allenamines very difficult to handle.

If the nitrogen functionality containing an electron withdrawing group, such a carbonyl group in particular, is the substituted group on the alkenes or allenes, enamides or allenamides, respectively, are obtained. In comparison to enamines, enamides exhibit a much diminished enaminic reactivity, because the *N*-electron-withdrawing group, the carbonyl group, alleviates the delocalization of the lone-pair electrons of the nitrogen atom into the C=C double bond. The lone pair conjugates with the carbonyl group leading to decreasing electron density of the C=C double bond. Therefore, enamides show a good balance of stability and reactivity, a combination which accounts for their increasing importance in organic synthesis and medicinal chemistry.[50] The stability of enamides is well demonstrated, for instance, by the occurrence of stable enamide structures in many natural products and drug candidates.[51] The enamide group is an important substructure that is often found in natural products and synthetic drugs.

Similarly, allenamides possess the right balance between stability and reactivity that are more rewarding than allenamines for the same reasons that make enamides more stable than enamines. These nitrogen-containing structures represent a versatile functional group that can be utilized as a useful building block in a variety of synthetic transformations, leading to complex structures that are useful for constructing natural and unnatural products.

Both enamides and allenamides offer a wide variety of alternatives for the inclusion of nitrogen-based moiety into organic systems. Nitrogen-containing structures are prevalent

among medicinally interesting natural and unnatural products and, thus, are useful in developing new therapeutics. For instance, the enamide group is an important substructure that is often found in natural products and synthetic drugs that have, amongst others, sedative, cytotoxic, or anti-inflammatory, anti-parasitic and anti-cancer properties.[50,52] Therefore, efforts in developing the chemistry of these compounds can be significant and rewarding, especially to synthetic chemists and medicinal chemists.[10]

Detailed reviews of enamides are given in chapter three while that of allenamides are in chapter four. These include the synthetic routes for the two functional groups and some of the significant reactions each of the two undergoes.

Carbon–carbon and carbon-heteroatom bond-forming reactions constitute one of the foundations in organic synthesis and have attracted extensive exploration since the dawn of organic chemistry.[1] For instance, the direct C–H activation (or functionalization) of organic compounds with transition metals has recently received much attention across the chemistry fields.[2] These C-H functionalization often involves generation of reactive radical intermediates.

Reactions *via* radical intermediates are widely used in organic synthesis.[1] However, the generation of these highly reactive species under mild conditions and in a predictable way, in accordance with the general principles of Green Chemistry,[2] is not an easy task. The principles of green chemistry include, among others, prevention of waste or by products, maximum incorporation of the reactants into the final product and prevention of hazardous products. Photochemistry is the elective method, since the absorption of a photon leads to the selective delivery of a large amount of energy into an absorbing molecule and leaves no waste to get rid of after the process, thus offering a smart way to generate reactive intermediates under controlled conditions.[3] Moreover, the emerging strategy for the visible-light photoredox-catalysed C–C bond forming reactions further enrich the realm of this transformation,[3] such as the visible-light photoredox catalysis. It is the intention of this research to evolve a reaction method to transform enamides and allenamides into synthetically useful compounds by the use of photoredox catalysis.

2.1   Enamides

We intended to explore the area of radical/cationic pathway using iridium 2-phenylpyridine 4,4'-di-tert-butyl-2,2'-bipyridine complex [Ir(ppy)$_2$(dtbbpy)]PF$_6$ as a photoredox catalyst to access the *N*-acyl-*N'*-aryl-*N,N'*-aminals in a one-pot three components reaction under mild reaction conditions and their subsequent cyclization to γ-lactams.

Studies made by Courant and Masson[53] have demonstrated that iridium polypyridyl complexes could be used as photoredox catalyst to initiate three-component domino synthesis of *N*-carbamoyl α-alkylated imines under mild conditions. In their work, Courant and Masson were able to initiate a non-reductive radical alkylation of secondary enamides using iridium poly pyridyl photoredox catalyst to obtain *N*-acyliminium cation intermediate which was trapped by ethanol as a nucleophile to generate β-alkylated β-amido ether (**Scheme 29**).[53] With this in mind, we envisaged that the same procedure could be used with tertiary enamides using arylamines as nucleophiles to trap the *N*-acyliminium cation intermediate that might be formed to obtain *N*-acyl-*N'*-aryl-*N,N'*-aminals. In other words, we intend to develop a novel approach using iridium polypyridyl complex photoredox catalyst to initiate a three-component domino transformation of enamides to *N*-acyl-*N'*-aryl-*N,N'*-aminals *via* photoredox catalysed β-alkylation of enamide intermediate and their subsequent trapping with an arylamine. It is our desire to obtain *N*-acyl-*N'*-aryl-*N,N'*-aminals of the type **81** by combining the enamide, diethyl 2-bromomalonate and arylamine *via* a one-pot three-component reaction conditions (**Scheme 30**). We thought, if this could be achieved, the *N,N'*-aminals so obtained would be first of its kind accessed through this approach.   The *N*-acyl-*N'*-aryl-*N,N'*-aminals would be synthetically useful precursors to valuable γ-lactams building blocks under a mild condition (**Scheme 30**).

Scheme 29: Courant and Masson work

42
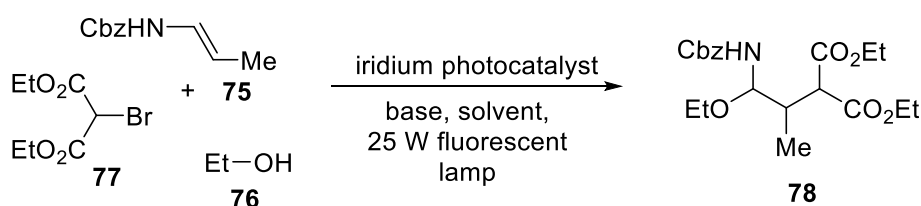
Scheme 30: Photoredox catalysed β-alkylation-α-amination of enamides
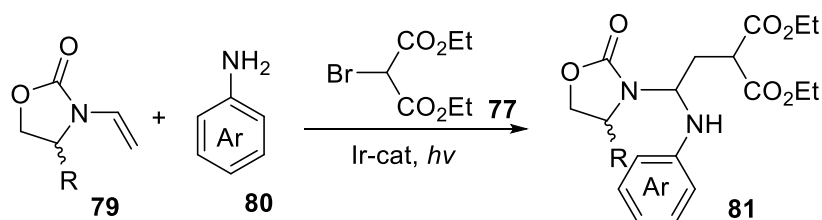
The *N*-acyl-*N'*-aryl-*N,N'*-aminal structural motif is prevalent within a wide range of biologically important compounds and have attracted considerable attention as building blocks for the synthesis of drug candidates. For example, the natural product evodiamine is an aminal-containing molecule with anti-inflammatory, antiobesity, and antitumor activities (**Figure 5**). In addition, aminal-containing molecules have also found a wide range of applications in optoelectronic materials.[54]

Figure 5: Some Aminal Containing Molecules

evodiamine   cholinesterase inhibitor
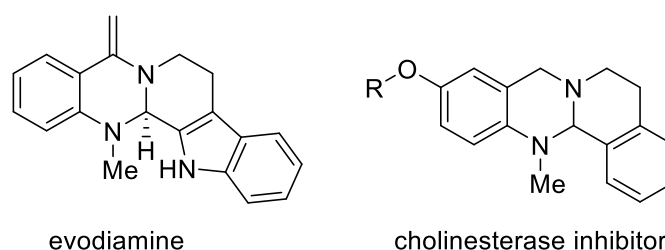
Typical approaches to the *N*-acyl-*N'*-aryl-*N, N'*-aminal motifs, whether cyclic or acyclic, have relied on the addition of an arylamine to an *N*-acyliminium species, or conversely, the addition of an amide or an equivalent to an *N*-aryliminium which are predicated on the successful formation of an *N*-acyl and *N*-aryliminium species. Another approach had been by means of Curtius and Hoffman rearrangements of protected amino acid derivatives. However, this often-multistep strategy has a limited substrate scope.[54] Therefore, the development of efficient and convenient methods for synthesizing aminals should be of great importance to the synthetic community.

Scheme 31: Some approaches to aminal preparation

Manzo *et al.* Au catalyzed procedure for the preparation of aminals[54]
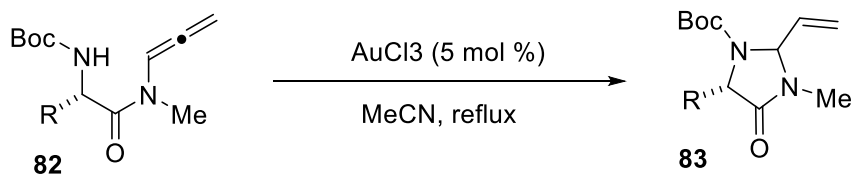
Toste *et al.* protocol for the preparation of cyclic aminals[54]
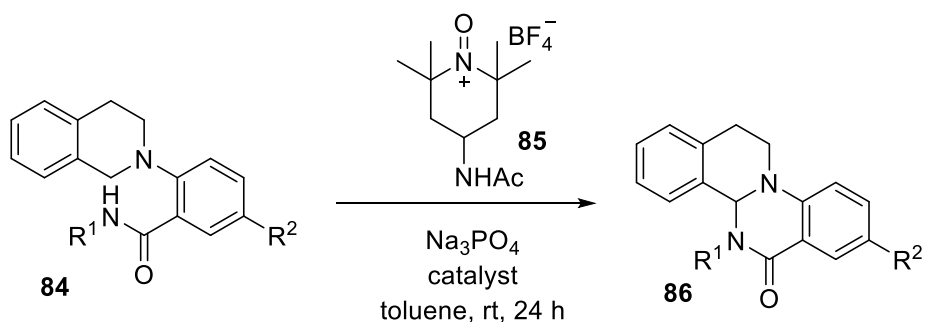
Wang *et al.* protocol for the preparation of aminals[54]
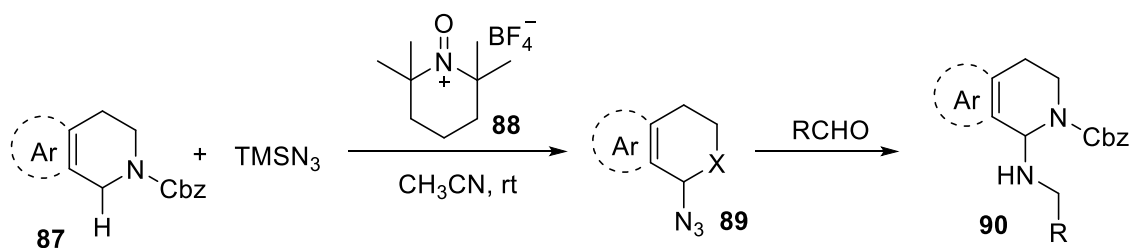
Aminal preparation *via* Curtius rearrangement of protected amino acid derivatives[55]
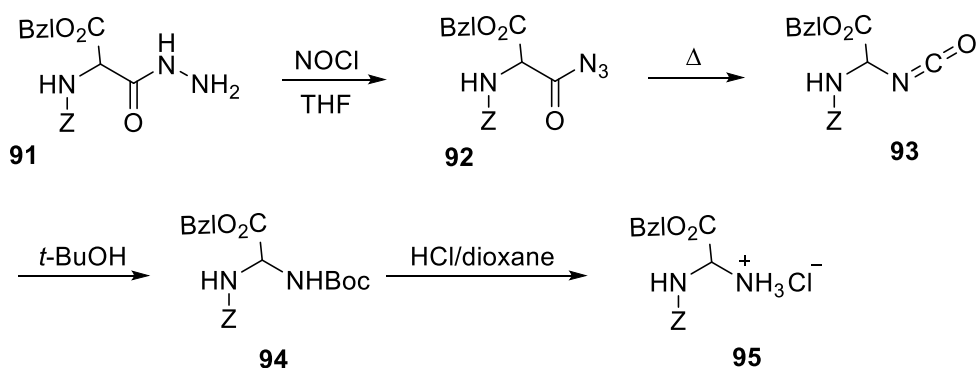
The γ-lactams should be obtained by intramolecular cyclization of the *N,N'*-aminals with the presence of a nucleophile *via* the lone pair of the nitrogen atom of the arylamine and an electrophilic carbon of the carbonyl carbon of the ester in the molecule (**Scheme 32**).

Scheme 32: Cyclization of *N,N'*-aminal to γ-lactam
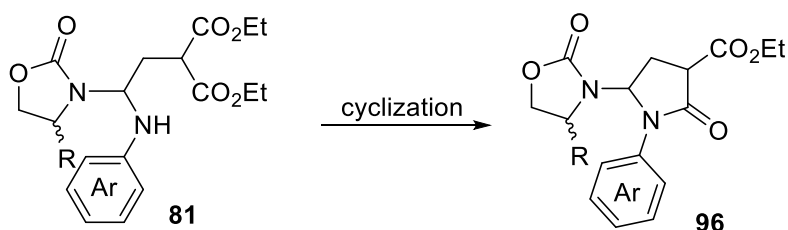
The γ-lactam moiety is part of the important structure of a large number of natural and non-natural compounds covering a broad spectrum of biological activities.[56] They are included in a large number of pharmaceutically active compounds with antibiotic, anti-inflammatory, and anti-tumoral functions.[57] The γ-lactam moiety is, therefore, a privileged structural subunit for the design of several pharmaceutical agents.[58,59] γ-Lactams also served as valuable building blocks for the synthesis of complex molecules due to their latent reactivity and the large panel of highly selective transformations they can undergo.[58] **Figure 6** shows rolipram, a selective inhibitor of phosphodiesterase (PDE) type IV possessing anti-inflammatory and antidepressant activities,[58] and some valuable γ-lactam ring containing natural products and pharmaceutical agents. Accordingly, products containing the γ-lactam core are important synthetic targets.

Figure 6: Some γ-lactam moiety containing natural products

rolipram   stemoamide   tuberostemospironine   (+)-clausenamide
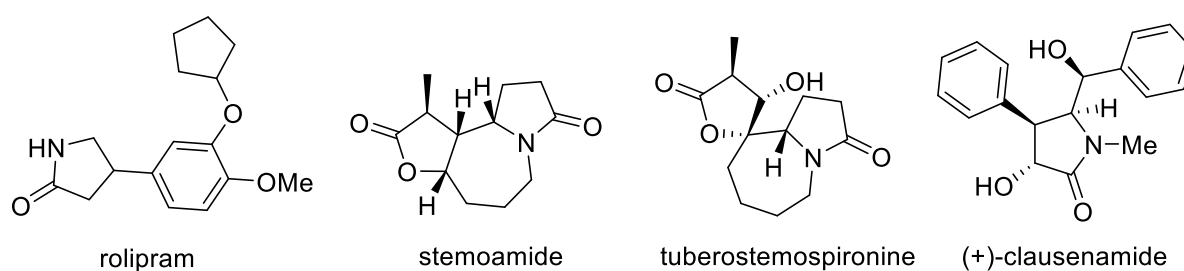
2.2   Allenamides

Allenamides possess the right balance between stability and reactivity of allenamines. The stability and reactivity are the result of the effects of the electron-withdrawing group, such as

carbonyl group, on the nitrogen atom which reduces the electron density on the allene moiety. Though it is less reactive than the allenamines, allenamides are more stable and still retain most of the allenaminic reactivities.[60]

Recently, allenamides with the similar classes of compounds have attracted considerable attention of the synthetic community due to their unique reactivity profiles.[61,62] The electron density on the central β-carbon is relatively higher than on the α- and γ-carbon atoms of the allene group of the allenamide as a result of the controlled electron donating ability of the nitrogen atom. This effect makes the central β-carbon a point of attack by a suitable electrophile. This can be harnessed in subsequent chemical transformation of allenamides leading to regiochemical confidence in the resulting products.

Importantly, this unique reactivity has led to the development of a variety of innovative transformations, including cycloadditions, Aldol additions, intramolecular cyclizations and intermolecular addition reactions, as well as the use of the allenamide building block in natural product synthesis. Despite this versatility of the allenamides to the synthetic community, no one has subjected these useful class of compounds to photoredox catalysis, at least to the best of our knowledge.

With the above in mind, we aimed to establish a novel atom-efficient and general photoredox catalyst mediated β-alkylation of allenamides building blocks utilising a one pot-component reaction. Then formation of a general route of arylamination at the α-position or γ-position forming a new carbon-nitrogen bond which may lead to *N,N'*-aminals in the case of α,β-addition products (**Scheme 33**). The presence of a C=C bond in the resulting adduct products can also be utilized in the subsequent transformations. We plan to achieve this by using iridium polypyridyl complex photoredox catalyst to initiate a three-component domino transformation of allenamides to *N*-acyl-*N'*-aryl-*N,N'*-aminals *via* photoredox catalysed β-alkylation and the subsequent trapping of the intermediate radical ion with a suitable nucleophile, namely an arylamine.

Scheme 33: Photoredox catalysed β-alkylation of allenamides
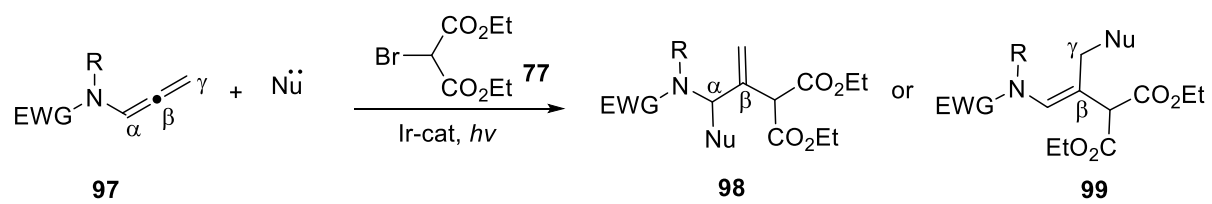
3.0   Enamides

3.1   Enamides: an Introduction

Enamines are unsaturated compounds derived by the condensation of aldehydes or ketones with secondary amines. If one of the nitrogen substituents of the enamine is a hydrogen atom, it is the tautomeric form of an imine (**Scheme 34**). This usually will rearrange to the imine; aniline being one of several exceptions to this. The enamine-imine tautomerism may be considered analogous to the keto-enol tautomerism. In both cases, a hydrogen atom switches its location between the heteroatom (oxygen in keto-enol or nitrogen in enamine-imine) and the second carbon atom. The high nucleophilicity of enamines can be ascribed to the electron-donating ability of the nitrogen lone pair to the C=C double bond, increasing its electron density.

Scheme 34: Condensation of carbonyl compounds and secondary amine
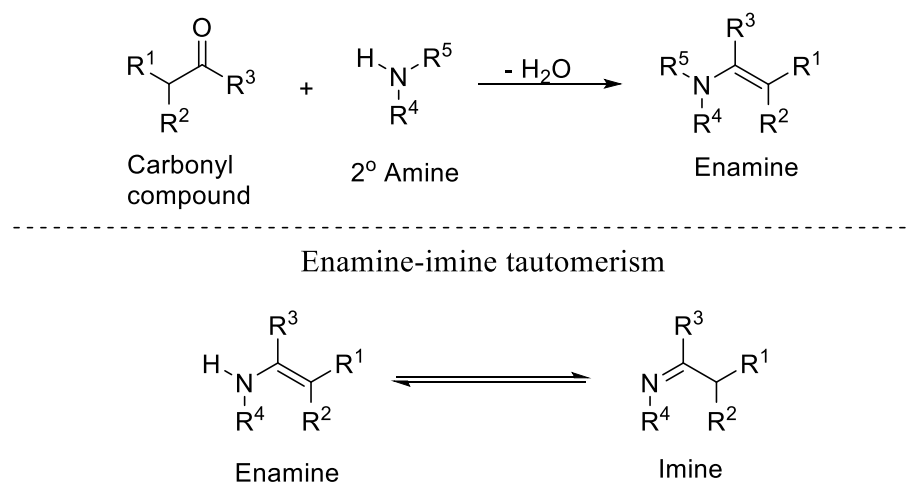
Figure 7. Comparison of enamines with enamides
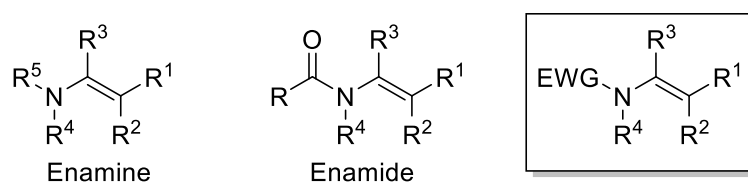
This electron rich C=C double bond makes enamines powerful synthetic intermediates and find wide applications in organic synthesis.[49] When one of the N-alkyl groups (R^4 or R^5 in Figure 7) of enamines is replaced by an electron-withdrawing group, such as an acyl, **enamides** are generated (**Figure 7**). Enamides are stable, highly polarized, electron rich double bonds that are excellent substrates for incorporation of nitrogen functionality.[50] In comparison to enamines, enamides exhibit a much diminished enaminic reactivity, because the N-electron-withdrawing group, the carbonyl group, alleviates the delocalization of the lone-pair electrons of the nitrogen atom into the C=C double bond. The lone pair conjugates with the carbonyl group leading to decreasing electron density of the C=C double bond. For this reason, enamides show a good balance of stability and reactivity, a combination which accounts for their increasing importance in organic synthesis and medicinal chemistry.[50] The stability of enamides is well demonstrated by the occurrence of stable enamide structures in many natural products and drug candidates.[49]

The enamide group is an important substructure that is often found in natural products and synthetic drugs that have, amongst others, sedative, cytotoxic, or anti-inflammatory, anti-parasitic and anti-cancer properties.[50,52] A majority of enamides bearing hydrogen on nitrogen are stable under air, are solid at room temperature, and can be purified by chromatography on silica gel. This stability contrasts with the corresponding enamines bearing hydrogen on nitrogen.[51]

The vast majority of synthetic applications of enamides documented in literature relate to their asymmetric reduction reactions. Indeed, enamides or dehydroamino acid derivatives are used as a testing ground for the study of the efficiency and enantioselectivity of the catalytic asymmetric hydrogenation of the carbon–carbon double bond.[49] Enamides offer a wide variety of alternatives for the inclusion of nitrogen-based moiety into organic systems.

Figure 8. Enamides in natural products and drugs

Salicyhalamide A

Retinoic acid derivative

Lobatamide

Apicularen A

Crocacin A
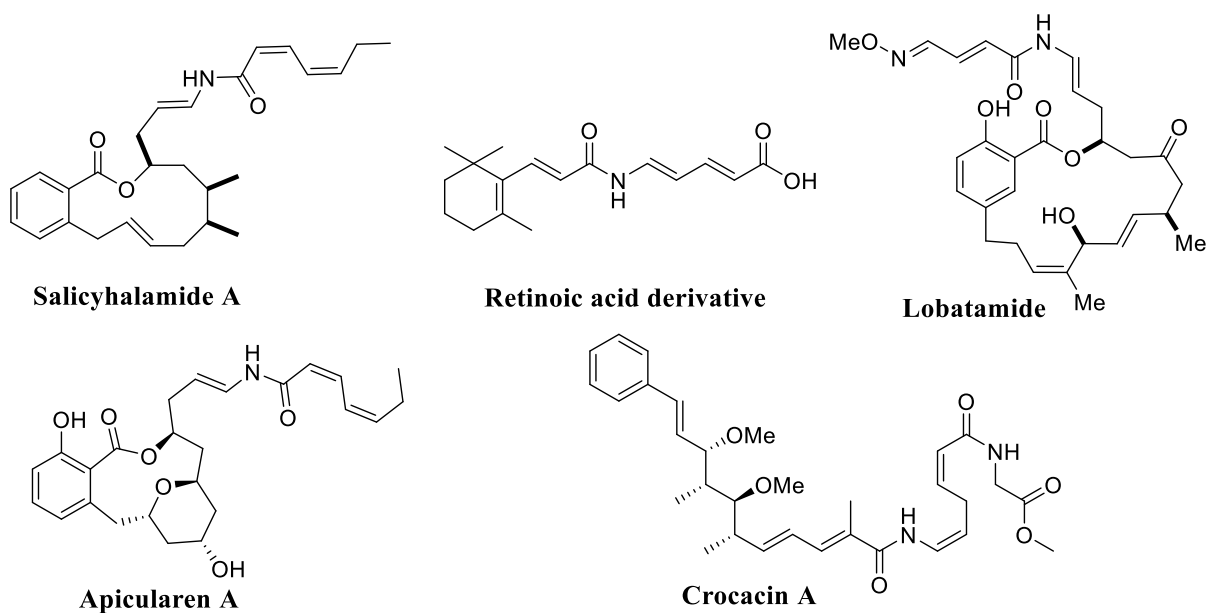
3.2 Synthetic Methods for Enamides

Retrosynthesis of enamides can theoretically be made in three major approaches as shown in **Figure 9** below.

Figure 9: Disconnections in enamides
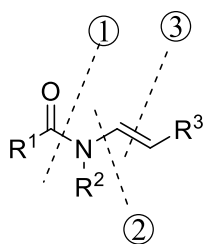
The first disconnection is straight forward. There is carbonyl group providing the electrophilic centre while the other section which is an enamine moiety provides the nucleophilic centre through the nitrogen atom. This suggests acylation of an enamine (**Scheme 35(a)**). The second disconnection involves the cleavage of an N-C bond. This gave an amide and an alkene synthons. This can be achieved by coupling reactions particularly transition metal coupling reactions like palladium catalysed N-C cross coupling reaction (**Scheme 35(b)**). The third scission is across the double bond. This may be achieved by 1,2-

elimination reaction from a saturated precursor, by metal catalysed isomerization of N-allylated amides or by Wittig reaction (**Scheme 35(c)**).

Scheme 35: Retrosynthesis of enamides
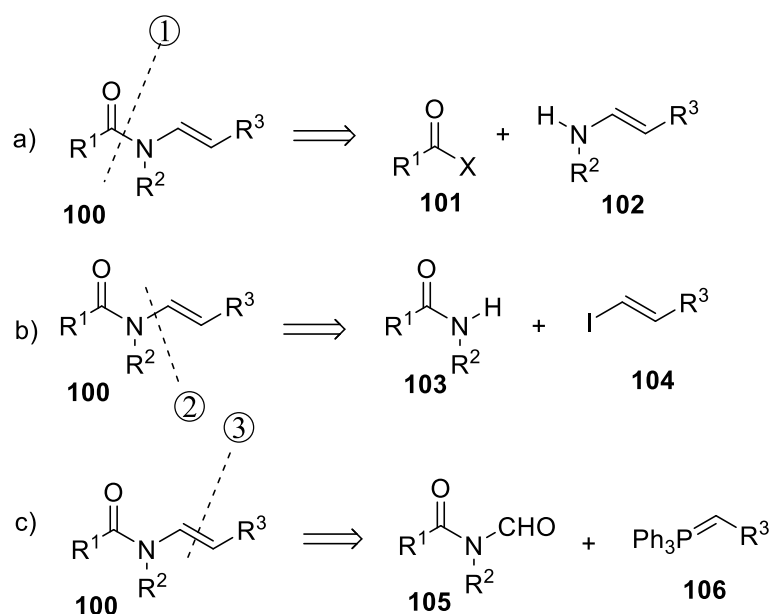
Several synthetic methods for enamides have been reported.[51] However, many of these synthetic methods have often been centered around condensation of an amide equivalent with the corresponding carbonyl functionality (**Scheme 36**).[51] One of such methods starts from nitriles, which are subjected to a Grignard reagent followed by treatment with acyl or alkoxy carbonyl cation equivalents (method I). This method can be used for the syntheses of aromatic ketone derived enamides and enecarbamates. Another method starts from α,β-unsaturated carboxylic acids, which are converted to acid azides followed by Curtius rearrangement to give isocyanates, which are treated with alcohols (method II). Most enecarbamates can be prepared *via* this method, although some of the corresponding α,β-unsaturated carboxylic acids are difficult to synthesize. An alternative method starts from the corresponding aldehydes, which are converted to *N,S*-acetals, followed by desulfonylation by treatment with bases (method III).

Scheme 36: Synthetic methods for enamides

However, more elaborate and novel methods such as organocuprate addition to isocyanates, acylation of *in situ* prepared imines and an *N*-acylation/Peterson elimination process have also been developed.[60] Complementing these methods, a number of transition-metal-catalysed approaches based on C-N bond-forming reactions (Pd, Cu), isomerizations of allyl amides (Fe, Rh, Ru), addition of amides to alkynes (Ru), organometallic additions to ynamides (Rh), Heck couplings (Pd), co-oligomerization of *N*-vinyl amides (Ru), and oxidative conjugate additions (Pd) have also been reported (**Scheme 37**).[60]

Scheme 37: Transition metal strategies in enamide synthesis
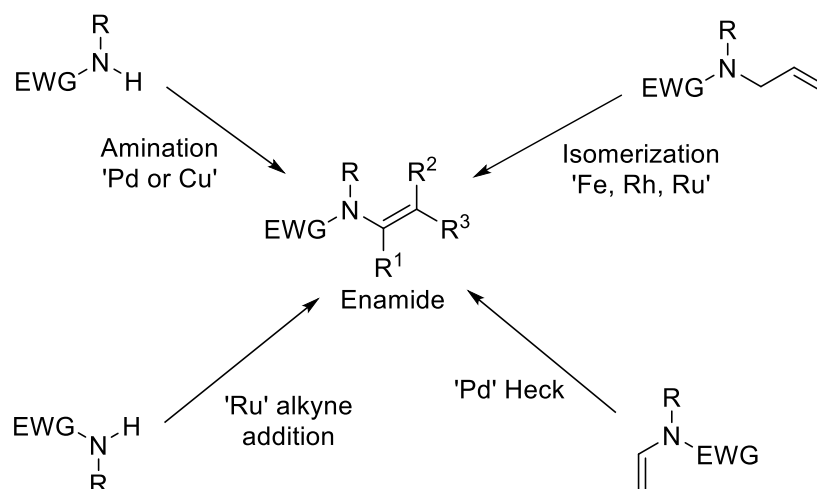
3.2.1 Palladium-Catalysed C-N Cross-coupling Reactions

Recent developments in palladium(0)-catalysed carbon-nitrogen bond formation have led to numerous useful synthetic methodologies, particularly for the cross-coupling of allyl, aryl, and vinyl halides and related electrophiles with amine and amide nucleophiles. Stahl *et al.*,[63] in 2004, reported the synthesis of enamides *via* vinyl transfer from vinyl ether to amides using the (DPP)Pd(OCOCF$_3$)$_2$ catalyst. Stahl *et al.* observed that ethyl vinyl ether undergoes nonoxidative transfer to the nitrogen nucleophile of the amides under the condition of the reaction. This reaction represents a C-N cross-coupling reaction with the vinyl ether as the electrophile partner.

Scheme 38: Palladium-catalysed C-N cross-coupling reaction
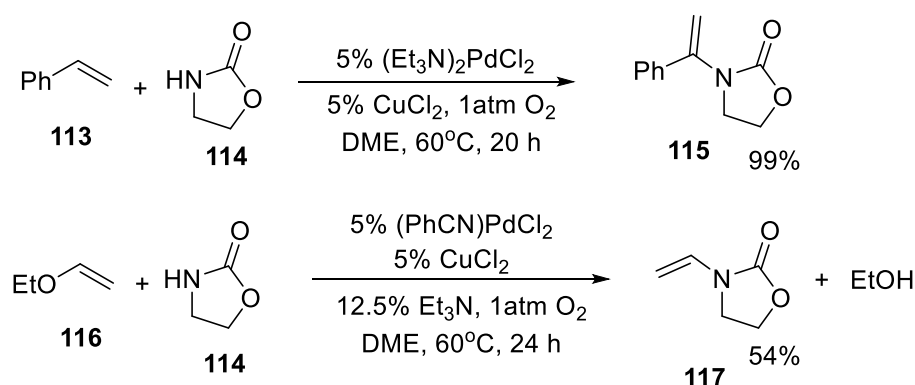
3.2.2 Conversion of Alkenylsilanes to Enamides

Fürstner *et al* reported, in 2001, the stereoselective synthesis of enamides under mild, aprotic and basic conditions. Fürstner's methodology is based on a silicon-directed epoxide ring opening with sodium azide, followed by reduction of the resultant azide to the corresponding amine, *N*-acylation and Peterson elimination to afford enamide (**Scheme 39**). The Peterson olefination (also called the Peterson reaction) is the chemical reaction of α-silyl carbanions with ketones (or aldehydes) to form a β-hydroxysilane that eliminates to form alkenes. This methodology offers great stereocontrol and broad scope, but has the disadvantage of requiring a multi-step sequence.[64]

Scheme 39: Conversion of (*E*)-alkenylsilanes into (*E*)-enamides
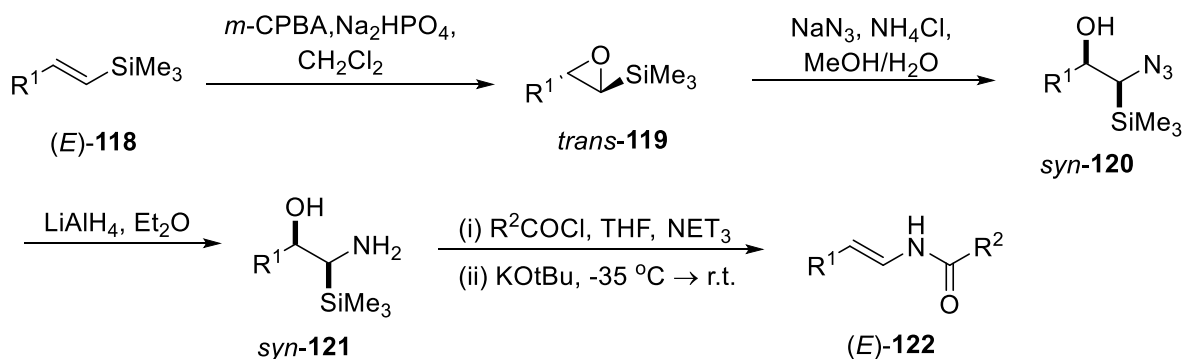
3.2.3 Enamide Synthesis from Primary Amides and Propargyl Aldehydes

In 2014, Hong *et al* reported a novel strategy for enamide synthesis from primary amides **123** and propargyl aldehydes **124** via Au(I)-catalysed tandem amide addition and Meyer–Schuster rearrangement (**Scheme 40**). *In situ* generated hemiaminals **126** were converted to the desired products under the optimized conditions. Enamide stereochemistry was controlled simply by changing solvents and adding a catalytic amount of acid. The developed synthetic strategy provides a new method to synthesize various β-substituted α,β-unsaturated carbonyl compounds.[65]

Scheme 40: Enamide synthesis from primary amides and propargyl aldehydes
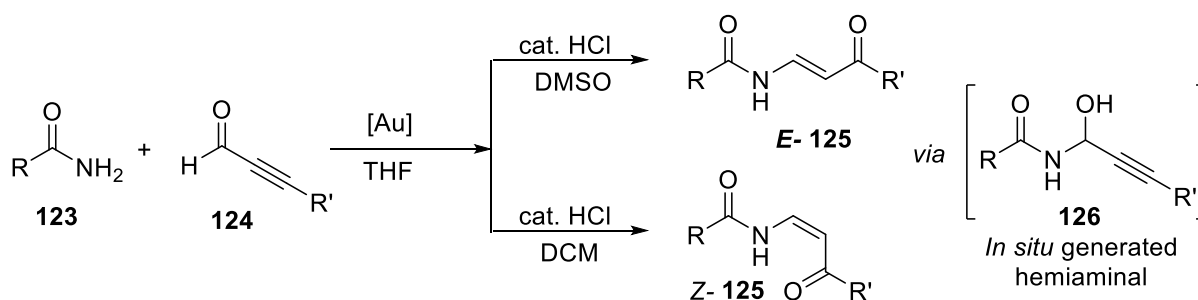
3.2.4 Hydroarylation of Allenamides

Hsung[61] and Kimber[66] reported a highly stereoselective transition metal catalysed hydroarylation of allenamides **127** to obtain a series of achiral and chiral oxazolidinone-derived *E*-enamides **129** via the 1,4-addition to *N*-acyl iminium intermediates **128** (**Scheme 41**). Au-catalysed hydroarylation took place relatively faster than their Pd- and Ru-catalysed counterparts.

Scheme 41: Kimber's stereoselective arylation of allenamides
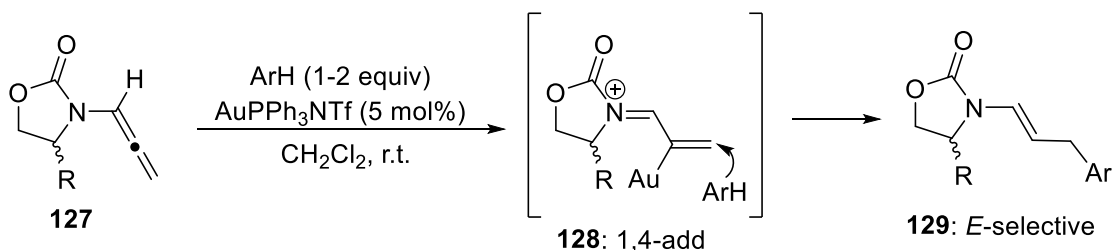
3.2.5 Dehydroalkoxylation of Hemiaminal

In 2002, Gaulon *et al.*[67] reported the preparation of cyclic enamides **96** in high overall yield by an easy two-step procedure based on the dehydroalkoxylation of an intermediate hemiaminal **131** using trimethylsilyl trifluoromethanesulfonate (TMSOTf) and triethylamine (TEA). The advantage of this method over others is that it is metal-free (**Scheme 42**).

Scheme 42: Gaulon preparation of enamide by dehydroalkoxylation of hemiaminal
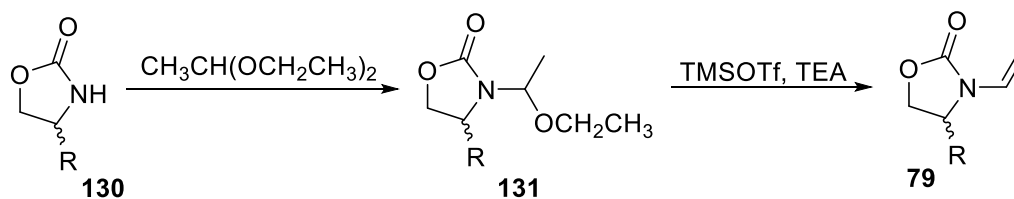
3.2.6   Isomerization of N-Allyl Amides To Form Substituted Enamides

The synthesis of geometrically defined enamides is problematic, especially the highly substituted and *Z*-enamides.   In 2017, Trost and co-workers reported a general atom economic method for the isomerization of a broad range of *N*-allyl amides **132** to form *Z*-di-, tri-, and tetrasubstituted enamides **133** with exceptional geometric selectivity (**Scheme 43**). A highly unsaturated precatalyst CpRu(CH₃CN)₃PF₆ was used.   The report represented the first examples of a catalytic isomerization of *N*-allyl amides to form nonpropenyl disubstituted, tri- and tetrasubstituted enamides with excellent geometric control.   The method was applied in the synthesis of *cis* vicinal amino alcohols and tetrasubstituted α-borylamido complexes.[50]

Scheme 43: Trost method of substituted enamides synthesis
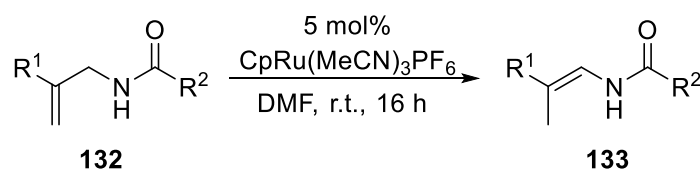
3.3   Chemistry of Enamides

Enamide moieties are contained in a number of natural product frameworks such as the chondriamides and salicylihalamides and within cyclic peptides.[66] The significant chemical stability of enamides as a result of the electron withdrawing functionality upon the nitrogen atom makes it less reactive than the enamines in spite the noticeable feature of nucleophilic character of the enamine.   Enamides often react similar to simple C=C bonds and offer further options for the incorporation of *N*-functionality into complex systems.[68]   They are commonly utilized in asymmetric hydrogenations, cycloadditions, cyclopropanations, halo functionalizations, heterocycle synthesis, carbonyl and imine additions, and transition metal mediated C−C bond formations. In addition, enamides are important pharmacophores in various bioactive natural products that display a range of anticancer, antifungal, and cytotoxic

properties.[48] The unique reactivity that enamides display has led to the development of a number of general and *E/Z* selective syntheses.

3.3.1 *Enamides as nucleophiles*

Enamides can be viewed as tuneable enamines and as such, it is no surprise that they participate in a number of interesting transformations with electrophiles. Ground breaking work in this area originated from the Kobayashi laboratory,[51] who reported the first enantioselective use of enamides as nucleophiles in reactions with aldehydes under Cu-catalysis. The Kobayashi laboratory has since demonstrated the use of C_2 symmetric diamine ligands with a range of electrophiles and enamides as nucleophiles, promoted by Cu(II)-catalysts in conjunction with iminophosphonates for the enantioselective formation of phosphonic acid systems,[69] diazodicarboxylates for enantioselective α-aminations and eventually demonstrated that some aldehydes (α-oxo-aldehydes) will participate as useful electrophiles. [51]

Addition of Enamides or Enecarbamates to Imines

The Kobayashi research group reported the first catalytic enantioselective nucleophilic addition of enamides and enecarbamates to imines. [70] Reaction of enamides **135** with imines **134** in the presence of a chiral copper catalyst prepared from Cu(OTf)$_2$ and the chiral diamine **136** gave the corresponding β-aminoimines **137** (**Scheme 44**).[71] Kobayashi's procedure proved to be a robust strategy for the synthesis of optically active 1,3-diamine derivatives, which are useful building blocks for the synthesis of natural products and drug candidates.

Scheme 44: Nucleophilic addition of enamides to imines

57
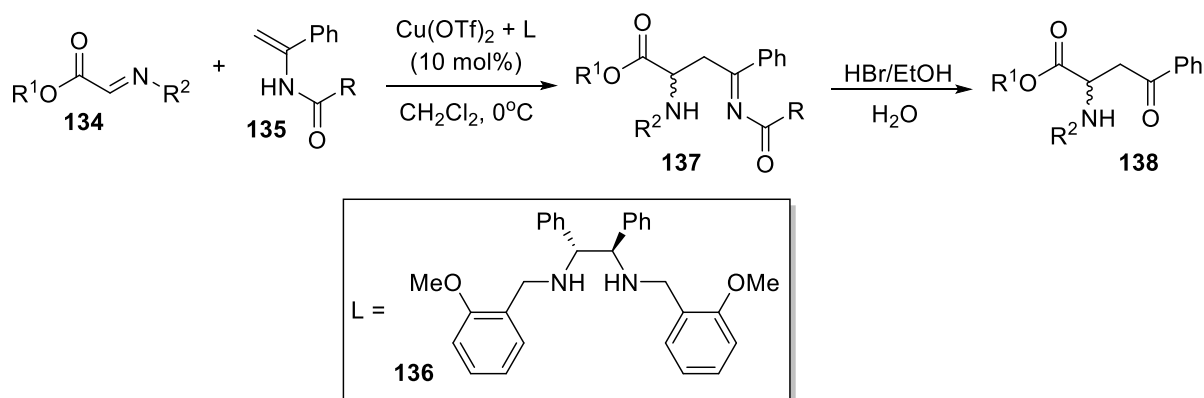
3.3.2 Nucleophilic Addition of 1,3-Dicarbonyl Compounds to Enamides

Nucleophilic addition to imines provides a facile synthetic route to nitrogen-containing compounds, many of which are of biological and chemical importance. Kobayashi and co workers reported, in 2006, that enamides and enecarbamates could be used as nucleophiles and that they react with several electrophiles in the presence of Lewis acids. They found that enamides and enecarbamates isomerize into imines surrogates in the presence of Lewis acids. The imines so formed then attack another molecule of the enamide being a very good nucleophile. Thus in the presence of Lewis acid such as TfOH, Sc(OTf)$_3$, or Cu(OTf)$_2$, enamides and enecarbamates undergo self-condensation or dimerise. To prevent enamides and enecarbamates from dimerizing under the acidic conditions, it is necessary to use nucleophiles that are more reactive than enamides and enecarbamates themselves. The group used 1,3-dicarbonyl compounds **139** such as β-ketoesters to trap the imine intermediate to form the adducts **140** (**Scheme 45**). This is a Mannich-type reaction of 1,3-dicarbonyl compounds with enecarbamates.[72]

Scheme 45: Lewis acid catalysed reaction of enamides with 1,3-dicarbonyl compounds
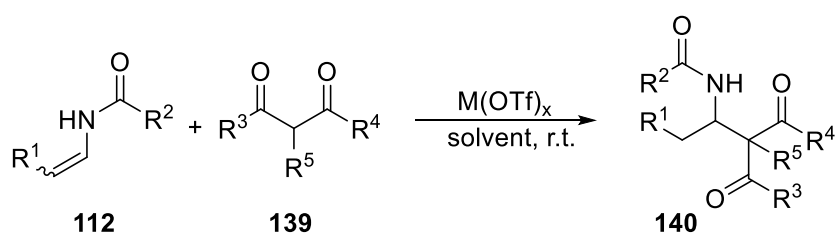
3.3.3 Transition metal mediated alkene transformations

Bennasar and co-workers[73], in 2006, reported the use of enamides in a number of transition metal mediated alkene transformations, especially in contexts where incorporation of nitrogen functionality is important, such as the ring-closing metathesis reaction (**Scheme 46**).

Scheme 46: Tandem Methylenation-Enamide Ring Closing Metathesis
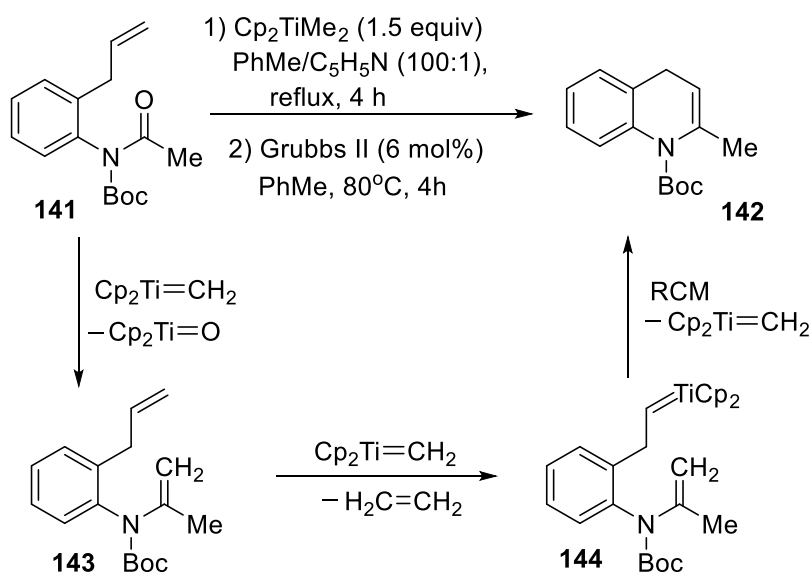
Bennasar demonstrated in this reaction that enamides could participate in ring closing metathesis reactions. Indeed, this example is a one-pot Petasis-methylenation of **141** followed by ring closing metathesis with the second generation Grubbs catalyst forming dihydroquinoline **142**.

3.3.4 Pericyclic reactions

Enamide substrates have also been used in many pericyclic reactions. Indeed, examples of cycloaddition, sigmatropic and electrocyclic chemistry have all been reported. In many instances, the C_{sp2}–N bond is transformed to a C_{sp3}–N bond as a result of the pericyclic reaction allowing the formation of new nitrogen stereocentres and an overall increase in molecular complexity. Rawal,[74] in 2000, reported a highly efficient and stereoselective Diels–Alder reaction using the conjugated enamide **145** as the reactive diene (**Scheme 47**). The reaction is promoted by Cr-salen complex **148** and yields synthetically useful cyclohexenyl carbamate **147** in high eneantiomeric excess.

Scheme 47: Enamides participate in Diels-Alder reactions
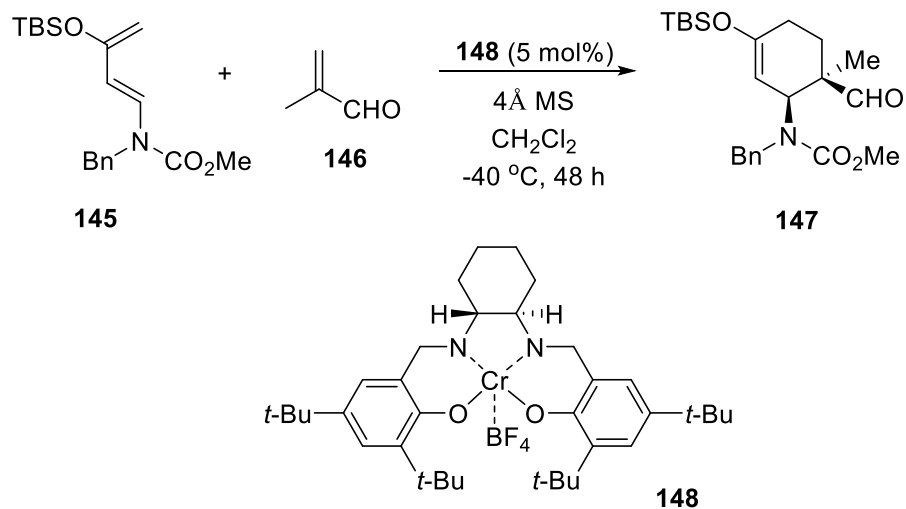
3.3.5 Radical reactions

In recent years there have been a number of reports detailing the utility of enamides in radical based transformations. In particular, Ishibashi (2008)[75] clearly showed the synthetic value of these enamide substrates through the synthesis of lennoxamine **151**. Enamide **149** was observed to undergo a regioselective 7–*endo* cyclization followed by subsequent homolytic aromatic substitution (**Scheme 48**). This single-pot process allows for the isolation of lennoxamine in 41%.

Scheme 48: Ishibashi's lennoxamine synthesis
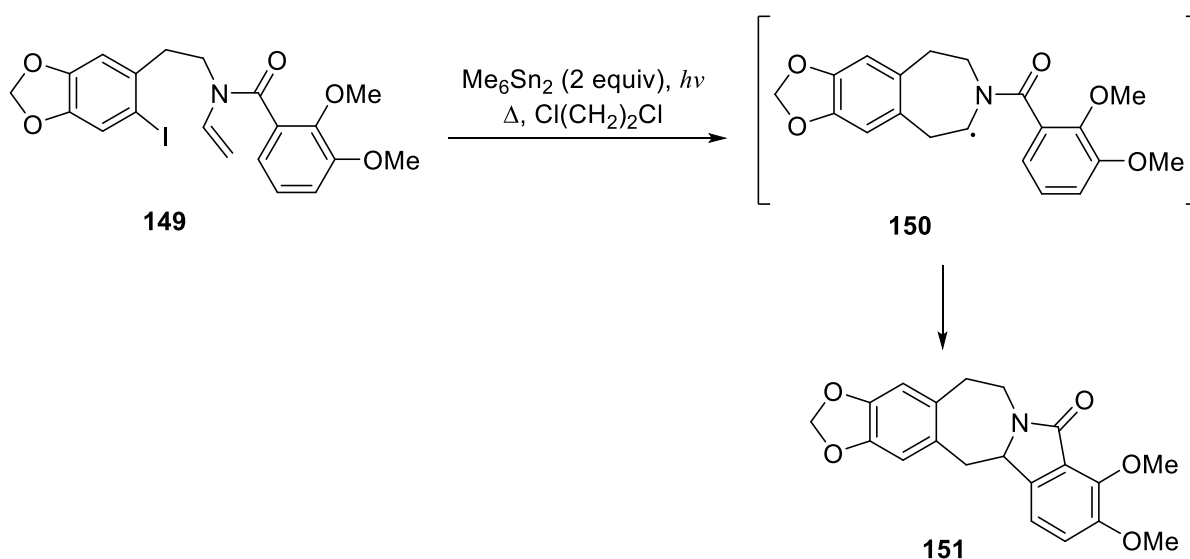
The Ishibashi group further demonstrated the value of enamide substrates in radical reactions by accomplishing syntheses of (±)-stemonamide and (±)-isostemonamide where the skeleton is formed through a key enamide radical reaction. In this instance, substrate **152** undergoes a double radical cascade cyclization initiated by 1,1'-azobis-cyclohexanecarbonitrile and terminated by Bu₃SnH (**Scheme 49**). Diastereomeric tricycles **153** are formed in moderate yield, albeit in a 1:1 ratio. Further elaboration of these tricycles allowed for succinct syntheses of these natural products.[76]

Scheme 49: A tandem radical cyclization entry to the stemonamide skeleton
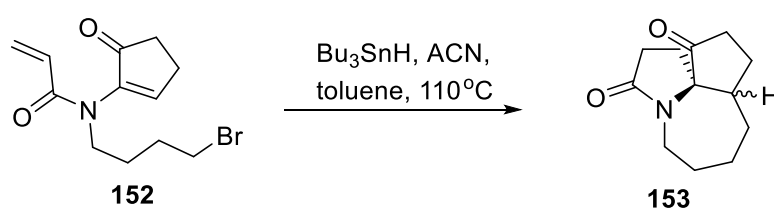
3.3.6 Photochemical reactions

Bach[77] demonstrated that enamides participate particularly well in the Paterno–Büchi photochemical reaction, forming amino oxetanes **156** in good yield with significant diastereo-selectivity (**Scheme 50**). Paterno–Büchi photochemical reaction is a photochemical reaction that forms four-membered oxetane rings **156** from a carbonyl **154** and alkene **155**.

Scheme 50: Enamide Paterno-Büchi reaction

cis **156**/*trans* **156** = 29:71
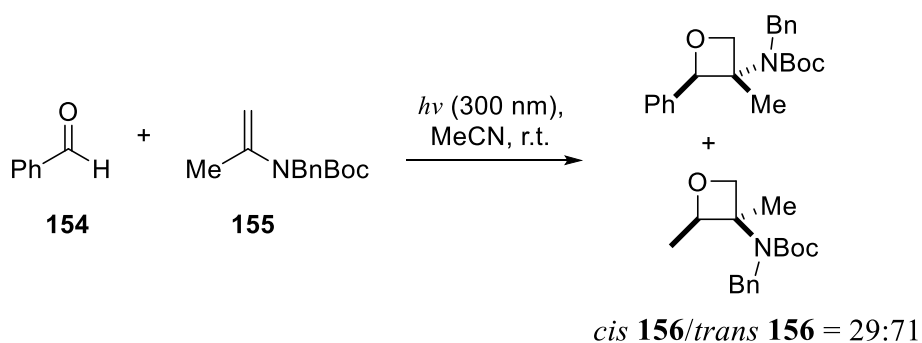
3.4   Enamides: Reactions, Results and Discussion

Our objective was to investigate the addition of bromide **77** to the electron rich enamide **79** by using photoredox catalysis. It was envisaged that upon formation of the malonate radical from **157**, and its addition to the enamide, that the subsequent radical would be oxidized in-line with Masson's findings to deliver the the iminium **160**. This iminium 146 can then be trapped with an arylamines to furnish the *N,N'*-aminal **81**; this can then be cyclized to deliver synthetically valuable γ-lactams (**96**) (**Scheme 51**).

Scheme 51: Synthetic pathway of the target molecule
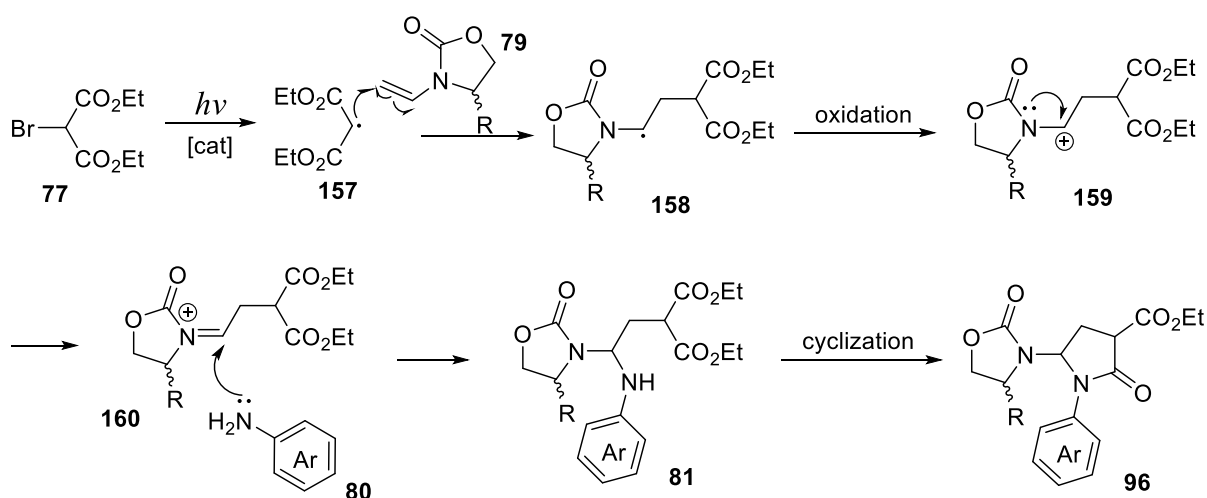
These γ-lactams have become sought after heterocycles and are ubiquitous molecular scaffolds in biologically-active natural products, including polyketides, alkaloids, steroids, and terpenes. Due to their occurrence in many biologically active compounds such as the acetogenins, lignans, and macrolides therefore they represent important synthetic targets.

In the proposed compound, there are nitrogen heterocycle, *N,N'*-aminal motif, γ-lactam moiety that are part of vitamins, and an aryl group. Levetiracetam, for example, an anticonvulsant drug used in the treatment of epileptic seizures contains pyrrolidinone moiety. Glimepiride is an antidiabetic sulfonylurea drug that increases insulin production in the pancreas and the activity of intracellular insulin receptors also contains some of the functional groups in the proposed molecule. Reutericyclin is a product of *Lactobacillus reuteri* bacteria that shows promising antibacterial activity against Grampositive strains, including *Clostridium difficile*, and is believed to have potential therapeutic value.[78] Another example is linezolid. Linezolid, an oxazolidinone antibacterial, is active against

Gram-positive bacteria including meticillin-resistant *Staphylococcus aureus* (MRSA), and glycopeptide-resistant enterococci.[79]   Linezolid is used for serious infections which are difficult to treat with other antibiotics. It is used to treat pneumonia, which is a serious lung infection. It is also used to treat skin and soft tissue infections caused by infection with MRSA bacteria. [79]
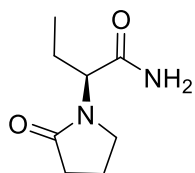
levetiracetam
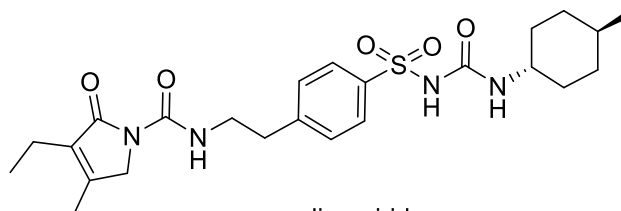
glimepiride
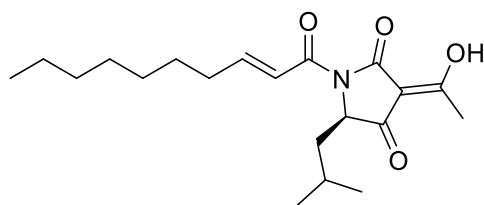
reutericyclin
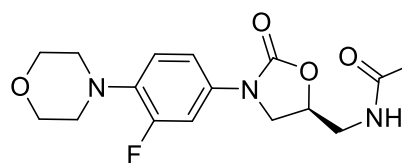
linezolid

As stated above, we aimed to establish a novel atom-efficient and general photoredox catalyst mediated β-alkylation of enamide utilising a one pot-component reaction. Then formation of a general route of arylamination at the α-position and its subsequent cyclization, thus forming a new nitrogen containing heterocycle into the molecule without the use of metal assisted cyclization reactions.

Therefore, our retrosynthetic route meant that we should first prepare the enamides **79** for the synthesis. Other components of the adducts are commercially available: the arylamines **80** and diethyl bromomalonate **77** (**Scheme 52**).

Scheme 52: Retrosynthetic scheme for the target molecule (**96**)
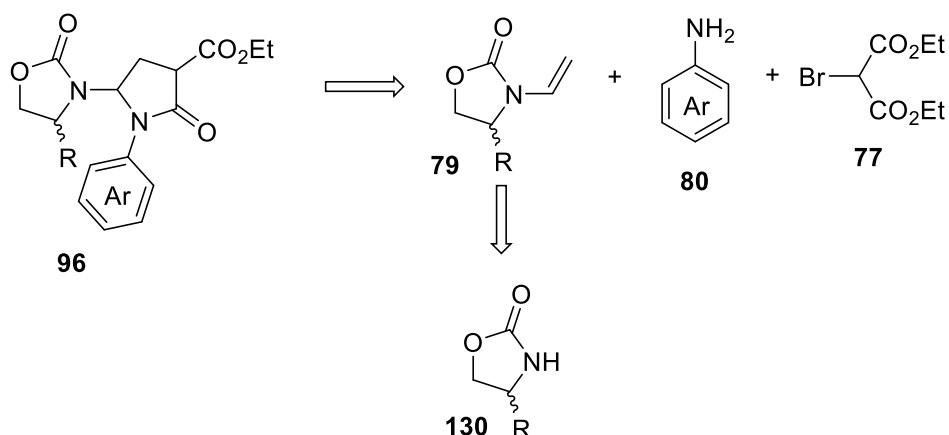
The initial reactions were to synthesize the enamides in sufficient quantities adopting the standard methods reported in the literatures by Gaulon *et al.*[67] and Liu.[80]

3.4.1 Enamides Synthesis

*Synthesis of N-Vinyl-2-oxazolidinone (**117**)*

In the preparation of the enamides, there are many options in the literature such as the use of palladium (II) catalysed reaction,[63] copper (I) catalysed reaction[81,82] and many other metal catalysed reactions. We opted for the procedure reported by Gaulon *et al.*[67] for its simplicity and high yield. The reaction was a two-step procedure based on the dehydroalkoxylation of the intermediate *hemi*-aminal obtained in the first step using trimethylsilyl trifluoromethanesulfonate (TMSOTf) and triethylamine (TEA). The first step as stated was the preparation of the *N,O*-acetal (or *hemi*-aminal) **161** (**Scheme 53**) that would be the starting material in the second and final step.

The desired product was obtained by the reaction of oxazolidin-2-one (**114**) and acetaldehyde diethyl acetal (acetal) in the presence of catalytic amount of DL-camphorsulfonic acid (CSA), with the acetal serving as both the reagent and solvent. It will be observed from Table 1 below that the optimum conditions for the reaction to obtain the highest yield was at temperature 55 °C with 7.0 mol% of CSA for a minimum of 18 h (98%, Table 1, entry 5), an increase in the amount of CSA to 10.0 mol% did not lead to any significant change in the yield (Table 1, entry 7). Getting the highest yield at 7.0 mol% was not in agreement with the 5.0 mol% reported in the literature (Table 1, entry 4 versus 5). When the reaction was carried

out at room temperature for 8 h, no product was obtained Table 1, (entry 1). We observed that the longer the reaction time the higher the yield until the maximum of 98% was obtained even when the reaction was run for 24 h which gave a comparable yield as at 18 h (Table 1, entry 5 versus 8). When the reaction was run in the absence of CSA, no product was formed the reactants were recovered; additionally, the TLC showed no significant change (Table 1, entry 9). One important observation was the huge reduction in the yield when the temperature was raised to 80 °C (34%, Table 1, entry 11).

Scheme 53: Preparation of *N-O*-acetal
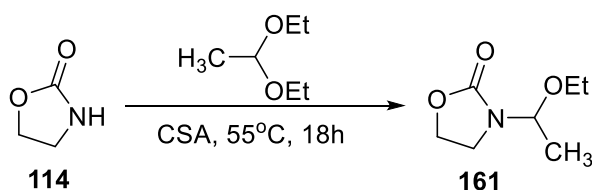
Table 1: Preparation of *N,O*-Acetal (**161**) Intermediate

Entry	Temp. [°C]	Time [h]	CSA (mol%)	Yield [%]
1	r.t.	8	5.0	0
2	55	5	5.0	18
3	55	8	5.0	46
4	55	18	5.0	86
5	55	18	7.0	98
6	55	18	1.0	32
7	55	18	10.0	92
8	55	24	7.0	97
9	55	16	--	0
10	80	6	7.0	10
11	80	16	5.0	34

The crude product was obtained as a colourless liquid and used without further purification for the second step of the reaction as indicated in the literature. The product was characterized and confirmed to contain the desired *N-O*-acetal (**161**) by the ^{1}H-NMR spectroscopy. The hydrogen atom near the nitrogen atom appeared at δ 5.12 ppm as a quartet

due to the coupling effect of the nearby methyl group hydrogen atoms which appeared at δ 1.26 ppm.

The mechanism of this reaction begins with the protonation of the oxygen of the ethoxy groups of the acetal **162**, thus making the carbon bearing the two oxygen atoms more electrophilic. The lone pair on the second oxygen now eliminates ethanol, as a leaving group, forming the intermediate oxonium ion **163**. Then the nucleophile, oxazolidin-2-one **114**, *via* its nitrogen lone pair, attacks the oxonium forming the *N*-acyl iminium ion **164**. This ion then loses a proton to the conjugate base of the acid CSA thereby completing the catalytic cycle of the acid CSA and the product **161** is formed (**Scheme 54**).

Scheme 54: Proposed mechanism for the formantion of the *N-O*-acetal (**161**)
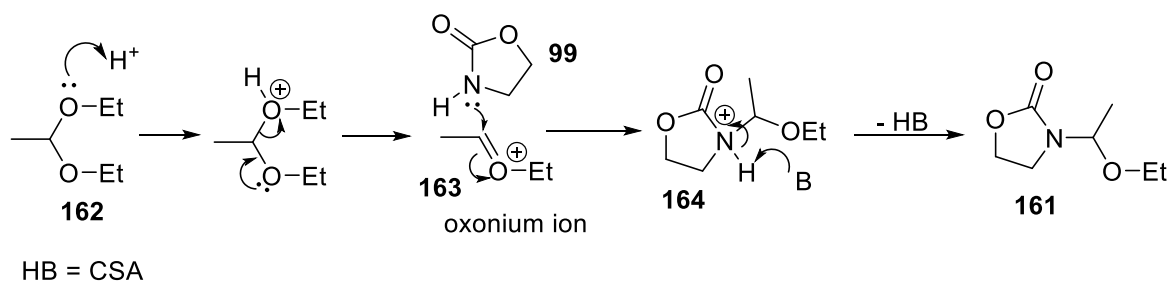
The second step in the synthesis of the enamide **117**, involves the use of the crude product obtained from the first step without its purification (**Scheme 55**). However, efforts were made to remove the solvent as much as possible from the reaction mixture. It was observed that if this solvent was still present in the reaction mixture in a substantial quantity, the final yield of the product would be significantly affected, and the reaction would not go into completion. The solvent, acetaldehyde diethyl acetal, will compete with the product in the reaction with trimethylsilyl triflate (trimethylsilyl trifluoromethanesulfonate, TMSOTf).

Initial attempts resulted in very low yields as a result of the residual solvent in the reaction mixture. The desired enamide **117** was eventually obtained as a pale yellow oily liquid. The optimum overall yield obtained was 76% with reaction time of 18 h. When the reaction was run at room temperature for 4 h, TLC did not indicate any change in the reaction mixture, no new spots were found on the plate (Table 2, entry 1). An increase in the reaction time to 16 h at room temperature gave only traces of the product (Table 2, entry 2) as indicated by the ^{1}H-NMR. The reaction proceeded to a relatively high yield at temperature of a mixture of ice and water (0 ºC) to 35% when run for 18 h (Table 2, entry 4). The best result were obtained

at temperature below -10 ℃ when the reaction flask was placed in a pot containing some dry ice and allowed to rise to room temperature gradually after the addition of all the reagents

Scheme 55: Synthesis of *N*-ethenyl-2-oxazolidinone (an enamide)
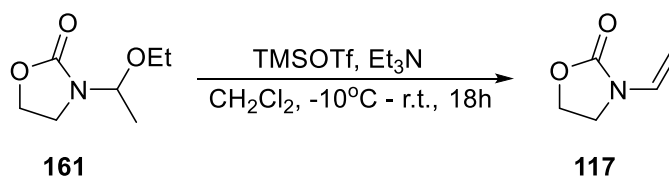
In addition to the temperature control and reaction time conditions, the status of the reagents used also affected the yield. The reaction performs well when the triethylamine (TEA) is distilled, fresh and importantly dry. We observed that trimethylsilyl trifluoromethanesulfonate (TMSOTf) has to be added in a dropwise manner to ensure that the reaction temperature remained low giving reproducible yields. Likewise, the rate at which the reaction temperature is brought to room temperature after the addition of TMSOTf affected the yield (Table 2, entry 7).

Table 2: Final Step Reaction Conditions for the Preparation of Enamide (**117**)

Entry	Temp. (℃)	Reaction Time [h]	Yield [%]
1	r.t.	4	0
2	r.t.	16	5
3	0	8	5
4	0	18	35
5	< -10	8	28
6	< -10	18	76
7[a]	< -10	18	44

[a] the temperature quickly brought to room temperature

After the completion of the reaction, the reaction was worked-up to remove the excess TMSOTf and the ammonium triflate salts by first treating the mixture with basic alumina followed by filtration through a pad of silica gel. Further purification was done by flash chromatography to afford the product. The purified liquid was characterized and confirmed

as the desired enamide by ^{1}H-NMR and ^{13}C-NMR analysis supported by IR and MS analysis. The ^{1}H-NMR resonance (signals) at δ 6.84, 4.40 and 4.27 ppm, respectively, confirmed the formation and presence of the terminal **-CH=CH$_2$** alkenyl group with the two germinal protons showing at δ 4.40 and 4.27 ppm, respectively. The proton on the carbon bonded to the nitrogen atom resonates at δ 6.84 ppm.

This reaction is believed to start with the attack on the lone pair on the oxygen of the ethoxide group by the electrophilic end of TMSOTf (the TMS) forming the TMS-oxonium ion **165.** This ion now eliminates TMS-OEt, as a leaving group, giving way to the formation of oxazolidinium ion **166**. Triflate ion or triethyl amine (TEA) then abstracts a proton from the oxazolidinium ion **166** to afford the product *N*-vinyl-2-oxazolidinone **117** (**Scheme 56**).

Scheme 56: Schematic representation of the mechanism of transformation of *N,O*-acetal to vinyl group.
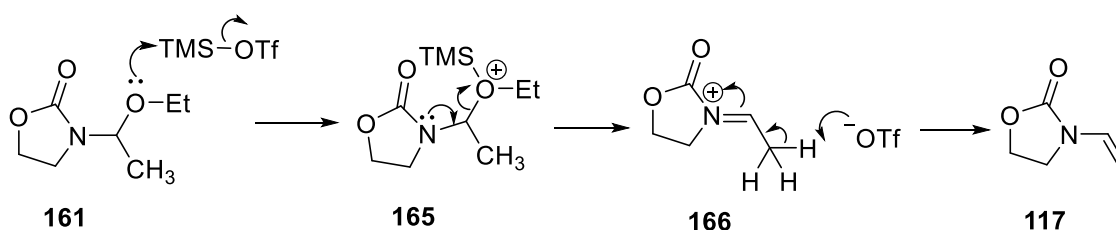
*Synthesis of (S)-4-benzyl-N-vinyl-2-oxazolidinone (**169**)*

Compound **169** is the chiral derivative of compound **117**. Its synthesis is very similar to the achiral derivative. The same method was used but with a little modification or variations in the reaction conditions. The reaction was also a two-step procedure based on the dehydroalkoxylation of the intermediate *hemi*-aminal as obtained in the achiral derivative. The first step was the preparation of the *hemi*-aminal, the reaction of (*S*)-4-benzyl-2-oxazolidinone **167** with acetaldehyde diethyl acetal in the presence of DL-camphorsulfonic acid (**Scheme 57**).

The desired product was obtained by the reaction of the reactants (*S*)-4-benzyloxazolidin-2-one (**167**) and acetaladehyde diethyl acetal (acetal) **162** in the presence of catalytic amount of DL-camphorsulfonic acid (CSA). The acetal **162** served as both reagent and solvent. From Table 3 it shows that the optimum conditions for the reaction was at temperature 55 °C with 7.0 mol% of CSA and 3 h reaction time (100%, Table 3, entry 3), an increase in the amount of CSA to 10.0 mol% has no significant effect on the yield (99% Table 3, entry 6). When the

reaction was carried out at room temperature for 20 h, no product was formed (Table 3, entry 1). In this case longer reaction time had great negative effect on the yield (56%, Table 3, entry 4). When the reaction was run in the absence of CSA, no product was formed the reactants were recovered and the TLC showed no discernable change (Table 3, entry 7). A higher temperature above 55 °C did not lead to an increase in the yield (60%, Table 3, entry 8).

Scheme 57: Preparation of Chiral Enamide Intermediate
(*N-O*-Hemi-aminal)
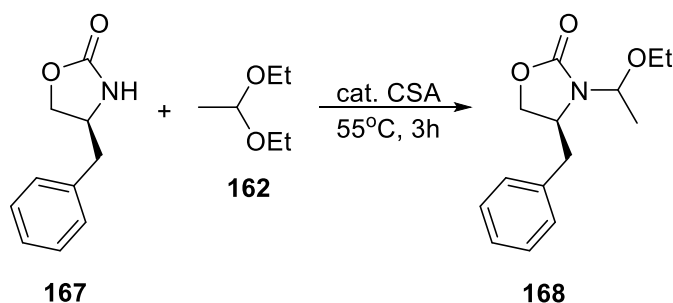
Table 3: Preparation of *N,O*-Acetal of the chiral Intermediate

Entry	Temp. [ºC]	Time [h]	CSA (mol%)	Yield [%]
1	r.t.	20	7.0	0
2	40	20	7.0	5
3	55	3	7.0	100
4	55	18	7.0	56
5	55	3	2.0	32
6	55	3	10.0	99
7	55	16	--	0
8	80	4	7.0	60
9	80	16	5.0	36

The crude product was obtained as a colourless liquid and used without further purification in the second step of the reaction (**Scheme 58**). The ^{1}H-NMR of the crude revealed the presence of the proton N-**CH**- at δ 5.32 ppm (q, *J* = 6.2 Hz, 1H), which coupled with **CH₃** at δ 1.52 ppm (d, *J* = 6.2 Hz, 3H) confirming the formation the *N,O*-acetal **168**.

The second step in the synthesis of compound **169**, the chiral enamide involves the conversion of **168** by reacting it with TMSOTf in the presence of TEA in dry DCM. The reaction conditions are similar to the transformation of **161** to **117.** The chiral enamide **169** was obtained as a white semi-solid. The optimum over all yield obtained was 72% with reaction time of 18 h. The reaction gave good result when run in inert atmosphere of nitrogen. Addition of dry TEA and TMSOTf was done in drop-wise manner and in that order at temperature -10 °C. After the addition of the reagents, the reaction mixture temperature was allowed to rise to room temperature gradually by itself. The ^{1}H-NMR analysis confirmed the formation of the product with the presence of the terminal -**CH=CH$_2$** group. The proton on the carbon bonded to the nitrogen atom appeared at δ 6.80 ppm while the two germinal protons of the methylene group showing at δ 4.57 and 4.54 ppm respectively.

Scheme 58: Preparation of chiral enamide from the intermediate
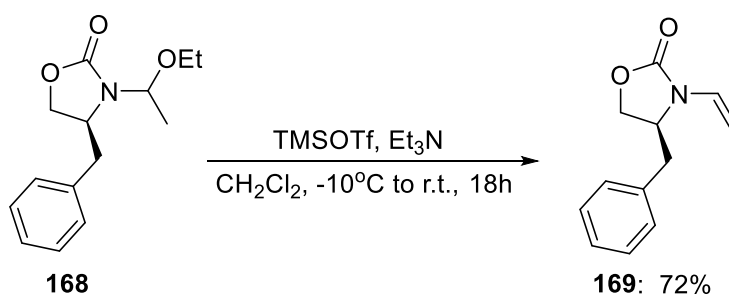
*Synthesis of (E)-3-(hex-1-en-1-yl)oxazolidin-2-one (**171**)*

A different synthetic route was used for the preparation of (*E*)-3-(hex-1-en-1-yl)-oxazolidin-2-one as the Gaulon's method could not be used. The synthetic route used as reported by Liu and Floreancig[80] offers a good avenue for the synthesis of enamides with substituent on the alkene group. It involves the condensation of aldehydes (hexanal in this case) with the carbamate, oxazolidin-2-one **114** to give enamide with the release of a water molecule (**Scheme 59**). This reaction occurs in the presence of an acid catalyst and it is reversible. To drive the reaction towards the product formation, the water molecule has to be removed from the reaction mixture. This was achieved with the use of a Dean-Stark trap apparatus and the enamide was obtained as pale yellow oily liquid.

Scheme 59: Synthesis of (*E*)-3-(hex-1-en-1-yl)oxazolidin-2-one
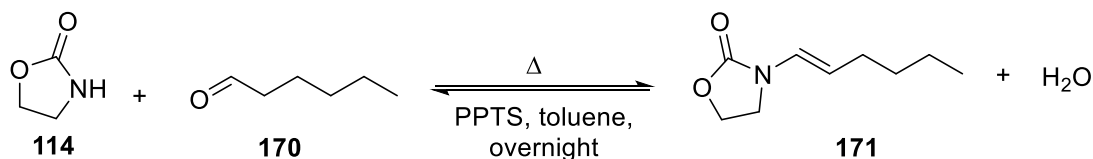
The formation of the product was confirmed from the ^{1}H NMR spectrum obtained, the terminal methyl -**CH₃** group hydrogen atoms on the hexyl moiety appeared at δ 0.83 ppm in triplet as a result of their coupling with the nearby –CH₂-. The hydrogen atom on the C=C bond next to the nitrogen atom in the ring -N-C**H**=C appeared at δ 6.56 ppm as doublet due to the coupling effect of the nearby hydrogen atom on the second *sp²* carbon which appeared at 4.81 – 4.70 ppm as multiplet, the coupling constant (*J* = 14.4 Hz) of this proton showed that it is trans to the coupled hydrogen, and the two –**CH₂**- groups of the ring were seen at δ 4.36 and 3.63 ppm as triplets, respectively. These were in agreement with literature reports.

The mechanism of the formation of the substituted enamide starts with the nucleophilic attack of the oxazolidin-2-one (**114**) on the aldehyde hexanal (**170**) with the lone pair of the nitrogen atom, on the electrophilic carbonyl carbon forming the intermediate ion **172**. The intermediate ion then rearranges *via* a proton transfer from the nitrogen atom to the oxygen atom to form 3-(1-hydroxyhexyl)-oxazolidin-2-one **173**. This is then protonated through the -OH group leading to the expulsion or removal of water and *N*-acyl iminium ion **174** formation. The deprotonation of the iminium ion by the conjugate base of the acid completes the catalytic cycle of the acid and the product, (*E*)-3-(hex-1-en-1-yl)-oxazolidin-2-one **171**, is obtained (**Scheme 60**).

Scheme 60: Mechanism of the aldehyde-carbamate condensation
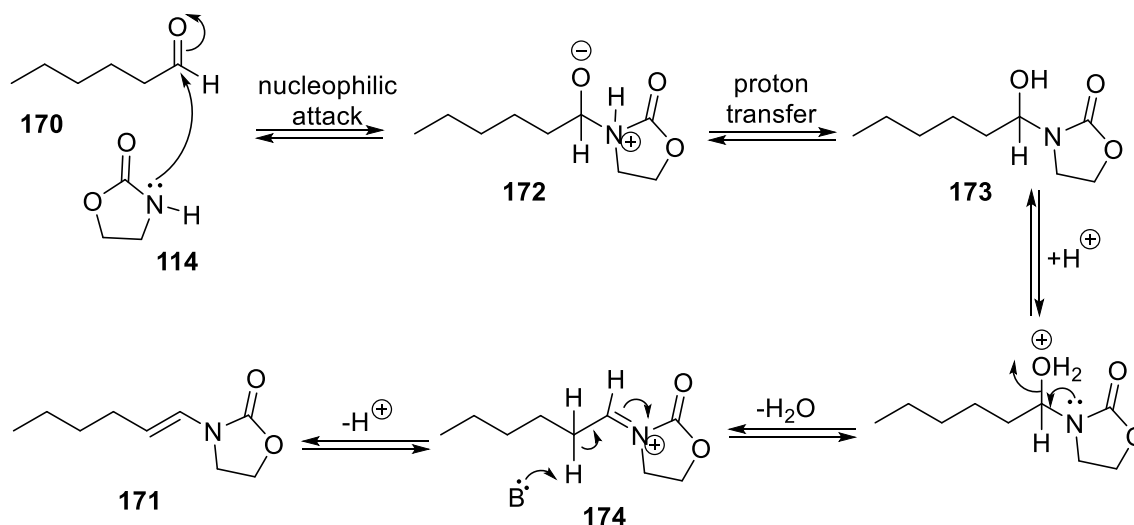
3.4.2 Enamides: Photoredox Catalytic Transformation Reactions

Carbon-carbon bond formation is the core of organic synthesis. Many organic synthetic methodologies to achieve this are based on the ease of generation of radicals. Generation of a radical is achieved traditionally by heating, irradiation by high-energy UV-light or a redox reaction.[5,6] These conventional methods are sometimes harmful and some are explosive as a result of uncontrollable rate of chain reactions that occur. In addition, the traditional methods often have a poor atom economy. During the process, considerable amounts of waste are generated which may cause environmental problems. In order to alleviate some of the problems mentioned above with the traditional methods of radical generation in organic synthesis, the use of a catalyst rather than a stoichiometric reagent is preferable. However, most of the catalysts used often are labile compounds, they react too fast, and require that carefully controlled conditions are used (e.g., with regard to the exclusion of air, moisture, impurities). In many cases co-catalysts and additives are also required.

Considering the environmental factor, the atom economy and energy requirement, new methods for the formation of the C-C bond have to be developed. These methods/protocols, according to the principles of "Green Chemistry", need to be easy and safe to use and are expected to be efficient (both in terms of energy and atoms) and selective in their outcomes.[6]

Nature's ability to use various visible light absorbing chromophores/photocatalysts for converting solar energy to chemical energy is a great option. The challenge to mimic and

understand enzymatic transformations, organocatalysis has now become an important tool in modern organic synthesis with new reactivity that complements that of enzyme and metal catalysis.[4,5,7]

Photochemical transformations/reactions, using photocatalysts, generally require mild conditions for substrate activation—ideally light alone—and are suitable for "green reactions".[4] This, therefore, is employed as a strategy especially with the recent development of photocatalysis that made (transition) metal polypyridyl complexes and organic dyes readily accessible to facilitate the conversion of visible light into chemical energy under exceptionally mild conditions.[15-17]

Literature reports have shown that small amounts of transition-metal polypyridyl complexes could be used as photoredox catalysts to accelerate photochemical transformations of compounds that ordinarily would not have undergone reactions under mild conditions. These complexes upon irradiation with visible light are excited and are involve in single electron transfer with some compounds thus making them strong oxidizing or reducing agents. Studies made by Courant and Masson[53] have demonstrated that iridium polypyridyl complexes could be used as photoredox catalyst to initiate three-component domino synthesis of *N*-carbamoyl α-alkylated imines under mild conditions.

In their previous work, Masson and co-workers[83] established that radical photoredox mediated addition of a -CF$_3$ equivalent, using the trifluoromethylating reagent **176**, to electron-rich styrene **113** derivatives followed by trapping of the intermediate carbocation by an electron-poor arylamine could lead to modest to good yields of the addition product of the type **175** (**Scheme 61**). In that report, they explored the use of easily oxidizable anilines such as *p*-anisidine where poor or little conversion to the desired products was observed.

Scheme 61: Masson's radical addition/cationic amination of styrene
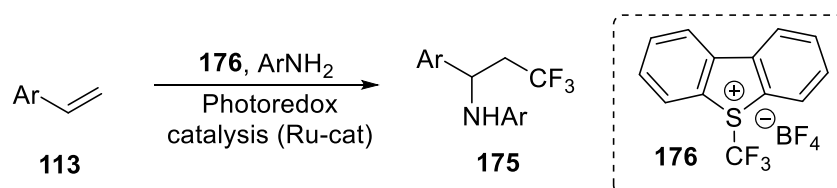
With this in mind, we therefore set to explore this area of radical/cationic pathway using iridium 2-phenylpyridine 4,4'-di-tert-butyl-2,2'-bipyridine complex [Ir(ppy)$_2$(dtbbpy)]PF$_6$ as

a photoredox catalyst starting with our enamides in the presence of arylamines, especially electron-rich arylamines to access *N,N'*-aminals. The *N,N'*-aminal structural motif is prevalent within a wide range of biologically important compounds.[84]

The initial experiment was focused on replicating the work of Courant and Masson[53] (**Scheme 62** and **Table 5**) on our prepared enamide, *N*-vinyl-2-oxazolidinone **117** using a strip of LED blue light instead of fluorescent light. We were able to get the desired three-component adduct after running the reaction for 16 hours, though the yield was very low at the first attempt. The reaction mixture was very difficult to purify because of the low yield of the product. The product **177** was confirmed by comparison of the its ^{1}H NMR with that previously reported by Masson.[53] A change of the lamp from the blue LED strip light to the Kessil® LED blue light (λ = 465 nm) gave the desired result as against low yield obtained from the former (12% Table 5, entry 1 vs 3). Then different reaction conditions: reaction time, bases and solvents were screened. To our delight the reaction proceeded in the two screened solvents: acetonitrile and dichloromethane. Higher yields were obtained in dry forms of both solvents than in bench stock solvent. However, higher yield was obtained in acetonitrile than in dichloromethane (42%, Table 5, entry 4 versus 8). The change in the nature of base from triethylamine to disodium hydrogenphosphate (Na_2HPO_4) greatly lowered the yield to nearly nothing (Table 5, entry 4). A reduced reaction time less than 6 h did not give reasonable yield, even in acetonitrile (Table 5, entry 6). The highest yield was obtained in about 15 h and it was in dry acetonitrile (Table 5, entry 8). Increase in the amount of the catalyst, [Ir(ppy)$_2$(dtbbpy)]PF$_6$ from 1.5 mol% to 2.0 mol% had no significant effect on the yield (Table 5, entry 10). The reaction was found not to occur in the dark (Table 5, entry 12), similarly it did not proceed without the photoredox catalyst (Table 5, entry 11). The presence of the base, triethylamine was essential as no reaction was recorded without it. (Table 5, entry 13).

Scheme 62: Photoredox of enamide (**117**) with ethanol

117

CHBr(CO$_2$Et)$_2$, EtOH

[Ir(ppy)$_2$(dtbbpy)]PF$_6$, Et$_3$N
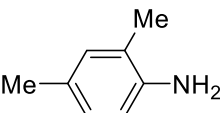
CH$_2$Cl$_2$, rt, blue light

177: 42%
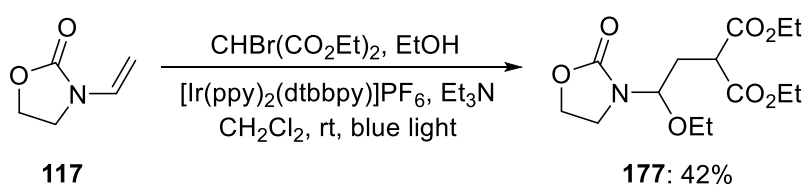
Table 5: Screening for the optimum conditions for photoredox reaction of *N*-Vinyl-2-oxazolindinone and ethanol.

Entry	Amount of Ir-Cat [mol%]	Light	Solvent	Base	Time [h]	Yield [%]
1	1.5	LED strip	CH_2Cl_2	Et_3N	6	2
2	1.5	LED strip	CH_2Cl_2	Et_3N	16	10
3	1.5	Kessil	CH_2Cl_2	Et_3N	6	12
4	1.5	Kessil	CH_2Cl_2	Et_3N	18	30
5	1.5	Kessil	CH_2Cl_2	Na_2HPO_4	18	0
6	1.5	Kessil	CH_3CN	Et_3N	5	--
7	1.5	Kessil	CH_3CN	Et_3N	7	8
8	1.5	Kessil	CH_3CN	Et_3N	15	42
9	1.5	Kessil	CH_3CN	Na_2HPO_4	15	4
10	2.0	Kessil	CH_3CN	Et_3N	15	41
11	0.0	Kessil	CH_3CN	Et_3N	20	0
12	1.5	No light	CH_3CN	Et_3N	15	0
13	1.5	Kessil	CH_3CN	----	15	0
14	1.5	Kessil	CH_3CN	Et_3N	15	--

Each of the experiments was carried out at least two times and the highest isolated yield was recorded. In the case where no light was stated, the reaction vessel was wrapped with three layers of aluminium foil. In entry 14, the bench trimethylamine solvent was used instead of dried/anhydrous solvent. Finally, (--) means no signal of the product could be obtained from the ^{1}H-NMR of the small residue obtained after the removal of the solvent from the reaction mixture.

The formation of the desired product was confirmed by ^{1}H-NMR with the disappearance of the signals at δ 6.84 ppm, 4.40 ppm, 4.27 ppm of the hydrogen atoms of the alkenyl moiety **CH=CH₂** of the enamide **117**, new signal at δ 5.08 ppm of the hydrogen atom of the carbon bearing the nitrogen atom of the ring and oxygen atom of the ethoxy group, the *N,O*-acetal carbon emerged in their place. This hydrogen appeared as triplet due to its coupling effect

with the two neighbouring hydrogen atoms that appeared at δ 2.37-2.28 (m, 1H) and 2.20-2.11 (m, 1H) ppm, respectively.

Having identified the optimum reaction conditions and confirming that the reaction worked within our laboratory environment, we then extended the scope of the reaction to different arylamines as the nucleophiles with aniline as our starting compound. To our delight we got the desired three-component adduct. The identification of the product was done using a combination of ^{1}H-NMR and ^{13}C-NMR with key diagnostic signals for the hydrogen and carbon atoms of -**CH**- aminal moiety with the hydrogen atom seen at δ 5.37 ppm appearing as triplet due to the coupling effect of the neighbouring two hydrogen atoms and δ 62.61 ppm for the carbon atom. This hydrogen signal appeared upfield of the spectrum than that of the hydrogen atom on the *N,O*-acetal carbon as a result of the electron withdrawing effect of the benzene ring.

We began by screening for the optimum conditions for the reaction with aniline **178** (Table 6). We found out that reaction went into completion at a very shorter time than for ethanol (Table 6, entry 1 vs 4). The reaction time reduced from 18 h to 3 h (Table 6, entry 5) and the amount of the nucleophile, aniline also reduced from 10.0 equivalent to 5.0 equivalent (Table 6, entries 3 and 5), ultimately giving the product in a higher isolated yield of 72%. A reduction to 2.0 equivalent of aniline had a detrimental effect in the yield (Table 6, entry 6).

Scheme 63: Photoredox amination of enamide (**117**) with aniline
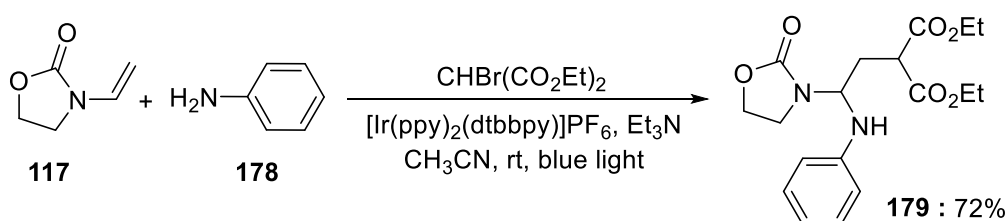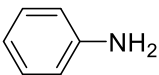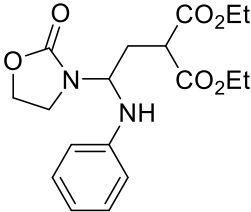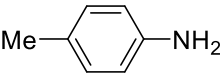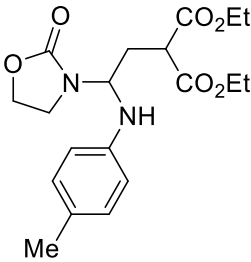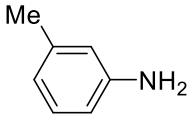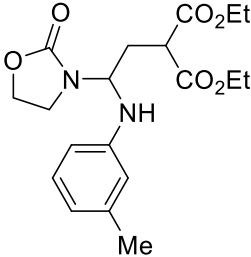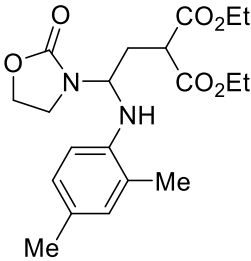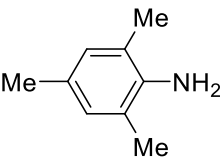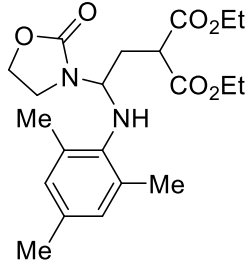
Table 6: Screening for the optimum condition for Photoredox Alkylation Enamide Using Aniline as the Nucleophile

Entry	Substrate	Time [h]	Amount [Equiv.]	Yield [%]
1	Ethanol	18	10.00	42
2	Aniline	18	10.00	56
3	Aniline	18	5.00	54

4	Aniline	6	5.00	61
5	Aniline	3	5.00	72
6	Aniline	3	2.00	38

Having established the optimum conditions for the reaction with aniline for the synthesis of **179**, the reaction was then extended to a range of arylamines to ascertain the substrate scope of the reaction. The results are as shown in Table 7. We started with *p*-toluidine which delivered the product **181** in a significantly higher yield (84%) than aniline, possibly due to its increased nucleophilicity; additionally, we were able to obtain suitable crystals for single crystal X-ray analysis. *m*-Toluidine also reacted giving **183** in 88% isolated yield. The 2,3- and 2,6-dimethylaniline gave **185** and **189** in 71% and 60% yields, respectively; furthermore, the sterically encumbered 2,4,6-trimethylaniline gave **187** in 64%. *o*-Anisidine furnished *N,N'*-aminal **203** in 76% yield, although, it was found that this product slowly degraded upon standing to give the imine, possibly due to the electron-rich nature of the aniline. However, we were able to obtain crystals of **203**, suitable for single-crystal X-ray analysis, which definitely assigned the structure as shown. The *o*-trifluoromethoxy (2-OCF$_3$) analogue **205** could also be obtained in 77% isolated yield, and this product **205** also demonstrated increased stability compared to **203**. The reaction accommodated electron withdrawing groups, highlighted by 3-trifluoromethylaniline and 3,5-bistrifluoromethyl aniline giving derivatives **191** and **193** in 62% and 61% yields, respectively. Anilines with halogen substitutions such as 3,4-dichloro, 4-bromo, 2-fluoro and 4-bromo-2-fluoro all performed well in this reaction with 58%, 70%, 75% and 79% isolated yield respectively, with the 4-bromoaniline and 2-fluoroaniline generating products with suitable crystals for single-crystal X-ray analysis. 3-(Ethoxycarbonyl)aniline also gave the desired adduct *N,N'*-aminal **207** in 70% isolated yield. *N*-alkyl substituted arylamines were also tolerated within the reaction conditions with no observed oxidation of the alkyl groups. *N*-Methylaniline gave the desired adduct **209** in 61% without oxidation of the methyl group; and finally, diphenylamine gave **211** in 56% isolated yield illustrating that sterically encumbered anilines were also tolerated. The ORTEP structures for **181**, **195**, **197**, **203** and **209** are shown in **Figure 10**.

Table 7: Results of the photoredox reactions of enamide **117** with different arylamines

Entry	Arylamine	Product	Yield (%)
1	**178**	**179**	72
2	**180**	**181**	84
3	**182**	**183**	88
4	**184**	**185**	71
5	**186**	**187**	64

#	Amine	Product	Yield
6	**188**	**189**	60
7	**190**	**191**	62
8	**192**	**193**	61
9	**194**	**195**	70
10	**196**	**197**	75
11	**198**	**199**	79
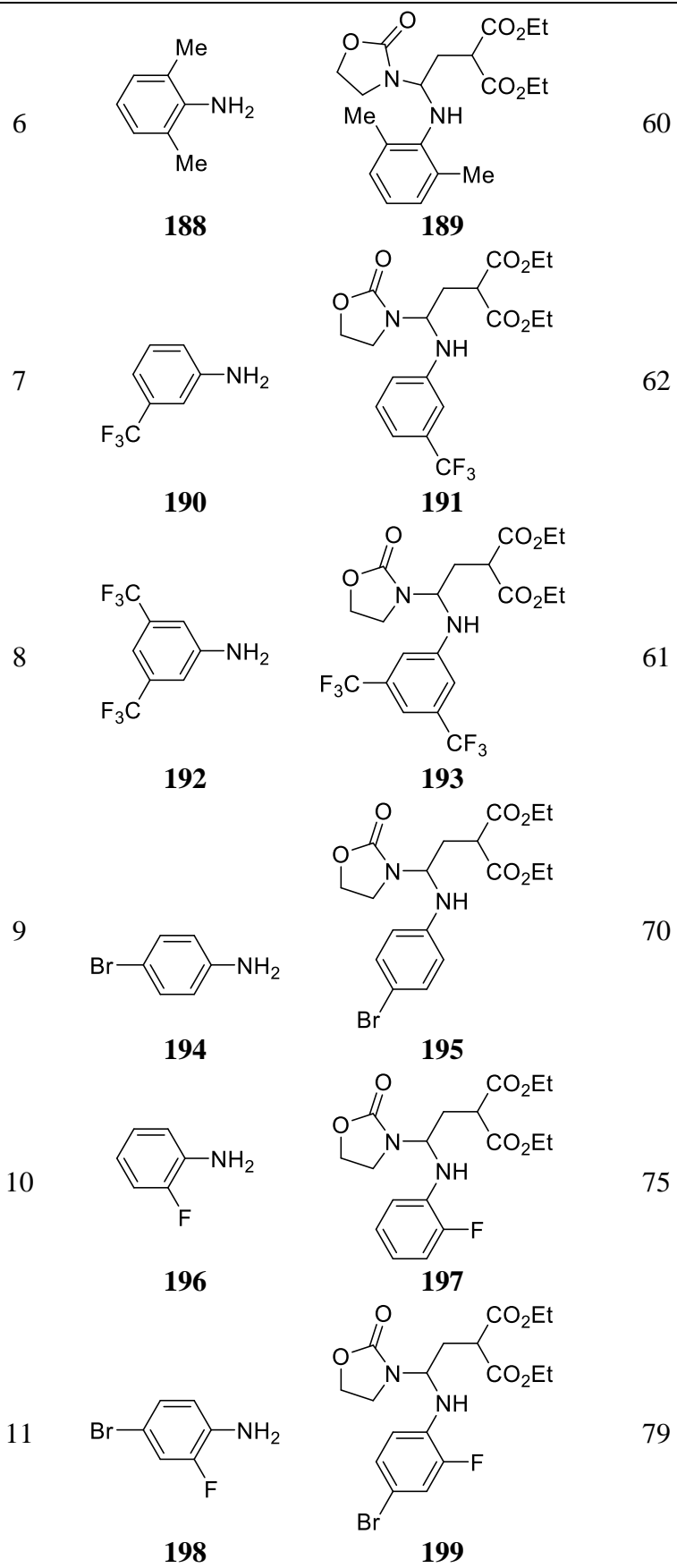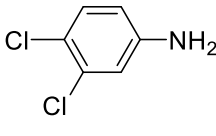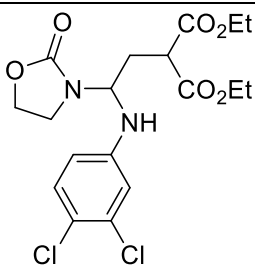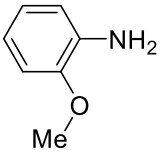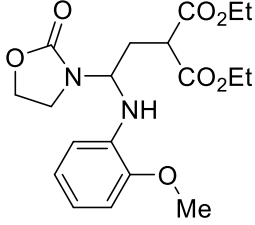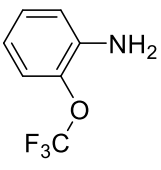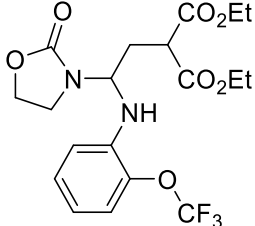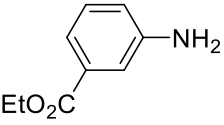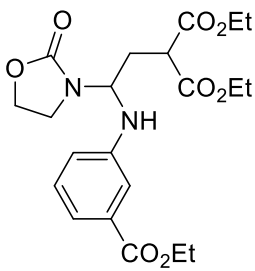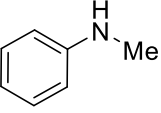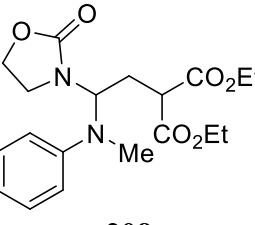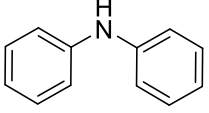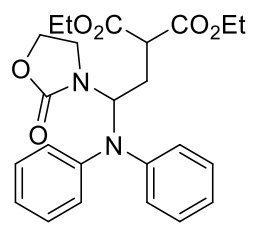
12	**200**	**201**	58
13	**202**	**203**	76
14	**204**	**205**	77
15	**206**	**207**	70
16	**208**	**209**	61
17	**210**	**211**	56

Figure 10: The structures of the compounds as shown by X-ray diffraction analysis

181

195

197

203

209
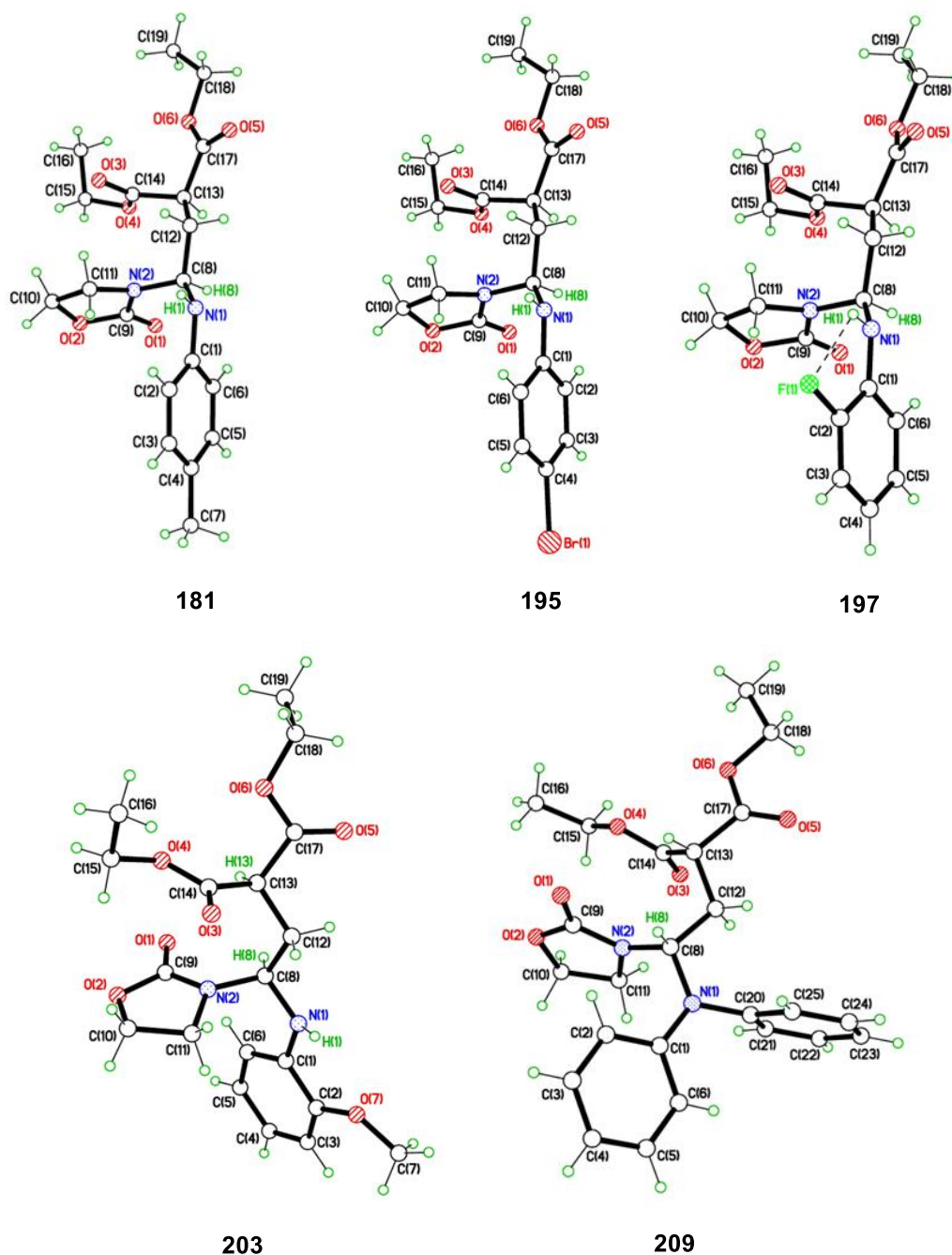
However, the reaction did not give the required result with *p*-methoxy-aniline (*p*-anisidine) **212**, whereas with *o*-anisidine **202** a yield of 76% was obtained. The *p*-anisidine reacts with the diethyl 2-bromomalonate rather than giving the desired three-component adduct **213**. The enamide was recovered unreacted (**Scheme 64**). This may be as a result of the electron donating property of the methoxy group on the ring that increases the electron density on the nitrogen atom. The lone pair on the nitrogen atom of the amino group are now much more readily available for nucleophilic attack in the *p*-anisidine than in *o*-anisidine due to the

relative steric hindrance of the methoxy group at the ortho position (the ortho effect). Diethyl 2-((4-methoxyphenyl)amino)malonate **214** was formed instead of diethyl 2-(2-((4-methoxyphenyl)amino)-2-(2-oxooxazolidin-3-yl)ethyl)malonate (**Scheme 64**).

Scheme 64: Photoredox amination of enamide (**117**) with *p*-anisidine (**212**)
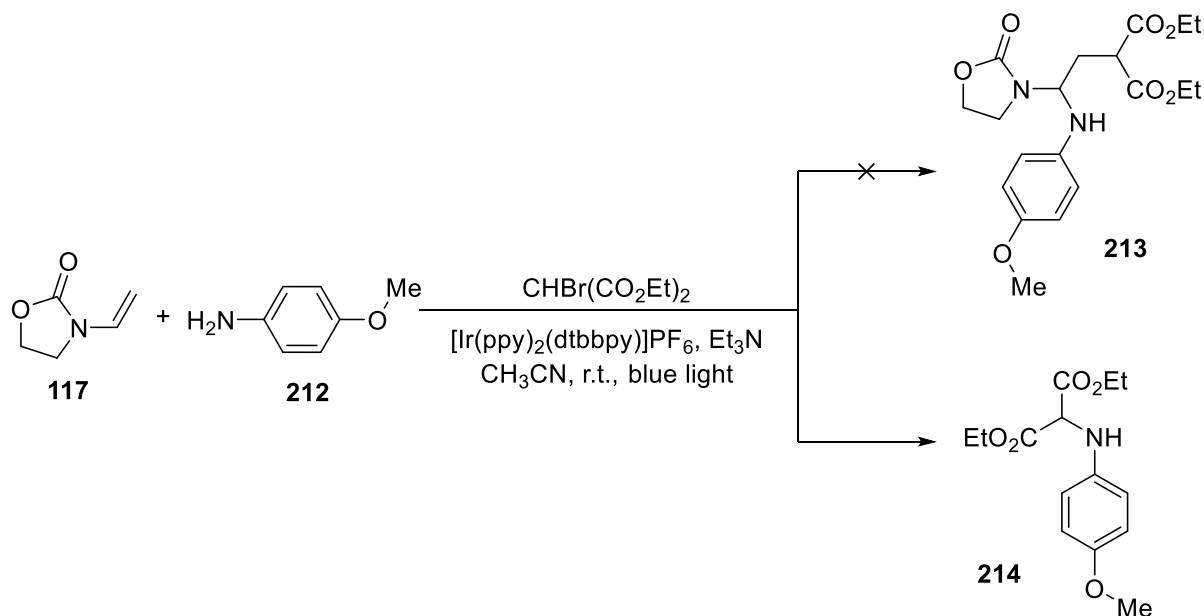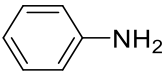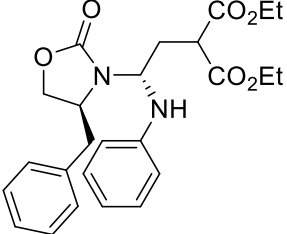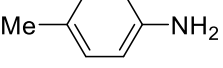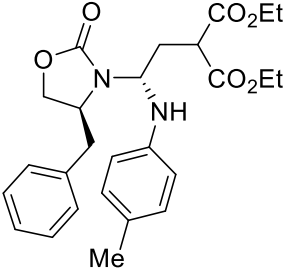
To investigate the diastereoselectivity of this transformation reaction, chiral enamide (**169**) and double bond substituted enamide (**171**) were then exposed to the reaction conditions and chiral bromide akylating agents were also employed. The chiral enamide, (*S*)-4-benzyl-3-vinyloxazolidin-2-one **169** reactions are shown in **Scheme 65** while those of the substituted enamide, (*E*)-3-(hex-1-en-1-yl)oxazolidin-2-one **171** and chiral bromide alkylating agent (1-bromoethyl)benzene **225** are shown in **Scheme 66**.
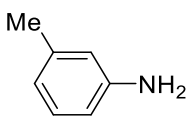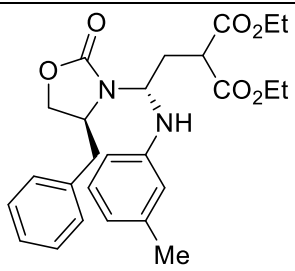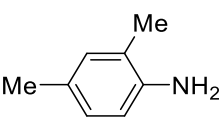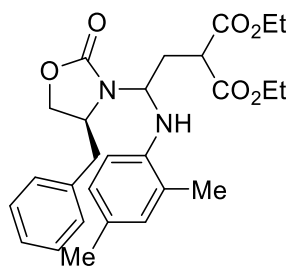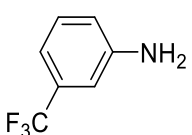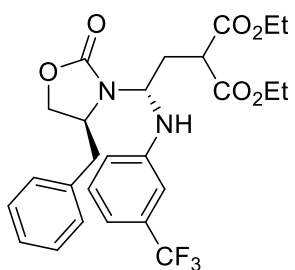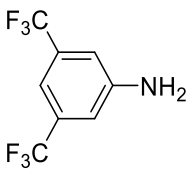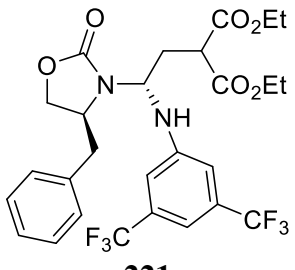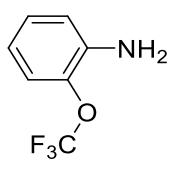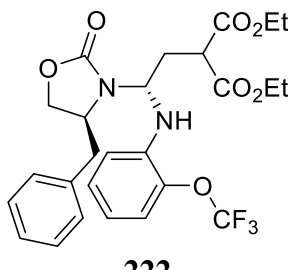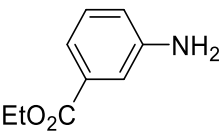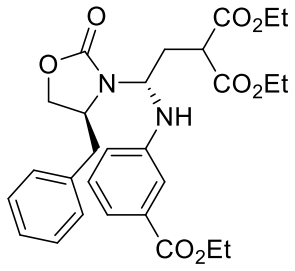
Scheme 65: Chiral enamide scope on the photoredox reaction

The reaction of (S)-4-benzyl-3-vinyloxazolidin-2-one **169** with aniline delivered the product **216** as a 52:48 mixture of diastereoisomers in overall yield of 56%. The diastereoisomers ratio was determined by the ^{1}H NMR using the chemical shift δ of the two hydrogen atoms of the bridging methylene between the aminal carbon and the carbon with the two carbonyl groups of the malonate moiety. The δ of these bridging methylene hydrogen atoms for the two diastereoisomers do not overlap. The ratio of the integration of their signals corresponds to the diastereoisomer ratio of the mixtures. Similar techniques and integrations were used to obtain the diastereoisomeric ratio of other adducts. *p*-Toluidine reacted to give the adduct **217** with the isolated yield of 58%, while *m*-toluidine and 2,4-dimethylaniline gave the products **218** and **219** in good isolated yields of 61% and 53% in that order with appreciably improved levels of diastereoselectivity. *p*-Toluidine gave product as a 87:13 mixture of diastereoisomers, *m*-toluidine gave 70:30 ratio and 2,4-dimethylaniline gave 50:50, respectively. A high level of diastereoselectivity was observed for electron withdrawing arylamine with 3-trifluoromethylaniline giving the product **220** as a mixture of 95:5 diastereoisomers with the total yield of 54% and 3,5-bistrifluoromethyaniline with product **221** isolated in 60% yield essentially as one single stereoisomer. *o*-(Trifluoromethoxy)aniline and ethyl 3-aminobenzoate gave the adducts **222** and **223** with isolated yields of 58% and 61% as mixtures of diastereoisomers of 75:25 and 55:45 ratios, respectively as shown by ^{1}H-NMR spectroscopy.

Table 8: Products of photoredox reaction of chiral enamide **155** with different arylamines

Entry	Arylamine	Product	Diastereomer Ratio (dr)	Yield (%)
1	**178**	**216**	52:48	69
2	**180**	**217**	87:13	58

Entry	Amine	Product	Ratio	Yield
3	**182**	**218**	70:30	61
4	**184**	**219**	50:50	53
5	**190**	**220**	95:5	54
6	**192**	**221**	95:5	60
7	**204**	**222**	75:25	58
8	**206**	**223**	55:45	61

Additionally, the double bond substituted enamide derived from hexanal, (*E*)-3-(hex-1-en-1-yl)oxazolidin-2-one **171** gave surprisingly good levels of diastereoselectivity in this reaction, giving **224** in 53% yield as a single stereoisomer as shown in **Scheme 66(a)**.

Further diastereoselectivity investigation with the use of chiral alkylating agents, (1-bromoethyl)benzene **225** and ethyl α-bromophenylacetate **228** were employed. The reaction was carried out with *p*-Toluidine **180** and enamide **117**. The chiral alkylating agent **225** gave the product **226** as a mixture of diastereoisomers in 50:50 ratio with the overall yield of 58% (**Scheme 66 (c)**) and **228** reacted, though at much longer time, to give the adduct **229** as a mixture of diastereoisomers in 50:50 dr with the overall isolated yield of 38% (**Scheme 66 (b)**). The product **227** obtained from the reaction of the sterically encumbered aniline, diphenylamine **210** was a mixture of diastereoisomers in 95:5 ratio with the overall yield of 53% (**Scheme 66(d)**).

In all of the additions described, the separation of the two diastereoisomers could not be undertaken, and the diastereoisomeric ratio most likely represents an equilibrium. One can then conclude from the observed diastereoselectivity that the stereoselectivity of the reaction is influenced by the nature of the substituents on the benzene ring of the aniline.

Scheme 66: Photoredox reactions of enamide **171** and enamide **117** with chiral alkaylating agents


(a) **171** → CHBr(CO₂Et)₂, *p*-toluidine / Ir-Cat (1.5 mol%), Et₃N / CH₃CN, r.t., blue light → **224**: 53% [95:5]

(b) **117** + **228** → Me—C₆H₄—NH₂ **180** / Ir-Cat (1.5 mol%), Et₃N / CH₃CN, r.t., blue light → **229**: 38% [50:50 mixture]

(c) **117** + **225** → Me—C₆H₄—NH₂ **180** / Ir-Cat (1.5 mol%), Et₃N / CH₃CN, r.t., blue light → **226**: 58% [50:50 mixture]

(d) **117** + **225** → Ph₂NH **210** / Ir-Cat (1.5 mol%), Et₃N / CH₃CN, r.t., blue light → **227**: 53% [95:5 mixture]
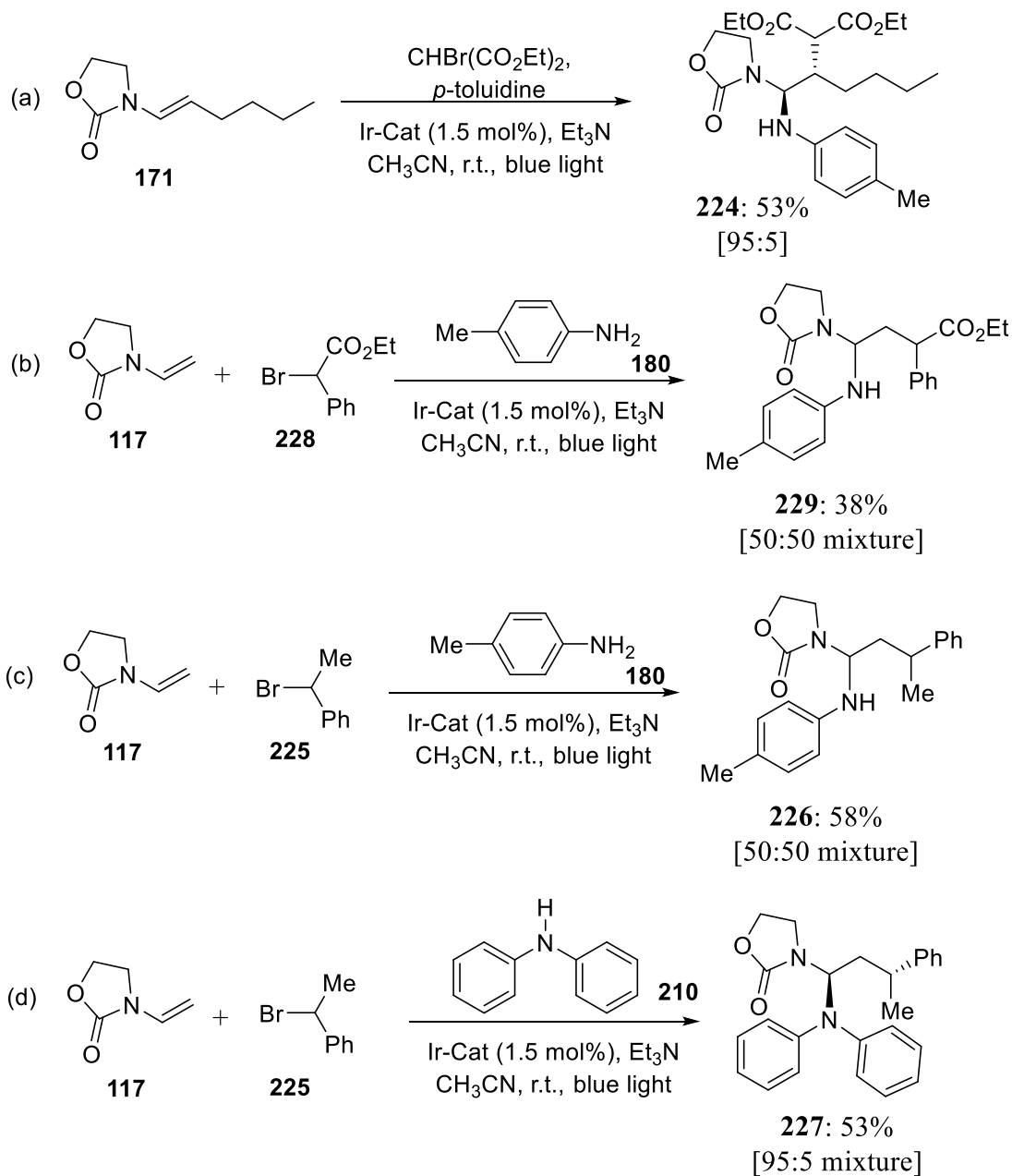
Proposed Mechanism of the Reaction

The proposed mechanism (**Scheme 67**) of the reaction starts with the absorption of photon by the photocatalyst Ir(ppy)$_2$(dtbbpy)PF$_6$ (represented as Ir-Cat$^+$) causing its excitation, then single electron transfer to the excited catalyst *Ir-Cat$^+$ from triethylamine **230**, forming the reduced Ir-Cat, a reductive quenching process, and the radical cation of triethylaminium **231** is also formed alongside. Reduction of the C–Br bond of the diethyl bromomalonate **77** by
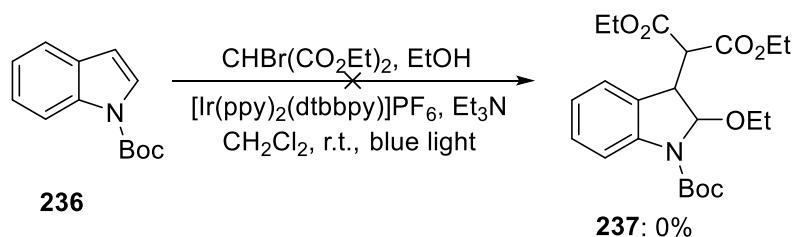
the reduced photocatalyst Ir-Cat, a strong reducing agent, forms radical **157** while regenerating the catalyst Ir-Cat$^+$ thereby completing the catalytic cycle of Ir(ppy)$_2$(dtbbpy)PF$_6$. Ir-Cat donates a single electron to the C–Br bond for easy exit of bromine, a good leaving group. The interaction of the enamide, *N*-ethenyl-2-oxazolidinone (**117**) with the electrophilic radical **157** produces the radical **232**. This radical could be oxidized by either the exited photocatalyst, *Ir-Cat$^+$ or the triethylaminium ion **231** by removing one electron from it to provide the intermediates *N*-acyl iminium cation **234**. The cation generated under this condition is then intercepted by the nucleophile, arylamine, as hypothesized by Stephenson and co-workers[34] to give the product **235**.

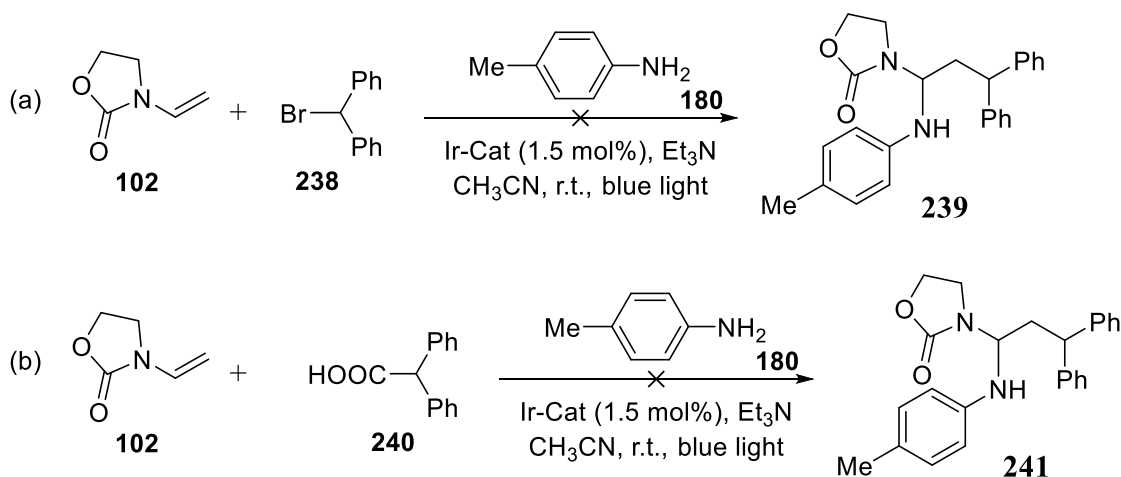**Scheme 67**: Proposed mechanism for the photoredox reaction
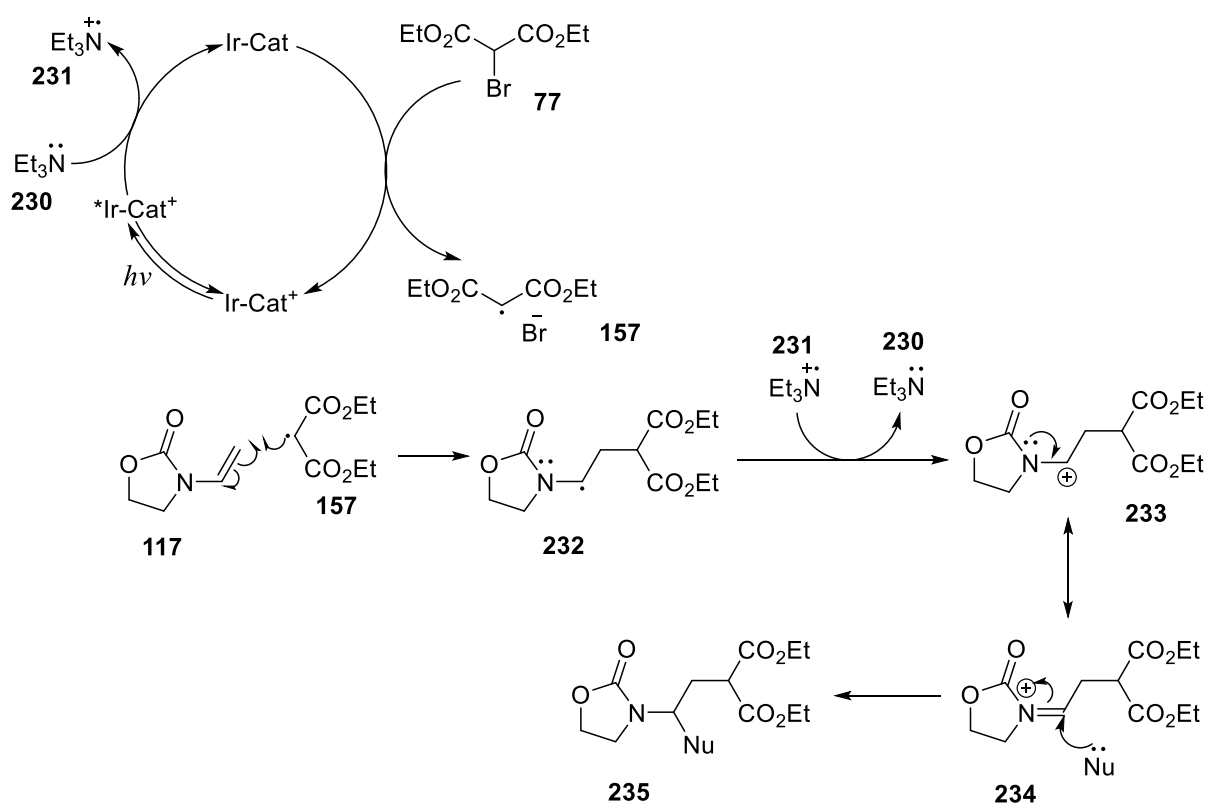
However, when *tert*-butyl 1*H*-indole-1-carboxylate (**236**) was used in place of *N*-vinyl-2-oxazolidinone (**117**) as an enamide in the above reaction, the compound **237** was not observed (**Scheme 68**). This might be as a result of the involvement of the π-electrons of the C=C bond and the lone pair on the nitrogen atom in the aromatic system of the ring. Going into such a reaction will destabilize the aromatic ring, which is highly un-favourable.

Scheme 68: Photoredox of **236** with ethanol

236 → **237**: 0%

Reagents: CHBr(CO$_2$Et)$_2$, EtOH / [Ir(ppy)$_2$(dtbbpy)]PF$_6$, Et$_3$N, CH$_2$Cl$_2$, r.t., blue light

The reaction did not also give the expected results with (bromomethylene)dibenzene **238** and 2,2-diphenylacetic acid **240** as the alkylating agents under the reaction conditions. The adduct **239** and **241** were not obtained as products. The starting material, enamide was recovered unreacted even after running the the reaction for over 30 hours.

Scheme 69: Pohotoredox reaction of enamide **117** with alkylating agents **238** and **240**

(a) **102** + **238** → **239**, conditions: **180**, Ir-Cat (1.5 mol%), Et$_3$N, CH$_3$CN, r.t., blue light

(b) **102** + **240** → **241**, conditions: **180**, Ir-Cat (1.5 mol%), Et$_3$N, CH$_3$CN, r.t., blue light

3.4.3 Cyclization of the Enamides Photoredox Catalysed Products to γ-lactams

The synthetic utility of the photoredox reaction products was tested by cyclizing some of the products to their corresponding γ-lactams (**Scheme 70**). The γ-lactam ring, also known as γ-butyrolactam, is part of the important structure of a large number of natural and non-natural compounds covering a broad spectrum of biological activities.[56] γ-Lactams find several applications in medicinal, synthetic, and material chemistry. They are included in a large number of pharmaceutically active compounds with antibiotic, anti-inflammatory, and anti-tumoral functions.[57] γ-Lactam moiety is a structural subunit for the design of several pharmaceutical agents.[58,59] γ-lactams also served as valuable building blocks for the synthesis of complex molecules due to their latent reactivity and the large panel of highly

selective transformations they can undergo.[58] Accordingly, products containing the γ-lactam core are important synthetic targets, so many synthetic strategies have been attempted and reported to make this valuable structural moiety and it is of primary interest in medicinal chemistry(**Figure 11**).[58,59,85,86]

Figure 11: Some natural products containing γ-lactam moiety

stemoamide   tetramic acid   jatropham   cynometrine
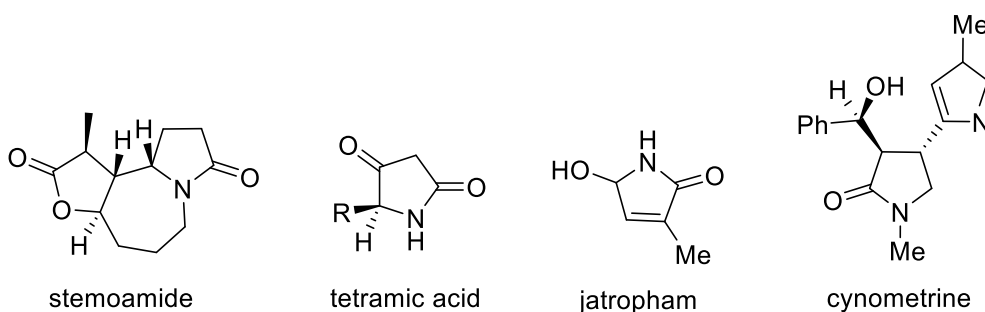
Initial attempt to cyclize these products into γ-lactams by stirring the adduct product in anhydrous toluene and heating to reflux for 24 hours resulted in zero yield as the starting material was recovered almost completely unreacted. Similarly, the addition products did not cyclize with the addition of potassium hydroxide, a base. The cyclization was however achieved with the addition of acetic acid and heating at 80 °C overnight.

Scheme 70: Cyclization of adduct products to γ-lactams
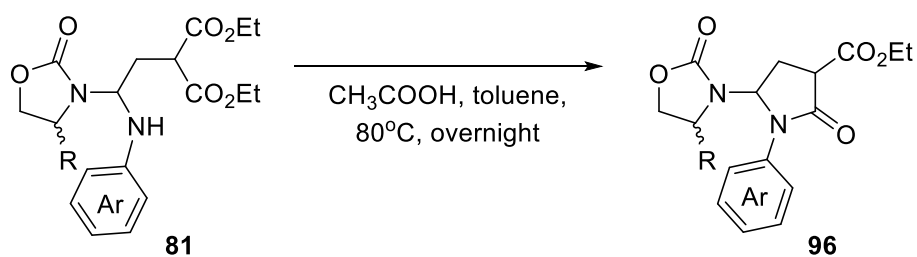
The yield of the corresponding γ-lactams, the products of cyclization, obtained ranges from 53% to 65%. The products were confirmed and characterized by ^{1}H NMR, ^{13}C NMR, and mass spectrometry techniques. X-ray crystallography, in addition to the NMR spectroscopy, was also used to analyze the product that formed crystals.
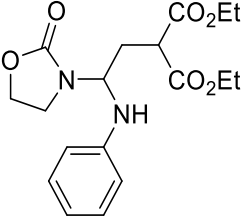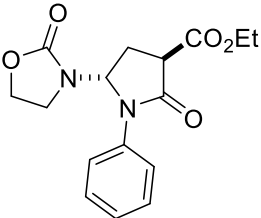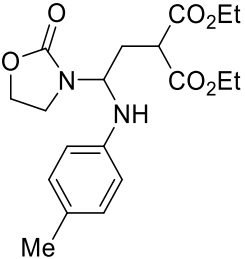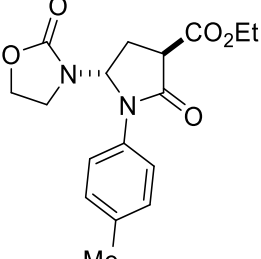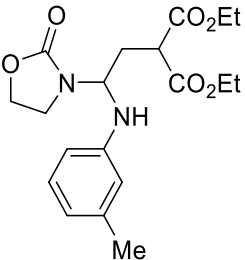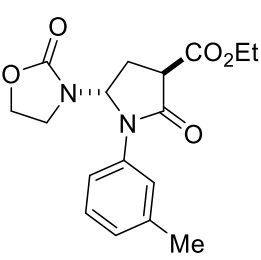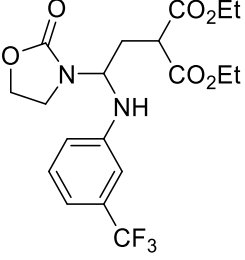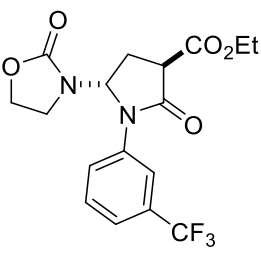
In each case, the cyclization proved effective, but regrettably, the products could not be separated into the different diastereoisomers. The major and minor diastereoisomers were, however, identified using a combination of ^{1}H-NMR and NOE experiments, and the
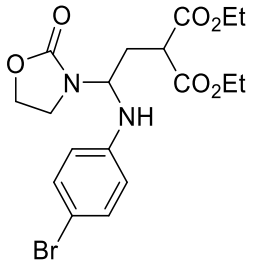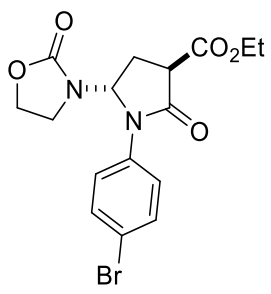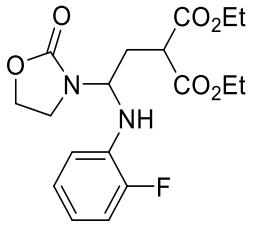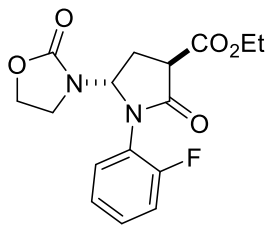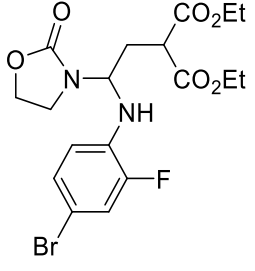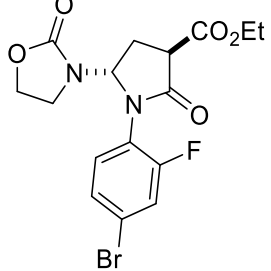
diastereoisomeric ratios of the mixtures were determined by the integration of the diagnostic signals in the γ-lactam ring. The NOE occurs through space thus enabling one to differentiate two diastereoisomers through the space interactions of protons that are not connected by chemical bonds. Using the γ-lactam **243** obtained from the photoredox reaction product **181** as a representative, the diastereomeric ratio was determined to be 53:47. The hydrogen atom on the carbon bearing the aminal moiety appear at δ 6.27 ppm and 6.23 ppm, respectively for the two diastereoisomers. The hydrogen atom on the carbon that bears the ester group appears at δ 3.65 ppm for a diastereoisomer while the signal for the other diastereomer appears at δ 3.47 ppm. The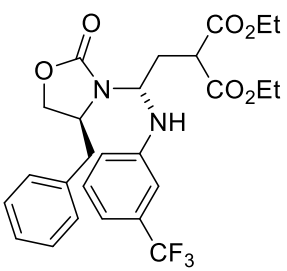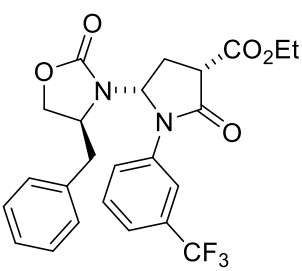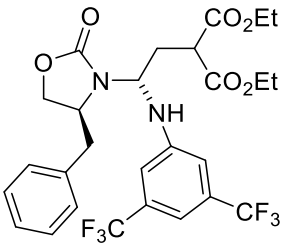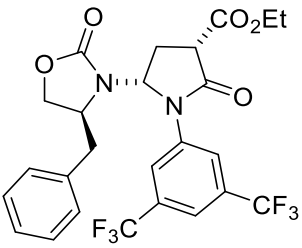 two hydrogen atoms of the methylene bridge in the lactam ring are diastereotopic. The diastereotopic methylene bridge hydrogen atoms of one the diastereoisomer appear at δ 2.93 ppm and 2.24 ppm while those of the other diastereoisomer appear at δ 2.78 ppm and 2.42 ppm.

Having confirmed the formation of the γ-lactam product **243** formed by the adduct product **181**, other adducts from tables 7 and 8 were treated under the same conditions to determine the scope of the reaction (Table 9, entry 2). The treatment of adducts **179** and **183** delivered the desired γ-lactams **242** and **244**, in 64% and 65% yield, respectively as 50:50 and 55:45 mixtures of diastereoisomers in that order (Table 9, entries 1 and 3). The adduct products with electron withdrawing substituents groups on the benzene ring also delivered their corresponding γ-lactam products in comparable yields. The adduct product with *m*-trifluoromethyl group **193** delivered γ-lactam **245** (Table 9, entry 4) with 65% yield while *p*-bromo derivative **195** gave lactam **246** in 53% yield (Table 9, entry 5) as mixtures of diastereoisomers with ratio 50:50 for the two. The treatment of adduct products o-fluoro-(**197**) and 4-bromo-2-fluoro derivatives (**199**), with acetic acid, delivered the desired γ-lactams **247** and **248**, in 61% and 60% yields, respectively and isolated as 57:43 and 57:43 mixtures of diastereoisomers.

Some chiral adduct products were also subjected to this acetic acid treatment and they delivered the desired γ-lactam products. Chiral adduct product **220** gave lactam **249** (54% yield) while adduct product **221** delivered the corresponding γ-lactam **250** (51% yield) with diastereoisomeric mixtures of 53:47 and 54:46, respectively (Table 9, entries 8 and 9).

Table 9: Products of cyclization of the adduct products of photoredox reaction

Entry	Adduct product	Cyclized Product	Diastereoisomeric ratio (dr)	Yield (%)
1	**179**	**242**	50:50	64
2	**181**	**243**	53:47	60
3	**183**	**244**	55:45	65
4	**193**	**245**	50:50	65

Entry			Ratio	Yield
5	**195**	**246**	50:50	53
6	**197**	**247**	57:43	61
7	**199**	**248**	57:43	60
8	**220**	**249**	55:45	54
9	**221**	**250**	58:42	51

Essentially, all the cyclized products exhibited a slight preference for the *syn*-product, with the one exception being the *p*-tolyl γ-lactam **243**. The diastereoselectivity ratio could also be partially influenced by the inclusion of an *ortho* substituent on the aryl ring, as exemplified by the 2-fluoroaryl γ-lactam **247**. We are delighted to obtain the 4-bromo-2-fluoro-tolyl γ-lactam **248** in crystal form upon standing overnight. The ORTEP structure for **248** is shown in **Figure 12.** There is possibility that the cyclized compound might epimerize in chloroform-d from the fact that when the crystal sample used for the X-ray analysis was re-run for the ^{1}H-NMR same diastereoisomeric ratio as when the sample was freshly isolated from the reaction mixture was observed.

Figure 12: The structure of γ–lactam **248** as shown by X-ray analysis

248

Plausible Mechanism of the Acid Catalysed Cyclization of the Adducts.

The reaction begins with the protonation of one of the lone pairs on the oxygen of one of the carbonyl carbons of the malonate moiety thereby making the carbon more susceptible to nucleophilic attack. The carbon atom is attacked by the lone pair on the nitrogen atom of the arylamine group forming arylaminium ion **252**. Next there is a proton transfer from the arylaminium ion to the oxygen atom of the ethoxy group which aids the loss of a molecule of ethanol as a leaving group and an oxonium ion **255** is formed. Then the oxonium ion loses the hydrogen atom to the ethanoate ion, the conjugate base of the acetic acid, to complete the catalytic cycle of the acid and the product, γ-lactam **242** is formed. All these processes or steps are reversible (**Scheme 71**).

3.4.4 *In situ* Bromination of Malonate

Use of bromomalonate derivatives in photoredox additions is ubiquitous within the literature. A report by Stephenson[87] on the photoredox catalysed Appel reaction, suggested that an *in situ* bromination of malonate by use of an external brominating reagent could be used as an alternative. With the successes achieved from the above reactions, we thought of trying some other alkylating agents/groups, especially non-activated alkyl groups, if the reaction conditions would accommodate them. Attempt was made to explore the use of a different radical source for the reaction to generate bromomalonate *in situ*. The first attempt was to use tetrabromomethane **257** as a source of bromine radical for the reaction to generate diethyl bromomalonate *in situ*. To our delight we obtained a desirable result of the adduct product when diethyl malonate **256** and tetrabromomethane were used in place of diethyl 2-bromomalonate with the enamide **117** and *p*-toluidine (**Scheme 72**). However, this has not been optimized.

Scheme 72: Photoredox reaction with carbon tetrabromide as a source of radical
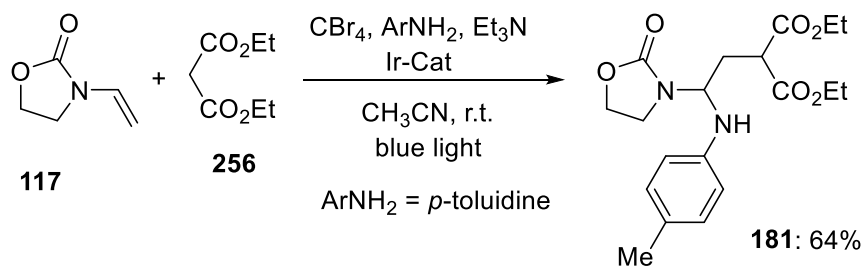
The Proposed Mechanism
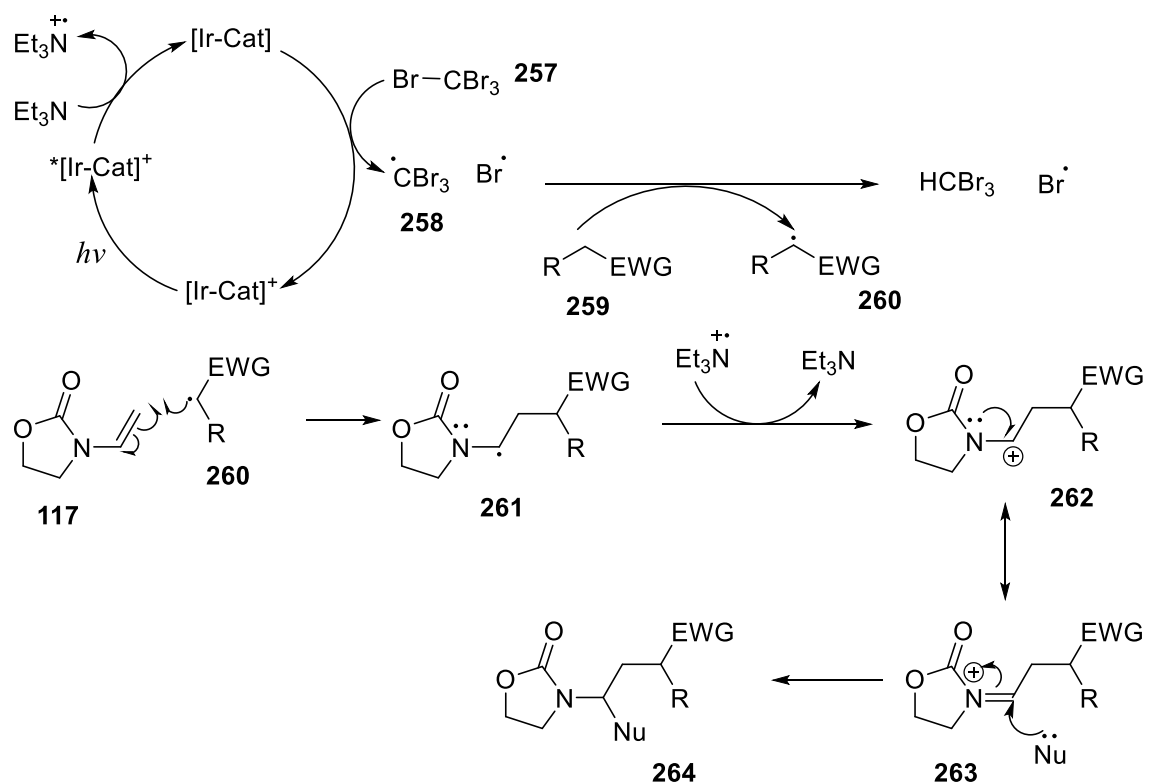
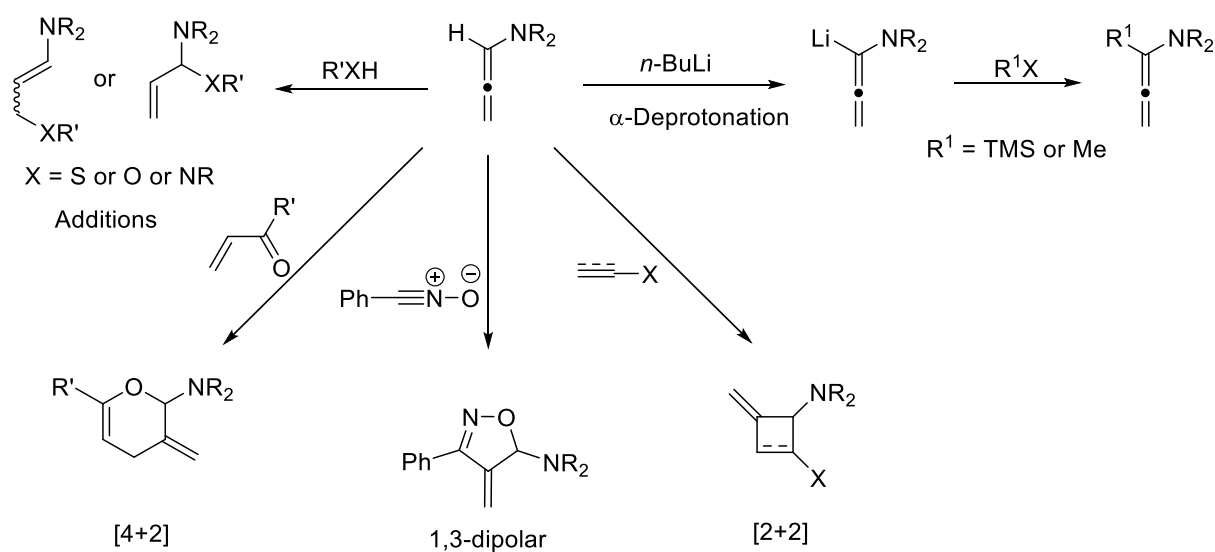## 4.0   Allenamides

4.1   Allenamides: an Introduction

Allenes, the cumulative dienes, is a functional group that can be exploited as a useful building block in synthetic transformations for the building of complex structures that are useful for constructing natural and unnatural products.[47,48,61] Subgroups of allenes are obtained when the terminal carbon has a heteroatom such as oxygen, sulfur, or nitrogen as a substuent (**Figure 13**).[48] When the heteroatom is nitrogen from an amine, we have an allenamine. The π-donating ability of nitrogen atom renders allenamines more electron-rich than simple allenes, thereby predisposing them to electrophilic activations. Hence, allenamines are synthetically useful. When nitrogen atom donates its lone pair toward the allenic moiety it renders transformations involving additions of electrophiles [E$^+$] and nucleophiles [Nu$^-$] highly regioselective.[48]

Figure 13: Allenes and Allene sub-groups

Allenes   Allenol ethers   Allenylsulfides   Allenamines
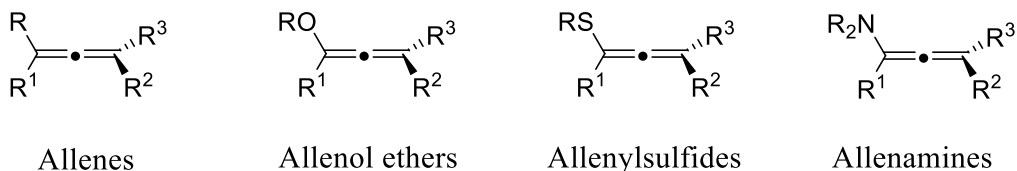
Synthetic transformations involving allenamines should therefore be useful in organic synthesis. They are useful in many reactions which include α- or γ-lithiation of allenamines, additions, 1,3-dipolar, [2+2]-cycloadditions, and hetero [4+2]-cycloadditions (**Scheme 73**). Other examples are cyclizations, dimerizations, and rearrangement reactions.[61]

The extent of synthetic applications of allenamines is limited, because they are sensitive to hydrolysis, polymerization, and isomerization even at low temperatures, thereby creating serious difficulties in their preparation and handling. However, the transformations involving allenamines often result in products possessing nitrogen functionalities and more importantly they are regio- and stereoselective.

Nitrogen-containing structures are prevalent among medicinally interesting natural and unnatural products and, thus, are useful in developing new therapeutics. Therefore, efforts in developing the chemistry of allenamines and identifying an allenamine-equivalent that possesses the right balance between stability and reactivity can be significant and rewarding, especially to synthetic chemists and medicinal chemists. The desired stability and reactivity can be achieved by having the appropriate electron-withdrawing group on the nitrogen atom of allenamines. One of such are the allenamides in which the nitrogen atom has the carbonyl group as the electron withdrawing group substituent (**Figure 14**).

Allenamides are less reactive, but more stable, than the allenamines because of the electron-withdrawing carbonyl group on the nitrogen atom that diminishes the electron donating ability of the nitrogen towards the allenic moiety.[48]

Figure 14: General Structure of Allenamides
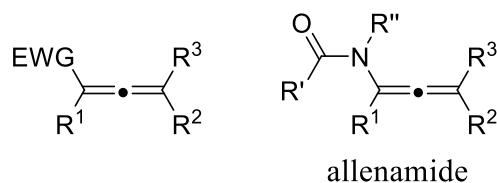
allenamide

The first preparation of allenamide, 1,2-propadienyl-2-pyrrolidinone, was reported in 1967 by Dickinson.[47,88] Dickinson coined the term "allenamide" to describe 1,2-propadienyl-2-pyrrolidinone he prepared based on the analogy of using enamides for Stork's *N*-acylated enamines, and afterwards there has been increased interest in the chemistry of allenamides ranging from medicinal studies, to materials using living polymerization, to synthetic methodologies. These efforts support the notion that allenamides are becoming a proven allenamine-equivalent with the right balance of stability and reactivity.

Figure 15: 1,2-propadienyl-2-pyrrolidinone
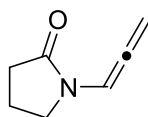

4.2   Synthetic Methods for Allenamides

There has not been a general reliable synthetic method for the preparation of various allenamides, however, the base-induced isomerization seems to be the most reliable and facile synthetic entry into these synthetically useful class of compounds. In 1967, Dickinson demonstrated that treatment of 2-pyrrolidinone **265** with NaH and propargyl bromide **266** led to the preparation of allenamide **268** as the major and stable product via prototropic isomerization pathway (**Scheme 74**).[73] It was also found that the same allenamide could be obtained from the ynamide **267**, which is believed to be an intermediate of the Dickinson's reaction, using NaOMe or NaH.[54] Interestingly, the allenamide did not undergo further isomerization to the ynamide **270** as one would have expected, although with further treatment with NaOMe and pyrrolidine, the allenamide **268** reacts further to give the amide **274** *via* ynamide intermediate.[89]
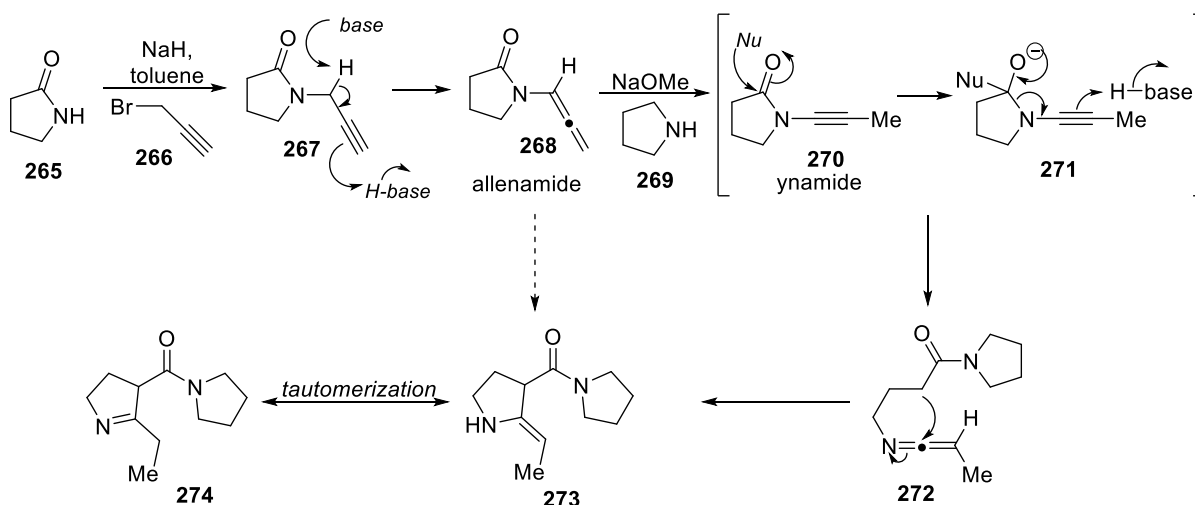
Bogentoft[90] in 1969 also reported the preparation of allenamide **276** *via* a base-induced isomerization of propargyl amide **275** in 50% yield. Oxazole **278** was also isolated, it is likely derived from allenamide **277** after ring opening of the quinazolone (**Scheme 75**).

**Scheme 75**: Bogentoft's base induced isomerization allenamide synthesis
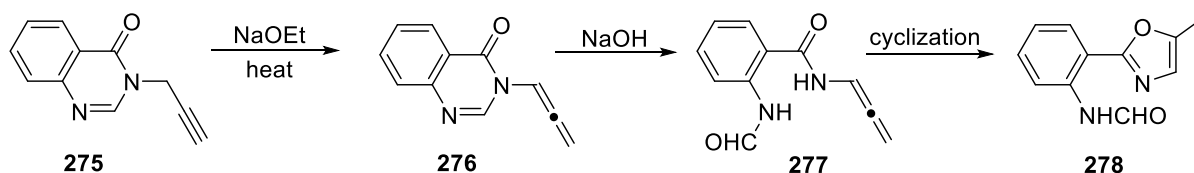
In 1976, Corbel[91] achieved the first synthesis of an acyclic allenamide **280** also via the base-induced isomerization of *N*-propargyl phosphoramidate [X = OEt]/phosphoramide [X = NMe$_2$] (**Scheme 76**). Ynamide **281** was found along with **280**, as a mixture when X = NMe$_2$.

Scheme 76: Corbel allenamide synthesis

X = OEt, **280** only
X = NMe$_2$, a mixture of **280** and **281**
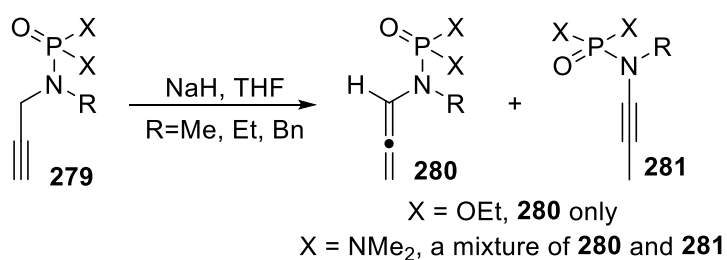
Overman[92] in 1979 reported the isolation of allenamides as a result of Claisen rearrangement of propargyl trichloroacetyl imidates **282**, though in a low yield of about 20%. Under the reaction condition, the allenamides **283** could further isomerize to 1-*Z*-3-*E*-dienamides **284** in a highly stereoselective manner. This method was used to synthesize highly substituted chiral allenamides. Similarly, Claisen-type rearrangement of propargyl thiol benzimidazole **285** gives allenamide **286** as an intermediate in its transformation to the compound **287** (**Scheme 77**).

Scheme 77: Overman's Claisen rearrangement
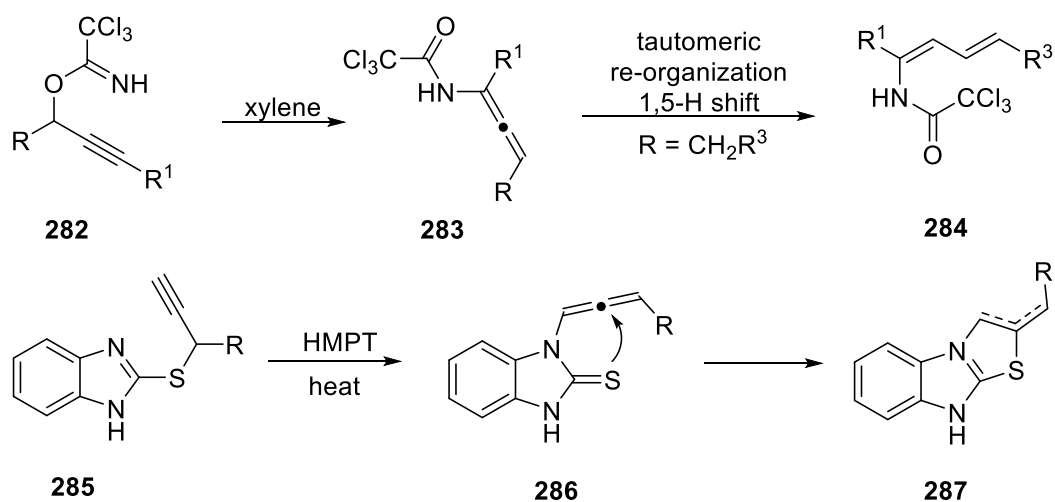
Recently, Morrill *et al.* reported the synthesis of a new class of allenamides, *N*-allenyl cyanamides in which the electron-withdrawing group on the nitrogen atom is the cyano group, through deoxycyanamidation-isomerization.[93] In their report, propargyl alcohol **288** was used to react with the corresponding cyanamide **289** via deoxycyanamidation and its subsequent base induced isomerization to *N*-allenyl cyanamide **290**. The two steps were carried out in one-pot (**Scheme 78**).

Scheme 78: Morrill's synthesis of *N*-allenyl cyanamides
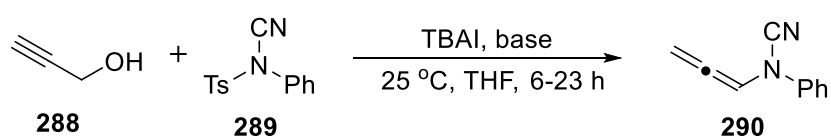
In 1981, Tamura and co-workers[94] reported the first example of [2,3]-sigmatropic rearrangement of sulfimine **293**, leading to allenamide **294** (**Scheme 79**). The rearranged

precursor **293** was obtained by acylating the propargyl sulfide **291** with *N*-triflate carbamate **272**

Scheme 79: Tamura's [2,3]-sigmatropic rearrangement
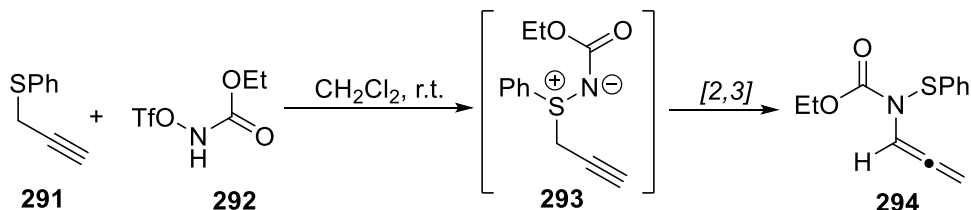
Allenamide can also be prepared through base-induced isomerization of propargyl amides. Padwa[95] in 1982 reported that at high temperature under basic conditions, propargyl amide **295** isomerizes to allenamide **296** (**Scheme 80**). Galons[96] also reported, in 1985, another example in which allenamides **298** and **300** were formed through a solid−liquid phase transfer catalyst-promoted reaction of imidazoles **297** and **299**, respectively with propargyl bromide **266** (**Scheme 81**).

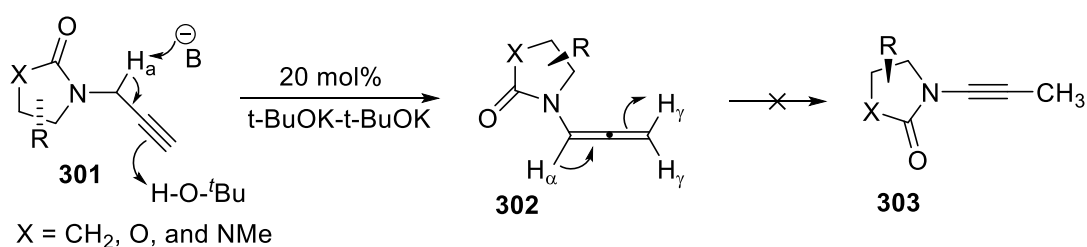**Scheme 80**: Padwa's preparation of allenamides
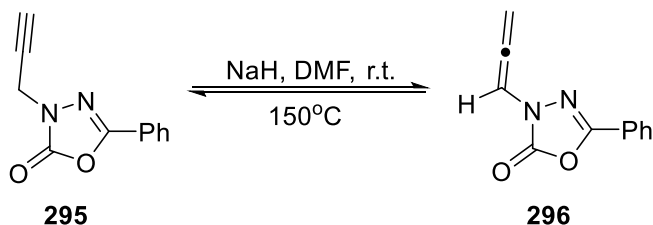
**Scheme 81**: Galons preparation of allenamides
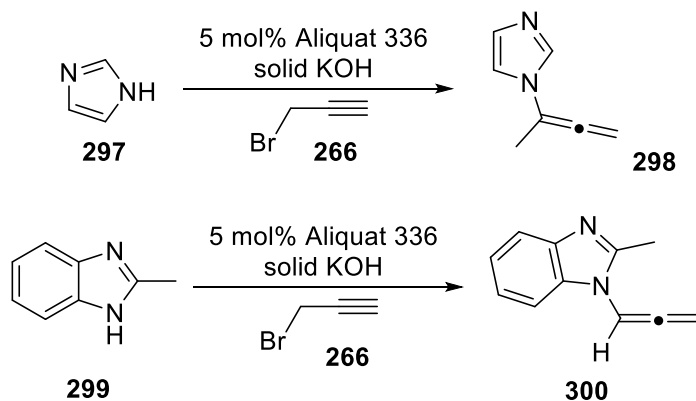
Hsung and co-workers in 2001 reported the isomerization of cyclic propargyl amides **301** to allenamides in their attempt to synthesize ynamides *via* the base-induced isomerization. They observed that instead of ynamides **303** to be formed, the isomerization gave allenamides **302** (**Scheme 82**). This happened to be the first chiral allenamides to be synthesized. Propargyl amides in which the nitrogen atom is part of aromatic heterocycle most often isomerize to the corresponding allenamides. There are very few examples of isomerization of propargyl amides resulting into the formation of ynamides. In most cases, isomerizations of propargyl amides provided only allenamides.[48,97]

Scheme 82: First chiral allenamides

Apart from the synthetic methods or approaches mentioned above, there are many other documented methods that have been used by different researchers for the preparation of allenamides, these include amongst others De Meijere's isomerization for acyclic *N*-tosyl allenamide,[98] Tanaka[99] and Farina's eliminations for preparations of β-lactam-based α,α-disubstituted allenamides from enol triflates.[100] While synthetic approaches to these substrates have been well documented, it is the base-catalysed rearrangement of propargyl amides that has stood out as a method of choice for their synthesis.[101] This method has a major drawback of reliance on the formation of the propargyl amide from the reaction of propargyl bromide with the appropriate amide under basic conditions. This drawback is, however, circumvented by the one-pot approach reported in 2015 by Kimber and co-workers[101] for the preparation of allenamides. The simple method involves one-pot preparation using a DMSO/*t*BuOK protocol. The procedure is experimentally simple and robust, and provides *N*-allenyl analogues, commonly used within the literature, in yields comparable to the two-step approach (**Scheme 83**).

Scheme 83: Kimber's one-pot protcol

114 → **304**: 65%
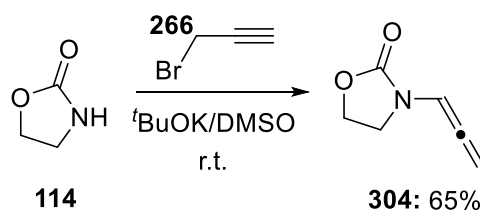
In 2016, Evano *et al.* reported the synthesis of allenamides derived from oxazolidinones and hydantoins by copper-catalysed coupling of propargylic bromides and nitrogen nucleophiles.[102] Copper thiophene carboxylate (CuTC)-2,2'-bipyridine complex was used as the coupling catalyst in the presence of an inorganic base Cs_2CO_3 or K_3PO_4. This method is suitable for the synthesis of trisubstituted allenamides which the Trost[62] and Hung group methods could not be used for their synthesis (**Scheme 84**).

Scheme 84: Evano Cu-catalysed allenamides synthesis

**130** + **305** → **306**
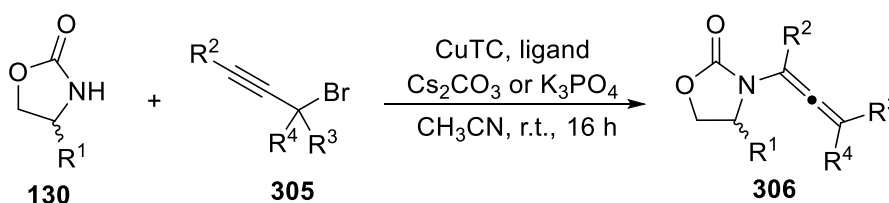
4.3   Chemistry of Allenamides

Allenamides are electron-deficient equivalents of allenamines. They represent interesting functional groups and useful in organic synthesis. Their chemical utility have been exploited by a number of research groups.[103] Allenamide subunit undergoes several versatile chemical reactions including highly regio- and stereoselective transformations offering useful building blocks in organic synthesis. Some of the reactions are deprotonation, addition reactions, cycloaddition reactions and cyclization like radical cyclization, acid-catalysed cyclization, palladium-mediated transformations, base-catalysed CO_2 capture, based-catalysed heterocyclizations, gold-mediated transformations and ruthenium-catalysed aminoallylations. When allenamides are involved in cyclization or cycloaddition transformation, they give rise to structurally diverse heterocycles, as well as to complex molecular architectures that are analogues of natural products and biologically relevant substrates.[103]
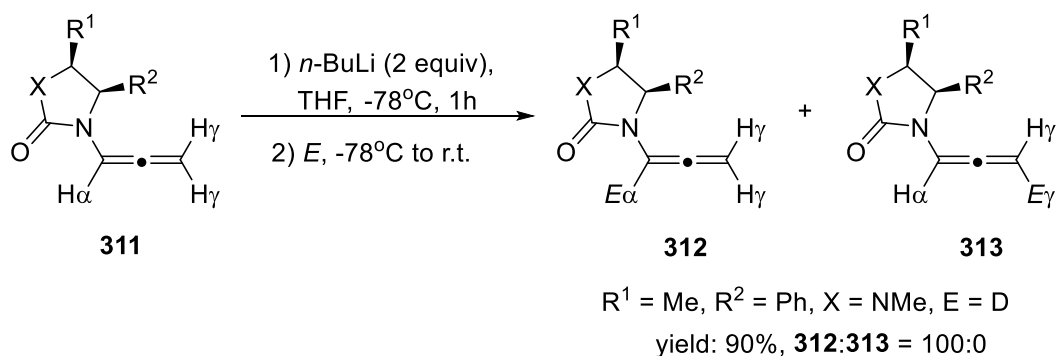
4.3.1 Deprotonations

Allenamide can undergo deprotonation in either α- or γ- position. The α-position seems to be more favourable than the γ-position. The reason could be as a result of the inductive effect of the α-carbon withdrawing the electrons on the bond toward itself thus making it relatively more nucleophilic than the γ-carbon. The inductive effect is as a result of the nitrogen atom directly bonded with it. Corbel[104] documented the first example of α-deprotonation of allenamide **307** to generate the lithiated allenamide **308**, which was trapped by electrophiles to afford α-substituted allenamides **309** (**Scheme 85**). Subsequent hydrolysis of **309** resulted in the corresponding unsaturated ketones **310**.

Scheme 85: Corbel deprotonation at α-position
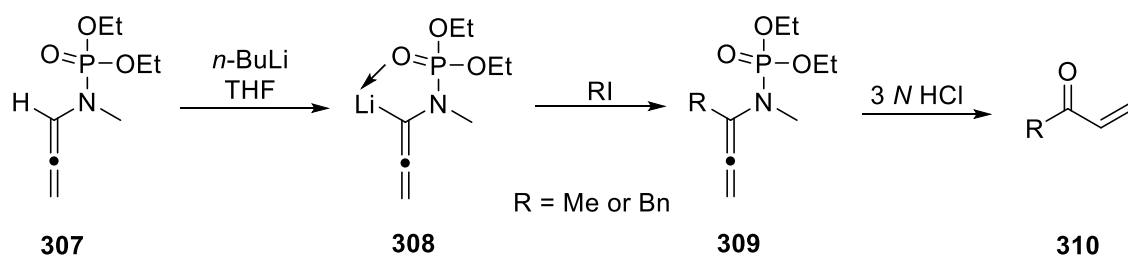
Hsung[105] also reported a regioselective α-deprotonation of allenamides **311** using *n*-BuLi (**Scheme 86**). The one-pot deprotonation/alkylation sequence that can be widely applicable to access a series of α-substituted allenamides **312**; the γ-deprotonation product **313** was not observed.

Scheme 86: Hsung selective α-deprotonation

R^1 = Me, R^2 = Ph, X = NMe, E = D
yield: 90%, **312**:**313** = 100:0

Hsung[105] further revealed that when *t*-BuLi was used, there was no α/γ selectivity. The deprotonation led to a 50:50 mixture of **315** and **316** (**Scheme 87**). However, the

deprotonation/D$_2$O trapping sequence of allenamide with the α-position blocked would occur at γ-position to afford **318** with moderate diastereoselectivity.

Scheme 87: Hsung selective α-deprotonation


315:316 = 50:50
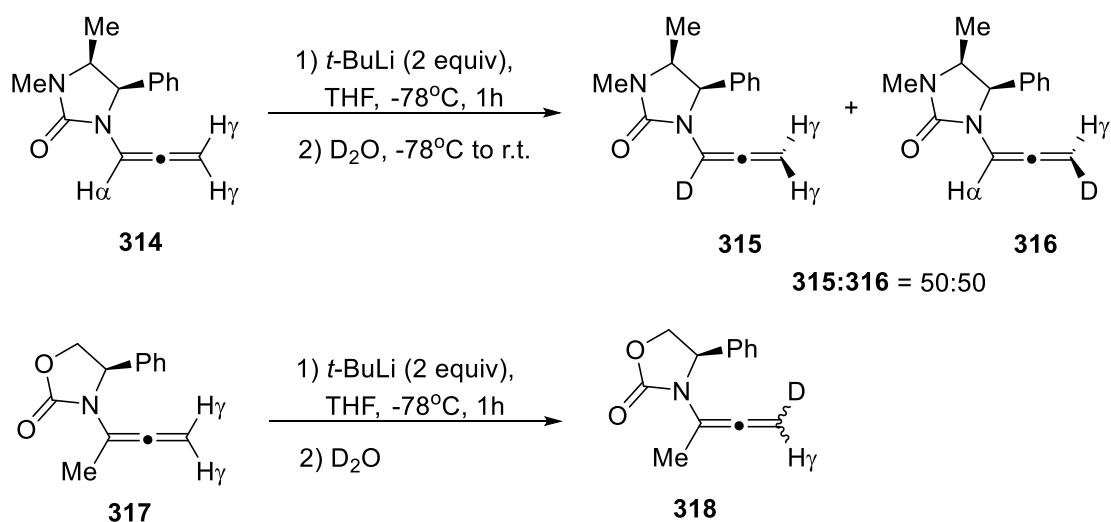
4.3.2 Addition Reactions

Hydroalkoxylations

Horino,[106] in 2008, found that hydroalkoxylations of allenamide **319** with alcohol **320** could take place at both γ- and α- positions to afford distal addition product **300** and proximal addition product **322**, respectively (**Scheme 88**). With an Au(I) catalyst, the hydroxylation of **319** could be achieved more selectively at the α-position to give **322** in high yield. Diene **322** was subsequently used to construct the spirodihydrofuran **323** through ring-closing metathesis (RCM). In contrast, the distal addition product **321** was more favoured under thermal conditions.

**Scheme 88**: Horino hydroalkoxylation of allenamides
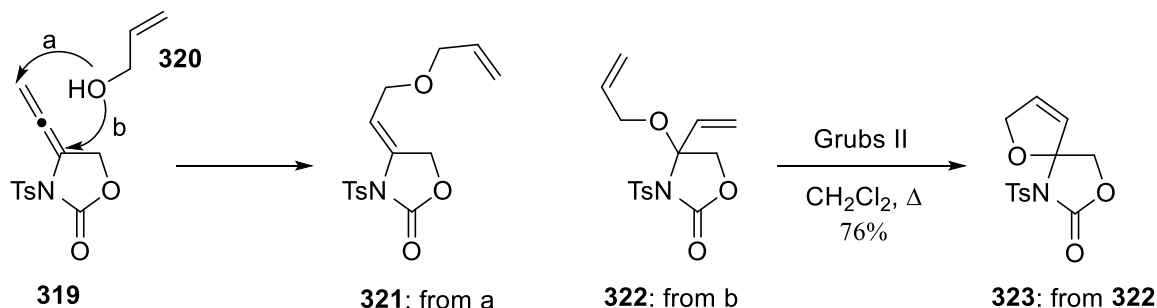
Hydroamination

In 2010, Kimber *et al.*[107] reported an intermolecular hydroamination of allenamides **324** with arylamines **325** under mild Au(I) catalytic conditions delivering allylamino *E*-enamides **326** stereoselectively in high yield *via* intermediate **327**. The reaction is made possible *via* a convenient method for conjugated *N*-acyliminium formation. The products of this reaction, allyl-aminoenamides, have the potential to be valuable building blocks in organic synthesis since they contain two vital functionalities, allyl amines and enamides, within one framework (**Scheme 89**).

**Scheme 89**: Kimber intermolecular hydroamination
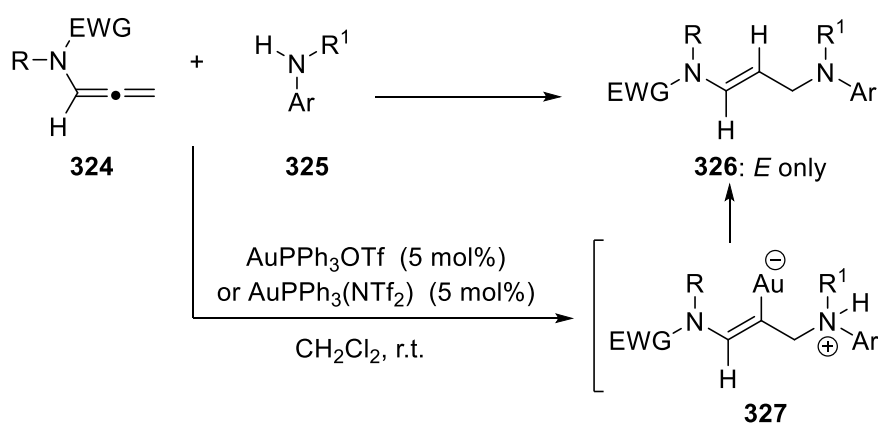
Broggini[108] also, in 2009, reported an Au(III)-catalysed intramolecular hydroamination of allenamides **328**, which afforded a mixture of *cis-* and *trans* 2-vinyl-imidazolidines **331** through the 5-exo-trig transition states **329** and **330**, respectively. Intriguingly, when R = Bn, only *cis*-**331** was isolated in good yield (**Scheme 90**).

Scheme 90: Broggini Au(I) catalysed intramolecular hydroamination of allenamides

cis-**331**   *trans*-**331**
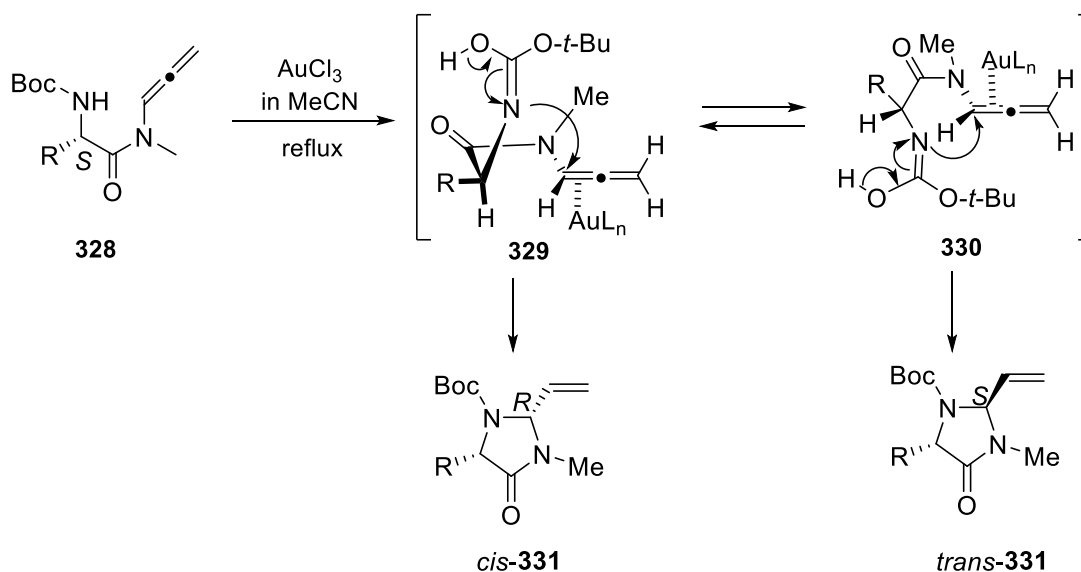
Broggini[109] also reported that allenamides **328** could be subjected to base-promoted intramolecular hydroamination, leading to heterocycles **332**, **333**, and/or **334** (**Scheme 91**). In most cases, the cyclization occurs effectively with microwave irradiation at the central allenic carbon to afford **333** thereby representing an umpolung addition reaction. However, no hydroamination products were observed when R = Ph.

Scheme 91: Broggini base-promoted intramolecular hydroamination of allenamides

|	**332**	**333**	**334**
Reaction at r.t.: R = *t*-Bu	9%	28%	25%
Microwave: R = *t*-Bu	0	89%	0
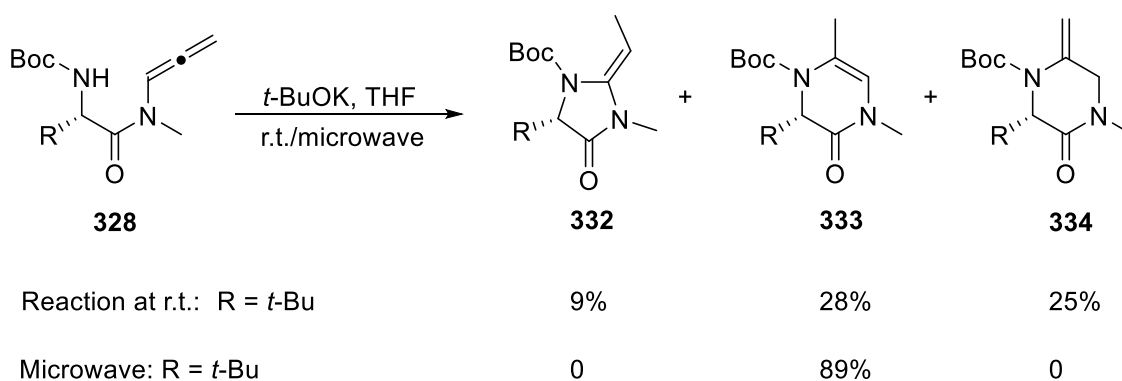
Hydroarylation

Ohno developed the first Au-catalysed intramolecular hydroarylation of allenamides for the formation of dihydroquinolines.[61,66] Kimber, in 2010, reported a highly stereoselective hydroarylation of allenamides **335** to obtain a series of achiral and chiral oxazolidinone-derived *E*-enamides **337** *via* the 1,4-addition to *N*-acyl iminium intermediates **336** (**Scheme**

92).[56] Bis-hydroarylation products could be obtained in some cases. For example, allenamide **335** reacted with furan twice through both 1,4- and 1,2-hydroarylation to give **338**. In another case, bis-hydroarylation afforded **339** when 2 equiv. of the allenamide **335** was used.

Scheme 92: Kimber stereoselective arylation of allenamides
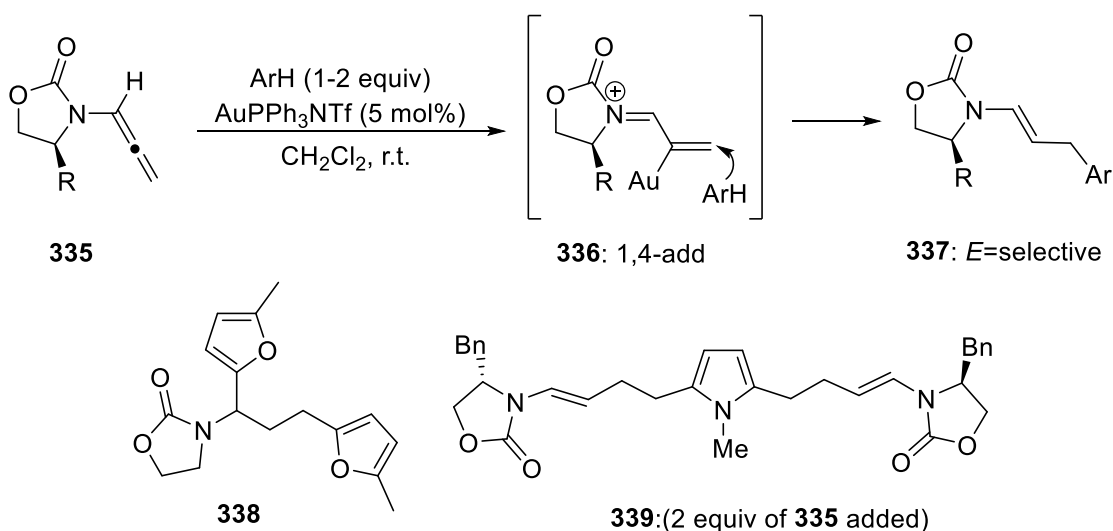

4.3.3 Cycloaddition Reactions

Allenamides, being electron-deficient equivalents of allenamines, can participate in a range of cycloaddition reactions giving rise to novel heterocycles and diverse molecular architectures similar to those obtained in natural products. Cycloadditions involving allenamides can be cycloadditions directly involving the allenamide olefin, and cycloadditions using the allenamides olefin as a precursor to a nitrogen-stabilized allyl cation.

Several research groups have carried out and reported studies of different kinds of cycloaddition reactions involving allenamides. These include [2+1]-cycloadditions by Hsung and co-workers,[110] [2+2]-cycloadditions by Tamaru,[111] Nair,[112] Chen,[113] Mascareñas[114] and González;[115] [2+2+1]-cycloadditions by Hsung[105] and Oh;[116] [3+2]-cycloadditions by Broggini and Zecchi;[117] and dipolar cycloaddition by Barluenga[118] and Piperno and Romeo.[119]
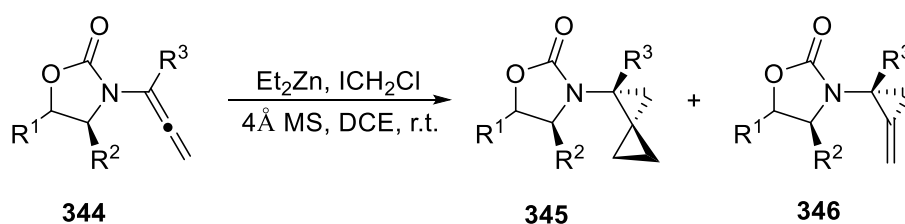
[2+1]-Cycloadditions.

Hsung[110] reported the first detailed studies on epoxidations of chiral allenamides **340** including ^{1}H-NMR studies of these reactions (**Scheme 93**). When Oxone® was used, isolation of cyclic ether **343** suggested that a more acidic medium during the oxidation can promote rapid ring-opening of allene oxide or epoxyallene **341** to provide the α,β-unsaturated *N*-acyl iminium intermediate **342**.

Scheme 93: Hsung's epoxidation of cyclic allenamide
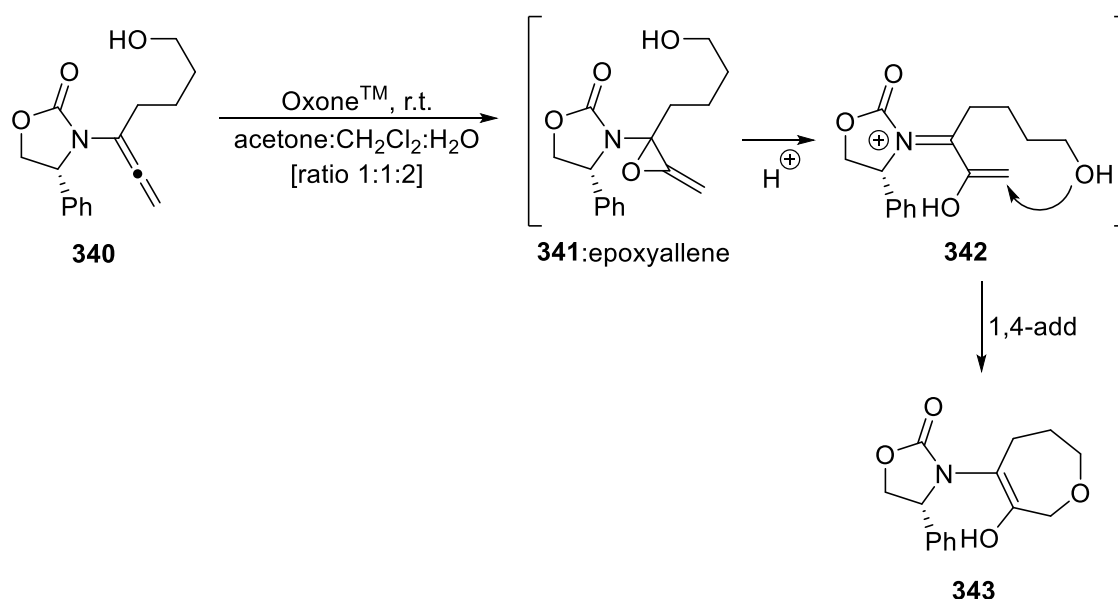
In 2009, Hsung[120] reported a detailed account of Simmons−Smith cyclopropanation of allenamides to generate amido-spiro[2,2]-pentanes (**Scheme 94**). For α-unsubstituted allenamides **344**, only bis-cyclopropanation products **345** were formed, while α-substituted allenamides resulted in mixtures of mono- and bis-cyclopropanation products **346** and **345**, though there was a lack of selectivity in the reaction.

**Scheme 94**:Hsung's cyclopropanation of allenamides

[2+2]-Cycloadditions

Studies of [2+2]-cycloaddition reactions involving allenamides were carried out by several research groups. Tamaru and co-workers[111] reported, in 1997, of the thermal [2+2] cycloaddition of allenamides was among the earliest of such reactions. Various allenamides **347** underwent [2+2]-cycloaddition reactions chemoselectively at the allenic β,γ-position with alkenes or alkynes to respectively furnish cyclobutanes **350** or cyclobutenes **351** regio- and stereoselectively (**Scheme 95**).[121] This methodology was reportedly to be limited to terminal alkenes and alkynes bearing not only electron-withdrawing and conjugating groups but also electron-donating groups with complete retention of the alkene double bond geometries.

Scheme 95:Tamaru's [2+2]-cycloaddition of allenamides
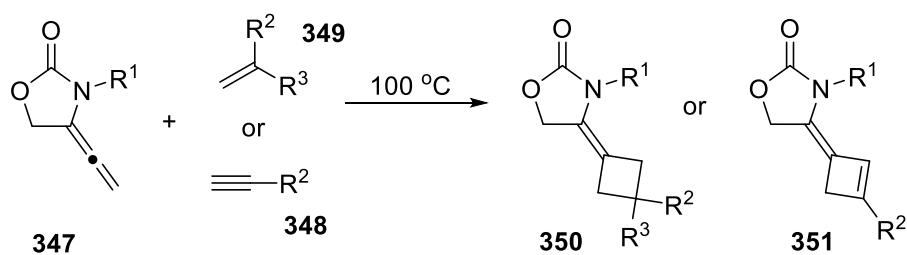
Nair[112] published, in 2002, a unique [2+2]-cycloaddition of allenamides **352** with [60]fullerene **353** to afford novel cyclobutane annulated fullerene derivatives **354** (**Scheme 96**). The reaction took place selectively on the internal double bond of allenamides.

Scheme 96: Nair's [2+2]-cycloaddition of allenamides with [60]fullerene
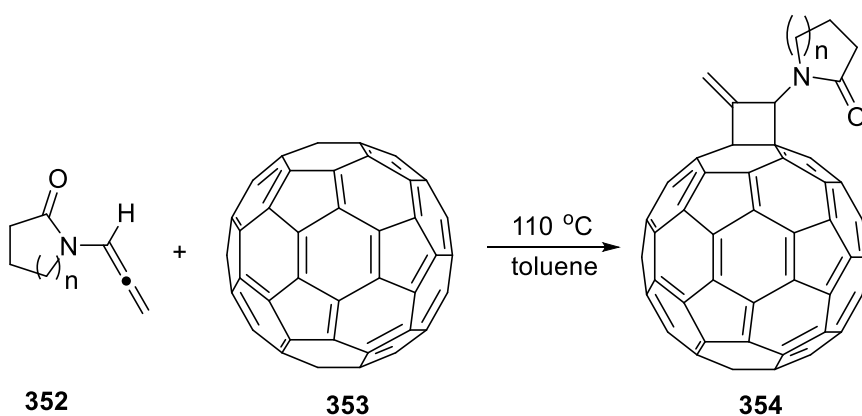
Chen[113] also reported in 2012 the first Au-catalysed [2+2]-cycloadditions of allenamides and later same year, Mascarenas[113] independently reported a gold-catalysed intermolecular [2+2]-cycloaddition of allenamide **304** with various alkenes **356** for the synthesis of cyclobutanes **357**. This reaction is highly regioselective with only the exo-double bond of the allenamides involves in the reactions (**Scheme 97**).

**Scheme 97**: Mascarenas's Au-catalysed [2+2]-cycloaddition of allenamides with alkenes
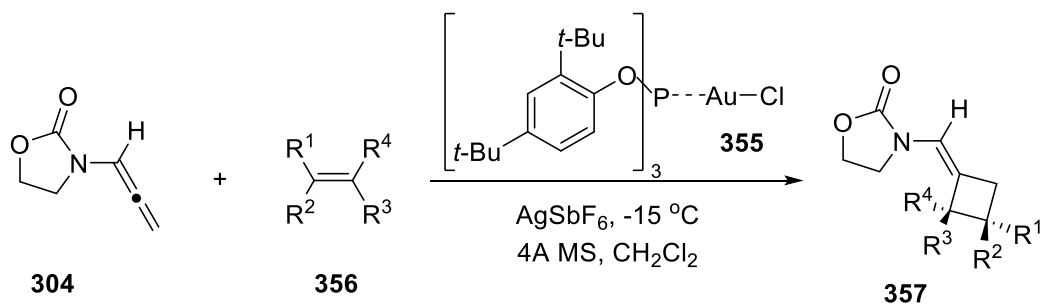
In addition, allenamides have also been reported to participate in many other types of cycloaddition reactions such as thermal intramolecular [4+2]-cycloadditions; torque-selective ring closures of allenamides; inverse-electron-demand Diel-Alder reactions; cycloisomerization like the Pauson-Khand reaction (PKR); cyclopropanation; and [4+3]-cycloadditions using nitrogen-substituted oxyallylcations.[103]

4.3.4 Cyclizations

Allenamides have been reported to undergo several types of cyclization both transition metal mediated and non-transition metal cyclization transformations. Some of the addition reactions of allenamides actually involve cyclizations, especially the intramolecular hydroamination and hydroarylation.

Hacksell[122] reported the first cyclization involving an allenamide. His attempts to methylate propargyl amides **358** led to isolation of the oxazole **359** when $R^2 = p$-NO$_2$Ph, and the desired allenamides **360** were isolated when $R^2 = p$-MeOPh or Ph (**Scheme 93**). This cyclization occurred for all substrates when MeI was not added, and presumably, **361** and **362** were key intermediates. Cyclization is actually faster than methylation when $R^2 = p$-NO$_2$Ph.

Scheme 98: Hacksell's cyclization

358: R^1 = CH_3, CF_3 359: R^2 = p-NO_2Ph 360: R^2 = p-MeOPh or Ph

361   362   363
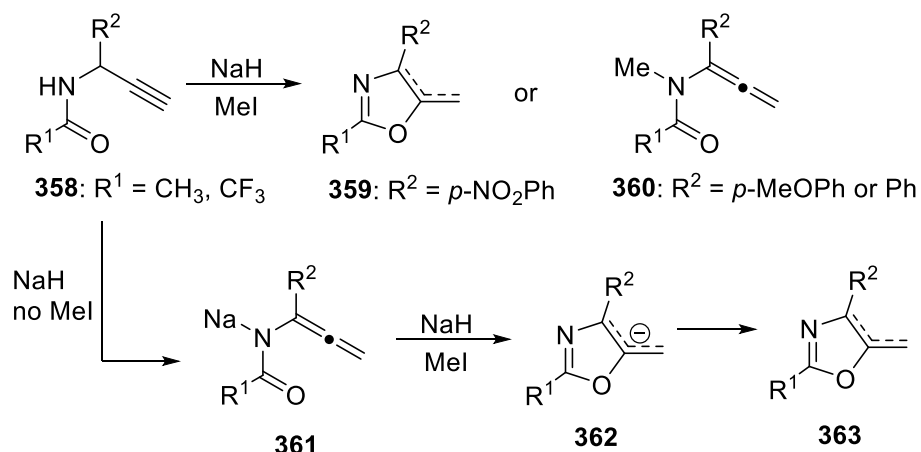
Motivated by the successes achieved in the Au(I) activation of allenamides and their subsequent reaction with electron-rich arenes and arylamines to give functionalised enamides, Kimber and co-workers then considered intramolecular arene cyclization of allenamides. Kimber,[123] in 2012, then reported the achievement of the construction of α-vinyl-substituted tetrahydroisoquinolines **365,** cyclized products, through an Au(I)-catalysed intramolecular hydroarylation of allenamides **364** (**Scheme 99**).

Scheme 99: Kimber's arene cyclization with allenamides

364   R = EWG or Me; X = CH_2 or C(O)   365
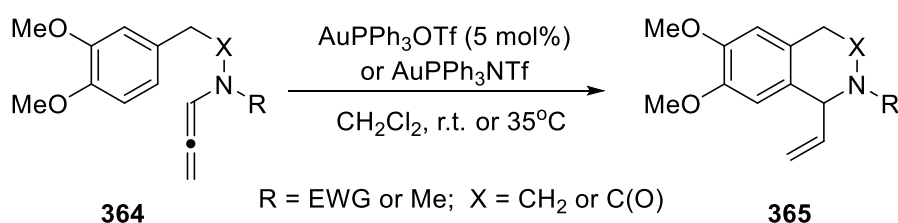
Liu and co-workers, in 2017, reported the use of allenamides in the metallo-ene/Suzuki coupling reaction catalysed by palladium. In this reaction, two new Csp^3–Csp^2 bonds were constructed in one pot providing a variety of polyfunctionalized 2,3-dihydropyrrole derivatives (**Scheme 100**). This reaction shows an excellent regioselectivity providing the terminal C_1 position coupling product without detection of the internal C_3 coupling product. The unique terminal alkene as one of the most easily functionalized groups endows these molecules with versatile transformations into much more complicated molecules.[124]

Scheme 100: Liu metallo-ene/Suzuki coupling reaction of allenamides
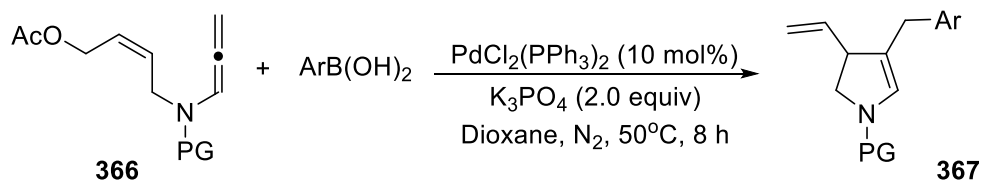
Shen and Hsung, in 2005, also reported the first radical cyclization reactions involving allenamides. The reactions are highly regioselective for the central carbon of the allenic moiety that led to the synthesis of nitrogen heterocycles such as isoquinolines and carbocycles such as indane and naphthalene (**Scheme 101(a)**). However, when highly constrained allenamides like **370** are used in the reaction, the formation of *exo*-cyclization products are favoured leading to the synthesis of isoindoles **371** (**Scheme 101(b)**).[125]

Scheme 101: Hsung's radical cyclizations of allenamides
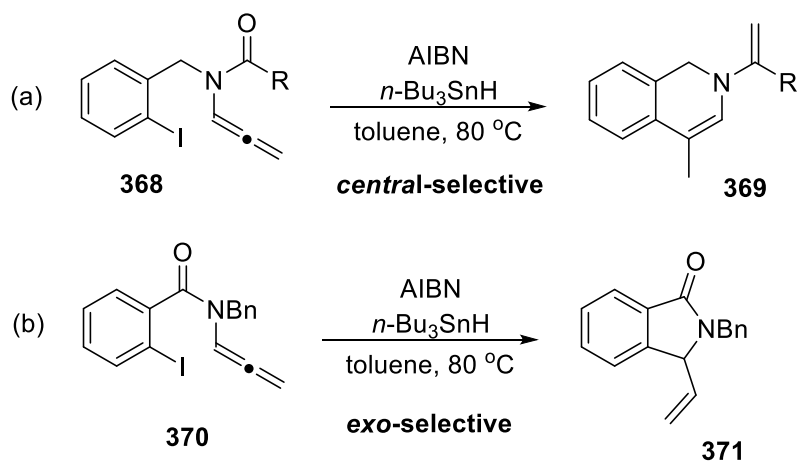
In conclusion, allenamides are versatile compounds that undergo useful reactions leading to varieties of compounds that can be used in the synthesis of natural compounds and for the development of new therapeutics. Therefore, efforts in developing the chemistry of these compounds can be significant and rewarding, especially to synthetic chemists and medicinal chemists as both offer a wide variety of alternatives for the inclusion of a nitrogen-based moiety into organic systems.

4.4   Allenamides: Reactions, Results and Discussion

The presence of the electron withdrawing group, the carbonyl group, on the nitrogen atom of the allenamides attached to the α-carbon of the allene moiety leads to the distinct reactivities display by this class of compounds from the traditional reactions of allenes. This substituent can donate electron density through the lone pair on the nitrogen atom into the allene, principally onto the central β-carbon. This can be harnessed in the chemical transformations of allenamides to obtain highly regioselective products. This distinct reactivity profile of allenamides had contributed to the recent attention enjoyed by this unique class of compounds in the synthetic community. They have been involved in variety innovative transformations, including cycloadditions, Aldol additions, intramolecular cyclizations and intermolecular addition reactions, as well as their uses as precursors in natural product synthesis.

Radical reactions represent a powerful tool in organic synthesis. The generation of radicals is achieved traditionally by heating, irradiation by light or a redox reaction. These conventional methods of radical generation often need the use of harmful or explosive reagents, use of high-energy UV radiation etc.[6,7] In other words, radical generation involves uncontrollable, harsh conditions and often have a poor atom economy. However, these environmentally unfriendly conditions can be avoided by using photoredox catalysed techniques which are mild and mostly have high atom and energy economy. The process generates less amounts of waste, environmentally friendly and above all no special equipment is required.

Reports of reactions involving the use of allenamides in radical reactions are limited so the single intermolecular radical cyclization as reported by Hsung.[125] There are no reports of radical photoredox reactions on allenamides is in the literature, at least to best of our knowledge. With this in mind, we intend to develop a general addition reaction for the transformation of allenamides using a mild condition of visible light photoredox catalysis as the main synthetic reaction.

Addition reactions of allenamides are typically promoted by the electrophilic activation of the β-carbon of the allenamide. The reaction of the allenamide with the electrophiles can promote the formation of a conjugated *N*-acyliminium that can subsequently undergo an addition reaction with a suitable nucleophile. The outcome of this nucleophilic addition reaction can be grouped into three distinct regiochemically divergent products (**Scheme 102**); (a) addition

over the α, β-double bond of the allene (**372**); (b) addition over the β, γ-double bond of the allene (**373**); and (c) addition at both the α- and γ-positions (**374**) by two nucleophiles. The thought process behind this approach is based on the intramolecular radical cyclization of allenamides reported by Hsung and co-workers.[125].

**Scheme 102**: Electrophilic activation of allenamides
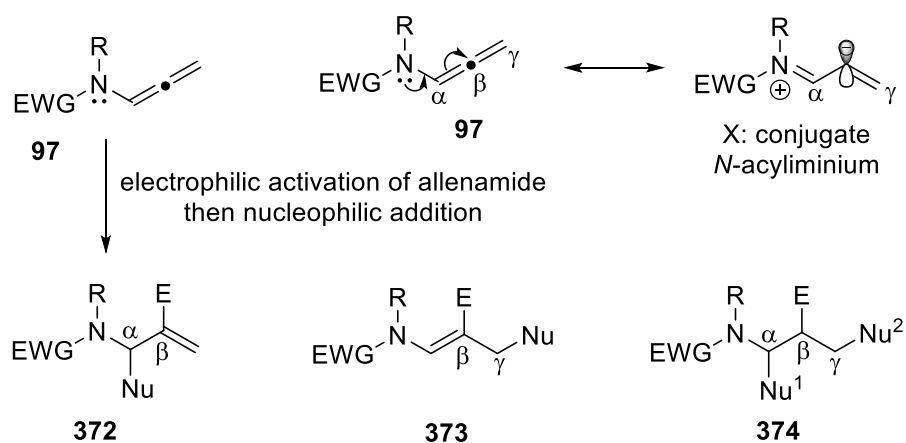
We envisage that the photoredox catalysed addition developed on enamides can be used on allenamides. However, unlike enamides the addition of the malonate radical to the allenamide, followed by oxidation to the iminium should furnish the conjugated *N*-acyl iminium ion **379** (**Scheme 103**). This intermediate can then be intercepted by an appropriate nucleophile, but importantly, this can occur at either the α- or γ-position, therefore leading ultimately to the products **98** and **99** (**Scheme 104**). Therefore, the three component domino reactions of allenamide, diethyl bromomalonate as the electrophile source and the nucleophile, which could be oxygen and nitrogen, will be examined.

Scheme 103: Photoredox catalysed generation of conjugated *N*-acyliminium ion
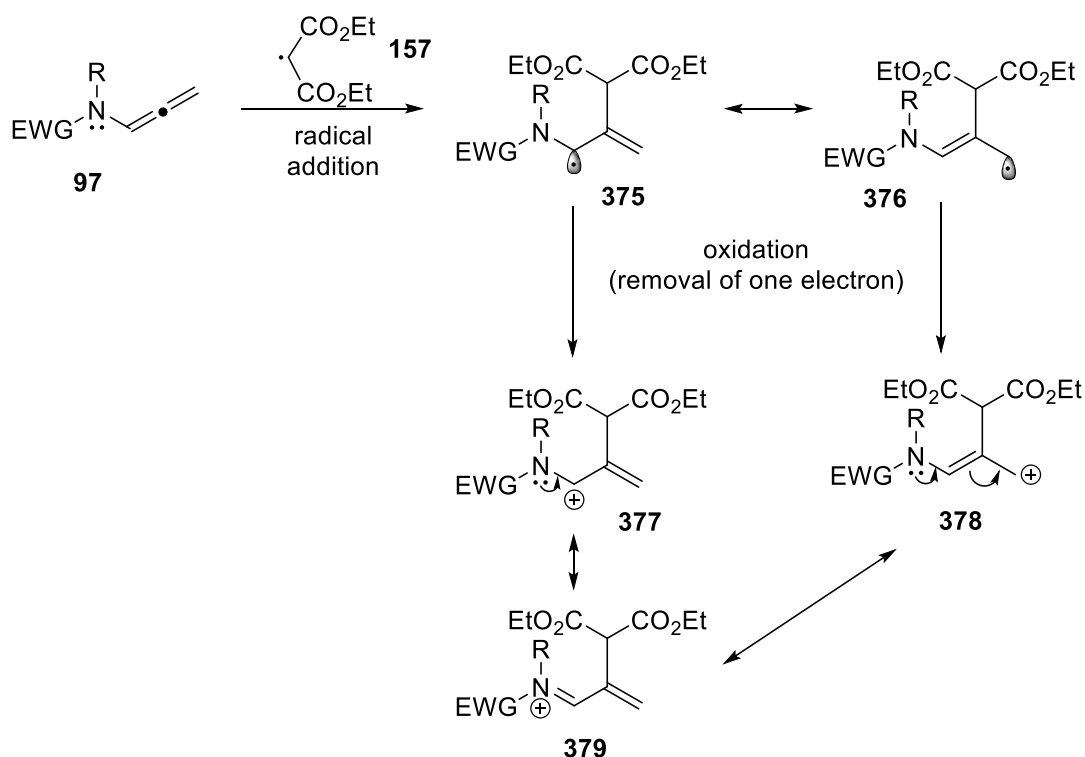
Scheme 104: Addition of nucleophile to the *N*-acyl iminium ion intermediate **379**
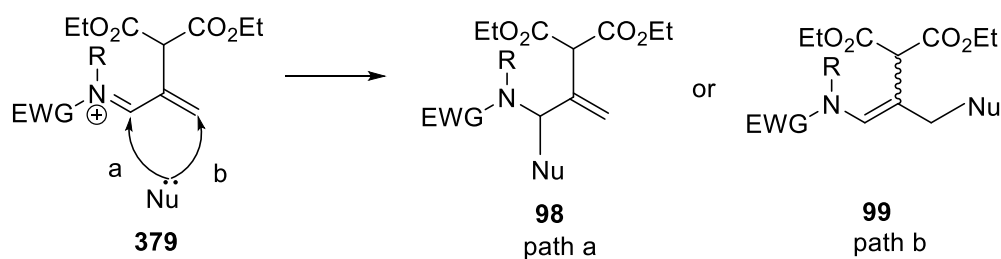
Therefore to test our hypothesis above we required sufficient amounts of allenamides precurosrs, which would be synthesized using the standard method reported in the literature by Kimber *et al.*[101]

4.4.1 Allenamides Synthesis

*Synthesis of N-Allenyl-2-oxazolidinone*

The allenamide was synthesized from oxazolidin-2-one **114** using the one-pot protocol reported earlier by the Kimber's research group (**Scheme 83**). There was no need for the reaction optimisation since this had been done by the previous members of the research

group, except when some challenges arose and the integrity of the reagents used had to be verified.

The reaction was carried out in dry/anhydrous dimethylsulfoxide DMSO under an inert atmosphere of argon. It involves the combination of all the reagents, oxazolidin-2-one, potassium tert-butoxide (*t*-BuOK) and propargyl bromide in one reaction pot. The yield was greatly affected by the dryness and freshness of the t-BuOK, with fresh, anhydrous *t*-BuOK giving higher yield of the product than the stock *t*-BuOK. The rate at which the propargyl bromide is added into the reaction mixture also has some effects on the final yield of the product. It was found that when the propargyl bromide was added too rapidly, a lot of heat was generated and a mixture of the allenamide and the propargyl amide was formed. In the initial attempt, the ratio of the allenamide to the propargyl amide formed was determined from the ^{1}H-NMR spectrum to be 81:19. The signals obtained from the ^{1}H-NMR indicated the presence of the two isomers: the ^{1}H-NMR signals of the hydrogen atoms of the allenyl group of the allenamide showing at δ 6.84 ppm for the hydrogen atom on the C=C next to the nitrogen atom of the ring appearing as triplet due to the coupling effect of the two terminal hydrogen atoms of the second C=C whose signal at δ 5.41 ppm appears as a doublet. The hydrogen atoms of the propargyl group for the propargyl amide fraction showed at δ 4.04 ppm for the two hydrogen atoms on the carbon next to the nitrogen appearing as doublet due to the coupling effect of the hydrogen atom on the terminal *sp*-carbon which appeared triplet at δ 2.28 ppm. However, when the propargyl bromide was added drop-wise over an extended period of time the ratio of the allenamide to the propargyl amide increased in favour of higher quantity of allenamide. The time frame of about 45 minutes drop-wise addition gave the allenamide with little or no propargyl amide isomer.

Having successfully prepared *N*-allenyloxazolidin-2-one **304**, we then extended the scope of the reaction to other different amide substrates for their conversion to allenamides. The substrates included *N*-methyl-*p*-toluenesulfonamide, (*S*)-4-benzyloxazolidin-2-one, (*S*)-4-isopropyloxazolidin-2-one, pyrrolidin-2-one, piperidin-2-one and ε-caprolactam all of which gave comparable yields (Table 10).

Scheme 83: Kimber's one-pot protocol
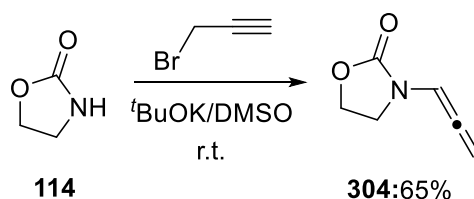
The reaction is thought to commence with the deprotonation of dimethyl sulfoxide **380** by the tert-butoxide ion **381** forming methylsulfinymethylide ion **382** that in turn deprotonate oxazolidin-2-one **114** to give the 2-oxooxazolidin-3-ide anion **383**. The 2-oxooxazolidin-3-ide anion then attacks the alkynyl carbon of propargyl bromide **266** in an S_N2 reaction pushing a pair of π-electron to move towards bromine for easy elimination as a bromide ion being a good leaving group to afford the intermediate 3-propargyl-2-oxazolidinone **384** from which the base abstracts a proton and isomerizes to the product **304** (**Scheme 105**).

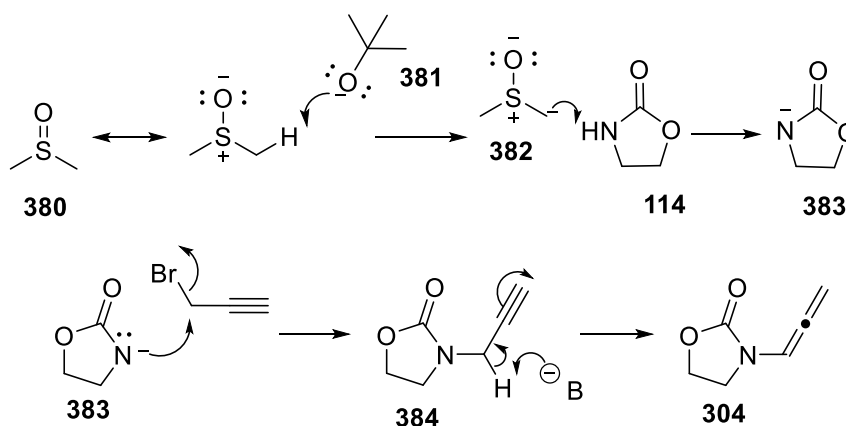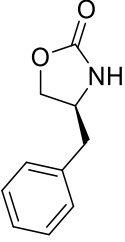**Scheme 105**: Proposed mechanism for the transformation
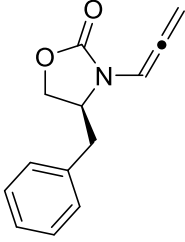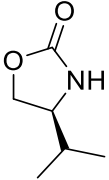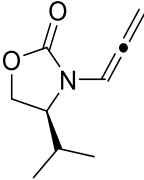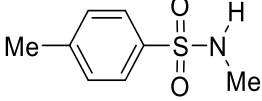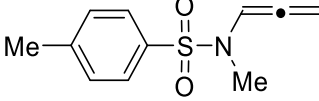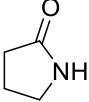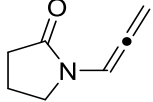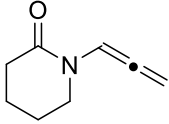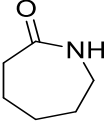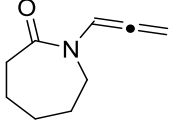
Table 10: Synthesis of allenamides

Entry	Substrate	Product	Yield [%]
1	**114**	**304**	72

118

2	**167**	**384**	51
3	**385**	**386**	60
4	**387**	**388**	78
5	**265**	**268**	61
6	**389**	**390**	68
7	**391**	**392**	80

4.4.2 Allenamides: Photoredox Catalysed Transformation Reactions

The considerable stability of the allenamides as compared to allenamines due to the presence of an electron withdrawing group attached to the nitrogen gives allenamides their characteristic reactivity profiles that attract attention of synthetic community in the recent time. Allenamides display distinct reactivity from the traditional allenes as a result of the presence of the nitrogen atom attached at the α-carbon. The nitrogen atom of the amide unit can donate electron density into the allene central β-carbon. This exclusive distinct characteristic profile can be harnessed in various chemical transformations and has led to its use in innovative transformations such as cycloadditions, Aldol additions, cyclizations and intermolecular addition reactions.

The versatility of the allenamide functional group has been exploited by a considerable number of researchers, as stated earlier. The radical cyclization reaction reported by Hsung and co revealed the chemical tra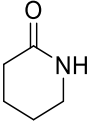nsformations of allenamides leading to regiochemical confidence in the resulting products. However, no one to our best knowledge has involved allenamide in photoredox transformation.

We started by subjecting our prepared allenamide **304**, 3-(propa-1,2-dien-1-yl)oxazolidin-2-one to the Courant and Masson[53] conditions of photoredox reaction just as we did with the enamide. We added our iridium photocatalyst and the allenamide in the reaction vessel with degassed anhydrous acetonitrile followed by the addition of the alkylating reagent, diethyl 2-bromomalonate, triethylamine and the nucleophile, etha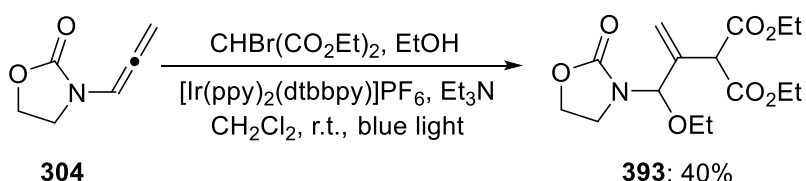nol. After the irradiation with the Kessil® LED blue light ($\lambda = 465$ nm), we obtained the adduct product **393** of the type (a) in the Scheme 97 where the addition is α,β-adduct with *exo*-methylene (**Scheme 106**).

**Scheme 106**: Photoredox of allenamide (**304**) with ethanol

The adduct product, diethyl 2-(3-ethoxy-3-(2-oxooxazolidin-3-yl)prop-1-en-2-yl)malonate (**393**) is very similar to the adduct product **177** of enamide **117** except that the carbon atom joining the *N,O*-acetal moiety and the malonate group is now an *sp²* hybridized carbon with a

double bond with another carbon. This feature is significant in its identification and confirmation. The formation of the desired product was confirmed by ^{1}H-NMR, ^{13}C NMR and mass spectrometry. The ^{1}H NMR revealed the disappearance of the signals of the hydrogen atoms of the allene group of the allenamide. The diagnostic signal of the adduct product at δ 5.60 ppm for the hydrogen atom of the carbon bearing the nitrogen atom of the ring and oxygen atom of the ethoxy group, i.e. the *N,O*-acetal carbon emerged as singlet and the two vinylic protons appeared in the ^{1}H NMR spectrum at δ 5.56 ppm and δ 5.42 ppm, respectively. The hydrogen atom on the carbon bearing the malonate moiety appeared at δ 4.05 ppm as singlet. The hydrogen atoms of the ethoxy group of the *N,O*-acetal moiety showed at δ 3.54 ppm for O-CH$_2$- which appeared as quadruplet due to the coupling effect of the neighbouring methyl group hydrogen atoms (-CH$_2$-CH$_3$) which appear as triplet at δ 1.18 ppm on the spectrum.

Having obtained the desired adduct product with the use of ethanol, we then decided to find out the scope of the reaction with other oxygen nucleophiles. We made use of isopropanol and methanol. Isopropanol also gave an adduct product with the isolated yield of 33%. However, the combination of COSY and HMQC experiments from the NMR, revealed that the nucleophilic addition did not occur at the α-carbon to give *hemi*-aminal product rather it was attached to the γ-carbon to give product **372**. Therefore this gave the β,γ-adduct product; that is the addition product of the path (b) as seen in **Figure 16** (**Scheme 107**).

Scheme 107: Photoredox of allenamide (**304**) with isopropanol
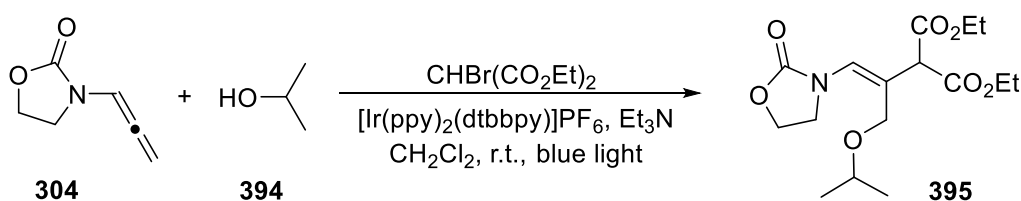
When methanol was used, the crude ^{1}H NMR showed peaks of the formation of the adduct product, however this product could not be isolated from the reaction matrix. The *hemi*-aminal product is unstable in acid condition and decomposed in silica gel, as it is slightly acidic. It protonates the oxygen of the methoxide group of the *hemi*-aminal and methanol is released as a leaving group (**scheme 108**). Therefore, it could not be isolated from the reaction mixture.

Scheme 108: Decomposition of methyl hemiaminal in silica gel
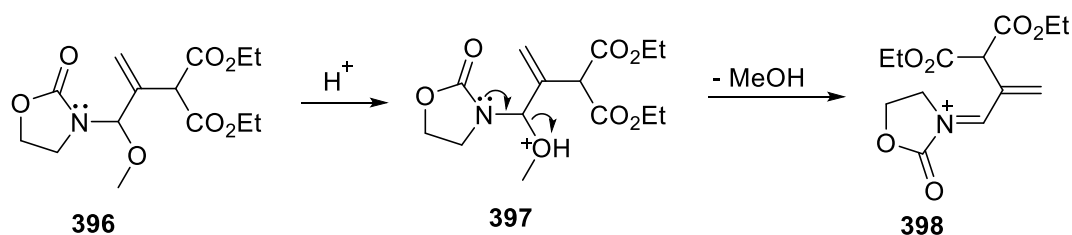
The allenamide **304** was then subjected to the reaction conditions to investigate its performance with a range of aryl amines (**Scheme 109**). We began with *p*-toluidine together with diethyl 2-bromomalonate **77** under our reaction conditions which gave the *exo*-methylene **399** as the only isolable product in 53% yield. This *exo*-methylene reaction product was conclusively identified by the characteristic vinylic protons within the ^{1}H NMR at δ 5.48 ppm and δ 5.45 ppm as doublets, respectively.
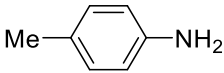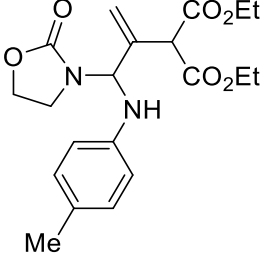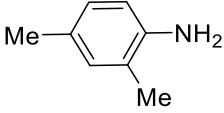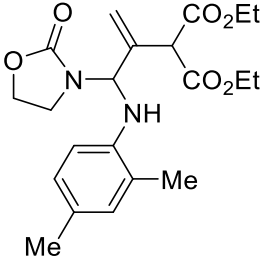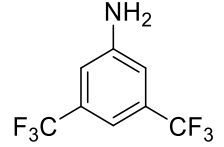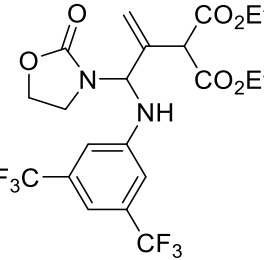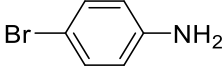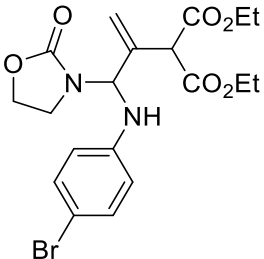
Scheme 109: Photoredox of Allenamide (**304**) with Aryl amines
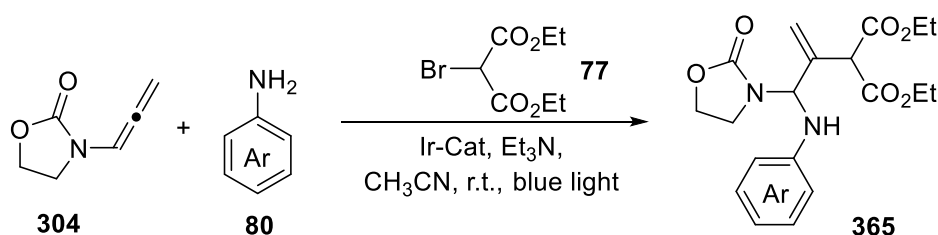
The reaction was then carried out on a range of electron donating and electron withdrawing aryl amines with all the adduct product isolated with *exo*-methylene products as the only isolable products. The results are as shown in **Table 11** below. 2,4-Dimethylaniline reacted giving the adduct product **400** with 57% yield. This yield was marginally higher than that of *p*-toluidine possibly because of its higher nucleophilicity as a result of the positive inductive effects of the two methyl groups on the benzene ring. Arylamine with electron withdrawing groups as substituents also undergo the reaction with the allenamide but with slightly reduced yield. 3,5-Bis(ditrifluoromethyl)aniline, *p*-bromoaniline and 4-bromo-2-fluoroaniline reacted to give products **401, 402** and **403** with isolated yields 45%, 49% and 46% respectively. However, o-anisidine and its 2-OCF$_3$ analogue reacted giving the products **404** and **405** with isolated yields of 51% and 53%, respectively. The higher yield obtained in these cases may be explained by the positive mesomeric effects over the inductive effects as observed in the cases of 3,5-bis(ditrifluoromethyl)aniline and 4-bromo-2-fluoroaniline. The contribution of

the lone pairs on the oxygen atoms in the increased electron density of the ring making the arylamine relatively more nucleophilic led to the increase in the yield.
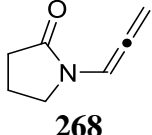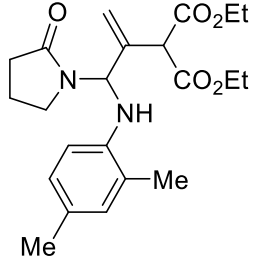
Table 11: Products of photoredox reaction of allenamide **304** with different arylamines

Entry	Nucleophile	Product	Yield (%)
1	Me⟶NH$_2$ **180**	**399**	53
2	Me, Me ⟶NH$_2$ **184**	**400**	57
3	NH$_2$, F$_3$C, CF$_3$ **192**	**401**	45
4	Br⟶NH$_2$ **194**	**402**	49

5	NH₂, F, Br **198**	**403**	46
6	NH₂, O-Me **202**	**404**	51
7	NH₂, O-CF₃ **204**	**405**	53
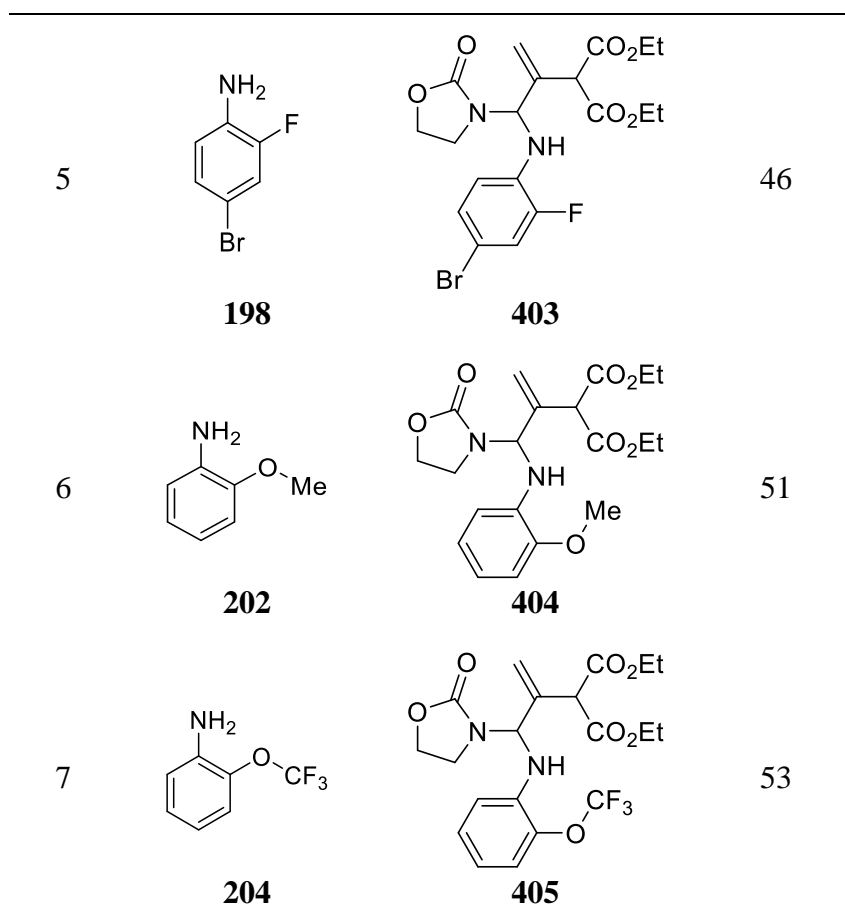
The reaction was also carried out on a range of different allenamides to investigate the generality of the reaction using the same arylamine, 2,4-dimethylaniline (**184**). Allenamides **268**, **390** and **392** gave the *N,N'*-aminal product with *exo*-methylene group **406**, **407** and **408** with the yield 54%, 41% and 43%, respectively as shown in **Table 12**.

Table 12: Photoredox reaction products with different allenamides

Entry	Allenamide	Product	Yield (%)
1	**268**	**406**	54

2	**390**	**407**	41
3	**392**	**408**	43
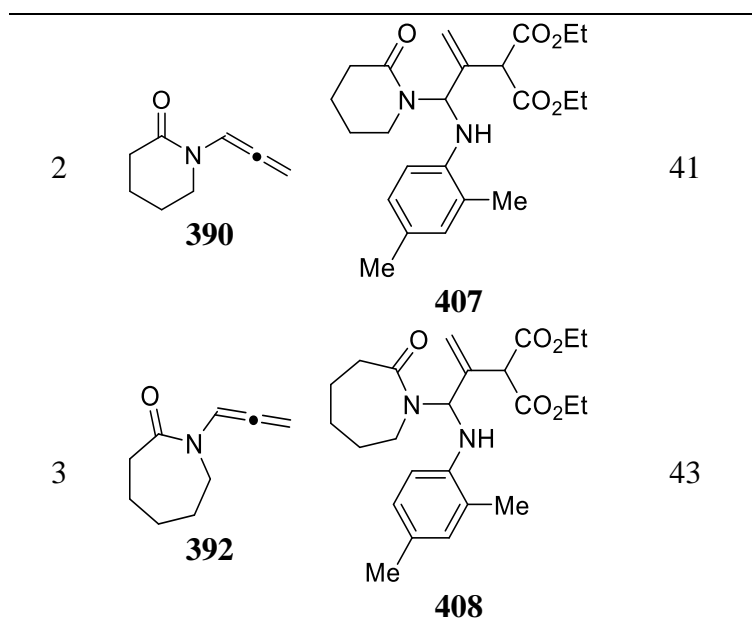
Allenamide **268** reacted with 4-bromo-2-fluoroaniline **198** and gave the adduct product **409** with 42% isolated yield (**Scheme 110**).

Scheme 110: Photoredox reaction of allenamide **268** with arylamine **198**
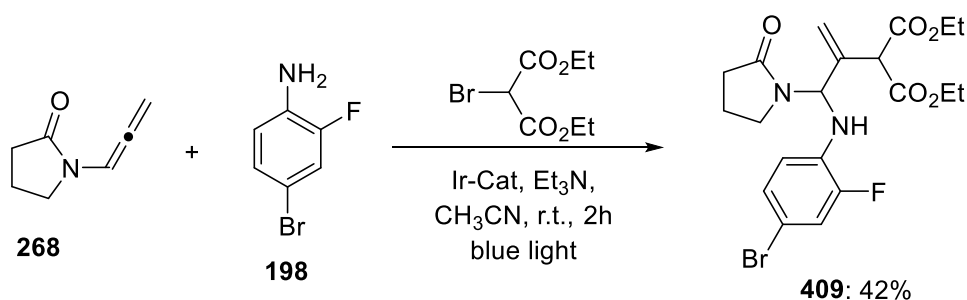
Attempt was also made to investigate the stereoselectivity of the reaction by using chiral allenamides **384** and **386**. We started with (*S*)-4-benzyl-3-(propa-1,2-dien-1-yl)oxazolidin-2-one **384**, adduct product of the β,γ-addition was obtained **410** with the isolated yield of 41% (**Scheme 111**).

Scheme 111 : Photoredox catalysed β-alkylation-γ-arylation of the chiral allenamide
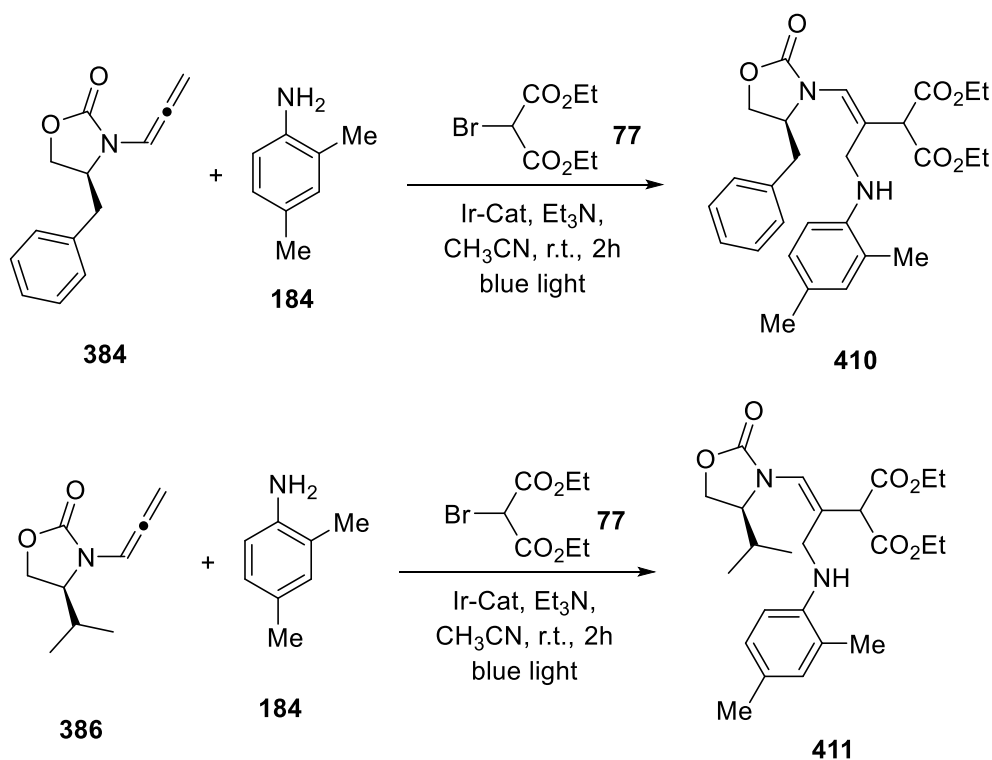
The structure of the product obtained from the reaction of **384** with **184** was determined using ^{1}H NMR, HMQC and NOE experiments. Analysis of the spectroscopic data confirmed the structure to be as shown. The NOE experiments showed a strong interaction (enhancement) between the hydrogen atom on the α-carbon (δ 6.38 ppm) and the hydrogen atom (δ 4.28 ppm) on carbon bearing the carbonyl groups of the malonate moiety when the hydrogen at δ 6.38 ppm was energized indicating that the two hydrogen atoms are on the same side of the C=C double bond adjacent to the nitrogen atom of the ring (**Figure 17**). Hence, the product is the Z-isomer. Similarly, chiral allenamide **386** reacted to give the adduct product **411** in the same way allenamide **384** reacted. **386** gave product **411** in isolated yield of 50%.

Figure 17: Result from the nOe experiments

(*E*)-**410**   (*Z*)-**410**
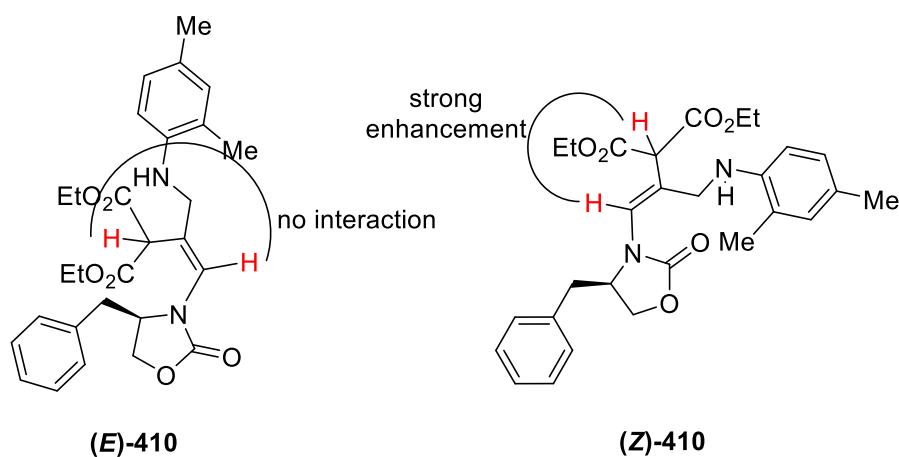
The mechanism of the reaction is presumed to be similar to that of the photoredox reactions of the enamide as described in **Scheme 67**. The product outcome observed in **Scheme 106** results from addition of electrophilic diethyl malonate radical **157** to the central allenic carbon of the allenamide **304** to give the radical **412**, this radical is then oxidized by losing an electron to either the triethylaminium radical ion **231** or the reduced form of the photoredox catalyst to afford the conjugated *N*-acyl iminium ion **398**. This is followed by addition of the nucleophile to either the α- or γ-position of the resultant conjugated *N*-acyl iminium ion species **398** (**Scheme 112**) leading to the observed products **415** or **416**, respectively. This approach therefore has the potential to open new opportunities in the application of allenamides in complex and total synthesis, outside of these classical activation pathways in which the nucleophile attacks only the γ-carbon.

Scheme 112: Proposed Mechanism for the Photoredox Reaction
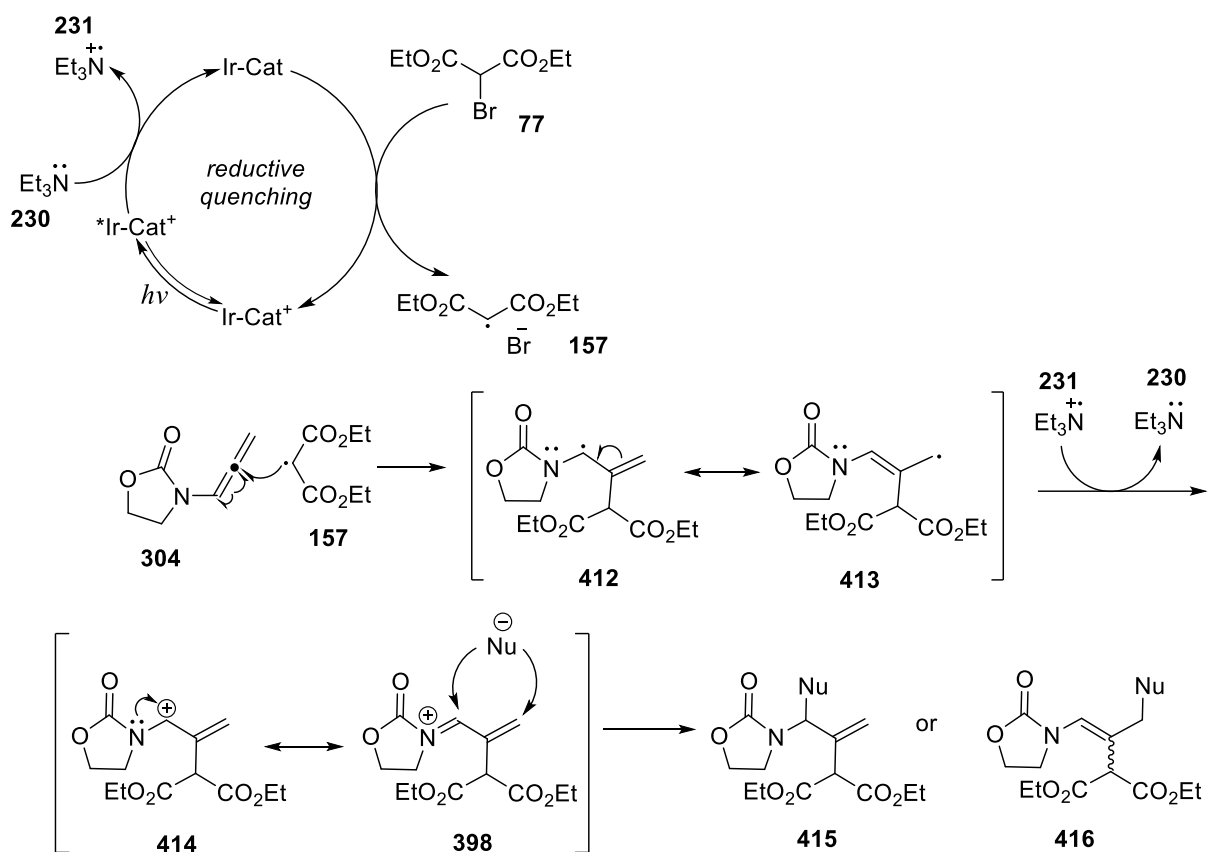
However, when carbon nucleophiles were used in this reaction, the desired adduct products were not obtained. For instance, when *N*-methyl-indole **417** was used, adduct product **418** was not isolated instead compounds **419** and **420** were obtained. Similarly, 1,3,5-trimethoxybenzene did not give the adduct product from the reaction. (**Scheme 113**)

Scheme 113: Photoredox reaction of allenamide (**304**) with *N*-methylindole
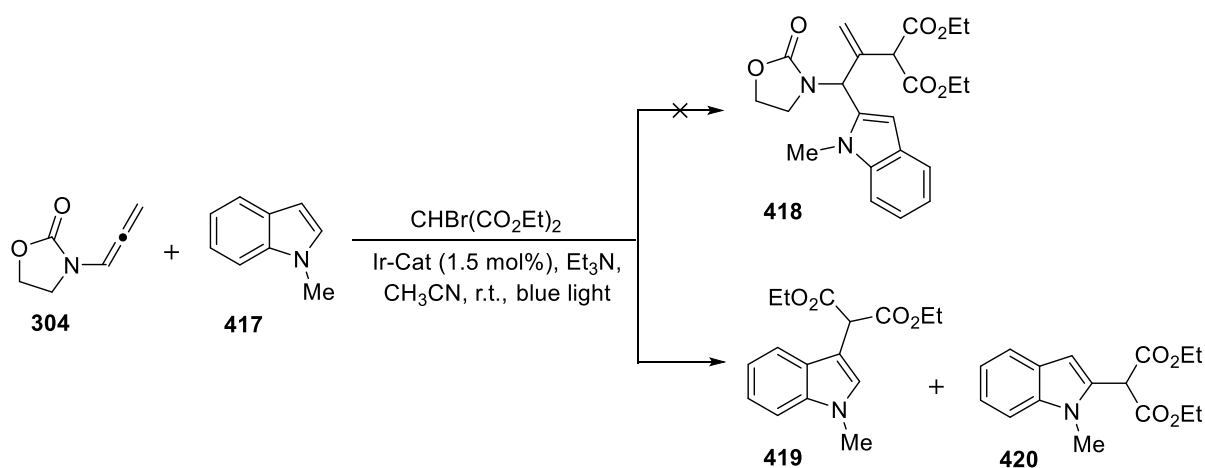
5.0 Future Work

The important impediments associated with the chemical industries are the exhaustion and nonrenewal of fossil fuels, and the global warming. The search for clean, renewable and environmentally friendly energy source[4,6] in the preparation of valuable synthetic building blocks and biologically important molecules has become essential. In this endeavour, photocatalysis using visible light represents a unique strategy because of its inherent "green chemistry" features.[40]

5.1 Enamides

The vast majority of biologically active molecules and pharmaceutical compounds contain nitrogen heterocycles.[126] The photoredox catalysed β-alkylation-α-amination of enamides had been developed and used to prepare many varieties of *N*-acyl-*N,N'*-aminals compounds which have also been cyclized into γ-lactams. These are compounds that contain nitrogen heterocycles. More analogues of these aminals and their corresponding γ-lactams need to be prepared to build a library and for biological testing that was the driving for the research project.

The reaction protocol can further be extended by varying the substituent groups around the enamides and using substituted malonate **422** to generate quaternary centres. Future work could also be done on the cyclized products, the γ-lactams, such as decarboxylation (**Scheme 114**).

Scheme 114: Proposed expansion of the reaction methodology on other substrates
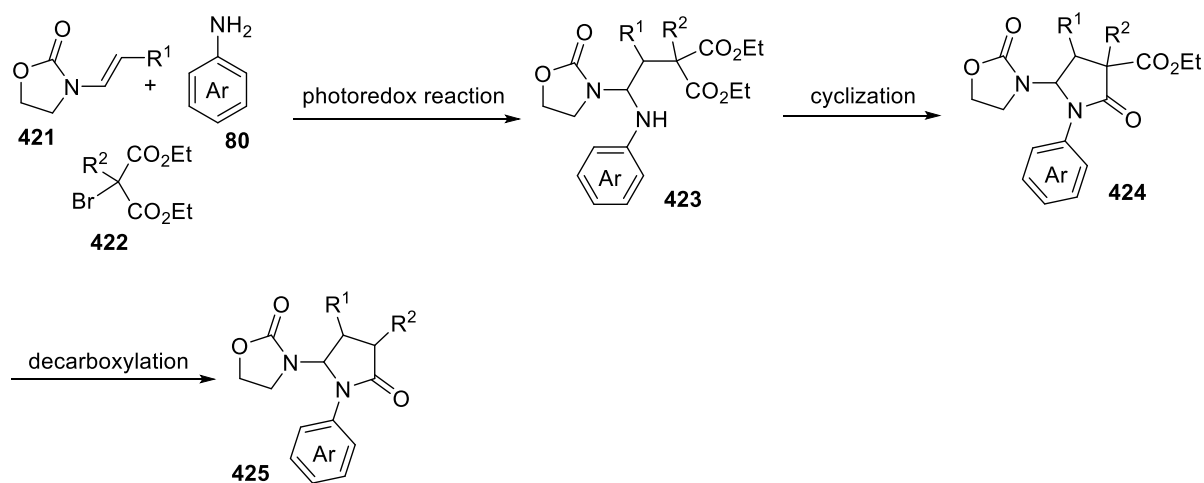
The application of this newly developed synthetic route could be exploited in the synthesis of lamellarins **434** (**Scheme 115**). Lamellarin alkaloids are a family of marine natural products that contain a pyrrolo[2,1-a]isoquinoline core. They were found to exhibit a wide spectrum of biological activities.[127]

The main steps in the lamellarin alkaloid shown in the scheme **115** below are the preparation of the enamide **430** and the subsequent photoredox catalysed β-alkylation of the enamide using diethyl bromomalonate as the alkylating agent (**Scheme 115**, steps c and d) to obtain the product **431** that can be cyclized to the γ-lactam containing product **432**. Since this reaction procedure tolerates many functional groups, it should be possible to achieve.

Scheme 115: Application of the photoredox catalysis in lamellarin synthesis
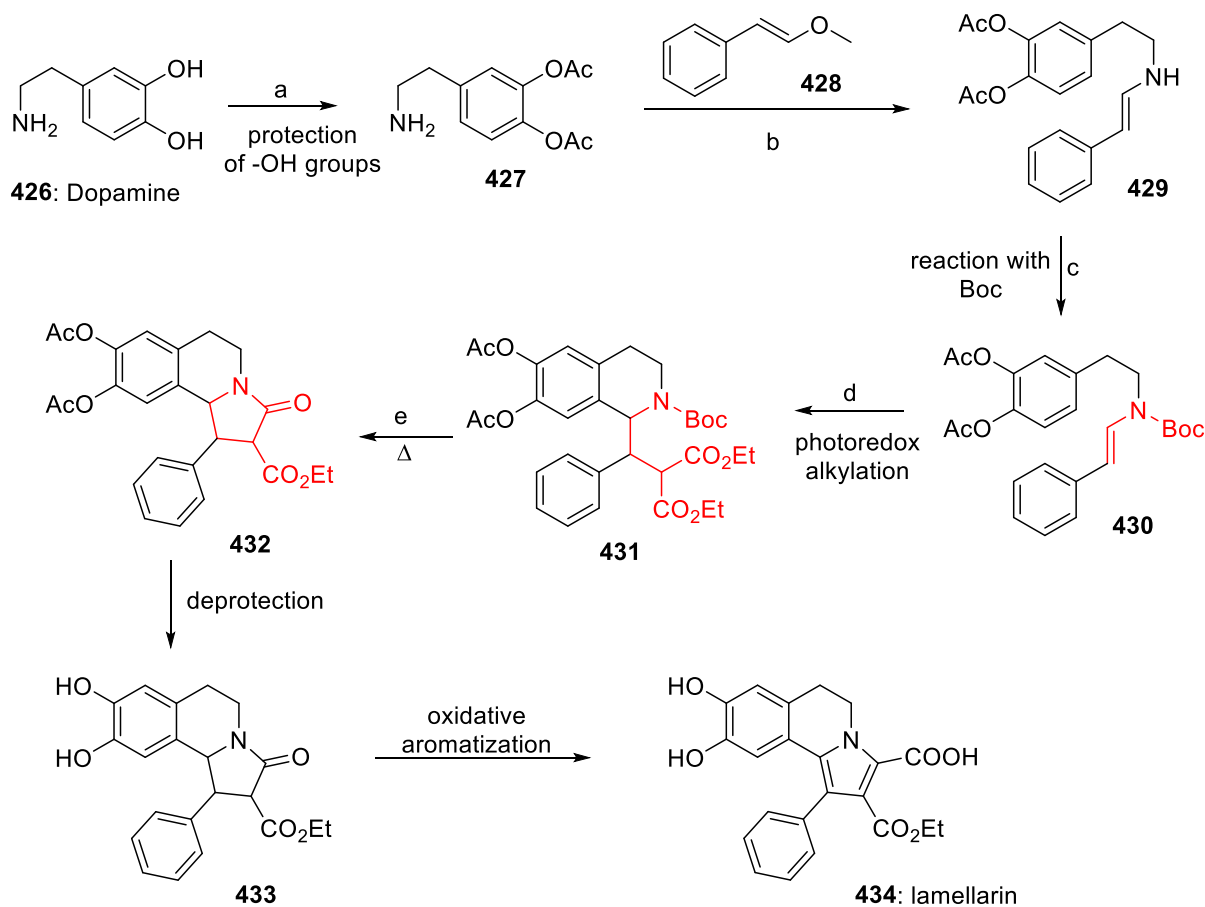
5.2 Allenamides

Addition reaction of allenamides using the photoredox catalysed electrophilic malonate radical activation of the central β-carbon of the allenamide with the formation of a conjugated *N*-acyliminium and its subsequent trapping arylamine nucleophiles is a unique and novel synthetic method in engaging allenamides in photoredox reactions. The outcome of this addition reaction was the formation of *N,N'*-aminals with exo-methylene group or double bond substituted enamides.

This approach therefore has the potential to open new opportunities in the application of allenamides in complex and total synthesis, outside of these classical activation pathways in which the nucleophile attacks only the γ-carbon.

For example, the *N,N'*-aminal products can be cyclized to give fully substituted lactams like the addition product of the enamides. The advantage of the exo-methylene double bond can

also be taken in synthesis. The use and transformation of the enamides has just been described, therefore the second group of the products from the addition reactions of allenamides can also be subjected to the same reactions to give rise to the synthesis of complex natural products.

Scheme 116: Possible future work on the addition products of allenamides
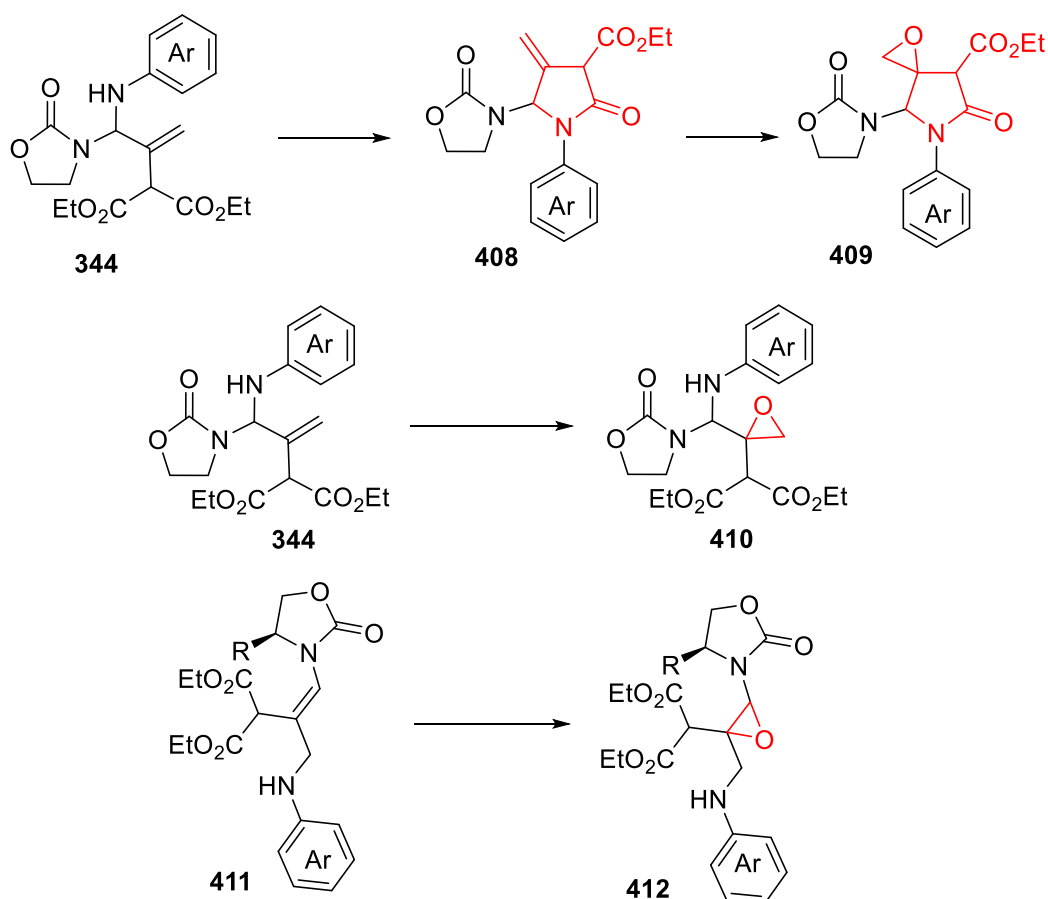
In this project we examined the addition of bromomalonate to enamides and allenamides. Masson has already demonstrated[83,128] the addition of CF_3 radical equivalents to enamides, and it therefore follows by analogy that similar CF_3 additions to allenamides could be accomplished (**scheme 110**). This would greatly expand this chemistry and give a method for the addition of the CF_3 group to the central allenic carbon of the allenamide which is not currently possible using current electrophilic activation methods.

Scheme 110: Proposed photoredox catalysed trifluoromethylation of allenamides
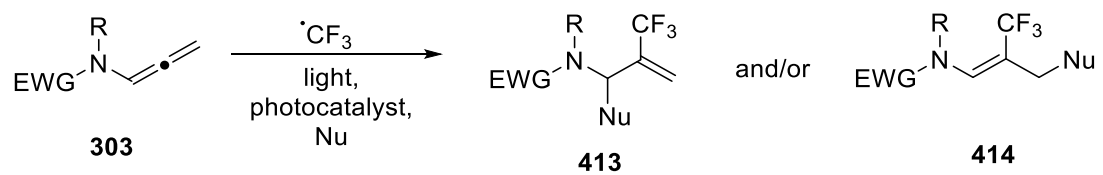
6.0 Experimental

All reactions were carried out using commercially available reagents and solvents throughout without further purification, except dichloromethane (CH_2Cl_2) and triethylamine (Et_3N) which were dried using 4Å molecular sieve. DMSO and acetonitrile were purchased dry from commercial suppliers. Light petroleum refers to the fraction with bp 40-60 °C. Thin layer chromatography was carried out on Merck Kieselgel 60 GF254 aluminum foil backed plates. The plates were visualized under UV light or with vallinin stain. Flash chromatography was carried out using Merck Kieselgel 60H silica or Matrix silica 60, with the eluent as specified in the individual syntheses. IR spectra were recorded using Perkin Elmer FTIR Spectrometer (Paragon 100) as solutions in CH_2Cl_2, unless otherwise stated. ^{1}H and ^{13}C NMR spectra were recorded using Bruker 400 MHz NMR machine and a JEOL ECS-400 MHz NMR machine; chemical shifts are quoted in ppm and coupling constants, *J*, are quoted in Hz; chloroform-d was used throughout unless otherwise stated. 13C-NMR spectra are recorded without 19F decoupling. For compounds containing fluorine line values are reported as multiplet signals could not easily be identified. High and low resolution mass spectra were carried out on a Thermofisher exactive (orbi) resolution mass spectrometer. All crystal data were measured using a Bruker APEX 2 CCD diffractometer equipped with Mo-Kα radiation (λ = 0.71073 Å) at 150K, except otherwise stated, with the assistance of Dr. Mark J. Elsegood.

Synthetic Procedures

N-(Ethenyl)-oxazolidin-2-one (117)
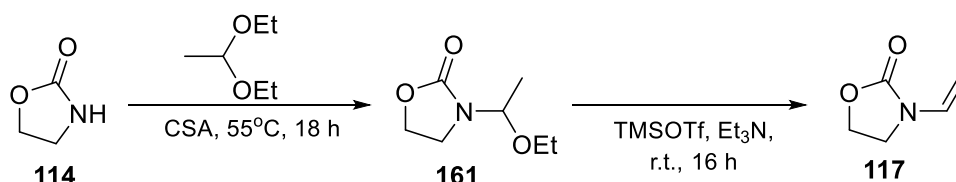
Step 1: Preparation of Intermediate *N*-(1-ethoxylethyl)-2-oxazolidinone (161)

A mixture of 2-oxazolidinone **114** (2.05 g, 23.4 mmol), acetaldehyde diethyl acetal (33 mL, 0.23 mol) and DL-camphorsulfonic acid (0.27 g, 1.17 mmol) was heated for 21 h at 55 °C.

After cooling, aq. NaHCO$_3$ (15 mL) was added and the reaction mixture extracted with Et$_2$O (3×10 mL). The organic layer was washed with brine and dried over MgSO$_4$ and filtered. Removal of solvent yielded crude *N,O*-acetal used without further purification (3.65 g, 98%). ^{1}H-NMR (400 MHz, CDCl$_3$) δ 5.12 (q, J = 6.0 Hz, 1H), 4.27 (dd, J = 13.0, 8.0 Hz, 2H), 3.46 (t, J = 8.0 Hz, 2H), 3.39 (dd, J = 12.4, 7.0 Hz, 2H), 1.26 (d, J = 6.2 Hz, 3H), 1.09 (t, J = 7.2 Hz, 3H). This is in agreement with literature.[67]

Step 2: Preparation of N-vinyl-2-oxazolidinone (117)

To a cooled solution (0 °C) of crude *N,O*-acetal (3.72 g, 23.4 mmol) in anhydrous CH$_2$Cl$_2$ under nitrogen (22 mL) were dropwise added distilled NEt$_3$ (4.9mL, 37.7mmol) and, trimethylsilyl triflate (5.5 mL, 30.4 mmol). After slow return to room temperature and stirring for 16 h, the mixture was filtered through basic alumina. Removal of solvent and purification by filtration (silica gel 4/1; ether) yielded enamide **117** as a pale yellow oil (2.02 g, 76%). ^{1}H-NMR (400 MHz, CDCl$_3$) δ 6.77 (dd, J = 15.9, 8.9 Hz, 1H), 4.39 (d, J = 9.5 Hz, 1H), 4.36 (t, J = 8.2 Hz, 2H), 4.23 (d, J = 15.7 Hz, 1H), 3.65 (t, J = 8.2 Hz, 2H) ppm. ^{13}C-NMR (100Mz, CDCl$_3$) δ 155.44, 129.69, 93.50, 62.39, 41.91; HRMS [M+H] calculated for C$_5$H$_8$NO$_2$ 114.0550 found 114.0550. This agreed with literature.[67]

(*E*)-*N*-(Hex-1-en-1-yl)-oxazolidin-2-one (171)
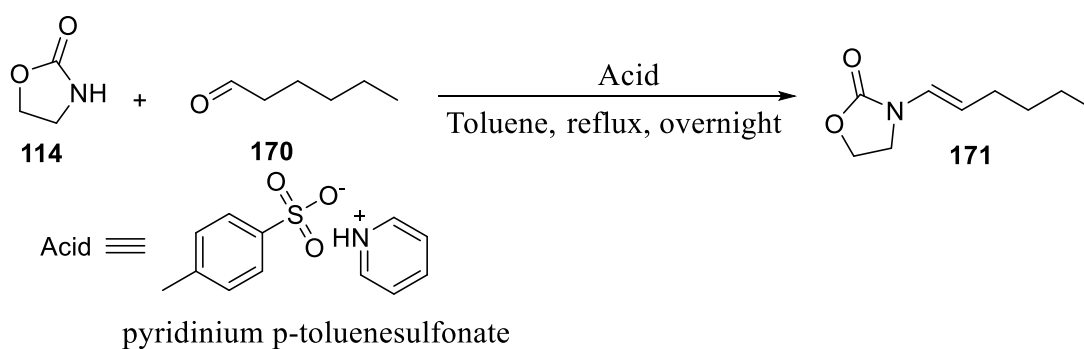
The procedure reported by Liu and Floreancig[78] was used for the synthesis of *E*-vinyl oxazolidinones: A solution of 2-oxazolidinone (0.91 g, 10.5mmol), hexanal (1.2 mL, 10.0mmol) and pyridinium *p*-toluenesulfonate (0.25 g, 1.0mmol) in toluene (50 mL) was heated at reflux in a 100 mL round bottom flask fitted with a Dean-Stark apparatus to trap water overnight. After the completion of the reaction, upon disappearance of the starting material monitored via TLC, the reaction mixture was allowed to cool to room temperature and concentrated *in vacuo*. Further purification was performed using silica gel flash column

chromatography (hexane/EtOAc 7:3) to afford the product **171** as a pale yellow oil (0.868g, 5.14 mmol). Yield 52%. ^{1}H-NMR (400 MHz, CDCl$_3$) δ 6.56 (d, J = 14.4 Hz, 1H), 4.81-4.70 (m, 1H), 4.36 (t, J = 8.0 Hz, 2H), 3.63 (t, J = 8.0 Hz, 2H), 2.00 (q, J = 7.1 Hz, 2H), 1.36-1.18 (m, 4H), 0.83 (t, J = 6.6 Hz, 3H) ppm; ^{13}C-NMR (100 MHz, CDCl$_3$) δ 155.53, 123.74, 111.43, 62.22, 42.68, 32.23, 29.50, 22.09, 13.93 ppm; HRMS [M+Na] Calculated for C$_9$H$_{15}$NO$_2$Na 192.0995, found 192.0995.

(*S*)-4-Benzyl-3-vinyloxazolidin-2-one (169)
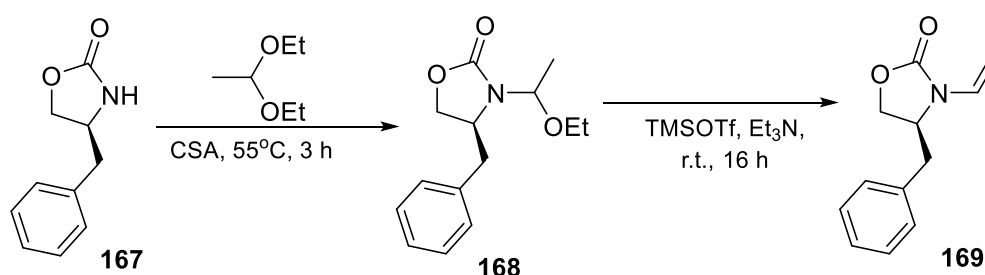
Step 1: Preparation of Intermediate (*S*)-4-Benzyl-3-(1-ethoxylethyl)-2-oxazolidinone (168)

A mixture of *S*-(-)-4-benzyl-2-oxazolidinone **167** (1.77g, 10 mmol), acetaldehyde diethyl acetal (14.1 mL, 100 mmol) and DL-camphorsulfonic acid (0.115g, 0.5 mmol) was placed in a 50 mL round bottom flask and heated for 3 hours at 55 °C. After cooling and dilution with Et$_2$O (40 mL), saturated aqueous NaHCO$_3$ solution (10 mL) was added and the organic phase separated from the mixture. The organic phase was then washed with brine (10 mL) and dried over MgSO$_4$ and filtered. Removal of solvent yielded a crude *N,O*-acetal which was used in the second step without further purification. (*S*)-4-benzyl-3-(1-Ethoxyethyl)-oxazolidin-2-one **168** was obtained as a colourless oil.

Step 2: Preparation of (4S)-4-Benzyl-3-vinyl-2-oxazolidinone (169)

To a cooled solution (0 °C) of crude *N,O*-acetal **2** (10 mmol) in anhydrous CH$_2$Cl$_2$ (10 mL) was added under nitrogen distilled Et$_3$N (15 mmol), then dropwise, TMSOTf (13 mmol). After slowly warming to r.t. and stirring for 18 h, the mixture was treated with basic alumina to remove the excess of TMSOTf. After removal of the solvent, the residue was filtered through silica gel (Et$_2$O) to remove the ammonium triflate salts and was purified by flash chromatography. The chromatographic purification (silica gel; cyclohexane-EtOAc, 7:3)

afforded the product **169** (*S*)-4-benzyl-3-vinyl-2-oxazolidinone (0.93 g, 90%) as a colourless viscous oily liquid. R_f 0.37 (Hexane-EtOAc, 7:3). ^{1}H-NMR (400 MHz, CDCl$_3$) δ 7.40-7.03 (m, 5H), 6.80 (ddd, *J* = 16.4, 9.0, 2.8 Hz, 1H), 4.65-4.42 (m, 2H), 4.37-3.96 (m, 3H), 3.18 (d, *J* = 14.0 Hz, 1H), 2.77 (ddd, *J* = 13.8, 8.7, 2.7 Hz, 1H) ppm; ^{13}C-NMR (100 MHz, CDCl$_3$) δ 155.18, 135.31, 129.42, 129.04, 128.90, 127.42, 94.22, 66.61, 54.42, 35.89 ppm; HRMS [M+H] calculated for C$_{12}$H$_{14}$NO$_2$ 204.1016, found 204.1019.

N-(Propa-1,2-dien-1-yl)-2-oxazolidinone (304)

A 100 mL round bottom flask was equipped with a magnetic stir bar and filled with argon to evacuate air. The flask was then charged with 2-oxazolidinone **114** (0.871 g, 10.0 mmol) in dry DMSO (20 mL) under an argon atmosphere and *t*-BuOK (1.683 g, 15.0 mmol) added, sealed with a rubber septum and filled with argon to provide an inert atmosphere. The mixture was stirred for 1 hour at room temperature. To this mixture was added propargyl bromide (1.25 mL, 80% solution in toluene, 11.0 mmol) dropwise over 40 minutes using syringe pump. After the addition was complete, the mixture was stirred at room temperature overnight under argon. The reaction mixture was then diluted with distilled water (50 mL) and extracted with EtOAc (3 × 50 mL). The combined organic extracts were washed with water (2 × 50 mL) and finally with brine (30 mL) to remove the residual DMSO that might still be present. The organic extracts were dried over Na$_2$SO$_4$, filtered and the solvent removed under vacuum. The crude reaction product was then purified by filtration through a pad of silica (EtOAc:/petroleum ether, 1:1) to afford the product **304** as a pale yellow solid (0.90 g, 72%). ^{1}H-NMR (400 MHz, CDCl$_3$) δ 6.84 (t, *J* = 6.4 Hz, 1H), 5.41 (d, *J* = 6.2 Hz, 2H), 4.39 (t, *J* = 8.2 Hz, 2H), 3.58 (t, *J* = 8.2 Hz, 2H) ppm; ^{13}C-NMR (100 MHz, CDCl$_3$) δ 201.47, 155.38, 97.02, 87.98, 62.37, 43.17 ppm; HRMS [M+H] Calculated for C$_6$H$_8$NO$_2$ 126.0549 found 126.0550.

(*S*)-4-benzyl-3-(propa-1,2-dien-1-yl)oxazolidin-2-one (384)
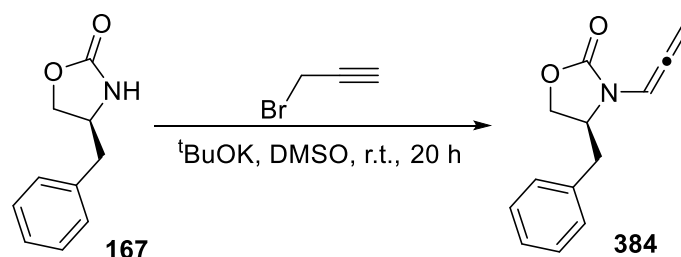
A 100mL round bottom flask was equipped with a magnetic stir bar and filled with argon to evacuate air. The flask was then charged with (*S*)-4-benzyloxazolidin-2-one **167** (1.77 g, 10.0 mmol) in dry DMSO (20 mL) under an argon atmosphere and *t*-BuOK (1.68 g, 15.0 mmol) added, sealed with a rubber septum and filled with argon to provide an inert atmosphere. The mixture was stirred for 1 h at room temperature. To this mixture was added propargyl bromide (1.25 mL, 80% solution in toluene, 11.0 mmol) dropwise over 40 minutes using syringe pump. After the addition was complete, the mixture was stirred at room temperature overnight under argon. The reaction mixture was then diluted with distilled water (50 mL) and extracted with EtOAc (3 × 50 mL). The combined organic extracts were washed with water (2 × 50 mL) and finally with brine (30 mL) to remove the residual DMSO that might still be present. The organic extracts were dried over MgSO$_4$, filtered and the solvent removed under vacuum. The crude reaction product was then purified by filtration through a pad of silica (EtOAc:/petroleum ether, 1:1) to afford the product **384** as pale-yellow liquid (oil) (1.08 g, 51%). ^{1}H-NMR (400 MHz, CDCl$_3$) δ 7.35-7.23 (m, 3H), 7.15 (d, *J* = 7.0 Hz, 2H), 6.89 (t, *J* = 6.6 Hz, 1H), 5.53 (ddd, *J* = 26.6, 10.1, 6.4 Hz, 2H), 4.23 (t, *J* = 8.4 Hz, 1H), 4.17-4.05 (m, 2H), 3.24 (dd, *J* = 13.8, 3.1 Hz, 1H), 2.72 (dd, *J* = 13.8, 8.9 Hz, 1H) ppm; ^{13}C-NMR (100 MHz, CDCl$_3$) δ 201.69, 155.06, 135.46, 129.38, 129.01, 127.38, 96.04, 88.07, 66.73, 55.72, 37.22 ppm; IR *v* (cm^{-1}) 3056, 2987, 1754, 1410, 1235, 1094, 1030; HRMS [M+Na] Calculated for C$_{13}$H$_{13}$NO$_2$Na 238.0838 found 238.0848.
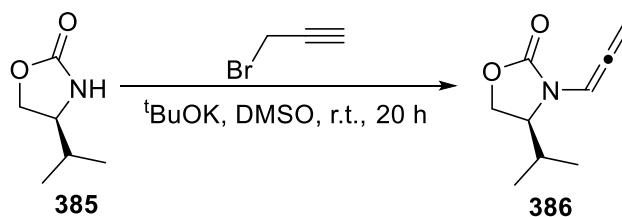
(S)-4-isopropyl-3-(propa-1,2-dien-1-yl)oxazolidin-2-one (386)

A 100mL round bottom flask was equipped with a magnetic stir bar and filled with argon to evacuate air. The flask was then charged with (S)-4-isopropyloxazolidin-2-one **385** (1.29 g, 10.0 mmol) in dry DMSO (20 mL) under an argon atmosphere and t-BuOK (1.68 g, 15.0 mmol) added, sealed with a rubber septum and filled with argon to provide an inert atmosphere. The mixture was stirred for 1 hour at room temperature. To this mixture was added propargyl bromide (1.25 mL, 80% solution in toluene, 11.0 mmol) dropwise over 40 minutes using syringe pump. After the addition was complete, the mixture was stirred at room temperature overnight under argon. The reaction mixture was then diluted with distilled water (50 mL) and extracted with EtOAc (3 × 50 mL). The combined organic extracts were washed with water (2 × 50 mL) and finally with brine (30 mL) to remove the residual DMSO that might still be present. The organic extracts were dried over MgSO$_4$, filtered and the solvent removed under vacuum. The crude reaction product was then purified by filtration through a pad of silica (EtOAc:/petroleum ether, 1:1) to afford product **386** as a pale-yellow liquid (oil) (1.00 g, 60%). ^{1}H-NMR (400 MHz, CDCl$_3$) δ 6.75 (t, J = 6.4 Hz, 1H), 5.34 (ddd, J = 25.2, 10.0, 6.5 Hz, 2H), 4.22 (t, J = 8.9 Hz, 1H), 4.13 (q, J = 4.4 Hz, 1H), 3.83-3.76 (m, 1H), 2.31-2.21 (m, 1H), 0.80 (dd, J = 11.9, 7.0 Hz, 6H) ppm; ^{13}C-NMR (100 MHz, CDCl$_3$) δ 201.40, 155.50, 95.69, 87.61, 63.12, 58.90, 26.97, 17.70, 13.79 ppm; IR v (cm^{-1}) 2968, 1749, 1409, 1138, 1009; HRMS [M+Na] Calculated for C$_9$H$_{13}$NO$_2$Na190.0838 found 190.0848.
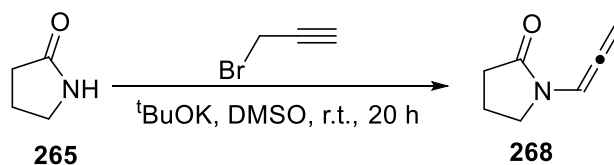
1-(Propa-1,2-dien-1-yl)pyrrolidin-2-one (268)

A 100mL round bottom flask was equipped with a magnetic stir bar and filled with argon to evacuate air. The flask was then charged with pyrrolidin-2-one **265** (0.851 g, 10.0 mmol) in dry DMSO (20 mL) under an argon atmosphere and *t*-BuOK (1.68 g, 15.0 mmol) added, sealed with a rubber septum and filled with argon to provide an inert atmosphere. The mixture was stirred for 1 h at room temperature. To this mixture was added propargyl bromide (1.25 mL, 80% solution in toluene, 11.0 mmol) dropwise over 40 minutes using syringe pump. After the addition was complete, the mixture was stirred at room temperature overnight under argon. The reaction mixture was then diluted with distilled water (50 mL) and extracted with EtOAc (3 × 50 mL). The combined organic extracts were washed with water (2 × 50 mL) and finally with brine (30 mL) to remove the residual DMSO that might be still present. The organic extracts were dried over MgSO$_4$, filtered and the solvent removed under vacuum. The crude reaction product was then purified by filtration through a pad of silica (EtOAc:/petroleum ether, 1:1) to afford product **268** as a pale yellow liquid (oil), (0.75 g, 61%). ^{1}H-NMR (400 MHz, CDCl$_3$) δ 6.96 (t, *J* = 6.4 Hz, 1H), 5.27 (d, *J* = 6.2 Hz, 2H), 3.30 (t, *J* = 7.2 Hz, 2H), 2.35 (t, *J* = 8.2 Hz, 2H), 2.03-1.91 (m, 2H) ppm; ^{13}C-NMR (100 MHz, CDCl$_3$) δ 202.68, 172.98, 95.80, 86.63, 45.76, 31.21, 17.43 ppm; IR *v* (cm^{-1}) 3018, 1747, 1682, 1415, 1216, 1021; HRMS [M+H] Calculated for C$_7$H$_{10}$NO 124.0757 found 124.0765.
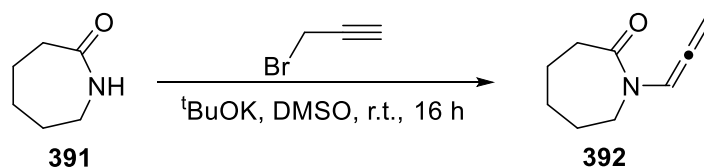
1-(Propa-1,2-dien-1-yl)piperidin-2-one (390)

A 100mL round bottom flask was equipped with a magnetic stir bar and filled with argon to evacuate air. The flask was then charged with piperidin-2-one **389** (0.99 g, 10.0 mmol) in dry DMSO (20 mL) under an argon atmosphere and *t*-BuOK (1.68 g, 15.0 mmol) added, sealed

with a rubber septum and filled with argon to provide an inert atmosphere. The mixture was stirred for 1 hour at room temperature. To this mixture was added propargyl bromide (1.25 mL, 80% solution in toluene, 11.0 mmol) dropwise over 40 minutes using syringe pump. After the addition was complete, the mixture was stirred at room temperature overnight under argon. The reaction mixture was then diluted with distilled water (50 mL) and extracted with EtOAc (3 × 50 mL). The combined organic extracts were washed with water (2 × 50 mL) and finally with brine (30 mL) to remove the residual DMSO that might be still present. The organic extracts were dried over MgSO$_4$, filtered and the solvent removed under vacuum. The crude reaction product was then purified by filtration through a pad of silica (EtOAc:/petroleum ether, 1:1) to afford product **390** as a pale yellow liquid (oil), (0.93 g, 68%). ^{1}H-NMR (400 MHz, CDCl$_3$) δ 7.57 (t, J = 6.6 Hz, 1H), 5.34 (d, J = 6.6 Hz, 2H), 3.27 (t, J = 6.0 Hz, 2H), 2.42 (t, J = 6.4 Hz, 2H), 1.80 (d, J = 42.8 Hz, 4H) ppm; ^{13}C-NMR (100 MHz, CDCl$_3$) δ 202.34, 168.20, 99.04, 87.07, 46.06, 32.81, 22.68, 21.06 ppm; IR v (cm^{-1}) 3056, 2953, 1717, 1638, 1414, 1267, 1019; HRMS [M+H] Calculated for C$_8$H$_{12}$NO 138.0913 found 138.0921.

1-(Propa-1,2-dien-1-yl)azepan-2-one (392)

A 100mL round bottom flask was equipped with a magnetic stir bar and filled with argon to evacuate air. The flask was then charged with ε-caprolactam **391** (1.13 g, 10.0 mmol) in dry DMSO (20 mL) under an argon atmosphere and *t*-BuOK (1.68 g, 15.0 mmol) added, sealed with a rubber septum and filled with argon to provide an inert atmosphere. The mixture was stirred for 1 hour at room temperature. To this mixture was added propargyl bromide (1.25 mL, 80% solution in toluene, 11.0 mmol) dropwise over 45 minutes using a syringe pump. After the addition was complete, the mixture was stirred at room temperature overnight under argon. The reaction mixture was then diluted with distilled water (50 mL) and extracted with EtOAc (3 × 50 mL). The combined organic extracts were washed with water (2 × 50 mL) and finally with brine (30 mL) to remove the residual DMSO that might be still present. The organic extracts were dried over MgSO$_4$, filtered and the solvent removed under vacuum. The crude reaction product was then purified by filtration through a pad of silica

(EtOAc:/petroleum ether, 1:1) to afford product **392** as a pale-yellow liquid (oil), (1.31 g, 87%). ^{1}H-NMR (400 MHz, CDCl$_3$) δ 7.37 (t, *J* = 6.6 Hz, 1H), 5.30 (d, *J* = 6.2 Hz, 2H), 3.41 (t, *J* = 4.9 Hz, 2H), 2.53 (t, *J* = 5.6 Hz, 2H), 1.75-1.52 (m, 6H) ppm; ^{13}C-NMR (100 MHz, CDCl$_3$) δ 201.58, 173.89, 99.57, 87.39, 46.05, 37.22, 29.67, 27.68, 23.47 ppm; IR *v* (cm^{-1}) 3043, 2931, 2857, 1958, 1736, 1719, 1215, 1082, 973; HRMS [M+H] Calculated for C$_9$H$_{14}$NO 152.1070 found 152.1053.

Procedure for the photoredox synthesis with ethanol:

Diethyl 2-(2-ethoxy-2-(2-oxooxazolidin-3-yl)ethyl)malonate (177)
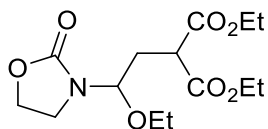
An oven dried 50 mL round bottom flask was filled with argon gas and charged with iridium photocatalyst (14 mg, 0.015 mmol) and anhydrous acetonitrile (10 mL) and seal with a rubber septum. The flask was evacuated of air and filled again with argon on a Schlenk line. *N*-Vinyl-2-oxazolidinone **117** (0.11 g, 1.0 mmol), diethyl bromomalonate (0.40 mL, 2.0 mmol), trimethylamine TEA (0.28 mL, 2.0 mmol) and ethanol (0.59 mL, 10.0 mmol) were added in that order to the solution in the flask under argon atmosphere. The flask was then irradiated with a Kessil blue light overnight for 16 hours with stirring at room temperature.

After the reaction has completed as monitored by TLC, the solvent was removed under a reduced pressure to obtain the crude product. The crude product was purified by flash chromatography on silica gel (hexane-EtOAc 4:1 to 1:1) to afford the product **177** as a pale yellow liquid (0.21 g, 66%); ^{1}H-NMR (400 MHz, CDCl$_3$) δ 5.06 (dd, *J* = 7.8, 5.8 Hz, 1H), 4.45-4.23 (m, 2H), 4.23-4.03 (m, 4H), 3.61-3.30 (m, 5H), 2.41-2.22 (m, 1H), 2.22-2.04 (m, 1H), 1.29-1.18 (m, 6H), 1.18-1.08 (m, 3H) ppm; ^{13}C-NMR (100 MHz, CDCl$_3$) δ 168.84, 158.17, 81.67, 64.27-63.71, 62.50, 61.78, 48.67, 38.76, 32.04, 15.10-14.54, 14.07 ppm; HRMS [M+H] Calculated for C$_{14}$H$_{24}$NO$_7$ 318.1541 found 318.1547.

General procedure for the photoredox syntheses with arylamines: An oven dried 50 mL three neck round bottom flask was filled with argon gas and charged with iridium photocatalyst (1.5mol%) enamide or allenamide (1.0 eq) and anhydrous acetonitrile (~ 0.1M) and seal with a rubber septum in the middle neck and the other two necks closed with glass stoppers. The flask was purged again with argon while one neck was opened. The middle neck was then fitted with an argon filled balloon. Diethyl bromomalonate (2.0 eq), trimethylamine TEA (2.0 eq) and arylamine (5.0 eq) were added in that order to the solution in the flask under the argon atmosphere. The flask was then irradiated with a Kessil blue light (λ = 467 nm) for 3 hours with stirring at room temperature. After the reaction had completed as monitored by TLC, the solvent was removed under reduced pressure to obtain

the crude product. The crude product was purified by flash chromatography on silica gel (hexane-EtOAc 4:1) to afford the product.

Diethyl 2-(2-(2-oxooxazolidin-3-yl)-2-(phenylamino)ethyl)malonate (179)
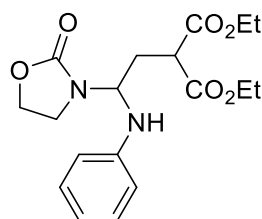
179

The crude product was purified by flash chromatography on silica gel (hexane-EtOAc 4:1) to afford the product **179** as pale yellow liquid (0.26 g, 72%). ^{1}H-NMR (400 MHz, CDCl$_3$) δ 7.18 (t, J = 8.0 Hz, 2H), 6.78 (t, J = 7.8 Hz, 1H), 6.65 (d, J = 8.7 Hz, 2H), 5.37 (t, J = 7.2 Hz, 1H), 4.44 (t, J = 8.0 Hz, 1H), 4.26-4.13 (m, 5H), 3.63 (t, J = 7.8 Hz, 1H), 3.53 (t, J = 6.6 Hz, 1H), 3.45 (dd, J = 14.6, 8.4 Hz, 1H), 3.36 (q, J = 8.5 Hz, 1H), 2.55-2.43 (m, 1H), 2.38-2.28 (m, 1H), 1.24 (dt, J = 18.5, 7.0 Hz, 6H) ppm; ^{13}C-NMR (100 MHz, CDCl$_3$) δ 169.37, 169.03, 157.84, 144.34, 129.70, 119.30, 113.57, 65.01, 62.61, 62.35, 62.16, 62.05, 49.09, 40.65, 39.26, 32.22, 14.07 ppm; IR v (cm^{-1}) 3357, 2983, 2956, 1736, 1708, 1601,1520, 1499, 1460, 1386, 1368, 1325, 1291, 1251, 1093. HRMS [M+H] calculated for C$_{18}$H$_{25}$N$_2$O$_6$ 365.1707 found 365.1701

Diethyl 2-(2-(2-oxooxazolidin-3-yl)-2-(p-tolylamino)ethyl)malonate (181)

181

The crude product was purified by flash chromatography on silica gel (hexane-EtOAc 4:1) to afford the product **181** as white solid substance (0.32 g, 84%) and it was recrystallized (CH$_2$Cl$_2$-Hexane 1:1) to give colourless crystals. ^{1}H-NMR (400 MHz, CDCl$_3$) δ 6.98 (d, J = 7.8 Hz, 2H), 6.56 (d, J = 8.2 Hz, 2H), 5.34 (q, J = 7.7 Hz, 1H), 4.24-4.07 (m, 6H), 3.53 (t, J = 6.6 Hz, 1H), 3.44 (td, J = 8.5, 6.2 Hz, 1H), 3.34 (q, J = 8.5 Hz, 1H), 2.53-2.43 (m, 1H), 2.37-

2.28 (m, 1H), 2.21 (s, 3H), 1.25 (dt, J = 16.6, 7.1 Hz, 6H) ppm; ^{13}C-NMR (400 MHz, CDCl$_3$) δ 169.38, 169.07, 157.88, 141.93, 130.17, 128.56, 113.68, 62.83, 62.35, 62.13, 62.03, 49.10, 39.27, 32.22, 20.50, 14.29 ppm; IR v (cm^{-1}) 3357, 2984, 2918, 1748, 1737, 1706, 1616, 1517, 1414, 1368, 1251, 1218 1178, 1082, 1008; HRMS [M+H] calculated for C$_{19}$H$_{27}$N$_2$O$_6$ 379.1864, found 379.1862.
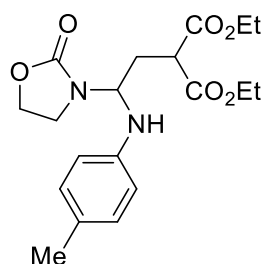
Diethyl 2-(2-(2-oxooxazolidin-3-yl)-2-(m-tolylamino)ethyl)malonate (183)

183

The crude product was purified by flash chromatography on silica gel (hexane-EtOAc 4:1) to afford the product **183** as pale yellow oil (0.33 g, 88%). ^{1}H-NMR (400 MHz, CDCl$_3$) δ 7.06 (t, J = 7.6 Hz, 1H), 6.59 (d, J = 7.4 Hz, 1H), 6.46 (dd, J = 10.7, 2.1 Hz, 2H), 5.36 (q, J = 7.7 Hz, 1H), 4.25-4.07 (m, 8H), 3.52 (t, J = 6.8 Hz, 1H), 3.44 (td, J = 8.4, 6.5 Hz, 1H), 3.36 (q, J = 8.5 Hz, 1H), 2.54-2.40 (m, 1H), 2.40-2.27 (m, 1H), 2.24 (s, 3H), 1.24 (dt, J = 17.2, 7.1 Hz, 6H) ppm; ^{13}C-NMR (100 MHz, CDCl$_3$) δ 169.36, 169.06, 157.83, 144.38, 139.54, 129.57, 120.18, 114.42, 110.58, 62.35, 62.14, 62.03, 49.08, 39.27, 32.22, 21.65, 14.07 ppm; IR v (cm^{-1}) 3366, 2980, 1738, 1704, 1607, 1528, 1367, 1249, 1217, 1125, 1080; HRMS [M+H] calculated for C$_{19}$H$_{27}$N$_2$O$_6$ 379.1864, found 379.1861.

Diethyl 2-(2-((2,4-dimethylphenyl)amino)-2-(2-oxooxazolidin-3-yl)ethyl)malonate (185)

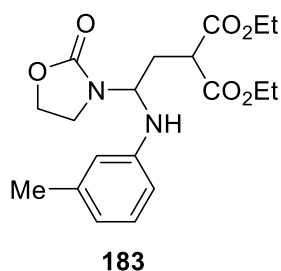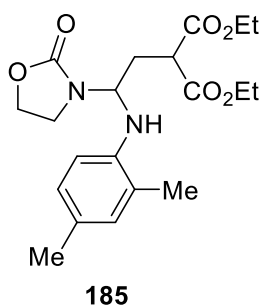**185**

The crude product was purified by flash chromatography on silica gel (hexane-EtOAc 4:1) to afford the product **185** as a pale yellow oil (0.35 g, 91%). ^{1}H-NMR (400 MHz, CDCl$_3$) δ

145

6.89 (t, J = 7.6 Hz, 2H), 6.58 (d, J = 8.2 Hz, 1H), 5.39 (q, J = 7.6 Hz, 1H), 5.23 (q, J = 6.0 Hz, 0H), 4.41-4.29 (m, 1H), 4.27-4.08 (m, 6H), 3.99 (d, J = 8.2 Hz, 1H), 3.60-3.41 (m, 4H), 3.26 (dd, J = 17.3, 7.8 Hz, 1H), 2.60-2.50 (m, 1H), 2.40-2.30 (m, 1H), 2.20 (s, 3H), 2.09 (s, 3H), 1.25 (dt, J = 16.5, 7.2 Hz, 6H) ppm; ^{13}C-NMR (100 MHz, CDCl$_3$) δ 169.54, 169.13, 157.79, 139.93, 131.36, 128.06, 127.97, 122.23, 111.37, 62.57, 62.33, 62.12, 62.04, 49.11, 39.17, 38.62, 32.13, 20.42, 19.32, 17.47, 15.08, 14.08 ppm; IR v (cm^{-1}) 3337, 1743, 1722, 1621, 1589, 1300, 1243, 1183, 1080, 1028; HRMS [M+H] calculated for C$_{20}$H$_{29}$N$_2$O$_6$ 393.2020, found 393.2018.

Diethyl 2-(2-(mesitylamino)-2-(2-oxooxazolidin-3-yl)ethyl)malonate (187)

187

The crude product was purified by flash chromatography on silica gel (hexane-EtOAc 4:1) to afford the product **187** as yellow oil (0.26 g, 64%). ^{1}H-NMR (400 MHz, CDCl$_3$) δ 6.76 (s, 2H), 4.94 (t, J = 7.4 Hz, 1H), 4.25-4.08 (m, 6H), 3.62 (t, J = 7.2 Hz, 1H), 3.48-3.38 (1H), 3.28 (q, J = 8.4 Hz, 1H), 2.70-2.57 (m, 1H), 2.57-2.44 (m, 1H), 2.27-2.20 (6H), 2.18 (s, 3H), 1.30-1.21 (m, 6H) ppm; ^{13}C-NMR (100 MHz, CDCl$_3$) δ 169.30, 169.14, 157.39, 139.28, 132.01, 129.96, 129.20, 66.77, 62.28, 61.89, 49.41, 43.28, 32.50, 20.60, 18.71, 14.10 ppm; IR v (cm^{-1}) 3368, 2981, 1726, 1483, 1444, 1391, 1370, 1275, 1260, 1096, 1028; HRMS [M+H] calculated for C$_{21}$H$_{31}$N$_2$O$_6$ 407.2177, found 407.2156.
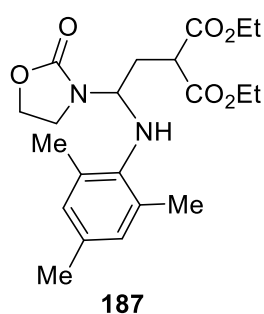
Diethyl 2-(2-((2,6-dimethylphenyl)amino)-2-(2-oxooxazolidin-3-yl)ethyl)malonate (189)

189

The crude product was purified by flash chromatography on silica gel (hexane-EtOAc 4:1) to afford the product **189** as 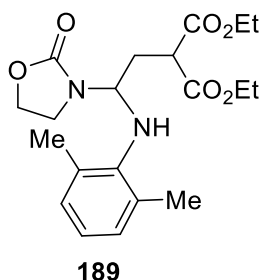a pale yellow oil (0.23 g, 60%). ^{1}H-NMR (400 MHz, CDCl$_3$) δ 6.94 (d, J = 7.4 Hz, 2H), 6.81 (t, J = 7.6 Hz, 1H), 5.22 (q, J = 6.0 Hz, 1H), 5.00 (s, 1H), 4.25-4.06 (m, 7H), 3.63 (t, J = 7.0 Hz, 1H), 3.41 (q, J = 7.7 Hz, 1H), 3.27 (q, J = 8.4 Hz, 1H), 2.69-2.59 (m, 1H), 2.57-2.48 (m, 1H), 2.29-2.24 (6H), 1.30-1.22 (m, 6H) ppm; ^{13}C-NMR (100 MHz, CDCl$_3$) δ 169.29, 169.12, 157.33, 141.90, 129.35, 129.05, 122.65, 66.52, 62.28, 61.92, 49.37, 43.29, 32.53, 18.85, 14.11 ppm; IR v (cm^{-1}) 2981, 2359, 2341, 2253, 1739, 1594, 1558, 1445, 1372, 1247, 1099, 1030; HRMS [M+H] calculated for C$_{20}$H$_{29}$N$_2$O$_6$ 393.2020, found 393.2017.

Diethyl 2-(2-(2-oxooxazolidin-3-yl)-2-((3-(trifluoromethyl)phenyl)amino)ethyl)malonate (191)

191

The crude product was purified by flash chromatography on silica gel (hexane-EtOAc 4:1) to afford the product **191** as a yellow liquid (0.21 g, 97%). ^{1}H-NMR (400 MHz, CDCl$_3$) δ 7.29 (t, J = 7.8 Hz, 1H), 7.01 (d, J = 7.8 Hz, 1H), 6.85 (t, J = 8.0 Hz, 2H), 5.39 (q, J = 7.6 Hz, 1H), 4.55 (d, J = 8.2 Hz, 1H), 4.29-4.11 (m, 6H), 3.53 (t, J = 6.8 Hz, 1H), 3.50-3.41 (m, 1H), 3.37 (q, J = 8.4 Hz, 1H), 2.56-2.45 (m, 1H), 2.40-2.29 (m, 1H), 1.27 (t, J = 7.2 Hz, 3H), 1.22 (t, J = 7.2 Hz, 3H) ppm; ^{13}C-NMR (100 MHz, CDCl$_3$) δ 169.29, 168.94, 157.78, 144.76, 130.40, 115.98, 115.73, 110.63, 62.45, 62.39, 62.28, 62.17, 49.00, 39.28, 32.01, 14.02 ppm; IR v (cm^{-}

**Diethyl   2-(2-((3,5-bis(trifluoromethyl)phenyl)amino)-2-(2-oxooxazolidin-3-yl)ethyl)
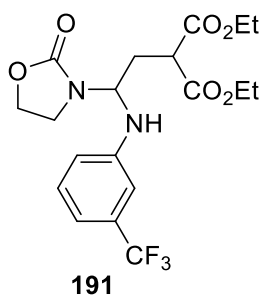malonate (193)**
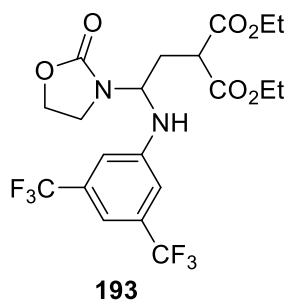
193

The crude product was purified by flash chromatography on silica gel (hexane-EtOAc 4:1) to
afford the product **193** as a pale yellow liquid (0.15 g, 61%). ^{1}H-NMR (400 MHz, CDCl$_3$) δ
7.23 (s, 1H), 7.10 (s, 2H), 5.42 (q, *J* = 7.4 Hz, 1H), 5.14 (d, *J* = 7.8 Hz, 1H), 4.32-4.25 (m,
2H), 4.25-4.11 (m, 5H), 3.58-3.46 (m, 3H), 3.46-3.32 (m, 1H), 2.59-2.47 (m, 1H), 2.43-2.33
(m, 1H), 1.77 (s, 1H), 1.26 (t, J = 7.0 Hz, 3H), 1.21 (t, J = 7.2 Hz, 3H) ppm; ^{13}C-NMR (100
MHz, CDCl$_3$) δ 169.21, 168.92, 157.82, 145.70, 135.37, 133.05, 132.71, 132.39, 124.73,
122.01, 113.01, 112.25, 62.44, 62.37, 62.25, 62.19, 48.90, 39.28, 31.74, 14.00 ppm; IR *v*
(cm^{-1}) 3330, 2985, 2360, 1732, 1622, 1526, 1475, 1277, 1134, 1029.   HRMS [M+Na]
calculated for $C_{20}H_{22}F_6N_2O_6Na$ 523.1274, found 523.1267.

Diethyl 2-(2-((4-bromophenyl)amino)-2-(2-oxooxazolidin-3-yl)ethyl)malonate (195)
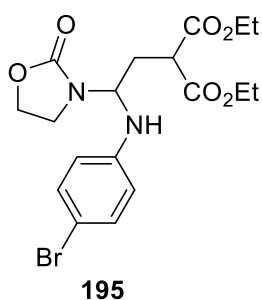
195

The crude product was purified by flash chromatography on silica gel (hexane-EtOAc 4:1) to
afford the product **195** as light brown solid (0.31 g, 70%) which was recrystallized (CH$_2$Cl$_2$-
hexane 1:1) to give colourless crystals. ^{1}H-NMR (400 MHz, CDCl$_3$) δ 7.26 (d, *J* = 7.4 Hz,
2H), 6.54 (d, *J* = 8.7 Hz, 2H), 5.32 (q, *J* = 7.6 Hz, 1H), 4.32-4.08 (m, 6H), 3.52 (t, *J* = 6.8 Hz,

1H), 3.45 (dd, J = 14.8, 8.7 Hz, 1H), 3.37-3.28 (1H), 2.53-2.43 (m, 1H), 2.37-2.27 (1H), 1.65 (s, 1H), 1.30-1.20 (6H) ppm; ^{13}C-NMR (100 MHz, CDCl$_3$) δ 169.29, 168.96, 157.82, 143.39, 132.47, 115.26, 111.26, 62.55, 62.37, 62.23, 62.13, 49.01, 39.20, 32.05, 14.07 ppm; IR v (cm^{-1}) 3356, 2984, 2917, 1736, 1704, 1593, 1370, 1323, 1250, 1083, 1006; HRMS [M+H] calculated for C$_{18}$H$_{24}$BrN$_2$O$_6$ 443.0812, found 443.0805.

Diethyl 2-(2-((2-fluorophenyl)amino)-2-(2-oxooxazolidin-3-yl)ethyl)malonate (197)

197

The crude product was purified by flash chromatography on silica gel (hexane-EtOAc 4:1) to afford the product **197** a pale yellow solid (0.28 g, 75%) which was recrystallized (CH$_2$Cl$_2$-hexane 1:1) to give colourless crystals. ^{1}H-NMR (400 MHz, CDCl$_3$) δ 7.03-6.89 (m, 2H), 6.82 (t, J = 8.4 Hz, 1H), 6.76-6.65 (m, 1H), 5.41 (q, J = 7.6 Hz, 1H), 4.42 (d, J = 6.2 Hz, 1H), 4.30-4.11 (m, 6H), 3.52 (t, J = 7.0 Hz, 1H), 3.49-3.44 (m, 1H), 3.34 (q, J = 8.4 Hz, 1H), 2.59-2.48 (m, 1H), 2.43-2.33 (m, 1H), 1.32-1.18 (m, 6H) ppm; ^{13}C-NMR (100 MHz, CDCl$_3$) δ 169.07, 168.91, 157.82, 152.55, 150.17, 132.74, 132.64, 125.25, 118.92, 114.89, 114.71, 113.79, 62.38, 62.20, 62.07, 49.05, 38.82, 32.09, 14.07 ppm; IR v (cm^{-1}) 3382, 2984, 1724, 1620, 1519, 1418, 1331, 1258, 1156, 1029; HRMS [M+Na] calculated for C$_{18}$H$_{23}$FN$_2$O$_6$Na 405.1432 Found 405.1430.
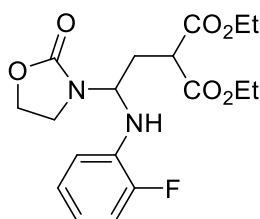
Diethyl 2-(2-((4-bromo-2-fluorophenyl)amino)-2-(2-oxooxazolidin-3-yl)ethyl)malonate (199)

199

The crude product was purified by flash chromatography on silica gel (hexane-EtOAc 4:1) to afford the product **199** as a colourless solid. (0.37 g, 79%, M.P. 102.5 – 104.3 °C). It was recrystallized (CH$_2$Cl$_2$-hexane 1:1) to afford colourless crystals. ^{1}H-NMR (400 MHz, CDCl$_3$) δ 7.16-7.08 (m, 2H), 6.72 (t, J = 9.1 Hz, 1H), 5.37 (t, J = 7.4 Hz, 1H), 4.31-4.11 (m, 6H), 3.54-3.44 (m, 2H), 3.32 (q, J = 8.4 Hz, 1H), 2.58-2.48 (m, 1H), 2.42-2.31 (m, 1H), 1.31-1.20 (m, 6H) ppm; ^{13}C-NMR (100 MHz, CDCl$_3$) δ 169.01, 168.83, 157.82, 152.26, 149.83, 132.03, 128.13, 127.47, 118.46, 118.25, 114.89, 109.67, 65.02, 62.17, 48.97, 40.67, 38.78, 31.91, 14.07 ppm; IR v (cm^{-1}) 3020, 2434, 1748, 1514, 1392, 1216, 760; HRMS [M+Na] calculated for C$_{18}$H$_{22}$BrFN$_2$O$_6$Na 483.0537 Found 483.0519.

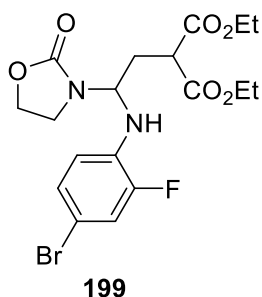**Diethyl 2-(2-((3,4-dichlorophenyl)amino)-2-(2-oxooxazolidin-3-yl)ethyl)malonate (201)**

201

The crude product was purified by flash chromatography on silica gel (hexane-EtOAc 4:1) to afford the product **201** a pale yellow liquid which turned solid upon standing (0.25 g, 58%). The solid was recrystallized (CH$_2$Cl$_2$-Hexane 1:1) into colourless crystals. ^{1}H-NMR (400 MHz, CDCl$_3$) δ 7.18 (d, J = 8.7 Hz, 1H), 6.75 (d, J = 2.5 Hz, 1H), 6.51 (dd, J = 8.7, 2.9 Hz, 1H), 5.29 (q, J = 7.6 Hz, 1H), 4.63 (d, J = 8.2 Hz, 1H), 4.29-4.09 (m, 6H), 3.57-3.40 (2H), 3.34 (q, J = 8.5 Hz, 1H), 2.53-2.39 (1H), 2.39-2.26 (m, 1H), 1.30-1.18 (m, 6H) ppm; ^{13}C-

NMR (100 MHz, CDCl$_3$) δ 169.16, 168.94, 157.87, 144.17, 133.12, 131.16, 121.95, 115.41, 112.94, 62.44, 48.92, 39.20, 31.88, 14.06 ppm; IR v (cm^{-1}) 3331, 2984, 1725, 1598, 1370, 1274, 1259, 1050.   HRMS [M+Na] calculated for C$_{18}$H$_{22}$^{35}Cl$_2$N$_2$O$_6$Na 455.0747 Found 455.0744.

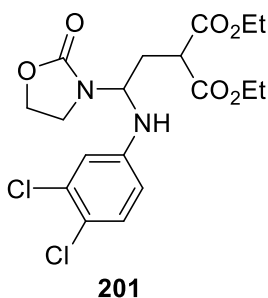**Diethyl 2-(2-((2-methoxyphenyl)amino)-2-(2-oxooxazolidin-3-yl)ethyl)malonate (203)**

203

The crude product was purified by flash chromatography on silica gel (hexane-EtOAc 4:1) to afford the product **203** a pale yellow oil which crystallised upon standing (0.30 g, 76%). The solid was recrystallized (CH$_2$Cl$_2$-hexane 1:1) to afford colourless crystals. ^{1}H-NMR (400 MHz, CDCl$_3$) δ 6.85 (dd, J = 8.2, 6.6 Hz, 1H), 6.80-6.62 (m, 3H), 5.41 (t, J = 7.0 Hz, 1H), 4.44 (t, J = 8.2 Hz, 1H), 4.28-4.10 (m, 5H), 3.82 (s, 3H), 3.62 (t, J = 7.8 Hz, 1H), 3.54 (t, J = 6.6 Hz, 1H), 3.49-3.35 (m, 1H), 3.27 (q, J = 8.5 Hz, 1H), 2.60-2.45 (m, 1H), 2.40 (q, J = 7.0 Hz, 1H), 1.33-1.16 (m, 6H) ppm; ^{13}C-NMR (100 MHz, CDCl$_3$) δ 169.06, 157.93, 146.62, 133.99, 121.80, 118.53, 111.67, 109.73, 65.01, 62.33, 62.05, 55.56, 49.09, 38.76, 32.33, 14.08 ppm; IR v (cm^{-1}) 3386, 2975, 2934, 1746, 1723, 1602, 1512, 1250, 1210, 1144, 1016; HRMS [M+H] calculated for C$_{19}$H$_{27}$N$_2$O$_7$ 395.1813 Found 395.1806.

Diethyl2-(2-(2-oxooxazolidin-3-yl)-2-((2-trifluoromethoxy)phenyl)amino)ethyl)malonate (205)

205

The crude product was purified by flash chromatography on silica gel (hexane-EtOAc 4:1) to afford the product **205** as a yellow oily liquid (0.34 g, 77%). ^{1}H-NMR (400 MHz, CDCl$_3$) δ

7.13 (t, J = 7.4 Hz, 2H), 6.83 (d, J = 7.4 Hz, 1H), 6.76-6.70 (m, 1H), 5.41 (q, J = 7.7 Hz, 1H), 4.68 (d, J = 8.2 Hz, 1H), 4.29-4.10 (m, 6H), 3.53-3.43 (m, 2H), 3.27 (q, J = 8.5 Hz, 1H), 2.59-2.49 (m, 1H), 2.40-2.30 (m, 1H), 1.24 (dt, J = 14.0, 6.4 Hz, 6H) ppm; ^{13}C-NMR (100 MHz, CDCl$_3$) δ 169.06, 168.94, 157.84, 136.86, 136.11, 128.37, 121.21, 118.67, 113.49, 62.41, 62.13, 61.72, 48.89, 38.61, 31.82, 14.04 ppm; IR v (cm^{-1}) 3394, 2982, 2360, 1726, 1612, 1482, 1420, 1215, 1158, 1026; HRMS [M+H] calculated for C$_{19}$H$_{24}$F$_3$N$_2$O$_7$ 449.1530, found 449.1525.
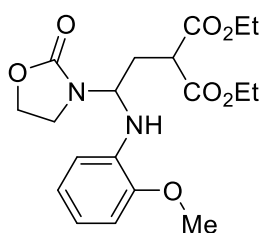
Diethyl 2-(2-((3-(ethoxycarbonyl)phenyl)amino)-2-(2-oxooxazolidin-3-yl)ethyl)malonate (207)

207

The crude product was purified by flash chromatography on silica gel (hexane-EtOAc 4:1) to afford the product **207** as a yellow liquid (0.15 g, 70%). ^{1}H-NMR (400 MHz, CDCl$_3$) δ 7.42 (d, J = 7.8 Hz, 1H), 7.33 (s, 1H), 7.23 (t, J = 8.2 Hz, 1H), 6.86 (dd, J = 8.2, 2.5 Hz, 1H), 5.39 (q, J = 7.7 Hz, 1H), 4.61 (d, J = 8.7 Hz, 1H), 4.30 (q, J = 7.1 Hz, 2H), 4.25-4.06 (m, 5H), 3.56-3.50 (1H), 3.49-3.42 (1H), 3.38-3.29 (1H), 2.54-2.44 (m, 1H), 2.41-2.31 (m, 1H), 1.34 (t, J = 7.0 Hz, 3H), 1.24 (t, J = 7.0 Hz, 3H), 1.20 (t, J = 7.0 Hz, 3H) ppm; ^{13}C-NMR (100 MHz, CDCl$_3$) δ 169.21, 169.02, 166.74, 157.86, 144.59, 131.68, 129.84, 120.21, 117.21, 115.23, 62.44, 62.12, 61.08, 49.01, 39.29, 32.06, 14.36, 14.06 ppm; IR v (cm^{-1}) 2986, 2254, 1734, 1607, 1591, 1276, 1259, 1049; HRMS [M+H] calculated for C$_{21}$H$_{29}$N$_2$O$_8$ 437.1918, found 437.1915.
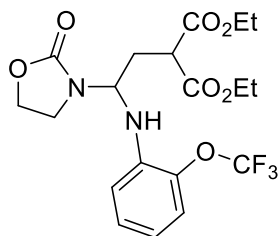
Diethyl 2-(2-(methyl(phenyl)amino)-2-(2-oxooxazolidin-3-yl)ethyl)malonate (209)

209

The crude product was purified by flash chromatography on silica gel (hexane-EtOAc 4:1) to afford the product **209** as a yellow oil (0.113 g, 61%). ^{1}H-NMR (400 MHz, CDCl$_3$) δ 7.25 (t, J = 8.0 Hz, 2H), 6.89 (d, J = 7.8 Hz, 2H), 6.82 (t, J = 7.2 Hz, 1H), 5.58 (dd, J = 8.2, 6.6 Hz, 1H), 4.27-4.07 (m, 6H), 3.59-3.47 (m, 2H), 3.32 (q, J = 8.2 Hz, 1H), 2.93 (s, 3H), 2.69-2.60 (m, 1H), 2.54 (dt, J = 14.3, 6.1 Hz, 1H), 1.27-1.19 (m, 6H) ppm; ^{13}C-NMR (100 MHz, CDCl$_3$) δ 169.14, 168.86, 157.76, 148.31, 129.50, 119.22, 114.18, 67.74, 62.16, 61.96, 60.49, 49.00, 41.78, 32.72, 30.42, 14.05 ppm; IR v (cm^{-1}) 2981, 1724, 1599, 1506, 1414, 1390, 1370, 1225, 1095, 1029; HRMS [M+Na] calculated for C$_{19}$H$_{26}$N$_2$O$_6$Na 387.1527, found 387.1527.

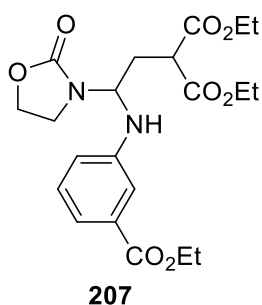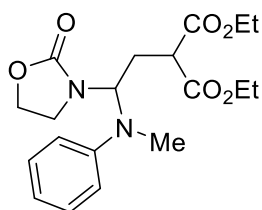**Diethyl 2-(2-(diphenylamino)-2-(2-oxooxazolidin-3-yl)ethyl)malonate (211)**
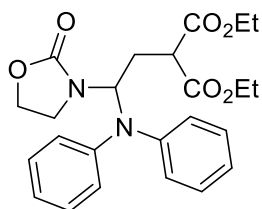
211

The crude product was purified by flash chromatography on silica gel (hexane-EtOAc 4:1) to afford the product **211** as a yellow oil which solidified upon standing (0.12 g, 56%). The solid was recrystallized (CH$_2$Cl$_2$-hexane 1:1) to give colourless crystals. ^{1}H-NMR (400 MHz, CDCl$_3$) δ 7.28 (t, J = 7.6 Hz, 3H), 7.05 (t, J = 6.8 Hz, 2H), 6.97-6.91 (4H), 5.92 (t, J = 7.4 Hz, 1H), 4.46-4.39 (m, 1H), 4.24-4.07 (m, 5H), 3.69 (t, J = 8.0 Hz, 1H), 3.56-3.43 (m, 2H), 3.23 (q, J = 8.2 Hz, 1H), 2.22 (t, J = 6.8 Hz, 2H), 1.23 (td, J = 7.1, 1.8 Hz, 6H) ppm; ^{13}C-NMR (100 MHz, CDCl$_3$) δ 169.26, 168.69, 158.01, 145.19, 129.66, 123.56, 93.57, 65.97, 62.34, 61.97, 48.76, 41.99, 40.56, 31.65, 14.05 ppm; IR v (cm^{-1}) 2981, 1741, 1637, 1589,

1493, 1370, 1330, 1248, 1097, 1077, 1028; HRMS [M+Na] calculated for $C_{24}H_{28}N_2O_6Na$ 463.1840, found 463.1836.

Diethyl 2-((R)-2-((S)-4-benzyl-2-oxooxazolidin-3-yl)-2-(phenylamino)ethyl)malonate (216)

216

The crude product was purified by flash chromatography on silica gel (hexane-EtOAc 5:1) to afford the product **216** as a mixture of diastereomers (dr 52:48) as yellow oil (0.13 g, 56%). ^{1}H-NMR (400 MHz, CDCl$_3$) δ 7.34-7.16 (m, 5H), 7.09 (t, J = 6.6 Hz, 2H), 6.86-6.76 (m, 1H), 6.73 (d, J = 7.4 Hz, 1H), 6.62 (d, J = 7.8 Hz, 1H), 5.36-5.23 (m, 1H), 4.59 (d, J = 7.8 Hz, 1H), 4.26-4.12 (m, 3H), 4.01-3.85 (m, 2H), 3.65-3.54 (m, 1H), 3.29 (dd, 13.5, 3.8 Hz, 1H), 2.83-2.73 (m, 1H), 2.63-2.52 (m, 1H), 2.49-2.38 (m, 1H), 1.32-1.18 (m, 6H) ppm; ^{13}C-NMR (100 MHz, CDCl$_3$) δ 169.65, 169.41, 169.10, 158.29, 157.57, 145.40, 144.97, 135.59, 129.73, 129.05, 127.32, 119.67, 114.79, 113.89, 67.48, 64.45, 64.04, 62.05, 57.23, 54.62, 49.15, 40.62, 39.77, 34.08, 32.91, 14.07 ppm; IR v (cm^{-1}) 3318, 2981, 1730, 1708, 1601, 1499, 1411, 1367, 1259, 1180, 1097, 1021; HRMS [M+Na] calculated for $C_{25}H_{30}N_2O6Na$ 477.1996, found 477.1995.

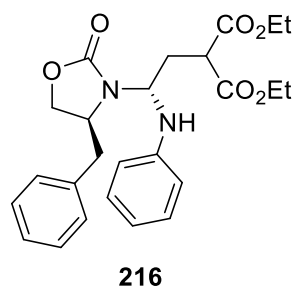**Diethyl 2-((R)-2-((S)-4-benzyl-2-oxooxazolidin-3-yl)-2-(p-tolylamino)ethyl)malonate (217)**
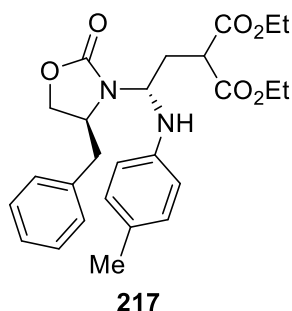
217

The crude product was purified by flash chromatography on silica gel (hexane-EtOAc 5:1) to afford the product **217** as a mixture of diastereomers (dr 87:13) as yellow oil (0.27 g, 58%). ^{1}H-NMR (400 MHz, CDCl$_3$) δ 7.32-7.23 (m, 2H), 7.09 (d, J = 7.0 Hz, 2H), 7.00 (d, J = 8.2 Hz, 2H), 6.65 (d, J = 8.7 Hz, 2H), 5.23 (td, J = 10.0, 5.2 Hz, 1H), 4.48 (d, J = 10.7 Hz, 1H), 4.27-4.12 (m, 4H), 4.03-3.83 (m, 3H), 3.59 (t, J = 7.0 Hz, 1H), 3.32 (dd, J = 13.4, 3.9 Hz, 1H), 2.82-2.70 (m, 1H), 2.55 (dd, J = 13.6, 9.9 Hz, 1H), 2.44 (qd, J = 7.1, 4.9 Hz, 1H), 2.24 (s, 3H), 1.25 (q, J = 7.3 Hz, 6H) ppm; ^{13}C-NMR (100 MHz, CDCl$_3$) δ 169.42, 169.14, 157.54, 143.05, 135.66, 130.13, 129.02, 127.29, 115.17, 67.41, 64.62, 61.96, 57.47, 49.20, 39.77, 32.95, 20.57, 14.13 ppm; IR v (cm^{-1}) 3348, 3027, 2979, 2872, 2359, 1727, 1637, 1232, 1155, 1030; HRMS [M+H] calculated for C$_{26}$H$_{32}$N$_2$O$_6$ 469,2333, found 469.2334.

Diethyl 2-((R)-2-((S)-4-benzyl-2-oxooxazolidin-3-yl)-2-(m-tolylamino)ethyl)malonate (218)
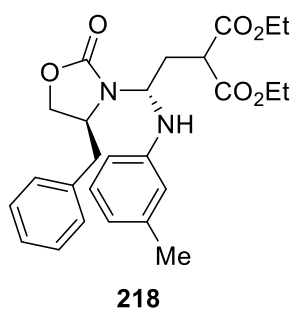

218

The crude product was purified by flash chromatography on silica gel (hexane-EtOAc 5:1) to afford the product **218** as a mixture of diastereomers (dr 70:30) as a yellow oil (0.14 g, 61%) ^{1}H-NMR (400 MHz, CDCl$_3$) δ 7.34-7.17 (m, 3H), 7.12-7.05 (m, 2H), 6.62 (d, J = 7.8 Hz, 1H), 6.54 (d, J = 6.2 Hz, 1H), 6.43 (d, J = 10.7 Hz, 1H), 5.28 (td, J = 9.7, 5.4 Hz, 1H), 4.58

(d, J = 10.7 Hz, 1H), 4.31-4.12 (m, 4H), 3.97 (t, J = 8.2 Hz, 1H), 3.92-3.83 (m, 1H), 3.64-3.53 (m, 1H), 3.34 (dd, J = 13.6, 4.1 Hz, 1H), 2.82-2.72 (m, 1H), 2.64-2.51 (m, 1H), 2.50-2.37 (m, 1H), 2.27 (s, 3H), 1.39-1.15 (m, 6H) ppm; ^{13}C-NMR (100 MHz, CDCl$_3$) δ 169.63, 169.39, 169.12, 158.31, 157.59, 145.48, 139.46, 135.69, 129.48, 129.01, 127.30, 120.61, 115.70, 111.71, 67.46, 63.99, 61.98, 57.33, 49.19, 39.77, 32.91, 21.68, 14.11 ppm; IR v (cm^{-1}) 3365, 2980, 2359, 1731, 1606, 1592, 1175, 1095, 1027, 905; HRMS [M+H] calculated for C$_{26}$H$_{33}$N$_2$O$_6$ 391.1864, found 391.1860.

Diethyl 2-((R)-2-((S)-4-benzyl-2-oxooxazolidin-3-yl)-2-((2,4-dimethylphenyl)amino) ethyl)malonate (219)
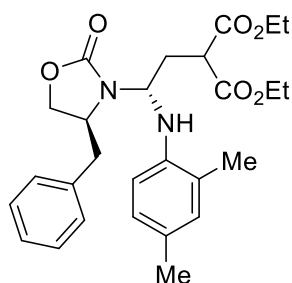
219

The crude product was purified by flash chromatography on silica gel (hexane-EtOAc 5:1) to afford the product **219** as a mixture of diastereomers (dr 50:50) as a yellow oil (0.11 g, 53%). ^{1}H-NMR (400 MHz, CDCl$_3$) δ 7.33-7.19 (m, 4H), 7.12-7.02 (m, 2H), 6.96-6.86 (m, 2H), 6.74-6.69 (1H), 6.47-6.42 (1H), 5.35-5.24 (m, 1H), 4.53-4.45 (m, 1H), 4.29-4.14 (m, 4H), 4.11 (q, J = 7.1 Hz, 2H), 3.99-3.84 (m, 1H), 3.64-3.57 (1H), 3.30 (dd, J = 13.4, 3.5 Hz, 1H), 2.90-2.80 (m, 1H), 2.70-2.41 (m, 2H), 2.28 (d, J = 3.3 Hz, 1H), 2.22, 2.21 (2 x Me, 3H), 2.18, 2.11 (2 x Me 3H), 1.29-1.23 (m, 6H) ppm; ^{13}C-NMR (100 MHz, CDCl$_3$) δ 171.25, 169.87, 169.51, 169.18, 158.26, 157.47, 140.98, 140.47, 135.64, 135.55, 131.64, 128.98, 128.63, 128.33, 127.94, 127.63, 127.29, 123.94, 122.83, 112.86, 111.46, 67.46, 64.30, 63.98, 62.10, 61.97, 60.49, 57.53, 54.51, 49.27, 40.87, 39.65, 33.98, 32.93, 21.15, 20.47, 17.53, 14.28, 14.08. HRMS [M+H] Calculated 483.2490 Found 483.2487.

Diethyl 2-((R)-2-((S)-4-benzyl-2-oxooxazolidin-3-yl)-2-((3-(trifluoromethyl)phenyl) amino)ethyl)malonate (220)
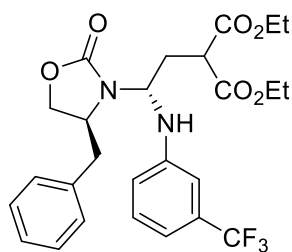
220

The crude product was purified by flash chromatography on silica gel (hexane-EtOAc 5:1) to afford the product **220** as a mixture of diastereomers (dr 95:5) as a yellow oil (0.18 g, 54%). ^{1}H-NMR (400 MHz, CDCl$_3$) δ 7.35-7.22 (m, 4H), 7.11 (d, *J* = 7.0 Hz, 2H), 7.04 (d, *J* = 7.4 Hz, 1H), 6.90 (d, *J* = 7.4 Hz, 1H), 5.28 (qd, *J* = 10.0, 5.3 Hz, 1H), 4.85 (d, *J* = 9.9 Hz, 1H), 4.26-4.06 (m, 4H), 4.06-3.98 (m, 1H), 3.95-3.88 (m, 1H), 3.53 (t, *J* = 6.8 Hz, 1H), 3.32 (dd, *J* = 13.6, 4.5 Hz, 1H), 2.83-2.73 (m, 1H), 2.65-2.52 (m, 1H), 2.45 (qd, *J* = 7.1, 5.1 Hz, 1H), 1.30-1.18 (6H) ppm; ^{13}C-NMR (100 MHz, CDCl$_3$) δ 169.27, 168.96, 157.58, 145.77, 135.41, 130.32, 129.14, 128.94, 127.44, 117.46, 116.05, 110.78, 67.52, 63.55, 62.10, 57.07, 49.09, 40.10, 32.75, 14.05 ppm; IR v (cm^{-1}) 2984, 2254, 1727, 1616, 1497, 1447, 1370, 1339, 1164, 1124, 1095, 1071, 1029; HRMS [M+H] calculated for C$_{26}$H$_{30}$F$_3$N$_2$O$_6$ 523.2050, found 523.2044.

Diethyl 2-((R)-2-((S)-4-benzyl-2-oxooxazolidin-3-yl)-2-((3,5-bis(trifluoromethyl)phenyl) amino)ethyl)malonate (221)
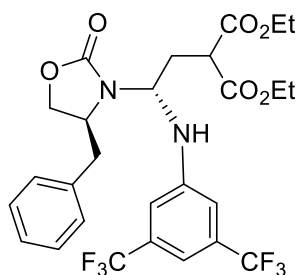
221

The crude product was purified by flash chromatography on silica gel (hexane-EtOAc 5:1) to afford the product **221** as a single of stereoisomes as a pale yellow oil (0.18 g, 60%). ^{1}H-NMR (400 MHz, CDCl$_3$) δ 7.39-7.20 (m, 3H), 7.12 (d, *J* = 7.8 Hz, 3H), 5.43-5.11 (m, 1H),

4.42-3.99 (m, 5H), 3.95 (dd, J = 8.7, 6.2 Hz, 1H), 3.50 (t, J = 6.8 Hz, 1H), 3.31 (dd, J = 13.6, 4.5 Hz, 1H), 2.94-2.69 (m, 1H), 2.62 (dd, J = 13.6, 9.5 Hz, 1H), 2.53-2.34 (m, 1H), 1.35-1.12 (m, 6H) ppm; ^{13}C-NMR (100 MHz, CDCl$_3$) δ 169.18, 168.86, 157.63, 146.46, 135.25, 132.88, 129.21, 128.87, 127.56, 124.75, 122.04, 113.46, 112.38, 67.59, 63.03, 62.21, 56.76, 48.98, 40.07, 32.50, 14.01 ppm; IR v (cm^{-1}) 3329, 2983, 1724, 1621, 1551, 1388, 1274, 1169, 1127, 1095, 1029; HRMS [M+Na] calculated for C$_{27}$H$_{28}$F$_6$N$_2$O$_6$Na 613.1744, found 613.1740.

Diethyl 2-((R)-2-((S)-4-benzyl-2-oxooxazolidin-3-yl)-2-((2-(trifluoromethoxy)phenyl) amino)ethyl)malonate (222)

222

The crude product was purified by flash chromatography on silica gel (hexane-EtOAc 5:1) to afford the product **222** as a mixture of diastereomers (dr 75:25) as a yellow oil (0.15 g, 58%). ^{1}H-NMR (400 MHz, CDCl$_3$) δ 7.36-7.21 (m, 4H), 7.21-7.11 (m, 3H), 7.08 (d, J = 7.0 Hz, 2H), 7.05-6.98 (1H), 6.81-6.74 (m, 1H), 5.51-5.30 (m, 1H), 4.95 (d, J = 8.7 Hz, 1H), 4.30-4.08 (m, 5H), 4.08-4.03 (m, 1H), 3.99 (t, J = 8.2 Hz, 0H), 3.91 (dd, J = 8.7, 6.2 Hz, 1H), 3.61-3.49 (m, 1H), 3.40-3.26 (1H), 2.87-2.76 (m, 1H), 2.72-2.57 (m, 1H), 2.51-2.38 (m, 2H), 1.31-1.21 (m, 6H) ppm; ^{13}C-NMR (100 MHz, CDCl$_3$) δ 169.46, 169.26, 168.95, 157.65, 137.60, 137.39, 136.65, 136.29, 135.62, 135.32, 129.04, 128.91, 128.49, 128.17, 127.30, 121.23, 118.88, 114.15, 67.56, 67.28, 66.92, 63.51, 63.05, 62.15, 55.43, 54.02, 49.02, 40.86, 40.28, 39.46, 32.16, 19.18, 14.05 ppm; IR v (cm^{-1}) 3382, 2984, 1730, 1612, 1519, 1411, 1274, 1257, 1216, 1165, 1095, 1028. HRMS [M+H] calculated for C$_{26}$H$_{33}$N$_2$O$_7$ 539.2000, found 539.2000.

Diethyl 2-((R)-2-((S)-4-benzyl-2-oxooxazolidin-3-yl)-2-((3-(ethoxycarbonyl)phenyl) amino)ethyl)malonate (223)
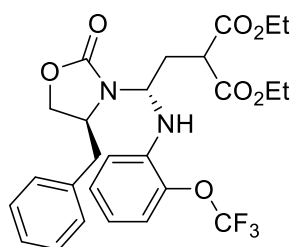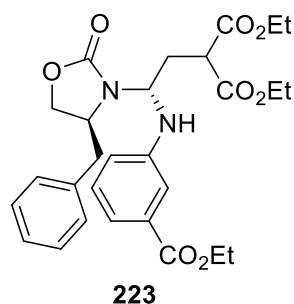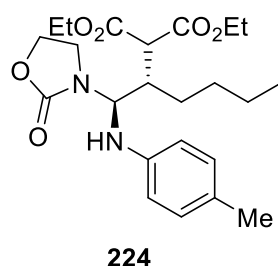

223

The crude product was purified by flash chromatography on silica gel (hexane-EtOAc 5:1) to afford the product **223** as a mixture of diastereomers (dr 55:45) as a yellow oil (0.16 g, 61%). ^{1}H-NMR (400 MHz, CDCl$_3$) δ 7.47 (d, J = 7.8 Hz, 1H), 7.39 (s, 1H), 7.34 (s, 1H), 7.31-7.17 (3H), 7.10 (q, J = 6.7 Hz, 2H), 5.29 (qd, J = 9.7, 5.3 Hz, 1H), 4.84 (dd, J = 26.2, 9.7 Hz, 1H), 4.45-4.26 (m, 2H), 4.26-4.03 (4H), 4.03-3.85 (m, 2H), 3.58 (dt, J = 23.5, 6.9 Hz, 1H), 3.41-3.20 (m, 1H), 2.88-2.73 (m, 1H), 2.65-2.51 (m, 1H), 2.51-2.38 (m, 1H), 1.35 (tt, J = 7.1, 2.3 Hz, 3H), 1.30-1.18 (m, 6H) ppm; ^{13}C-NMR (100 MHz, CDCl$_3$) δ 169.49, 169.26, 169.03, 166.66, 158.24, 157.51, 145.50, 145.16, 135.47, 131.79, 129.80, 129.02, 127.35, 120.69, 118.90, 117.86, 115.20, 67.51, 64.21, 63.62, 62.09, 61.11, 57.36, 54.89, 49.10, 40.32, 39.86, 33.69, 32.87, 14.35, 14.10 ppm; IR v (cm^{-1}) 3376, 2981, 1715, 1605, 1590, 1392, 1367, 1276, 1260, 1232, 1103, 1022; HRMS [M+Na] calculated for C$_{28}$H$_{34}$N$_2$O$_8$Na 549.2207, found 549.2215.

Diethyl 2-((1S,2S)-1-(2-oxooxazolidin-3-yl)-1-(p-tolylamino)hexan-2-yl)malonate (224)

224

The crude product was purified by flash chromatography on silica gel (hexane-EtOAc 5:1) to afford the product **224** as a single diastereoisomer as a pale yellow viscous liquid which turned solid on drying. Recrystallization with hexane-DCM 1:1 gave colourless crystals. (0.23 g, 53%). ^{1}H-NMR (400 MHz, CDCl$_3$) δ 6.99 (d, J = 8.2 Hz, 2H), 6.58 (d, J = 8.2 Hz,

2H), 5.30 (t, J = 9.3 Hz, 1H), 4.31-4.05 (m, 8H), 3.64 (d, J = 7.4 Hz, 1H), 3.38 (t, J = 8.0 Hz, 2H), 2.71-2.61 (m, 1H), 2.22 (s, 3H), 1.70-1.54 (m, 3H), 1.39-1.29 (m, 3H), 1.26 (td, J = 7.1, 1.4 Hz, 6H), 0.84 (t, J = 7.2 Hz, 3H) ppm; ^{13}C-NMR (100 MHz, CCl$_3$D) δ 169.11, 168.83, 158.36, 142.63, 130.63, 130.24, 128.53, 113.91, 66.75, 62.47, 61.79, 53.12, 42.26, 41.72, 29.01, 28.86, 23.08, 20.50, 14.06 ppm; IR v (cm^{-1}) 2252, 1737, 1699, 1514, 1389, 1249, 1178, 1037. HRMS [M+Na] calculated for C$_{23}$H$_{24}$N$_2$O$_6$Na 457.2309, found 457.2305.

3-((1*S*,3*R*)-3-phenyl-1-(*p*-tolylamino)butyl)oxazolidin-2-one (226)
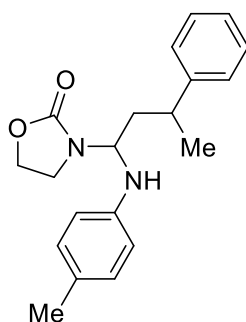
226

The crude product was purified by flash chromatography on silica gel (hexane-EtOAc 5:1) to afford the product **226** a mixture of diastereomers (dr 50:50) as a yellow liquid (0.15 g, 48%). ^{1}H-NMR (400 MHz, CCl$_3$D) δ 7.00 (d, J = 8.2 Hz, 3H), 6.85 (t, J = 7.8 Hz, 1H), 6.77 (s, 1H), 6.60 (d, J = 8.7 Hz, 3H), 6.45 (d, J = 8.2 Hz, 1H), 5.45 (t, J = 6.0 Hz, 1H), 5.28 (q, J = 6.0 Hz, 1H), 4.36 (t, J = 8.0 Hz, 2H), 4.31-4.15 (m, 2H), 3.87 (d, J = 4.9 Hz, 1H), 3.57-3.42 (m, 2H), 3.39 (t, J = 8.0 Hz, 2H), 3.36-3.24 (m, 1H), 2.21 (d, J = 11.5 Hz, 6H), 2.03 (qd, J = 6.2, 2.1 Hz, 1H), 1.70 (q, J = 11.8 Hz, 1H), 1.47 (d, J = 6.2 Hz, 3H), 1.22 (t, J = 6.0 Hz, 3H); ^{13}C-NMR (400 MHz, CCl$_3$D) δ 159.02, 157.58, 143.70, 142.37, 130.14, 129.26, 128.21, 127.24, 118.41, 115.17, 113.49, 62.25, 62.19, 59.89, 50.30, 47.11, 39.75, 38.82, 34.30, 22.37, 20.67, 20.50, 19.68.   IR v (cm^{-1}) 3350, 2918, 1730, 1617, 1506, 1482, 1423, 1304, 1251, 1171, 1077, 1057, 1028; HRMS [M+Na] calculated for C$_{20}$H$_{24}$N$_2$O$_2$Na 347.1730, found 347.1739.

3-((1S,3R)-1-(Diphenylamino)-3-phenylbutyl)oxazolidin-2-one (227)
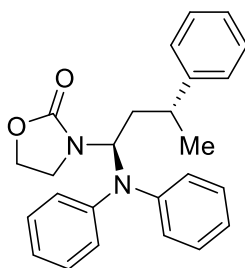
227

The crude product was purified by flash chromatography on silica gel (hexane-EtOAc 5:1) to afford the product **227** as a mixture of diastereomers (95:5) as a yellow oil (0.21 g, 53%). ^{1}H-NMR (400 MHz, CDCl$_3$) δ 7.42 (d, J = 8.2 Hz, 1H), 7.33-7.17 (m, 6H), 7.08 (d, J = 8.2 Hz, 2H), 6.96-6.84 (m, 2H), 5.43 (q, J = 7.1 Hz, 1H), 4.31 (q, J = 8.5 Hz, 1H), 4.22 (td, J = 9.1, 5.6 Hz, 1H), 3.59 (td, J = 8.8, 5.6 Hz, 1H), 3.26 (q, J = 8.7 Hz, 1H), 1.67-1.57 (m, 3H) ppm; ^{13}C-NMR (100 MHz, CDCl$_3$) δ 158.98, 143.55, 141.98, 129.31, 128.79, 127.82, 126.80, 120.62, 120.43, 118.80, 117.82, 62.50, 46.36, 39.73, 16.93 ppm; IR v (cm^{-1}) 3319, 2980, 2247, 1716, 1593, 1496, 1424, 1306, 1251, 1130, 1053, 1021; HRMS [M+H] calculated for C$_{25}$H$_{27}$N$_2$O$_2$ 387.2067, found 387.2083.

General Procedure for the Cyclization of the Adduct products to the γ-Lactams
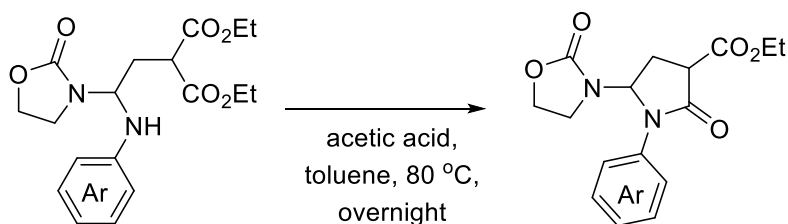
In a 25 mL round bottom flask, a solution of the diethylmalonate product (0.15 mmol) and acetic acid (0.15 mL) in toluene (2.5 mL) was heated to 80ºC and stirred overnight. The reaction was cooled to room temperature, saturated aqueous sodium bicarbonate (1.5 mL) was added and the solution extracted by ethyl acetate (5 mL × 2). The combined organic layer was dried over anhydrous sodium sulphate. The solvent was removed *in vacuo* and the crude mixture was purified via flash chromatography (EtOAc-hexanes 0:1 to 1:1) to yield the product as a mixture of diastereomers as a pale yellow oil.

Ethyl (3R,5R)-2-oxo-5-(2-oxooxazolidin-3-yl)-1-phenylpyrrolidine-3-carboxylate (242)
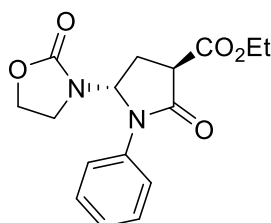
242

In a 25 mL round bottom flask, a solution of diethyl 2-(2-(2-oxooxazolidin-3-yl)-2-(phenylamino)ethyl)malonate (**179**) (55 mg, 0.15 mmol) and acetic acid (0.15 mL) in toluene (2.5 mL) was heated to 80ºC and stirred overnight. The reaction was cooled to room temperature, saturated aqueous sodium bicarbonate (1.5 mL) was added and the solution extracted by ethyl acetate (5 mL × 2). The combined organic layer was dried over anhydrous sodium sulphate and filtered. The solvent was removed *in vacuo* and the crude mixture was purified via flash chromatography (EtOAc-hexanes 3:7 to 1:1) to yield the product (**242**) as a mixture of diastereomers (dr 54:46) as a pale yellow oil (31 mg, 64%). ^{1}H-NMR (400 MHz, CDCl$_3$) δ 7.50-7.34 (m, 8H), 7.27-7.24 (1H), 7.22 (d, J = 7.0 Hz, 1H), 6.35-6.24 (m, 2H), 4.34-4.19 (m, 6H), 4.11 (td, J = 9.0, 6.7 Hz, 1H), 4.04 (td, J = 9.1, 6.2 Hz, 1H), 3.76 (td, J = 9.6, 6.7 Hz, 2H), 3.66 (dd, J = 10.3, 7.4 Hz, 1H), 3.53-3.43 (m, 1H), 3.32-3.23 (m, 1H), 3.18

(td, J = 9.0, 7.1 Hz, 1H), 3.00-2.90 (m, 1H), 2.88-2.74 (m, 1H), 2.43 (qd, J = 7.2, 5.3 Hz, 1H), 2.31-2.21 (m, 1H), 2.16 (d, J = 2.1 Hz, 1H), 1.35 (t, J = 7.2 Hz, 3H), 1.30 (t, J = 7.2 Hz, 3H), 1.23 (s, 1H) ppm; ^{13}C-NMR (100 MHz, CDCl$_3$) δ 170.22, 168.84, 168.11, 167.78, 157.569, 157.17, 135.56, 135.13, 129.48, 129.40, 126.94, 126.92, 123.20, 122.98, 67.56, 66.35, 52.40, 62.35, 62.04, 48.58, 47.85, 39.40, 38.74, 29.35, 27.14, 25.74, 14.26, 14.22 ppm; IR v (cm^{-1}) 3019, 2927, 2400, 1753, 1710, 1648, 1598, 1500, 1391, 1334; 1215, 1117, 1043; HRMS [M+Na] calculated for C$_{16}$H$_{18}$N$_2$O$_5$Na 341.1108, found 341.1106.

Ethyl (3R,5R)-2-oxo-5-(2-oxooxazolidin-3-yl)-1-(p-tolyl)pyrrolidine-3-carboxylate (243)

243

In a 25 mL round bottom flask, a solution of diethyl 2-(2-(2-oxooxazolidin-3-yl)-2-(p-tolylamino)ethyl)malonate (**181**) (56 mg, 0.15 mmol) and acetic acid (0.15 mL) in toluene (2.5 mL) was heated to 80ºC and stirred overnight. The reaction was cooled to room temperature, saturated aqueous sodium bicarbonate (1.5 mL) was added and the solution extracted by ethyl acetate (5 mL × 2). The combined organic layer was dried over anhydrous sodium sulphate and filtered. The solvent was removed *in vacuo* and the crude mixture was purified via flash chromatography (EtOAc-hexanes 3:7 to 1:1) to yield the product **223** as a mixture of diastereomers (dr 50:50) as a pale yellow oil (29 mg, 60%). ^{1}H-NMR (400 MHz, CDCl$_3$) δ 7.32 (dd, J = 12.2, 8.4 Hz, 2H), 7.18 (d, J = 7.8 Hz, 2H), 6.29-6.20 (m, 1H), 4.33-4.19 (m, 3H), 4.17-4.01 (m, 1H), 3.80-3.71 (m, 1H), 3.65 (dd, J = 10.5, 7.2 Hz, 1H), 3.53-3.41 (m, 1H), 3.33-3.16 (m, 1H), 3.00-2.88 (m, 1H), 2.85-2.73 (m, 1H), 2.42 (qd, J = 7.3, 5.4 Hz, 1H), 2.31 (s, 3H), 2.29-2.20 (m, 1H), 1.32 (dt, J = 18.1, 7.2 Hz, 3H) ppm; ^{13}C-NMR (100 MHz, CDCl$_3$) δ 170.12, 168.92, 167.82, 157.39, 136.90, 132.68, 130.03, 123.12, 67.66, 66.46, 62.19, 48.51, 47.80, 39.40, 38.76, 27.14, 25.74, 21.11, 14.24 ppm; IR v (cm^{-1}) 3376, 2980, 2916, 1732, 1700, 1614, 1516, 1500, 1391, 1252, 1177, 1031; HRMS [M+Na] calculated for C$_{17}$H$_{20}$N$_2$O$_5$Na 355.1264, found 355.1262.

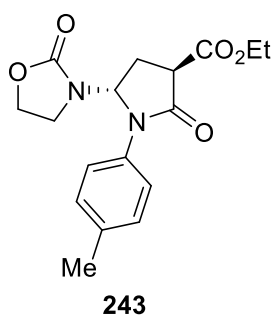**Ethyl (3*R*,5*R*)-2-oxo-5-(2-oxooxazolidin-3-yl)-1-(*m*-tolyl)pyrrolidine-3-carboxylate (244)**
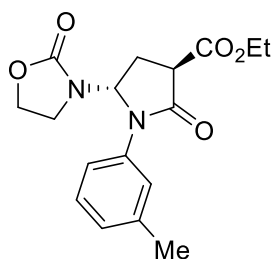
244

In a 25 mL round bottom flask, a solution of diethyl 2-(2-(2-oxooxazolidin-3-yl)-2-(m-tolylamino)ethyl)malonate (**183**) (55 mg, 0.15 mmol) and acetic acid (0.25 mL) in toluene (2.5 mL) was heated to 80ºC and stirred overnight. The reaction was cooled to room temperature, saturated aqueous sodium bicarbonate (1.5 mL) was added and the solution extracted by ethyl acetate (5 mL × 2). The combined organic layer was dried over anhydrous sodium sulphate and filtered. The solvent was removed *in vacuo* and the crude mixture was purified *via* flash chromatography (EtOAc-hexanes 3:7 to 1:1) to yield the product **244** as a mixture of diastereomers (dr 55:45) as a pale yellow oil (32 mg, 65%). ^{1}H-NMR (400 MHz, CDCl$_3$) δ 7.35-7.15 (m, 7H), 7.04 (d, *J* = 7.4 Hz, 2H), 6.32-6.21 (m, 2H), 4.34-4.19 (m, 7H), 4.17-4.10 (m, 1H), 4.10-4.00 (m, 1H), 3.80-3.70 (m, 2H), 3.65 (dd, *J* = 10.3, 7.4 Hz, 1H), 3.47 (dd, *J* = 15.2, 8.7 Hz, 1H), 3.33-3.15 (m, 2H), 2.98-2.89 (m, 1H), 2.84-2.73 (m, 1H), 2.42 (qd, *J* = 7.3, 5.4 Hz, 1H), 2.33 (s, 6H), 2.31-2.19 (m, 1H), 2.18-2.14 (1H), 1.32 (dt, *J* = 18.4, 7.1 Hz, 6H) ppm; ^{13}C-NMR (100 MHz, CDCl$_3$) δ 170.08, 168.90, 168.13, 167.67, 157.56, 157.17, 139.46, 139.39, 135.47, 135.03, 129.24, 129.16, 127.82, 127.78, 124.00, 123.75, 120.17, 120.04, 67.66, 66.44, 62.37, 62.34, 62.31, 62.04, 48.59, 47.85, 39.45, 38.76, 27.16, 25.76, 21.57, 14.24 ppm; IR v (cm^{-1}) 3475, 3019; 2980, 2400, 1750, 1706, 1606, 1520, 1493, 1392, 1215, 1113, 1043; HRMS [M+Na] calculated for C$_{17}$H$_{20}$N$_2$O$_5$Na 355.1264, found 355.1271.

Ethyl (3*R*,5*R*)-2-oxo-5-(2-oxooxazolidin-3-yl)-1-(3-(trifluoromethyl)phenyl)pyrrolidine-3-carboxylate (245)
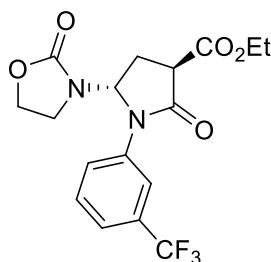
245

In a 25 mL round bottom flask, a solution of diethyl 2-(2-(2-oxooxazolidin-3-yl)-2-((3-(trifluoromethyl)phenyl)amino)ethyl)malonate (**193**) (65 mg, 0.15 mmol) and acetic acid (0.15 mL) in toluene (2.5 mL) was heated to 80ºC and stirred overnight. The reaction was cooled to room temperature, saturated aqueous sodium bicarbonate (1.5 mL) was added and the solution extracted by ethyl acetate (5 mL × 2). The combined organic layer was dried over anhydrous sodium sulphate and filtered. The solvent was removed *in vacuo* and the crude mixture was purified via flash chromatography (EtOAc-hexanes 3:7 to 1:1) to yield the product **245** as a mixture of diastereomers (dr 53:47) as a pale yellow oil (36 mg, 62%). ^{1}H-NMR (400 MHz, CDCl$_3$) δ 7.96 (s, 1H), 7.89 (s, 1H), 7.65-7.56 (m, 2H), 7.50 (q, J = 8.0 Hz, 4H), 6.35 (q, J = 4.0 Hz, 1H), 6.31 (dd, J = 8.2, 5.4 Hz, 1H), 4.20-4.13 (m, 1H), 4.13-4.04 (m, 1H), 3.83-3.74 (m, 2H), 3.68 (dd, J = 10.5, 7.6 Hz, 1H), 3.55-3.47 (m, 1H), 3.29-3.21 (m, 1H), 3.13 (td, J = 9.1, 7.4 Hz, 1H), 2.97 (qd, J = 7.4, 6.6 Hz, 1H), 2.88-2.77 (m, 1H), 2.46 (qd, J = 7.3, 5.4 Hz, 1H), 2.29 (ddd, J = 14.0, 9.5, 3.7 Hz, 1H), 1.35 (t, J = 7.2 Hz, 3H), 1.30 (t, J = 7.2 Hz, 3H) ppm; ^{13}C-NMR (100 MHz, CDCl$_3$) δ 169.68, 168.42, 167.87, 157.48, 157.12, 136.29, 135.86, 131.83, 130.03, 125.30, 123.41, 122.29, 120.25, 119.81, 67.26, 66.14, 62.53, 62.07, 53.86, 48.51, 47.79, 39.36, 38.70, 31.81, 31.00, 29.34, 26.98, 25.55, 14.21 ppm; IR v (cm^{-1}) 3020, 2976, 2400, 1753, 1713, 1598, 1521, 1389, 1216, 1180, 1135, 1043; HRMS [M+Na] calculated for C$_{17}$H$_{17}$N$_2$O$_5$Na 409.0982, found 409.0974.

Ethyl (3*R*,5*R*)-1-(4-bromophenyl)-2-oxo-5-(2-oxooxazolidin-3-yl)pyrrolidine-3-carboxylate (246)
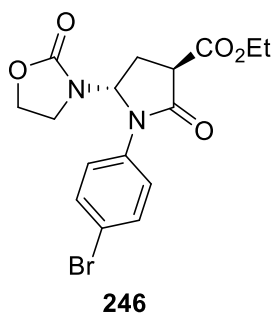
246

In a 25 mL round bottom flask, a solution of diethyl 2-(2-((4-bromophenyl)amino)-2-(2-oxooxazolidin-3-yl)ethyl)malonate (**195**) (65 mg, 0.15 mmol) and acetic acid (0.25 mL) in toluene (2.5 mL) was heated to 80ºC and stirred overnight. The reaction was cooled to room temperature, saturated aqueous sodium bicarbonate (1.5 mL) was added and the solution extracted by ethyl acetate (5 mL × 2). The combined organic layer was dried over anhydrous sodium sulphate and filtered. The solvent was removed *in vacuo* and the crude mixture was purified via flash chromatography (EtOAc-hexanes 3:7 to 1:1) to yield the product **246** as a mixture of diastereomers (dr 50:50) as a pale yellow oil (31 mg, 53%). ^{1}H-NMR (400 MHz, CDCl$_3$) δ 7.32 (dd, *J* = 12.2, 8.4 Hz, 2H), 7.18 (d, *J* = 7.8 Hz, 2H), 6.29-6.20 (m, 1H), 4.33-4.19 (m, 3H), 4.17-4.01 (m, 1H), 3.80-3.71 (m, 1H), 3.65 (dd, *J* = 10.5, 7.2 Hz, 1H), 3.53-3.41 (m, 1H), 3.33-3.16 (m, 1H), 3.00-2.88 (m, 1H), 2.85-2.73 (m, 1H), 2.42 (qd, *J* = 7.3, 5.4 Hz, 1H), 2.31 (s, 3H), 2.29-2.20 (m, 1H), 1.32 (dt, *J* = 18.1, 7.2 Hz, 3H) ppm; ^{13}C-NMR (100 MHz, CDCl$_3$) δ 170.12, 168.92, 167.82, 157.39, 136.90, 132.68, 130.03, 123.12, 67.66, 66.46, 62.19, 48.51, 47.80, 39.40, 38.76, 27.14, 25.74, 21.11, 14.24 ppm; IR *v* (cm^{-1}) 2981, 1739, 1705, 1589, 1491, 1384, 1288, 1179, 1093, 1036, 1010; HRMS [M+Na] calculated for C$_{16}$H$_{17}$N$_2$O$_5$Na 419.0213, found 419.0213.

Ethyl (3R,5R)-1-(2-fluorophenyl)-2-oxo-5-(2-oxooxazolidin-3-yl)pyrrolidine-3-carboxylate (247)
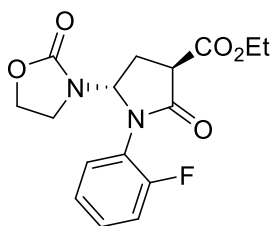
247

In a 25 mL round bottom flask, a solution of diethyl 2-(2-((2-fluorophenyl)amino)-2-(2-oxooxazolidin-3-yl)ethyl)malonate (**197**) (56 mg, 0.15 mmol) and acetic acid (0.25 mL) in toluene (2.5 mL) was heated to 80ºC and stirred overnight. The reaction was cooled to room temperature, saturated aqueous sodium bicarbonate (1.5 mL) was added and the solution extracted by ethyl acetate (5 mL × 2). The combined organic layer was dried over anhydrous sodium sulphate and filtered. The solvent was removed *in vacuo* and the crude mixture was purified via flash chromatography (EtOAc-hexanes 3:7 to 1:1) to yield the product **247** as a mixture of diastereomers (dr 53:47) as a pale yellow oil (29 mg, 61%). ^{1}H-NMR (400 MHz, CDCl$_3$) δ 7.40-7.26 (m, 4H), 7.23-7.11 (m, 4H), 6.16 (q, J = 4.5 Hz, 1H), 6.12 (dd, J = 8.2, 3.3 Hz, 1H), 4.36-4.18 (m, 7H), 4.18-4.09 (m, 1H), 3.86-3.75 (m, 2H), 3.68 (dd, J = 10.5, 6.8 Hz, 1H), 3.60-3.45 (m, 3H), 3.08-2.97 (m, 1H), 2.90-2.79 (m, 1H), 2.61 (s, 1H), 2.52 (qd, J = 7.1, 5.0 Hz, 1H), 2.40-2.29 (m, 1H), 2.15 (t, J = 3.1 Hz, 8H), 1.86 (d, J = 1.2 Hz, -1H), 1.37-1.32 (m, 3H), 1.32-1.27 (m, 3H), 1.23 (s, 3H) ppm; ^{13}C-NMR (100 MHz, CDCl$_3$) δ 169.65, 168.78, 168.32, 167.78, 157.41, 157.08, 130.30, 128.58, 128.33, 125.13, 122.83, 116.98, 69.59, 68.47, 67.33, 62.40, 62.11, 53.86, 47.53, 47.08, 39.80, 39.01, 31.83, 31.03, 29.35, 27.39, 25.80, 14.20 ppm; IR v (cm^{-1}) 2982, 2133, 2011, 2003, 1978, 1745, 1706, 1609, 1591, 1506, 1499, 1428, 1393, 1176, 1092, 763, 757; HRMS [M+Na] calculated for C$_{16}$H$_{17}$FN$_2$O$_5$Na 359.1014, found 359.0999.
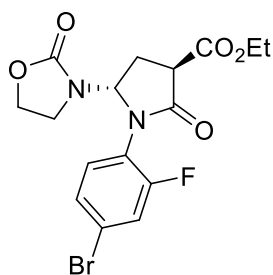
Ethyl (3R,5R)-1-(4-bromo-2-fluorophenyl)-2-oxo-5-(2-oxooxazolidin-3-yl)pyrrolidine-3-carboxylate (248).

248

In a 25 mL round bottom flask, a solution of diethyl 2-(2-((4-bromo-2-fluorophenyl)amino)-2-(2-oxooxazolidin-3-yl)ethyl)malonate (**199**) (70 mg, 0.15 mmol) and acetic acid (0.25 mL) in toluene (2.5 mL) was heated to 80ºC and stirred overnight. The reaction was cooled to room temperature, saturated aqueous sodium bicarbonate (1.5 mL) was added and the solution extracted by ethyl acetate (5 mL × 2). The combined organic layer was dried over anhydrous sodium sulphate and filtered. The solvent was removed *in vacuo* and the crude mixture was purified via flash chromatography (EtOAc-hexanes 3:7 to 1:1) to yield the product **248** as a mixture of diastereomers (dr 54:46) as a white solid substance (37 mg, 60%, M.P. 100.7 – 102.4ºC). ^{1}H-NMR (400 MHz, CDCl$_3$) δ 7.41-7.29 (m, 4H), 7.23-7.12 (m, 2H), 6.13 (q, J = 4.5 Hz, 1H), 6.09 (q, J = 3.8 Hz, 1H), 4.37-4.07 (m, 9H), 3.87-3.72 (m, 2H), 3.67 (dd, J = 10.7, 6.6 Hz, 1H), 3.57-3.47 (m, 2H), 3.43 (dd, J = 16.1, 9.1 Hz, 1H), 3.07-2.95 (m, 1H), 2.90-2.78 (m, 1H), 2.57-2.47 (m, 1H), 2.41-2.30 (m, 1H), 1.36-1.31 (m, 3H), 1.31-1.27 (m, 3H) ppm; ^{13}C-NMR (100 MHz, CDCl$_3$) δ 169.48, 168.62, 168.27, 167.69, 159.05, 157.44, 157.08, 156.50, 129.62, 129.22, 128.61, 128.45, 122.69, 122.12, 120.72, 68.26, 67.10, 62.45, 62.13, 47.45, 47.02, 39.81, 39.03, 27.35, 25.74, 14.20 ppm; IR v (cm^{-1}) 3155, 2986, 2254, 1757, 1719, 1603, 1498, 1389, 1181, 1042, 987, 732; HRMS [M+Na] calculated for C$_{16}$H$_{16}$BrFN$_2$O$_5$Na 437.0119, found 437.0102.

Ethyl (3*S*,5*R*)-5-((*S*)-4-benzyl-2-oxooxazolidin-3-yl)-2-oxo-1-(3-(trifluoromethyl)phenyl) pyrrolidine-3-carboxylate (249)
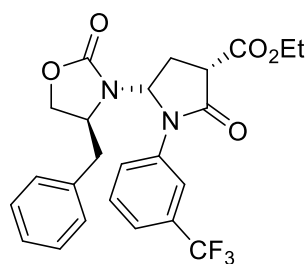
249

In a 25 mL round bottom flask, a solution of diethyl 2-(2-((*S*)-4-benzyl-2-oxooxazolidin-3-yl)-2-((3-(trifluoromethyl)phenyl)amino)ethyl)malonate (**220**) (51 mg, 0.10 mmol) and acetic acid (0.15 mL) in toluene (2.5 mL) was heated to 80ºC and stirred overnight. The reaction was cooled to room temperature, saturated aqueous sodium bicarbonate (1.5 mL) was added and the solution extracted by ethyl acetate (5 mL × 2). The combined organic layer was dried over anhydrous sodium sulphate and filtered. The solvent was removed *in vacuo* and the crude mixture was purified via flash chromatography (EtOAc-hexanes 3:7 to 1:1) to yield the product **249** as a mixture of diastereomers (dr 55:45) as a pale yellow oil (21 mg, 44%). ^{1}H-NMR (400 MHz, CDCl$_3$) δ 7.97 (s, 1H), 7.78-7.73 (m, 1H), 7.69-7.61 (m, 1H), 7.59-7.49 (m, 3H), 7.39-7.20 (m, 6H), 7.17-7.10 (m, 2H), 7.09-7.03 (m, 1H), 6.47 (t, J = 7.4 Hz, 1H), 5.75-5.54 (m, 1H), 4.51-4.40 (m, 1H), 4.32-4.18 (m, 1H), 4.15-4.05 (m, 1H), 4.04-3.93 (m, 1H), 3.87 (ddd, J = 20.0, 9.1, 6.0 Hz, 2H), 3.81-3.72 (m, 1H), 3.24 (dd, J = 13.2, 4.1 Hz, 1H), 2.95 (q, J = 6.6 Hz, 1H), 2.91-2.80 (m, 2H), 2.64-2.48 (m, 1H), 2.03 (d, J = 3.7 Hz, 1H), 1.97 (dd, J = 13.0, 11.3 Hz, 1H), 1.44-1.35 (m, 3H), 1.35-1.27 (m, 3H) ppm; ^{13}C-NMR (100 MHz, CDCl$_3$) δ 169.78, 169.33, 168.79, 167.37, 157.68, 156.51, 136.30, 135.11, 134.88, 129.81, 127.91, 127.46, 125.67, 119.99, 68.77, 67.40, 67.05, 66.84, 62.75, 62.29, 57.44, 53.57, 48.69, 47.96, 40.64, 39.09, 27.76, 24.11, 14.29, 14.22 ppm; IR v (cm^{-1}) 3020, 2938, 1752, 1712, 1615, 1596, 1497, 1329, 1216, 1172, 1131; HRMS [M+Na] calculated for C$_{17}$H$_{17}$F$_3$N$_2$O$_5$Na 499.1451, found 499.1461.
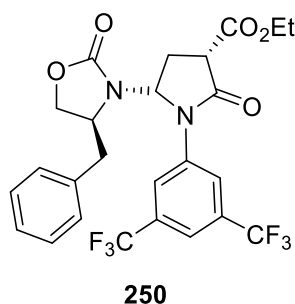
Ethyl (3*S*,5*R*)-5-((*S*)-4-benzyl-2-oxooxazolidin-3-yl)-1-(3,5-bis(trifluoromethyl)phenyl)-2-oxopyrrolidine-3-carboxylate (250)

250

In a 25 mL round bottom flask, a solution of diethyl 2-(2-((*S*)-4-benzyl-2-oxooxazolidin-3-yl)-2-((3,5-bis(trifluoromethyl)phenyl)amino)ethyl)malonate (**221**) (58 mg, 0.10 mmol) and acetic acid (0.25 mL) in toluene (2.5 mL) was heated to 80ºC and stirred overnight. The reaction was cooled to room temperature, saturated aqueous sodium bicarbonate (1.5 mL) was added and the solution extracted by ethyl acetate (5 mL × 2). The combined organic layer was dried over anhydrous sodium sulphate and filtered. The solvent was removed *in vacuo* and the crude mixture was purified via flash chromatography (EtOAc-hexanes 3:7 to 1:1) to yield the product **250** as a mixture of diastereomers (dr 58:42) as a pale yellow oil (8 mg, 15%). ^{1}H-NMR (400 MHz, CCl$_3$D) δ 8.17 (s, 3H), 7.98 (s, 2H), 7.77 (s, 2H), 7.42-7.21 (m, 12H), 7.12 (q, *J* = 6.7 Hz, 5H), 6.51 (t, *J* = 7.2 Hz, 1H), 5.74 (dd, *J* = 8.9, 2.7 Hz, 1H), 4.55-4.43 (m, 1H), 4.32-4.18 (m, 3H), 4.15-3.99 (m, 3H), 3.92 (ddd, *J* = 27.8, 9.1, 5.6 Hz, 3H), 3.21 (dd, *J* = 13.0, 3.9 Hz, 1H), 3.02-2.81 (m, 5H), 2.61 (dd, *J* = 13.6, 7.8 Hz, 1H), 2.57-2.46 (m, 1H), 2.16 (s, 4H), 2.06-1.91 (m, 2H), 1.61 (d, J = 38.7 Hz, 11H), 1.39 (t, *J* = 7.2 Hz, 4H), 1.35-1.20 (m, 8H) ppm; ^{13}C-NMR (100 MHz, CDCl$_3$) δ 169.38, 168.80, 167.50, 157.56, 156.38, 137.86, 137.21, 134.71, 134.60, 132.97, 132.79, 132.64, 132.45, 129.43, 129.06, 128.97, 128.72, 127.99, 127.50, 124.25, 123.39, 122.56, 121.54, 68.11, 67.31, 66.97, 66.69, 62.86, 62.42, 57.10, 53.40, 48.64, 47.83, 40.65, 39.05, 30.94, 27.70, 23.91, 14.21 ppm; IR *υ* (cm^{-1}) 3020, 2254, 1794, 1755, 1716, 1602, 1474, 1389, 1279, 1216, 1145, 1097; HRMS [M+Na] calculated for C$_{18}$H$_{16}$F$_6$N$_2$O$_5$Na 567.1325, found 567.1335.

General procedure for the photoredox reaction of allenamides with different nucleophiles: An oven dried 50 mL three neck round bottom flask was filled with argon gas and charged with iridium photocatalyst (1.5 mol%) allenamide (1.0 eq) and anhydrous acetonitrile (~ 0.1 M) and seal with a rubber septum in the middle neck and the other two necks closed with glass stoppers. The flask was purged again with argon while one neck was opened. The middle neck was then fitted with an argon filled balloon. Diethyl bromomalonate (2.0 eq), trimethylamine TEA (2.0 eq) and the nucleophile (5.0 eq) were added in that order to the solution in the flask under the argon atmosphere. The flask was then irradiated with a Kessil blue light (λ = 467 nm) for 3 - 10 h with stirring at room temperature. After the reaction has completed as monitored by TLC, the solvent was removed under a reduced pressure to obtain the crude product. The crude product was purified by flash chromatography on silica gel (hexane-EtOAc 4:1) to afford the product.

Diethyl 2-(3-ethoxy-3-(2-oxooxazolidin-3-yl)prop-1-en-2-yl)malonate (393)
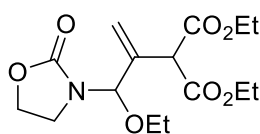
393

The crude product was purified by flash chromatography on silica gel (hexane-EtOAc 2:1) to afford the product **393** as a pale-yellow oil (65 mg, 40%). ^{1}H-NMR (400 MHz, CDCl$_3$) δ 5.61 (d, J = 1.6 Hz, 1H), 5.56 (s, 1H), 5.43-5.41 (1H), 4.39-4.25 (m, 2H), 4.22-4.15 (m, 4H), 4.05 (s, 1H), 3.61-3.47 (m, 2H), 3.43 (dd, J = 8.7, 7.4 Hz, 2H), 1.27 (dt, J = 18.0, 7.1 Hz, 6H), 1.19 (t, J = 7.0 Hz, 3H) ppm; ^{13}C-NMR (100 MHz, CDCl$_3$) δ 168.46, 167.62, 167.49, 158.63, 136.87, 118.48, 83.06, 64.34, 63.58, 62.70, 61.99, 61.89, 54.48, 39.00, 14.87, 14.05 ppm; IR v (cm^{-1}) 3329, 2969, 2931, 2882, 2657, 1745, 1466, 1378, 1305, 1159, 1127, 1107; HRMS [M+Na] calculated for C$_{15}$H$_{23}$NO$_7$Na 352.1367, found 352.1367.

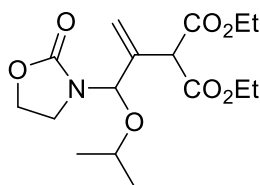**Diethyl 2-(3-isopropoxy-3-(2-oxooxazolidin-3-yl)prop-1-en-2-yl)malonate (395)**

395

The crude product was purified by flash chromatography on silica gel (hexane-EtOAc 2:1) to afford the product **395** as a pale yellow oil (55 mg, 33%). ^{1}H-NMR (400 MHz, CDCl$_3$) δ 6.27 (d, J = 7.8 Hz, 1H), 5.42 (d, J = 18.1 Hz, 1H), 4.41 (t, J = 7.8 Hz, 2H), 4.22-4.14 (m, 4H), 4.07-4.04 (1H), 3.89 (t, J = 8.0 Hz, 2H), 2.42-2.39 (2H), 1.30-1.20 (m, 12H) ppm; ^{13}C-NMR (100 MHz, CDCl$_3$) δ 168.14, 157.08, 138.35, 126.52, 123.26, 118.90, 62.68, 61.96, 57.05, 55.98, 45.84, 28.00, 14.07 ppm; IR v (cm^{-1}) 3055, 2987, 2306, 1755, 1667, 1265, 1155, 1035; HRMS [M+Na] calculated for C$_{16}$H$_{25}$NO$_7$Na 366.1523, found 366.1411.

Diethyl 2-(3-(2-oxooxazolidin-3-yl)-3-(p-tolylamino)prop-1-en-2-yl)malonate (399)

399

The crude product was purified by flash chromatography on silica gel (hexane-EtOAc 3:7) to afford the product **399** as a pale yellow oil (98 mg, 53%). ^{1}H-NMR (400 MHz, CDCl$_3$) δ 6.98 (d, J = 8.2 Hz, 3H), 6.60 (d, J = 8.7 Hz, 2H), 6.52 (d, J = 8.2 Hz, 1H), 5.96 (d, J = 9.5 Hz, 1H), 5.47 (dd, J = 8.2, 1.6 Hz, 1H), 4.93 (d, J = 9.5 Hz, 1H), 4.31-4.02 (6H), 3.79 (s, 1H), 3.50-3.31 (m, 2H), 2.21 (s, 3H), 1.31-1.20 (m, 6H) ppm; ^{13}C-NMR (100 MHz, CDCl$_3$) δ 169.01, 168.63, 167.70, 158.34, 141.86, 137.58, 130.12, 128.64, 118.53, 113.80, 113.27, 65.33, 62.25, 62.03, 55.53, 39.50, 31.66, 22.73, 20.51, 14.05 ppm; IR v (cm^{-1}) 3328, 2969, 2931, 1750, 1684, 1595, 1466, 1378, 1367, 1306, 1127, 1107, 950; HRMS [M+H] calculated for C$_{20}$H$_{27}$N$_2$O$_6$ 391.1864, found 391.1860.
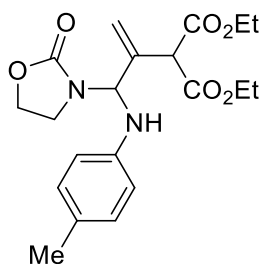
Diethyl 2-(3-((2,4-dimethylphenyl)amino)-3-(2-oxooxazolidin-3-yl)prop-1-en-2-yl)malonate (400)
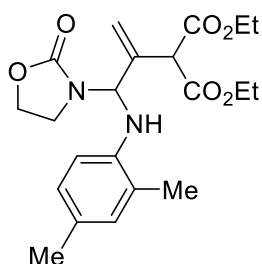
400

The crude product was purified by flash chromatography on silica gel (hexane-EtOAc 3:7) to afford the product **400** as a pale yellow oil (109 mg, 57%). ^{1}H-NMR (400 MHz, CDCl$_3$) δ 7.07-6.79 (m, 2H), 6.68-6.59 (m, 1H), 6.04 (s, 1H), 5.48 (q, *J* = 2.2 Hz, 1H), 4.94 (d, *J* = 6.6 Hz, 1H), 4.34-4.01 (m, 6H), 3.81 (s, 1H), 3.47 (td, *J* = 8.8, 5.5 Hz, 1H), 3.30 (q, *J* = 8.8 Hz, 1H), 2.22 (t, *J* = 4.7 Hz, 3H), 2.11 (d, *J* = 9.5 Hz, 3H), 1.27 (dt, *J* = 28.3, 7.1 Hz, 6H) ppm; ^{13}C-NMR (100 MHz, CDCl$_3$) δ 169.34, 168,74, 167.84, 158.31, 139.83, 137.65, 131.37, 131.11, 127.85, 127.30, 122.84, 118.73, 111.01, 109.92, 64.73, 62.70, 62.30, 58.17, 55.64, 44.44, 42.21, 39.22, 20.45, 17.74, 17.55, 14.07 ppm; IR *v* (cm^{-1}) 3342, 2969, 2930, 2881, 1738, 1517, 1466, 1378, 1305, 1159, 1128, 1034, 950; HRMS [M+H] calculated for C$_{21}$H$_{29}$N$_2$O$_6$ 405.2020, found 405.2017.

Diethyl 2-(3-((3,5-bis(trifluoromethyl)phenyl)amino)-3-(2-oxooxazolidin-3-yl)prop-1-en-2-yl) malonate (401)
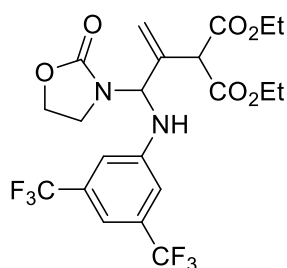
401

The crude product was purified by flash chromatography on silica gel (hexane-EtOAc 7:3) to afford the product **401** as a pale yellow liquid (113 mg, 45%). ^{1}H-NMR (400 MHz, CDCl$_3$) δ 7.27-7.21 (m, 1H), 7.11 (s, 2H), 6.17 (d, *J* = 8.7 Hz, 1H), 6.07 (d, *J* = 8.7 Hz, 1H), 5.51 (q, *J* = 1.8 Hz, 2H), 4.37-4.18 (m, 4H), 4.03-3.94 (m, 2H), 3.54-3.39 (m, 2H), 1.31 (t, *J* = 7.2 Hz, 3H), 1.11 (t, *J* = 7.0 Hz, 3H) ppm; ^{13}C-NMR (100 MHz, CDCl$_3$) δ 169.66, 167.09, 158.22,

145.63, 136.38, 133.33, 133.01, 132.67, 132.35, 124.73, 122.02, 120.34, 113.19, 112.30, 64.34, 62.66, 62.52, 55.92, 39.45, 14.02, 13.90 ppm; IR v (cm^{-1}) 3332, 2969, 2931, 1741, 1622, 1466, 1378, 1306, 1160, 1128, 1107, 1036; HRMS [M+Na] calculated for $C_{21}H_{22}F_6N_2O_6Na$ 535.1274, found 535.1276.

Diethyl 2-(3-((4-bromophenyl)amino)-3-(2-oxooxazolidin-3-yl)prop-1-en-2-yl)malonate (402)

402

The crude product was purified by flash chromatography on silica gel (hexane-EtOAc 3:7) to afford the product **402** as a pale yellow liquid (108 mg, 49%). ^{1}H-NMR (400 MHz, CDCl$_3$) δ 7.24 (d, J = 8.7 Hz, 2H), 6.57 (d, J = 8.7 Hz, 2H), 5.95 (d, J = 9.1 Hz, 1H), 5.46 (s, 2H), 5.37 (d, J = 9.5 Hz, 1H), 4.33-4.00 (m, 6H), 3.49-3.30 (m, 2H), 1.22 (t, J = 7.2 Hz, 3H), 1.15 (t, J = 7.0 Hz, 3H) ppm; IR v (cm^{-1}) 3370, 2970, 1723, 1593, 1490, 1160, 1098, 1073, 1030, 1014; HRMS [M+H] calculated for $C_{19}H_{24}BrN_2O_6$ 455.0812, found 455.0811.

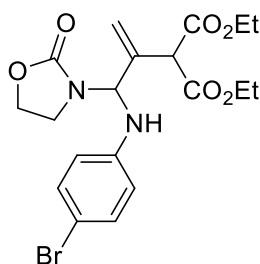**Diethyl 2-(3-((4-bromo-2-fluorophenyl)amino)-3-(2-oxooxazolidin-3-yl)prop-1-en-2-yl)malonate (403)**
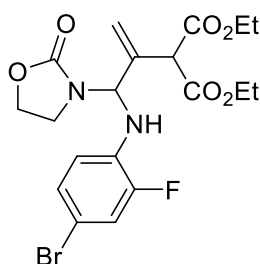
403

The crude product was purified by flash chromatography on silica gel (hexane-EtOAc 7:3) to afford the product **403** as a pale yellow liquid (102 mg, 46%). ^{1}H-NMR (400 MHz, CDCl$_3$) δ 7.16-7.09 (m, 2H), 6.80-6.73 (m, 1H), 6.01 (d, J = 9.1 Hz, 1H), 5.50 (dd, J = 7.2, 1.9 Hz,

2H), 5.44 (dd, J = 9.1, 2.9 Hz, 1H), 4.34-4.17 (6H), 4.12-4.05 (2H), 3.47 (dd, J = 14.6, 8.0 Hz, 1H), 3.35 (q, J = 8.8 Hz, 1H), 1.29 (t, J = 7.2 Hz, 3H), 1.17 (t, J = 7.2 Hz, 3H) ppm; ^{13}C-NMR (100 MHz, CDCl$_3$) δ 168.85, 167.33, 160.07, 158.26, 136.73, 132.06, 128.09, 119.47, 118.52, 118.30, 114.76, 109.81, 64.30, 62.43, 55.63, 39.12, 14.00 ppm; IR v (cm^{-1}) 3155, 2985, 1793, 1748, 1614, 114, 1194, 1096, 1034; HRMS [M+Na] calculated for C$_{19}$H$_{22}$BrN$_2$O$_6$Na 495.0537, found 495.0559.

Diethyl 2-(3-((2-methoxyphenyl)amino)-3-(2-oxooxazolidin-3-yl)prop-1-en-2-yl) malonate (404)

404

The crude product was purified by flash chromatography on silica gel (hexane-EtOAc 3:7) to afford the product **404** as a pale yellow liquid (99 mg, 51%). ^{1}H-NMR (400 MHz, CDCl$_3$) δ 6.87-6.67 (m, 4H), 5.98 (d, J = 8.7 Hz, 1H), 5.52 (d, J = 14.0 Hz, 2H), 5.16 (d, J = 9.5 Hz, 1H), 4.30-4.07 (m, 7H), 3.81 (s, 3H), 3.43 (td, J = 8.5, 5.5 Hz, 1H), 3.33-3.23 (1H), 1.24 (dt, J = 23.8, 7.1 Hz, 6H) ppm; ^{13}C-NMR (100 MHz, CDCl$_3$) δ 168.21, 167.76, 158.40, 147.08, 137.44, 134.03, 121.75, 118.82, 118.01, 111.72, 109.99, 65.04, 62.45, 62.16, 55.67, 55.13, 39.22, 14.05 ppm; IR v (cm^{-1}) 3331, 2969, 2931, 2882, 1739, 1466, 1378, 1367, 1340, 1305, 1159, 1127, 1031, 950; HRMS [M+H] calculated for C$_{20}$H$_{27}$N$_2$O$_7$ 407.1812, found 407.1811.

Diethyl 2-(3-(2-oxooxazolidin-3-yl)-3-((2-(trifluoromethoxy)phenyl)amino)prop-1-en-2-yl)malonate (405)
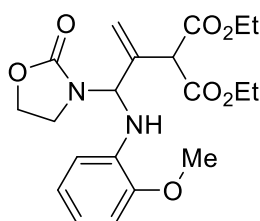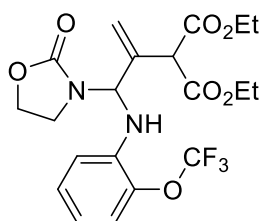

405

The crude product was purified by flash chromatography on silica gel (hexane-EtOAc 7:3) to afford the product **405** as a pale yellow liquid (117 mg, 53%). ^{1}H-NMR (400 MHz, CDCl$_3$) δ 7.16 (t, J = 7.6 Hz, 2H), 6.89 (d, J = 7.4 Hz, 1H), 6.76 (td, J = 7.7, 1.4 Hz, 1H), 6.07 (d, J = 9.1 Hz, 1H), 5.71-5.61 (m, 1H), 5.50 (dd, J = 13.0, 1.9 Hz, 2H), 4.33-4.01 (m, 6H), 3.48 (td, J = 8.7, 5.6 Hz, 1H), 3.31 (q, J = 8.9 Hz, 1H), 1.71 (s, 1H), 1.29 (t, J = 7.2 Hz, 3H), 1.16 (t, J = 7.0 Hz, 3H) ppm; ^{13}C-NMR (100 MHz, CDCl$_3$) δ 168.92, 167.50, 158.34, 136.94, 136.80, 136.50, 128.37, 121.36, 119.18, 118.78, 113.37, 64.09, 62.34, 55.39, 38.99, 14.00 ppm; IR v (cm^{-1}) 3337, 2969, 2931, 1739, 1613, 1466, 1378, 1308, 1159, 1128, 1107, 1034; HRMS [M+H] calculated for C$_{20}$H$_{24}$F$_3$N$_2$O$_7$ 461.1530, found 461.1532.

Diethyl 2-(3-((2,4-dimethylphenyl)amino)-3-(2-oxopyrrolidin-1-yl)prop-1-en-2-yl)malonate (406)
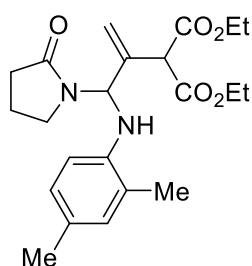
406

The crude product was purified by flash chromatography on silica gel (hexane-EtOAc 4:1) to afford the product **406** as a pale yellow liquid (106 mg, 54%). ^{1}H-NMR (400 MHz, CDCl$_3$) δ 6.87 (d, J = 7.4 Hz, 2H), 6.52 (d, J = 8.2 Hz, 1H), 6.20 (d, J = 9.9 Hz, 1H), 5.42 (d, J = 2.1 Hz, 1H), 5.35 (d, J = 1.6 Hz, 1H), 4.79 (d, J = 10.3 Hz, 1H), 4.31 (s, 1H), 4.29-4.17 (m, 2H), 4.12-4.02 (m, 2H), 3.28 (td, J = 8.9, 3.7 Hz, 1H), 3.09-3.00 (m, 1H), 2.46-2.37 (2H), 2.20 (s,

3H), 2.09 (s, 3H), 2.00-1.85 (m, 2H), 1.29 (t, J = 7.2 Hz, 3H), 1.15 (t, J = 7.2 Hz, 3H) ppm; ^{13}C-NMR (100 MHz, CDCl$_3$) δ 175.90, 169.19, 168.08, 140.19, 137.65, 131.24, 127.70, 122.73, 117.83, 110.96, 62.65, 62.14, 55.43, 41.53, 31.37, 20.45, 18.04, 17.53, 14.08 ppm; IR v (cm^{-1}) 3018, 2941, 1727, 1677, 1420, 1176, 1096, 1035; HRMS [M+H] calculated for C$_{22}$H$_{31}$N$_2$O$_5$ 425.2047, found 425.2068.

Diethyl 2-(3-((2,4-dimethylphenyl)amino)-3-(2-oxopiperidin-1-yl)prop-1-en-2-yl)malonate (407)

407

The crude product was purified by flash chromatography on silica gel (hexane-EtOAc 4:1) to afford the product **407** as a pale yellow liquid (86 mg, 41%). ^{1}H-NMR (400 MHz, CDCl$_3$) δ 6.86 (d, J = 6.6 Hz, 2H), 6.77 (d, J = 10.3 Hz, 1H), 6.50 (d, J = 9.1 Hz, 1H), 5.40-5.38 (1H), 5.30 (d, J = 2.1 Hz, 1H), 4.93 (d, J = 10.3 Hz, 1H), 4.33 (s, 1H), 4.32-3.99 (4H), 3.18-3.09 (m, 1H), 2.94-2.85 (m, 1H), 2.50-2.41 (m, 2H), 2.20 (s, 3H), 2.09 (s, 3H), 1.82-1.51 (m, 4H), 1.30 (t, J = 7.2 Hz, 3H), 1.15 (t, J = 7.2 Hz, 3H) ppm; ^{13}C-NMR (100 MHz, CDCl$_3$) δ 170.71, 169.45, 168.15, 140.25, 137.59, 131.28, 127.55, 122.55, 117.47, 111.07, 64.01, 62.44, 55.44, 40.55, 32.38, 22.97, 20.63, 17.55, 14.06 ppm; IR v (cm^{-1}) 3018, 2984, 1731, 1660, 1216, 1371, 1033; HRMS [M+Na] calculated for C$_{23}$H$_{32}$N$_2$O$_5$Na 439.2203, found 439.2217.

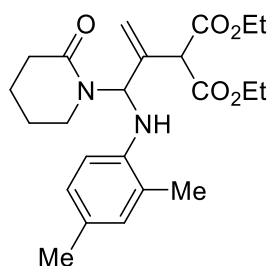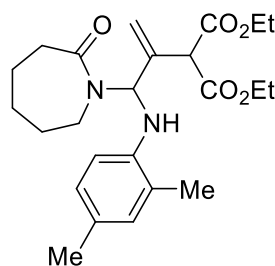**Diethyl 2-(3-((2,4-dimethylphenyl)amino)-3-(2-oxoazepan-1-yl)prop-1-en-2-yl)malonate (408)**

408

The crude product was purified by flash chromatography on silica gel (hexane-EtOAc 4:1) to afford the product **408** as a pale yellow liquid (92 mg, 43%). ^{1}H-NMR (400 MHz, CDCl$_3$) δ 6.89-6.82 (m, 2H), 6.70 (d, J = 9.9 Hz, 1H), 6.56 (d, J = 8.2 Hz, 1H), 5.36 (d, J = 2.1 Hz, 1H), 5.29 (d, J = 2.1 Hz, 1H), 5.03 (t, J = 4.9 Hz, 1H), 4.31 (s, 1H), 4.29-4.17 (m, 3H), 4.02 (dd, J = 8.9, 7.2 Hz, 1H), 3.30-3.11 (m, 3H), 2.63-2.42 (m, 3H), 2.19 (s, 3H), 2.08 (s, 4H), 1.77-1.61 (m, 4H), 1.47-1.36 (m, 2H), 1.30 (t, J = 7.2 Hz, 3H), 1.14 (t, J = 7.2 Hz, 3H) ppm; ^{13}C-NMR (100 MHz, CDCl$_3$) δ 176.77, 169.54, 168.12, 140.61, 138.50, 131.08, 127.69, 127.27, 122.21, 117.78, 111.21, 64.96, 62.17, 62.12, 55.43, 43.52, 37.99, 30.21, 28.01, 23.44, 20.49, 17.66, 14.10, 14.02 ppm; IR v (cm^{-1}) 3386, 3096, 2981, 2934, 2735, 1736, 1636, 1522, 1311, 1176, 1036; HRMS [M+Na] calculated for C$_{24}$H$_{34}$N$_2$O$_5$Na 453.2360, found 453.2309.

Diethyl 2-(3-((4-bromo-2-fluorophenyl)amino)-3-(2-oxopyrrolidin-1-yl)prop-1-en-2-yl)malonate (409)
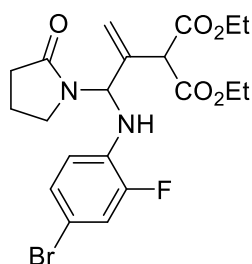
409

The crude product was purified by flash chromatography on silica gel (hexane-EtOAc 4:1) to afford the product **409** as a pale yellow liquid (97 mg, 42%). ^{1}H-NMR (400 MHz, CDCl$_3$) δ 7.14 (d, J = 2.1 Hz, 1H), 7.12-7.06 (2H), 6.65 (t, J = 8.9 Hz, 1H), 6.18 (d, J = 9.9 Hz, 1H), 5.46 (d, J = 2.1 Hz, 1H), 5.37 (d, J = 1.6 Hz, 1H), 5.33 (dd, J = 9.9, 2.9 Hz, 1H), 4.30-4.16

(m, 3H), 4.10 (q, J = 7.1 Hz, 3H), 3.31-3.23 (m, 1H), 3.13-3.05 (m, 1H), 2.49-2.33 (m, 2H), 2.01-1.90 (m, 2H), 1.29 (t, J = 7.2 Hz, 3H), 1.18 (t, J = 7.0 Hz, 3H) ppm; ^{13}C-NMR (100 MHz, CDCl$_3$) δ 176.09, 168.78, 167.59, 152.56, 150.14, 136.62, 132.33, 127.93, 118.67, 118.39, 118.18, 114.64, 109.34, 62.33, 61.90, 55.34, 41.47, 31.20, 18.07, 14.05 ppm; IR v (cm^{-1}) 3054, 728, 1686, 1614, 1421, 1265, 1154, 1035; HRMS [M+Na] calculated for C$_{20}$H$_{24}$BrFN$_2$O$_5$Na 493.0745, found 493.0767.

**Diethyl (*S,Z*)-2-(1-(4-benzyl-2-oxooxazolidin-3-yl)-3-((2,4-dimethylphenyl)amino)prop-1-en-2-yl)malonate (410)**

410

The crude product was purified by flash chromatography on silica gel (hexane-EtOAc 7:3) to afford the product **410** as a pale yellow liquid (97 mg, 41%). ^{1}H-NMR (400 MHz, CDCl$_3$) δ 7.28-7.21 (m, 3H), 7.09 (d, J = 6.2 Hz, 2H), 6.90 (t, J = 7.8 Hz, 2H), 6.51 (d, J = 8.2 Hz, 1H), 6.38 (s, 1H), 4.39-4.31 (m, 1H), 4.28 (s, 1H), 4.22-4.05 (m, 6H), 3.93 (d, J = 9.1 Hz, 2H), 3.17 (dd, J = 13.8, 3.5 Hz, 1H), 2.71-2.64 (1H), 2.22 (s, 3H), 2.09 (s, 3H), 1.60 (s, 1H), 1.27-1.19 (m, 6H) ppm; ^{13}C-NMR (100 MHz, CDCl$_3$) δ 168.36, 156.35, 143.79, 135.09, 131.10, 129.15, 127.10, 126.14, 123.32, 110.02, 77.12, 66.70, 62.07, 57.90, 56.53, 43.76, 38.42, 20.43, 17.49, 14.12 ppm; IR v (cm^{-1}) 3031, 2985, 1756, 1731, 1516, 1302, 1266, 1032; HRMS [M+H] calculated for C$_{28}$H$_{35}$N$_2$O$_6$ 495.2490, found 495.2487.

Diethyl (S,Z)-2-(3-((2,4-dimethylphenyl)amino)-1-(4-isopropyl-2-oxooxazolidin-3-yl) prop-1-en-2-yl)malonate (411)
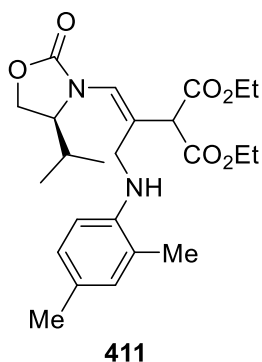
411
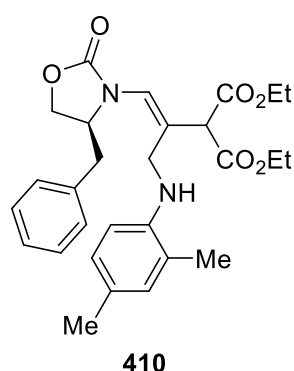
The crude product was purified by flash chromatography on silica gel (hexane-EtOAc 4:1) to afford the product **411** as a pale yellow liquid (107 mg, 50%). ^{1}H-NMR (400 MHz, CDCl$_3$) δ 6.91-6.84 (m, 2H), 6.47 (d, J = 7.8 Hz, 1H), 6.24 (s, 1H), 4.29-4.22 (m, 2H), 4.20-4.04 (m, 5H), 4.01-3.94 (m, 1H), 3.89 (d, J = 13.6 Hz, 1H), 3.79 (d, J = 13.6 Hz, 1H), 2.20 (s, 3H), 2.08 (s, 3H), 2.10-2.07 (1H), 1.27-1.17 (m, 6H), 0.87 (t, J = 6.6 Hz, 6H) ppm; ^{13}C-NMR (100 MHz, CDCl$_3$) δ 168.41, 168.33, 156.68, 143.90, 131.04, 127.24, 126.65, 126.22, 124.34, 123.06, 109.97, 63.85, 61.98, 61.63, 57.00, 43.77, 29.38, 20.41, 17.91, 17.44, 15.14, 14.03 ppm; IR v (cm^{-1}) 3157, 2982, 2253, 1746, 1664, 1467, 1261, 1095, 1033; HRMS [M+H] calculated for C$_{24}$H$_{35}$N$_2$O$_6$ 447.2490, found 447.2510.

REFERENCES

1. Castellote, M.; Bengtsson, N. *RILEM State of the Art Report* **2011,** *5*, 5.

2. Serpone, N.; Emeline A. V.; *Int. J. Photoenergy*, **2002,** *4*, 91.

3. Serpone, N.; Salinaro, A. *Pure & Appl. Chem.* **1999**, *71*, 303.

4. Cismesia, M. A.; Yoon T. P. *Chem. Sci.* **2015**, *6*, 5426.

5. Koike, T.; Akita M. *Synlett.* **2013**, *24*, 2492.

6. König, B. *Eur. J. Org. Chem.* **2017**, 1979.

7. Zeitler, K. *Angew. Chem. Int. Ed.* **2009**, *48*, 2.

8. Narayanam, J. M. R.; Stephenson, C. R. J. *Chem. Soc. Rev.* **2011**, *40*, 102.

9. Gust, D.; Moore, T. A. *Science* **1989**, *244*, 35.

10. Meyer, T. J. *Acc. Chem. Res.* **1989**, *22*, 163.

11. Gust, D.; Moore, T. A.; Moore, A. L. *Acc. Chem. Res.* **1993**, *26*, 198.

12. Balzani, V.; Credi, A.; Venturi, M. *ChemSusChem* **2008**, *1*, 26.

13. Kalyanasundaram, K. *Coord. Chem. Rev.* **1982**, *46*, 159.

14. Xi, Y.; Yi, H.; Lei, A. *Org. Biomol. Chem.*, **2013**, *11*, 2387.

15. Shaw, M. H.; Twilton, J.; MacMillan, D. W. C. *J. Org. Chem.* **2016**, *81*, 6898.

16. Kärkäs, M. D.; Porco, J. A.; Stephenson, C. R. J. *Chem. Rev.* **2016**, *116*, 9683.

17. Romero, N. A.; Nicewicz, D. A. *Chem. Rev.* **2016**, *116*, 10075.

18. Juris, A.; Balzani, V.; Barigelletti, F.; Campagna, S.; Belser, P.; von Zelewsky, A. *Coord. Chem. Rev*. **1988**, *84*, 85.

19. Prier, C. K.; Rankic, D. A.; MacMillan, D. W. C., *Chem. Rev.* **2013**, *113*, 5322.

20. Campagna, S.; Puntoriero, F.; Nastasi, F.; Bergamini, G.; Balzani, V. *Top. Curr. Chem.* **2007**, *280*, 117.

21. McCusker, J. K. *Acc. Chem. Res*. **2003**, *36*, 876.

22. Kavarnos, G. J.; Turro N. J. *Chem. Rev.* **1986**, *86*, 401.

23. Scandola, F.; Baizani, V. *J. Chem. Educ.* **1983,** *60*, 814.

24. Fagnoni, M.; Dondi, D.; Ravelli, D.; Albini A. *Chem. Rev.* **2007,** *107*, 2725.

25. Zhou, L.; Hossain, M. L.; Xiao, T. *Chem. Rec.* **2016**, *16*, 319.

26. Reckenthalera, M.; Griesbecka, A. G. *Adv. Synth. Catal.* **2013,** *355*, 2727.

27. Fukuzumi, S.; Mochizuki, S.; Tanaka, T. *J. Phys. Chem.* **1990,** *94*, 722.

28. Staveness, D.; Bosque, I.; Stephenson, C. R. J. *Acc. Chem. Res.* **2016**, *49*, 2295.

29. Hoffmann, N. *Chem. Rev*. **2008,** *108*, 1052.

30. Cambie, D.; Bottecchia, C.; Straathof, N. J. W.; Hessel, V.; Noel, T. *Chem. Rev.* **2016**, *116*, 10276.

31. Ischay, M. A.; Yoon, T. P. *Eur. J. Org. Chem.* **2012,** *18*. 3359.

32. Xuan, J.; Xiao, W.-J. *Angew. Chem. Int. Ed.* **2012**, *51*, 6828.

33. Nguyen, J. D.; D'Amato, E. M.; Narayanam, J. M. R.; Stephenson, C. R. J. *Nat. Chem.* **2012,** *4*, 854.

34. Tucker, J. W; Nguyen, J. D; Narayanam, J. M. R; Krabbe, S. W.T; Stephenson, C. R. J. *Chem. Commun.* **2010,** *46*, 4985.

35. Furst, L.; Narayanam, J. M. R.; Stephenson, C. R. J. *Angew. Chem. Int. Ed.* ***2011, 50, 9655.***

36. Kleinnijenhuis, R. A.; Timmer, B. J. J.; Lutteke, G.; Jan M. M. Smits, J. M. M.; Gelder, R. ; Maarseveen, J. H.; Hiemstra, H. *Chem. Eur.J.* **2016**, *22*, 1266.

37. Crimmins, M. T.; Pace, J. M.; Nantermet, P. G.; Kim-Meade, A. S.; Tomas, J. B.; Watterson, S. H.; Wagman, A. S. *J. Am. Chem. Soc.* **2000**, *122*, 8453.

38. Mangion, I. K.; MacMillan, D. W. C. *J. Am. Chem. Soc*. **2005,** *127*, 3696.

39. Hedstrand, D. M.; Kruizinga, W. M.; Kellogg, R. M. *Tetrahedron Lett*. **1978**, *19*, 1255.

40. Cano-Yelo, H.; Deronzier, A. *Tetrahedron Lett*. **1984**, *25*, 5517.

41. Dai C.; Meschini F.; Narayanam J. M. R.; Stephenson C. R. J. *J. Org. Chem.* **2012**, *77*, 4425.

42. Condie, A. G.; González-Gómez, J. C.; Stephenson, C. R. J. *J. Am. Chem. Soc.* **2010**, *132*, 1464.

43. Adrio, J.; Carretero, J. C. *Chem. Commun.*, **2011**, *47*, 6784.

44. Nguyen, J. D.; Tucker, J. W.; Konieczynska, M. D.; Stephenson, C. R. J. *J. Am. Chem. Soc.* **2011**, *133*, 4160.

45. Barton, D. H. R.; Csiba, M. A.; Jaszberenyi, J. C. *Tetrahedron Lett.* **1994**, *35*, 2869.

46. Wallentin, C. -J.; Nguyen, J. D.; Finkbeiner, P.; Stephenson, C. R. J. *J. Am. Chem. Soc.* **2012**, *134*, 8875.

47. Brasholz, M.; Reissig, H.-U.; Zimmer, R. *Acc. Chem. Res*. **2009**, *42*, 45.

48. Wei, L.-L.; Xiong, H.; Hsung, R. P. *Acc. Chem. Res*. **2003**, *36*, 773.

49. Wangab, M. *Chem. Commun.* **2015**, *51*, 6039.

50. B. M. Trost, J. J. Cregg, N. Quach, *J. Am. Chem. Soc.*, **2017**, *139*, 5133.

51. Matsubara, R.; Kobayashi, S. *Acc. Chem. Res*. **2008**, *41*, 292.

52. Gooßen, L. J.; Rauhaus, J. E.; Deng, G. *Angew Chem*. **2005**, *117*, 4110.

53. Courant, T.; Masson, G. *Chem. Eur. J.* **2012**, *18*, 423.

54. Dong, J; Xia, Q; Yan, C; Song, H; Liu, Y; Wang, Q. *J. Org. Chem.* **2018,** *83*, 4516.

55. Goodman, M.; Chorev, M. *Acc. Chem. Res*. **1979**, *12*, 1.

56. Ye, L. -W.; Shu, C.; Gagosz, F. *Org. Biomol. Chem*. **2014**, *12*, 1833.

57. https://phys.org/news/2018-03-successful-synthesis-gamma-lactam-hydrocarbons.html#jCp (accessed in August 2018)

58. Caruano, J.; Muccioli, G. G.; Robiette, R. *Org. Biomol. Chem.* **2016**, *14*, 10134.

59. Armanino, N.; Carreira, E. M. *J. Am. Chem. Soc.* **2013**, *135*, 6814.

60. Kimber, M. C. *Org. Lett.* **2010**, *12*, 1128.

61. Lu, T.; Lu, Z.; Ma, Z.; Zhang, Y.; Hsung, R. P. *Chem. Rev.* **2013**, *113*, 4862.

62. Trost, B. M.; Stiles, D. T. *Org. Lett.* **2005**, *7*, 2117.

63. Brice, J. L.; Meerdink, J. E.; Stahl, S. S. Org. Lett. **2004**, 6, 1845.

64. Furstner, A.; Brehm, C.; Cancho-Grande, Y. *Org. Lett.* **2001**, *24*, 3955.

65. Kim, S. M.; Lee, D.; Hong, S. H. *Org. Lett.* **2014**, *16*, 6168.

66. Watanabe, T.; Oishi, S.; Fujii, N.; Ohno, H. *Org. Lett.* **2007**, *9*, 4821.

67. Gaulon, C.; Gizecki, P.; Dhal, R.; Dujardin, G. *Synlett.* **2002**, *6*, 952.

68. Carbery, D. R. *Org. Biomol. Chem.* **2008**, *6*, 3455.

69. Kiyohara, H.; Matsubara, R.; Kobayashi, S. *Org. Lett*. **2006**, *8,* 5333.

70. Matsubara, R.; Nakamura, Y.; Kobayashi, S. *Angew. Chem., Int. Ed.* **2004**, *43*, 1679.

71. Kagan, H. B.; Dang, T.-P. *J. Am. Chem. Soc.* **1972**, *94*, 6429.

72. Kobayashi, S.; Gustafsson, T.; Shimizu, Y.; Kiyohara, H; Matsubara, R. *Org. Lett.* **2006**, *8*, 4923.

73. Bennasar, M. L.; Roca, T.; Monerris, M.; Garcia-Diaz, D. *J. Org. Chem.* **2006**, *71*, 7028.

74. Huang, Y.; Iwama, T.; Rawal, V. H., *J. Am. Chem. Soc*. **2000**, *122*, 7843.

75. Taniguchi, T.; Iwasaki, K.; Uchiyama, M.; Tamura, O.; Ishibashi, H., *Org. Lett.* **2005**, *7*, 4389.

76. Taniguchi, T.; Tanabe, G.; Muraoka, O.; Ishibashi, H. *Org. Lett*. **2008**, *10*, 197.

77. Bach, T.; Schroder, J. *Synthesis* **2001**, *8*, 1117.

78. Newman, D.J.; Cragg, G.M.; Snader, K.M. *Nat. Prod. Rep.* **2000**, *17*,215.

79. *Patient,*   https://patient.info/medicine/linezolid-for-infection-zyvox *(accessed June 2018).*

80. Liu, L.; Floreancig, P. E. *Org. Lett.* **2009**, *11*, 3152.

81. Nguyen, T. B.; Martel, A.; Robert Dhal, R.; Dujardin, G. *J. Org. Chem.* **2008**, *73*, 2621.

82. Tang, Y.; Babiash, E. S. C.; Feltenberger, J. B.; Hayashi, R. *Org. Lett.* **2009**, *11*, 3666.

83. Dagousset, G.; Carboni, A.; Magnier, E.; Masson, G. *Org. Lett*. **2014**, *16*, 4340.

84. Young, I. S.; Thornton, P. D.; Thompson, A. *Nat. Prod. Rep*. **2010**, *27*, 1801.

85. Zheng, X.; Dai, X. -J.; Yuan, H. -Q.; Ye, C. -X.; Ma, J.; Huang, P. -Q. *Angew. Chem. Int. Ed.*, **2013**, *52*, 3494.

86. Martelli, G.; Orena, M.; Rinaldi, S. *Curr. Org. Chem.*, **2014**, *18*, 1373.

87. Dai, C.; Narayanam, J. M. R.; Stephenson, C. R. J. *Nature Chem*. **2011**, *3*, 140.

88. Dickinson, W. B.; Lang, P. C. *Tetrahedron Lett*. **1967**, *8*, 3035.

89. DeKorver, K.; Li, H.; Lohse, A.; Hayashi, R.; Lu, Z.; Zhang, Y.; Hsung, R. *Chem. Rev.* **2010**, *110*, 5064.

90. Bogentoft, C.; Ericsson, O.; Stenberg, P.; Danielsson, B. *Tetrahedron Lett*. **1969**, *10*, 4745.

91. Corbel, B.; Paugam, J.-P.; Dreux, M.; Savignac, P. *Tetrahedron Lett*. **1976**, *17*, 835.

92. Overman, L. E.; Marlowe, C. K.; Clizbe, L. A. *Tetrahedron Lett*. **1979**, *20*, 599.

93. Ayres, J. N.; Williams, M. T. J.; Tizzard, G. J.; Coles, S. J.; Ling, K. B.; Morrill, L. C. *Org. Lett*. **2018**, *20*, 5282.

94. Tamura, Y.; Ikeda, H.; Mukai, C.; Morita, I.; Ikeda, M. *J. Org. Chem.* **1981**, *46*, 1732.

95. Padwa, A.; Caruso, T.; Nahm, S.; Rodríguez, A. *J. Am. Chem. Soc.* **1982**, *104*, 2865.

96. Galons, H.; Bergerat, I.; Combet-Farnoux, C.; Miocque, M.; Decodts, G.; Bram, G. *J. Chem. Soc., Chem. Commun.* **1985**, 1730.

97. Zaugg, H. E.; Swett, L. R.; Stone, G. R. *J. Org. Chem*. **1958**, *23*, 1389.

98. Van Boxtel, L. J.; Körbe, S.; Noltemeyer, M.; De Meijere, A. *Eur. J. Org. Chem*. **2001**, 2283.

99. Tanaka, H.; Kameyama, Y.; Sumida, S.; Yamada, T.; Tokumaru, Y.; Shiroi, T.; Sasaoka, M.; Taniguchi, M.; Torii, S. *Synlett* **1991**, 888.

100. Farina, V.; Kant, J. *Tetrahedron Lett*. **1992**, *33*, 3559.

101. Bousfield, T. W.; Kimber, M. C. *Tetrahedron Letters* **2015**, *56*, 350.

102. Demmer, C. S.; Benoit, E.; Evano, G. *Org. Lett*. **2016**, *18*, 1438.

103. Standen, P. E.; Kimber, M. C. *Curr. Opin. Drug Devel*. **2010**, *13*, 645.

104. Corbel, B.; Paugam, J.-P.; Dreux, M.; Savignac, P. *Tetrahedron Lett*. **1976**, *17*, 835.

105. Xiong, H.; Hsung, R. P.; Wei, L.-L.; Berry, C. R.; Mulder, J. A.; Stockwell, B. *Org. Lett*. **2000**, *2*, 2869.

106. Horino, Y.; Takata, Y.; Hashimoto, K.; Kuroda, S.; Kimurab, M.; Tamaru, Y. *Org. Biomol. Chem*. **2008**, *6*, 4105.

107.   Hill, A. W.; Elsegood, M. R. J.; Kimber, M. C. *J. Org. Chem.* **2010**, *75*, 5406.

108.   Manzo, A. M.; Perboni, A. D.; Broggini, G.; Rigamonti, M. *Tetrahedron Lett.* **2009**, *50*, 4696.

109.   Broggini, G.; Galli, S.; Rigamonti, M.; Sottocornola, S.; Zecchi, G. *Tetrahedron Lett.* **2009**, *50*, 1447.

110.   Rameshkumar, C.; Xiong, H.; Tracey, M. R.; Berry, C. R.; Yao, L. J.; Hsung, R. P. *J. Org. Chem.* **2002**, *67*, 1339.

111.   Kimura, M.; Horino, Y.; Wakamiya, Y.; Okajima, T.; Tamaru, Y. *J. Am. Chem. Soc.* **1997**, *119*, 10869.

112.   Nair, V.; Sethumadhavan, D.; Nair, S. M.; Shanmugam, P.; Treesa, P. M.; Eigendorf, G. K. *Synthesis* **2002**, *12*, 1655.

113.   Li, X.-X.; Zhu, L.-L.; Zhou, W.; Chen, Z. *Org. Lett.* **2012**, *14*, 436.

114.   Faustino, H.; Bernal, P.; Castedo, L.; López, F.; Mascareñas, J. L. *Adv. Synth. Catal.* **2012**, *354*, 1658.

115.   Suárez-Pantiga, S.; Hernández-Díaz, C.; Piedrafita, M.; Rubio, E.; Gonzáleza, J. M. *Adv. Synth. Catal.* **2012**, *354*, 1651.

116.   Gupta, A. K.; Park, D. I.; Oh, C. H. *Tetrahedron Lett.* **2005**, *46*, 4171.

117.   Broggini, G.; Bruché, L.; Zecchi, G. *J. Chem. Soc.*, Perkin Trans. 1. **1990**, 533.

118.   Barluenga, J.; Vicente, R.; López, L. A.; Tomas, M. *J. Am. Chem. Soc.* **2006**, *128*, 7050.

119.   Piperno, A.; Rescifina, A.; Corsaro, A.; Chiacchio, M. A.; Procopio, A.; Romeo, R. *Eur. J. Org. Chem.* **2007**, *9*, 1517.

120.   Lu, T.; Hayashi, R.; Hsung, R. P.; DeKorver, K. A.; Lohse, A. G.; Song, Z.; Tang, Y. *Org. Biomol. Chem.* **2009**, *7*, 3331.

121.   Horino, Y.; Kimura, M.; Tanaka, S.; Okajima, T.; Tamaru, Y. *Chem.-Eur. J.* **2003**, *9*, 2419.

122.   Nilsson, B. M.; Hacksell, U. *J. Heterocycl. Chem.* **1989**, *26*, 269.

123.   Singh, S.; Elsegood, M. R. J.; Kimber, M. C. *Synlett.* **2012**, *23*, 565.

124.   Liang, H.; Yan, F.; Dong, X.; Liu, Q.; Wei, X.; Liu, S.; Dong, Y.; Liu, H. *Chem. Commun.,* **2017**, *53*, 3138.

125.   Shen, L.; Hsung, R. P. *Org. Lett.* **2005**, *7*, 775.

126.   Carey, J. S.; D. Laffan, D.; Thomson, C.; Williams, M. T. *Org. Biomol. Chem.* **2006**, *4*, 2337.

127.   Bailly, C. *Curr. Med. Chem. Anti-Cancer Agents* **2004**, *4*, 363.

128. Carboni, A.; Dagousset, G.; Magnier, E.; Masson, G. *Org. Lett.* **2014**, *16*, 1240.